CLINICAL, CELLULAR, AND BIOCHEMICAL CONSEQUENCES OF XYLOSYLTRANSFERASE DEFICIENCY: IMPACT OF ISOFORMS AND CELLULAR EXPRESSION

By

NABIN POUDEL

Bachelors of Veterinary Science and Animal Husbandry
Tribhuvan University
Kathmandu, Nepal
2009

Submitted to the Faculty of the
Graduate College of the
Oklahoma State University
in partial fulfillment of
the requirements for
the Degree of
DOCTOR OF PHILOSOPHY
May, 2018

CLINICAL, CELLULAR, AND BIOCHEMICAL CONSEQUENCES OF XYLOSYLTRANSFERASE DEFICIENCY: IMPACT OF ISOFORMS AND CELLULAR EXPRESSION

Dissertation Approved:

Dr. Myron E Hinsdale

Dr. Lin Liu

Dr. Antonio G. Oomens

Dr. Steven Hartson

ACKNOWLEDGEMENTS

I have been continuously supported, encouraged and motivated by so many amazing people, throughout my graduate study, research activity and dissertation writing, without whom, this work would not have been possible.

My first and foremost acknowledgement goes to my research advisor and committee chair, Dr Myron Hinsdale, who believed in me and provided me opportunity to study and perform my doctoral dissertation research under his guidance. Dr Hinsdale, I would like to thank you for all of your efforts to carve me from a naïve student into a scientific person. I am indebted to you for your mentoring, encouragement, motivation, and positive attitude towards me and my research throughout my graduate study. Thank you for teaching me scientific research skills, good writing skills, and in becoming a good scientist as well as for providing me financial support throughout my graduate study without which this whole PhD would not have been possible. Thank you for shaping me into a good researcher.

I would also like to thank my committee members, Dr Lin Liu, Dr Antonio G Oomens, and Dr Steven D Hartson for your discussions and suggestion during each and every committee meeting. Those discussions and suggestions always helped me to better design my experiments to come up with more solid and logically sound conclusions of my research findings.

I would also like to thank OSU CVHS, VBSC graduate program and Department of Physiological Sciences for all the help and support throughout my doctoral study. I would like to shout special thanks to Michelle Kuehn, Dr Pamela Lovern, and Dr Ken Clinkenbeard for helping me with all the never ending administrative work during my PhD study. Michelle! Without you I don’t know where we all would have been. I would also like to thank OSU Graduate college for

the financial support and scholarships that were provided to me during my graduate study.

My sincere gratitude goes towards all the people from Dr Hinsdale's laboratory. I would like to thank Cristina, Pulav, Huan, Girija, Mallika, Adane, and Willie for helping me with my experiments during my busy teaching schedule. I will always be thankful to Cristina for always finding time to discuss research and many other problems. I would also like to thank Cristina, Pulav and Mallika for helping me directly with performing some of my experiments. It was a pleasure working with all of you amazing people who helped me during each and every day and constantly providing me warm and pleasant work environment.

I would also like to thank our collaborators, especially Dr Frank Rauch, Dr Craig Munns and Somayyeh Fahiminiya for providing us with the human patient samples for the second part of my dissertation. I would like to take a moment to acknowledge those three patients and their parents for their contribution and support for the science. I would also like to thank Robert Silasi-Mansat and Dr Florea Lupu from OMRF for helping with the microscopy imaging and histological analysis and Oklahoma Center for Respiratory and Infectious Diseases for providing cDNA samples from mouse lungs as well as different cell types present in a mouse lung. I would also like to thank Bo Zhai and Dr Pamela Lovern for providing cDNA from Human Coronary Artery Endothelial Cells. Sincere thanks goes to OSU DNA/ protein core facility for all plasmid sequencing and verifications. I would also like to thank all the funding agencies, including but not limited to OSU-CVHS Research Advisory Counsil, NIH-NIDDK, and PKD Foundation.

Last, but not the least I would like to thank my family for their continuous and selfless support to me. I am indebted to my father, Mr Madhav Prasad Sharma, and my mother, Mrs Ganga Devi Sharma for dreaming of a more educated family. This dissertation goes to you for all the sacrifices that you have made to make our dream come true. I would also like to thank my siblings, Pravin and Pramila for all the care, motivation, encouragement, and support that you have provided me. It is not possible to explain in words how much I am grateful to both of you. And Finally, I would not have been able to finish this without constant courage, encouragement,

and support from my wife Binu. You have been the one who had to adapt to my chaotic schedule and take care of the family and make home a better place for all along You have been there for all the ups and downs during this and I am thankful to you for everything.

Finally, I would like to acknowledge everybody who helped me directly and indirectly throughout to make my doctoral work a success.

Name: NABIN POUDEL

Date of Degree: MAY, 2018

Title of Study: CLINICAL, CELLULAR, AND BIOCHEMICAL CONSEQUENCES OF XYLOSYLTRANSFERASE DEFICIENCY: IMPACT OF ISOFORMS AND CELLULAR EXPRESSION

Major Field: VETERINARY BIOMEDICAL SCIENCES

Abstract:

Proteoglycans (PGs) are components of extracellular matrix, cell membrane, and basement membrane of the cells and consist of repeating disaccharide units of amino sugar and uronic acid, also known as glycosaminoglycans (GAGs) covalently linked to a PG core protein serine via a linker tetrasaccharide structure. The assembly of GAGs begins with the assembly of a xylose onto designated serine residues of the core protein by xylosyltransferase (XylT). There are two distinct isoforms of XylT: Xylt1 and Xylt2. Xylt2 is ubiquitously present while Xylt1 is limited to some organs. PGs and their GAG chains are very diverse in nature due to the variation in GAG length as well as due to post polymerization modifications including epimerization, deacetylation, and sulfation. This diversity makes PGs highly versatile molecules that can regulate multiple signaling pathways during growth, differentiation, proliferation and pathophysiology. Here in this study, using two distinct Xylt isoform knockout mice models in addition to human patients with mutations in XYLT2, we gain understanding of the roles of PGs during development, renal and pulmonary homeostasis and pathophysiology. We show that Spondyloocular syndrome, a rare congenital genetic disorder affecting musculoskeletal system, sensorineural system and cardiovascular syndrome, is caused by mutations in XYLT2. Using isoform-specific knockout mouse models, we show that XylT2 is critical in maintaining renal nephron physiology where reduced PG glycosylation in XylT2 deficiency results in proteinuria due to glomerular and tubular dysfunction mimicking many chronic kidney disease phenotypes. We also show that, despite XylT1 being the minor isoform in the lungs, XylT1 deficiency causes reduced pulmonary function and increased susceptibility to endotoxin-induced acute lung injury possibly due to reduced PG core protein expression, altered surfactant biology, and hyper-activation of NFkB signaling pathway.

TABLE OF CONTENTS

Chapter Page

Chapter Page

Chapter Page

LIST OF TABLES

Table Page

CHAPTER I

CHAPTER II

CHAPTER III

CHAPTER IV

LIST OF FIGURES

Figure Page

CHAPTER I

CHAPTER II

CHAPTER III

Figure Page

CHAPTER IV

LIST OF ABBREVIATIONS

AEC	Alveolar Epithelial cells
ALG	Asparagine-linked glycosyltransferase
AV	Atrio-ventricular
BALF	Bronchoalveolar lavage fluid
BMP	Bone morphogenic protein
CCL	Chemokine (C-C motif) ligand
CD	Cluster of diferentiation
CDC	Centers for Disease Control and Prevention
CSPG	Chondroitin sulfate proteoglycans
CXCL	Chemokine (C-X-C motif) ligand
DCT	Distal convoluted tubule
DSPG	Dermatan sulfate proteoglycans
ECM	Extracellular matrix
EMT	Epithelial mesenchymal transtion
EXT	Exostosin
GAGs	Glycosaminoglycans
GalNAc	N-acetyle galactosamine
GALT6	Polypeptide N-Acetylgalactosaminyltransferase 6
GALT7	Polypeptide N-Acetylgalactosaminyltransferase 7
GAT3A	Beta-1,3-Glucuronyltransferase 3
GBM	Glomerular basement membrane

GlcA	Glucuronic acid
GlcNAc	N-acetyle glucosamine
HSPG	Heparan sulfate Proteoglycans
ICAM	Intercellular adhesion molecule
IduA	Iduronic acid
IL	Interleukins
IRAK	Interleukin 1 receptor associated kinase
JAM	Junctional adhesion molecule
KC	Keratinocyte derived chemokine
LBP	Lipopolysaccharide binding protein
LFA	Integrin subunit beta 2
LH	Loop of Henle
LLO	Lipid-linked oligosaccharide
LPS	Lipopolysaccharide
MAPK	Mitogen activated protein kinase
MD-2	Myeloid differentiation protein 2
MIM	Mendelian inheritence in man
MIP	Macrophage inflammatory protein
MMP	Matrix metalloprotease
MyD88	Myeloid differentiation primary response 88
NDST-1	N-deacetylase and N-sulfotransferase I
NF-kB	Nuclear factor kappa B subuin
OST	Oligosaccharidetrasnsferase
PCT	Proximal convoluted tubule
PECAM	Platelet and endothelial cell adhesion molecular

PG	Proteoglycans
PTK	Protein tyrosin kinase
RANTES	Regulated upon activation, normally T-expressed, and presumably secreted
SGBS	simpson-golabi-behemel-syndrome
SLRP	Simple leucin rich repeats
SOS	Spondyloocular syndrome
SP	Surfactant associated protein
TGFβ	transforming growth factor beta
TIR	Toll interleukin 1 receptor
TIRAP	Toll interleukin 1 receptor domain containing adaptor protein
TJ	Tight junction
TLR	Toll like receptor
TNF	Tumor necrosis factor
TRAM	Translocation associated membrane protein
TRIF	TIR domain containing adaptor inducing inteferon beta
VCAM	Vascular adhesion molecule 1
VLA	Integrin subunit alpha 2
XYLT	Xylosyltransferase

CHAPTER I

LITERATURE REVIEW

1.1. Protein Glycosylation

Glycosylation refers to the addition of sugar molecule to the protein backbone. Protein glycosylation is the co-translational and/or post-translational addition of sugar monomers from the corresponding uridine-diphosphate nucleotide sugars to designated amino acid residues of the protein, catalyzed by groups of enzymes each specific for each monomer and collectively termed glycosyltransferases. Protein glycosylation is predominantly considered an Endoplasmic Reticulum (ER)-Golgi compartment event, but recently nucleocytoplasmic glycosylation has also been described (Hart & West, 2009). The fully mature glycoproteins are subsequently transported to the extracellular matrix (ECM) or to their cellular target that includes cellular organelles, cytoplasm, or nucleus.

Although there are total of 32 different types of glycan linkages, these can be subdivided into N-, C-, P-, and O-glycan linkages (Varki & Kornfeld, 2015). Furthermore, of these protein glycoconjugates there are three very broad and common categories: N-linked glycans, O-linked glycans, and Proteoglycans (PGs). N-linked glycosylation initiates via the addition of N-acetylglucosamine to an asparagine residue of the protein. O-linked glycosylation begins via the addition of N-acetylgalactosamine to the Serine and/or threonine residue of the protein. PGs constitute a group of glycoproteins that utilize both O-link and N-link glycoproteins. However the predominant glycan component is a disaccharide repeat and this disaccharide polymer is assembled onto specific cores or linkers of monosaccharides that subsequently are attached to the core protein. For example, heparan, chondroitin, and dermatan sulfate PGs are polysaccharides of disaccharide repeats assembled onto a specific tetrasaccharide linker that is attached to designated serine residues in the core protein (Lindahl, Couchman, Kimata, & Esko, 2015).

1.1.1 N-linked Glycosylation

N-linked glycosylation of proteins initiates at asparagine residues of the core protein specified by the consensus sequence N-X-S/T where X could be any amino acid residue besides proline (Bause, 1983). However, precision mapping of N-glycoproteomes in the mouse has detected about 26% of N-glycosylation in sites not having the previously thought consensus site (Zielinska, Gnad, Wisniewski, & Mann, 2010). N-linked glycosylation begins in the cytoplasm and completes in ER lumen (Dunphy & Rothman, 1983). The process occurs by stepwise addition of monosaccharides to ER membrane-bound phosphorylated polyisoprenols (dolichol or undecaprenol) to form a lipid-linked oligosaccharide (LLO) (Schwarz & Aebi, 2011). The oligosaccharide is formed by series of asparagine-linked glycosyltransferases (ALG) and then *en bloc* transferred to the asparagine residue of the protein at the N-X-S/T sequence by the enzyme oligosaccharyltransferase (OST) (Schwarz & Aebi, 2011). Further glycosidase trimmings and glycosylation additions complete N-linked glycosylation in the ER lumen. Significant interactions occur between these glycans and chaperone proteins calreticulin and calnexin to ensure proper glycoprotein folding (Freeze, Esko, & Parodi, 2009).

The very first step of N-linked glycosylation, the addition of N-acetylglucosamine phosphate to dolichol phosphate, is catalyzed by N-acetyl glucosamine-phosphate transferase or ALG7 which is followed by addition of β-1, 4 N-acetylglucosamine by UDP-N-acetylglucosaminyltransferase, a heteromeric enzyme complex of ALG13 and ALG14 (Gao, Tachikawa, Sato, Jigami, & Dean, 2005) (See Fig 1.1). β-1, 4 mannosyltransferase (ALG1) then transfers the first mannose residue to $GlcNAc_2$-P-P-Dol (Albright & Robbins, 1990; Couto, Huffaker, & Robbins, 1984) (See Fig 1.1). The subsequent branching mannose residues are added by α-1, 3/1, 6 mannosyltransferase encoded by gene *ALG2* (Aebi, 2013; Thiel et al., 2003) (See Fig 1.1). α−1, 2 mannose is then added to the Man_3-$GlcNAc_2$-P-P-Dol by enzyme α-1, 2

mannosyltransferase encoded by gene *ALG11* (See Fig 1.1). Once Man_5-$GlcNAc_2$-P-P-Dol or dolichol linked oligosaccharide (DLO) is formed it is then translocated inside ER lumen by Man_5-$GlcNAc_2$-P-P-Dol flippase. At present, the Man_5-$GlcNAc_2$-P-P-Dol flippase in eukaryotes is not known (Perez et al., 2015; Sanyal & Menon, 2010).

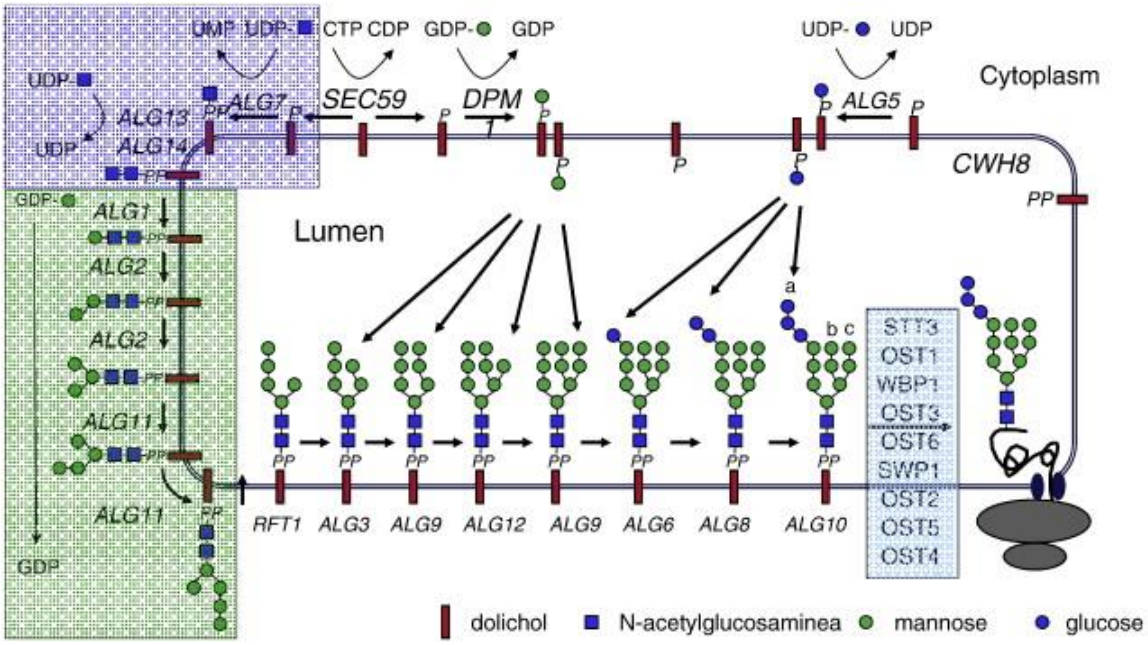

Figure 1. 1 Pathway of N-linked glycosylation
Reprinted from Biochemica et Biophysica Acta (BBA)-Molecular Cell Research vol 1883 , Aebi, Markus. "N-linked protein glycosylation in the ER". *Biochimica et Biophysica Acta (BBA)-Molecular Cell Research*1833.11 (2013): 2430-2437, with permission from Elsevier."

Translocation into the ER is critical for maturation of the DLO. Once the mDLO is translocated inside ER lumen, assembly of additional mannoses to the mannose polysaccharide results in three branches, referred to as antennae-a, b, and c (See Fig 1.1). Formation of the a-antenna is actually completed before the DLO is translocation into ER lumen. But the b- and c-antennae are assembled in the ER by a α-glycosidic linkages generated by a Dol-P-Man-dependent mannosyltransferases (Frank & Aebi, 2005). The b-antenna is formed by the sequential addition of two mannose molecules by ALG3 and ALG9 (Aebi, 2013). The c-antenna is

assembled by α-1, 6 mannosyltransferase encoded by *ALG12* and *ALG9* resulting in a Man_9-$GlcNAc_2$-P-P-Dol residue. Dol-P-Man dependent glucosyltransferases ALG6, ALG8, and ALG10 then subsequently glucosylate the a-antenna completing the formation of the tetradecosaccharide linked with dolichol (Glc_3-Man_9-$GlcNAc_2$-P-P-Dol) (Burda & Aebi, 1998; Reiss, te Heesen, Zimmerman, Robbins, & Aebi, 1996; Stagljar, te Heesen, & Aebi, 1994). The first and second glucose molecules are α−1, 3 linked while the terminal "capping" glucose molecule is α−1, 2 linked (Kornfeld & Kornfeld, 1985). This “capping” glucose establishes it as the substrate for Oligosaccharide transferase (OST) (Aebi, 2013).

Once completed the mDLO is transferred to the protein by the eukaryotic OST, a transmembrane multiprotein complex. In mammals, there are two distinct OST complexes, STT3A and STT3B where STT3A is the major OST complex (Shrimal, Cherepanova, & Gilmore, 2015) (See Fig 1.1). The transfer of oligosaccharide to the nascent polypeptide can be both co-translational and post-translational (Shrimal et al., 2015). Co-translational glycosylation is primarily mediated by STT3A complex. For those sites skipped by STT3A, STT3B complex will glycosylate (Shrimal et al., 2015). Further processing and modification within the Golgi of the N-glycosylated proteins creates variations in N-glycosylated proteins responsible for wide array of physiological and functional implications.

1.2.2 O-linked Glycosylation

Multiple forms of O-glycosylation are prevalent in eukaryotes. This linkage predominantely through the hydroxyl group of the amino acid side-chain of serine or threonine (S/T) residues includes O-N-Acetylgalactosaminylation (O-GalNAC), O-mannosylation (O-Man), O-fucosylation (O-Fuc), and O-Glucosylation (O-Glc) Another O-linkage O-galactosylation occurs on hydroxylysine and hydroxyproline (O-Gal). Unlike N-linked

glycosylations, many O-linked glycosylation events are a post-translational modification primarily in the Golgi apparatus and occurs by addition of monosaccharides instead of *en bloc* transfer of oligosaccharide to the S/T residue of the protein. Further, these modifications generally occur on a folded protein. O-GalNAc occurs in the Golgi catalyzed by N-acetyl galactosaminyltransferase (GalNAc-T) that transfers N-acetyl galactosamine (GalNAc) to designated S/T residues (Van den Steen, Rudd, Dwek, & Opdenakker, 1998). This GalNAc is then further elongated and modified by sialylation, sulfation, acetylation, fucosylation, and polylactosamine-extension. There are 20 GalNAc-T isoforms identified in eukaryotes so far (GalNAc-T 1 through GalNAc-T 20) (Bennett et al., 2012). O-GalNAc linked glycosylation has eight distinct core structures (Van den Steen et al., 1998). This is well exemplified by the mucin-type O-glycans. For the O-link glycosylations of O-α-fucose and O-β-glucose, a useful example is epidermal growth factor (Takeuchi, Kantharia, Sethi, Bakker, & Haltiwanger, 2012). These reactions are catalyzed by the respective O-fucosyl transferase and O-glucosyl transferase of which there are mutilple isoforms. For the O-man linkages account for one third of the linkages in the brain and are catalyzed by mannosyltransferases (POMT). Finally O-Galactosylation is another linkage that is found on hydroxyl-lysine and proline in collagen and may impact the rate of triple helix formation.

1.1.3 Proteoglycans

PGs consist of a core protein linked via a tetrasaccharide linker to a polysaccharide of repeating disaccharide units of hexuronic acids and amino hexose sugars referred to as glycosaminoglycans (GAGs). The four monosaccharides of the linker tetrasaccharide are assembled on the core protein at specific serine residues in Ser-Gly- sites. Unlike N-glycoproteins and O-glycoproteins, PGs are formed by assembly of GAGs onto the tetrasaccharide linker. After polymerization of the dissacchide chains, specific monosacchides are epimerized and sulfated

forming a structurally diverse and highly negatively charged polysacchaide. PGs are then translocated either to the plasma membrane, extracellular matrix, or intracellular vesicles.

1.1.3.1 Steps in PG Synthesis

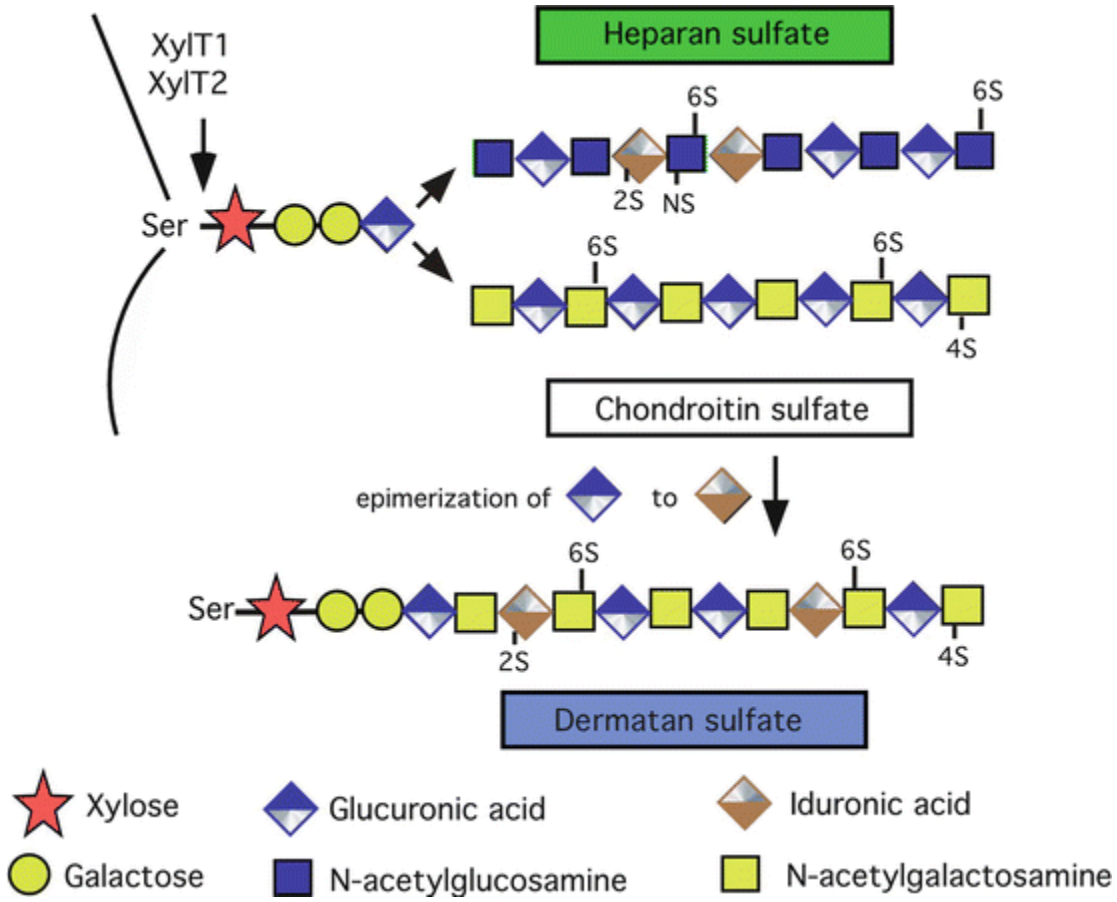

Figure 1. 2 Biosynthesis of Proteoglycans
Reprinted from Handbook of Glycosyltransferases and Related Genes vol 1 , Hinsdale, Myron E. "Xylosyltransferase I, II (XYLT1, 2)." *Handbook of Glycosyltransferases and Related Genes*. Springer Japan, 2014. 873-883., with permission from Springer Japan."

Synthesis of Proteoglycan Linker Tetrasaccharide

Formation of PG linker tetrasaccharide begins with the assembly of a xylose (Xyl) onto the serine residue of core protein by Xylosyltransferase (XYLT) (See Fig 1.2). There are two isoforms of XYLTs: XYLT1 and XYLT2 with XYLT2 being the predominant isoform in most tissues. XYLT transfers Xyl from a UDP- Xylose molecule to form a xyl-β1-O-Serine linkage

(Lindahl et al., 2015).This process occurs in the ER membrane. The protein then moves to *cis*-Golgi where two galactose (Gal) molecules are sequentially assembled by enzymes β1, 4-galactosyltransferase I (b3Galt7) and β1, 3-galactosyltransferase II (b3Galt6) in the *cis*-Golgi and *medial*-Golgi (Sugumaran, Katsman, & Silbert, 1992) (See Fig 1.2). This process is then followed by the assembly of Glucuronic acid by β1, 3-glucuronosyltransferase I (b3Gat3a) in the *medial*-Golgi forming the *D-GlcA-β1-3-Gal–β1-3-Gal-β1-4-Xyl-Ser* linker tetrasaccharide (See Fig 1.2). Disaccharide units of either heparan sulfate PGs (HSPG) or chondroitin sulfate PGs (CSPGs) are then polymerized onto the linker tetrasaccharide to form specific types of PGs, which are then modified by epimerization and sulfation at various carbon atoms of the monosaccharides of the repeating disaccharide chains.

Synthesis of HSPGs

HSPGs are formed by the assembly of repeating disaccharides polymers of N-acetylglucosamine (GlcNAc) and GlcA that constitute the GAG chain. Initiation of HSPG GAG chain polymerization begins by assembly of GlcNAc to the tetrasaccharide structure by α4-N-acetylglucosaminyltransferase (Lindahl et al., 2015). The oligomeric enzyme complex of EXT1/EXT2 (β4-glucuronyltransferase) then assembles the disaccharide polymer forming -$[4GlcA\text{-}\beta1\text{-}4\text{-}GlcNAc\text{-}\alpha1]_n$-4GlcA-β1-3-Gal-β1-3Gal-β1-4-Xyl-Serine. The HSPG GAG chains then undergo a series of sequential modifications including deacetylation, sulfation, and epimerization. GlcNAc is deacetylated and rapidly sulfated at Nitrogen molecule by the enzyme GlcNAc-deacetylase/N-sulfotransferase (NDST-1) forming N-sulfated Glucosamine ($GlcNSO_3$). This process does not deacetylate/sulfate all of the GlcNAc monosaccharides resulting in a mixture of $GlcNSO_3$ and GlcNAc in the HSPG GAG. Other modifications of HSPG GAGs include epimerization of C5 of GlcA and conversion of the monosaccharide into Iduronic acid (IduA) by Glucuronyl C5-Epimerase (Li, 2010), sulfation of C2 molecule of IduA adjacent to

reducing end of N-sulfated glucosamine by 2-O-sulfotransferase, and sulfation of C6 of $GlcNSO_3$ by 6-O-Sulfotransferase. 2-O-Sulfotransferase also sulfates some of the GlcA molecules.

Synthesis of CSPGs

CSPGs consist of repeating disaccharide units of GalNAc and GlcA. Once the linker tetrasaccharide structure is formed, the polymerization of the repeating disaccharide units of GalNAc and GlcA begins. The addition of GalNAc is catalyzed by β-1, 4-N-acetylgalactosaminyltransferase. The repeating disaccharide polymers are then assembled by the bifunctional enzyme complex collectively termed as chondroitin synthase forming -[4GalNac-α-4GlcA-β1]$_n$-4-GalNAc-α1-4GlcA-β1-3-Gal-β1-3Gal-β1-4-Xyl-Serine (Lindahl et al., 2015). ChSy acts as both β−1,4-N-acetylgalactosaminyltransferase and β−1,3-glucuronyltransferase to elongate the CSPG GAG chain (Lindahl et al., 2015). A new enzyme, chondroitin polymerization factor works in conjunction with Chondroitin synthase to elongate the CSPG GAG chain (Kitagawa, Izumikawa, Uyama, & Sugahara, 2003). After the CSPG GAG chain is attached to the core protein, similar to HSPG GAG chains, the GlcA at various positions in CSPG GAG chain is epimerized into IduA by glucuronyl C5-epimerase. C-4 and C-6 of GalNAc are sulfated by 4-O-sulfotransferase and 6-O-sulfotransferase respectively, and the C-2 of IduA adjacent to reducing end of GalNAc is sulfated by 2-O-sulfotransferase. The donor for the sulfate molecule during those sulfation processes is 3'-phosphoadenosine-5'-phosphosulfate (Cortes, Baria, & Schwartz, 2009). Since these modifications can result in various disaccharide units with various sulfation patterns, the CSPG GAGs are classified into five different groups of CSPG-A, CSPG-B, CSPG-C, CSPG-D, and CSPG-E. Mammalian CSPG GAGs with IduA are characterized as dermatan sulfate PG GAGs. These GAGs consist of mixtures of various types of CSPG disaccharides of the CSPG-A, -B, and -C groups and therefore are hybrid structures. The different groups of GAGs

can be distinguished by selective digestion using bacterial enzymes specific to each type of CSPG GAG disaccharide (Lindahl et al., 2015).

1.1.3.2 Heparan Sulfate Proteoglycans

HSPGs in Basement membrane

There are three primary HSPGs in basement membrane: Agrin, Perlecan and Collagen XVIII. The Agrin core protein is ~220kDa and with the GAG chains assembled it can be as large as ~400 kDa in size. Agrin has 2-3 putative HSPG binding domains, and it was first identified in basement membrane of neuromuscular junction where it aggregated the acetylcholine receptors (Nitkin et al., 1987), hence the name agrin. Since then, rigorous studies have established agrin as a predominant basement membrane proteoglycan, especially in the glomerular basement membrane, and in the fused basement membrane of endothelium and type I pneumocytes in lungs (Groffen et al., 1998). Alternative splicing at three different sites *x, y* and *z*, results in multiple isoforms of agrin with distinct functions in multiple tissues (Burgess, Nguyen, Son, Lichtman, & Sanes, 1999; Campanelli, Gayer, & Scheller, 1996; M. Gesemann et al., 1996; O'Toole et al., 1996; Ruegg et al., 1992). In kidneys, full-length agrin is localized in the glomerular basement membrane while the ot basement membranes of other nephron components consist of C-terminally truncated agrin that lacks the C-terminal agrin fragment (C. J. I. Raats et al., 1998). Agrin is proteolytically cleaved during pathological conditions (Daryadel et al., 2016; Drey et al., 2013). A high-resolution ultrastructural localization study using sub-diffraction resolution stochastic optical reconstruction microscopy on glomerular basement membranes shows agrin to be localized into two different layers of the glomerular basement membrane (Suleiman et al., 2013). This ultrastructural analysis (Suleiman et al., 2013) shows that the C-terminus of agrin is located more towards the cell membrane and N-terminus situated more towards the middle of the GBM. These findings reinforce the idea that agrin can bind with laminins in the ECM and integrins in the plasma membrane as well as α-dystroglycan in the

basement membrane (Denzer et al., 1998; Matthias Gesemann, Brancaccio, Schumacher, & Ruegg, 1998).

Perlecan is a ~400kDa proteoglycan consisting of five functional protein domains and three HS GAG binding sites (Paulsson, Yurchenco, Ruben, Engel, & Timpl, 1987). Perlecan has been studied extensively in the glomerular basement membrane as well as in the alveolar basement membrane in the lungs; however, it is present in most basement membranes. In addition to providing negative charge in the basement membrane, perlecan interacts with the fibrillin microfibrils (Tiedemann et al., 2005) and growth factors (Farach-Carson & Carson, 2007), stimulates angiogenesis and vasculogenesis (Aviezer et al., 1994).

Collagen XVIII is a type of non-fibrillar collagen with interspersed non-collagenous domains in between Gly-X-Y- repeats. The non-collagenous domains in collagen XVIII have sites for the N-glycosylation as well as for the HS GAG chains. There are three putative HS GAG serines in collagen XVIII. Alternative splicing of collagen XVIII results in three distinct isoforms of collagen XVIII (Suzuki et al., 2002). Genetic knockout/knockin studies reveal distinct functions and distinct expression patterns of each isoforms (Aikio et al., 2014; Kinnunen et al., 2011).

HSPGs in Cell membrane

Two distinct groups of HSPGs are localized in the cell membrane, glypicans and syndecans. Glypican family of HSPGs are glycosyl-phosphatidyl-inositol (GPI) anchored PGs and comprises six different glypicans: glypican-1 to glypican-6 (Filmus, Capurro, & Rast, 2008). Phylogenetically glypicans can be grouped into two broad families: glypican-3/5 that resemble drosophilla *dally* and glypican-1/2/4/6 that resemble *Drosophila dally* like protein (*dlp*) (Filmus et al., 2008). Early studies using molecular cloning and characterization showed a temporospatial distribution of glypicans in development as well in adult tissues. While glypican-1, glypican-4,

and glypican-6 are present in most of the tissues (David et al., 1990; Litwack, Stipp, Kumbasar, & Lander, 1994; Paine-Saunders, Viviano, & Saunders, 1999; Watanabe, Yamada, & Yamaguchi, 1995), glypican-2 is expressed during embryological development but is not detected in adult tissues (Stipp, Litwack, & Lander, 1994). Glypican-5 is primarily in the brain (Mark Veugelers et al., 1997) and glypican-3 is detected in kidneys, ovaries, mammary gland, lungs, and mesothelium (Pellegrini et al., 1998). Some glypicans are proteolytically cleaved and released from the cell surface and modulate various signaling pathways (De Cat et al., 2003). Furthermore, glypicans have been shown to developmentally regulate multiple signaling pathways including Wnt, Hedgehog, and Notch signaling in Drosophila as well as mammals by creating a morphogen gradient due to their ability to bind various growth factors and ligands (Capurro, Xiang, Lobe, & Filmus, 2005; Desbordes & Sanson, 2003; Y. Wu, Belenkaya, & Lin, 2010).

Syndecans are another type of membrane-associated PGs. Syndecans are type I transmembrane proteins with a short cytoplasmic domain, a hydrophobic transmembrane domain, and an N-terminal ectodomain with multiple HSPG GAG chain assembly serines (Carey, 1997). Four different syndecans have been identified in vertebrates (Tkachenko, Rhodes, & Simons, 2005) that can be broadly grouped into two subfamilies based on the protein sequence homology: syndecan-1/3 and syndecan-2/4 (Couchman, 2003). Like glypicans, there is a temporal and spatial distribution of syndecan expression at various stages of growth and development (Bernfield et al., 1992). Syndecan-1 and syndecan-2 are expressed in the mesenchymal tissue in the embryo and mostly in epithelial cells and plasma cells in the adults; syndecan-3 is typically present in the neuronal and musculoskeletal tissue. Syndecan-4 is ubiquitously present in most of the tissues (Bernfield et al., 1999). Syndecans regulate development, modulate various signaling pathways

including those for transforming growth factor beta (TGFβ) and fibroblast growth factor-2 and regulate cell adhesion and cell-extracellular matrix interaction (Tkachenko et al., 2005).

CD44 is a membrane-bound glycoprotein encoded by a single gene but present in multiple isoforms due to alternative splicing as well as post-translational modification (Screaton et al., 1992). Some isoforms of CD44 have HSPG as well as CSPG GAG chains assembled on them (Sleeman, Kondo, Moll, Ponta, & Herrlich, 1997). It can be a "part-time" PG meaning it may or may not have GAGs assembled on the core protein. CD44 is important in regulating growth and development, binding with multiple ligands such as hyaluronic acid, anchoring cells through cell adhesion, acting as co-receptor for signaling, controlling axonal guidance, as well as tumor metastasis (Ponta, Sherman, & Herrlich, 2003). As with most core proteins, the differential role that the core protein has versus the GAG chains in these activities is largely unknown.

Transforming growth factor beta receptor III (TGFβR-3) and neuropilin-1 are two membrane part-time PGs (Sarrazin, Lamanna, & Esko, 2011). TGFβR3 downregulates TGFβ signaling by inhibiting the TGFβ-1 and TGFβ-2 receptor complex formation and the GAG chains in TGFβR3 are required for the function of TGFβR3 as a regulator of TGFβ signaling (Eickelberg, Centrella, Reiss, Kashgarian, & Wells, 2002).

HSPGs in Cytoplasmic vesicles

Until now only serglycin has been detected as a cytoplasmic proteoglycan and known to have both HSPG and CSPG GAG chains (Kolset & Tveit, 2008). Serglycin is present in cytoplasmic vesicles in hematopoietic cells and endothelial cells (Kolset, Prydz, & Pejler, 2004) as well as in other cell types (Kolset & Tveit, 2008). In neutrophils and mast cells, serglycin is considered to be responsible for granule formation, proteases retention, and the release of the molecules from the granules (Kolset & Tveit, 2008). In macrophages, serglycin is present in the secretory vesicles and released during inflammatory events and binds with the inflammatory

cytokines and chemokines (Kolset, Mann, Uhlin-Hansen, Winberg, & Ruoslahti, 1996). Serglycin is also responsible for binding proteins and providing GAG in platelet α granule function. It was previously named "proteoglycan carrier protein for platelet factor 4 (PF4)" but was later sequenced as serglycin (Perin, Bonnet, Maillet, & Jolles, 1988).

1.1.3.3 Chondroitin/Dermatan Sulfate Proteoglycans

CSPGs have not been studied as extensively as HSPGs. Most of the CSPGs identified in mammals are extracellular matrix proteins. Syndecans, TGFβR3, CD44, and serglycin, which are primary HSPGs also have CS GAG chains attached to them in addition to their HS GAG chains (Lindahl et al., 2015). Broadly CSPGs can be divided into three distinct groups: Aggrecan family of CSPGs, Small Leucine-rich Proteoglycans (SLRPs) and other CSPGs.

Aggrecan Family of CSPGs

This family consists of large extracellular matrix CSPG. Most of these proteins are secreted in the extracellular matrix (ECM). They were initially characterized in cartilage, but were later found as predominant molecules in the brain and other tissues. Aggrecan family consists of four different large CSPGs: Aggrecan, versican, neurocan and brevican. The amino-terminal of Aggrecan family has hyaluronan binding sites, the central region has CS/keratin sulfate (KS) binding sites and the carboxy-terminal has lectin-like domains.

Aggrecan has more than 100 CSPG GAG chains assembled onto its core protein. In addition to CSPG GAG chains, aggrecan also contains N-linked and O-linked KS GAG chains (Iozzo & Murdoch, 1996; Kiani, Chen, Wu, Yee, & Yang, 2002). Aggrecan consists of three globular domains G1, G2 and G3. G1 domain is the binding site for hyaluronan while the G3 domain is the primary binding site for ECM proteins like fibrillin and tenascin-C (Day et al., 2004). It is the major constituent of cartilage ECM PG where it forms hydrated gel of aggrecan-hyaluronan aggregates (Kiani et al., 2002). These aggregates are important in chondrocyte-

chondrocyte interaction as well as chondrocyte-ECM environment interaction (Kiani et al., 2002). In addition to the cartilage, aggrecan is also present in nervous tissue serving an important role during various stages of development and differentiation.

Versican is a large ECM PG with approximately 20 GAG binding sites (Zimmermann & Ruoslahti, 1989). Versican has four distinct isoforms resulting from alternative splicing: V0-V3 of which V3 does not have any GAGs assembled onto it and is not considered as a PG (Shinomura, Nishida, Ito, & Kimata, 1993). Versican has similar structure and functions as of aggrecan, giving structure to the ECM framework through protein-protein interactions and binding with hyaluronan (Zimmermann & Ruoslahti, 1989). Decades of interaction studies of versican with other ECM proteins have shown versican to be an important regulator of cellular proliferation, migration, differentiation as well as sequestration and release of growth factors and various cytokines and inflammatory mediators (Hatano et al., 2017; Macri, Silverstein, & Clark, 2007; Wight, Kang, & Merrilees, 2014).

Small Leucine-rich Proteoglycans (SLRPs)

SLRPs are small proteoglycans with one to two CS/DS or KS GAG chains. The core protein of SLRPs consists of numerous 20-30 AA long leucine-rich repeats (Halper, 2014). Decorin and biglycan have 10 leucine-rich regions with CS/DS GAG chains while lumican and fibromodulin have 10 LRRs with KS GAG chains (Halper, 2014). The leucine rich repeats in SLRPs interact with fibrillar collagen and support fibrillogenesis (Heinegard, 2009). In addition, decorin and biglycan directly bind and inhibit TGFβ and they modulate the function of several growth factor receptors impacting multiple signaling pathways, cellular proliferation and the inflammatory response (Babelova et al., 2009; Halper, 2014; Hildebrand et al., 1994; Merline et al., 2011; Nastase, Young, & Schaefer, 2012).

Decorin is primarily produced by fibroblasts, smooth muscle cells, and endothelial cells and subsequently is ubiquitously present in multiple tissues (Neill, Schaefer, & Iozzo, 2012). Decorin interacts with various cytokines, ECM proteins, and Toll-like receptors (TLRs). It also sequesters multiple growth factors leading to inhibition of receptor tyrosine kinase family receptors (Halper, 2014; Hildebrand et al., 1994; Neill et al., 2012). Because of its diverse role, decorin is considered a potent tumor suppressor, cell proliferation regulator and immuno-suppressor (Neill et al., 2012; Yoon & Halper, 2005).

Biglycan possess two CSPG GAG assembly sites. It has similar functions as of decorin in sequestering various growth factors, activation of TLR-2/4 and purinergic P2X7 receptor, and mediating a sterile pro-inflammatory environment (Babelova et al., 2009; Hildebrand et al., 1994; Nastase et al., 2012). Biglycan, through it interaction with LRP6, modulates canonical Wnt signaling (Berendsen et al., 2011). During bone formation, biglycan regulates the process of ossification and mineralization of bone by influencing TGFβ/Bone Morphogenic Protein (BMP-4) signaling and canonical Wnt signaling (Berendsen et al., 2011; Parisuthiman, Mochida, Duarte, & Yamauchi, 2005).

Fibromodulin, lumican, and keratocan are of KSPGs (Halper, 2014), and they primarily bind collagen. These PGs have an additional N-terminal extension that consists of sulfated tyrosine residues (Heinegard, 2009). In addition to collagen binding, these PGs have been shown to interact with TGFβ (Hildebrand et al., 1994), IL10 as well as TLRs (Heinegard, 2009).

1.2. Spondylo-ocular syndrome

Spondylo-ocular syndrome (SOS) (MIM# 605822) is a rare genetic disorder characterized by developmental defects involving ocular structures, cardiovascular structures, and the musculoskeletal system. It was first defined by Schmidt et. al. (2001) for five siblings born

from consanguineous parents . The ocular phenotypes in those patients were studied in more details by Rudolph et al (2003) . A sixth case of a 5 year old boy with SOS phenotype was later reported by Alanay, Superti-Furga, Karel, and Tuncbilek (2006). Although cited by MIM in 2001 as distinct condition, gene mutations responsible for SOS were not identified until 2015 when Munns *et al* carried out whole exome sequencing followed by Sanger sequencing for three individuals consisting of two siblings and an unrelated individual with an SOS phenotype. Their findings demonstrated these individuals carried homozygous frameshift mutations in *XYLT2* (Munns et al., 2015). Later in 2016, a new report described four additional individuals of two siblings and two other unrelated patients, with additional novel mutations in XYLT2 gene causing SOS phenotypes (Taylan et al., 2016). A summary of phenotypes in described patients is included in Table 1.1.

1.2.1. PGs in SOS like phenotype

1.2.1.1. Musculoskeletal development

There are reports of mutations in almost every enzyme in the GAG assembly pathway each resulting in some form of musculoskeletal defect (Brown & Eames, 2016). Some of these syndromes were identified well before classical position cloning, gene mapping strategies, and whole genome sequencing were available. With the development of these new technologies, mutations in GAG assembly enzyme or the corresponding core protein have been readily matched with their associated musculoskeletal syndromes. Mutations in *XYLT1* (OMIM# 608124) result in Desbuquois dysplasia, *B3GALT7* (OMIM# 604327) in Type 1 Ehlers-Danlos Syndrome (EDS), *B3GALT6* (OMIM# 615291) in type 2 EDS type 1 spondyloepimetaphyseal dysplasia with joint laxity, *B3GAT3* (OMIM# 606374) in multiple joint dislocation, short stature, craniofacial dysmorphism and congenital heart defects. Hereditary Multiple Exostoses (HME), characterized by cartilaginous outgrowths in bones, results from mutations in HSPGs polymerizing enzymes

EXT1 (OMIM#608177), *EXT2* (OMIM#608210) and *EXTL3* (OMIM#600209). Chondroitin synthase (OMIM# 608183) mutations result in Tentamy preaxial brachydactyly syndrome.

In support of the congenital defects resulting from these mutations, animal models of GAG deficiency also show distinct musculoskeletal defects. GAG deficit zebrafish and mouse models show varying degrees of abnormal skeletal phenotypes (Eames et al., 2011; LeClair, Mui, Huang, Topczewska, & Topczewski, 2009; Mis et al., 2014; Wiweger et al., 2011). The mild skeletal phenotypes in total GAG knockout zebrafish *hi307* (mutation of *b3gat3*) suggest that only the core protein with substantially shortened GAG chains might be enough for the majority of skeletal development (Wiweger et al., 2011), which is supported by lack of a severe musculoskeletal phenotype observed in higher mammals such as the pug mouse that has a hypomorphic *Xylt1* allele causing early chondrocyte maturation, premature mineralization, and dwarfed overall body size (Mis et al., 2014).

Changes in PG core proteins also result in skeletal phenotypes. Glypican-4 knockout zebrafish (*knypek*) have distinct craniofacial dysmorphism as well as skeletal abnormalities (LeClair et al., 2009) and in humans, mutations in glypican-4 are associated with Simpson-Golabi-Behmel syndrome (SGBS), a rare genetic disorder involving multi-organ systems (Waterson, Stockley, Segal, & Golabi, 2010), so are mutations in glypican-3 (M. Veugelers et al., 2000). Mutation in aggrecan, a CSPG of the cartilage, results in Spondyloepiphyseal dysplasia characterized by shortening of trunk and limbs (Gleghorn, Ramesar, Beighton, & Wallis). Mutation in perlecan, a basement membrane HSPG is associated with Silverman-Handmaker type dyssegmental dysplasia (Arikawa-Hirasawa et al., 2001) and Schwartz-Jampel syndrome (Stum et al., 2006). Both of these syndromes have prominent musculoskeletal defects.

1.2.1.2 Ocular development

PGs are shown to be the crucial players during various stages of eye development and homeostasis. Immunolocalization studies have mapped HSPGs, CSPGs, and DSPGs in retina and choroid, while KSPGs are predominant in Sclera (Clark et al., 2011). Basement membrane HSPGS agrin, perlecan and collagen XVII are the principle HSPGs present in the retina (Keenan et al., 2012) towards the basal lamina while nervous tissue CSPGs neurocan and phosphocan are present in the extracellular matrix, in the nerve fiber-rich layers (Margolis, Rauch, Maurel, & Margolis, 1996). Neurocan mRNA expression undergoes extensive changes at the inner plexiform layer, nerve fiber layer and outer plexiform layers of the retina during retinal development (Masaru Inatani, Tanihara, Oohira, Honjo, & Honda, 1999), and during transient retinal ischemia (M. Inatani et al., 2000) suggesting some return to developmental profiles with tissue injury and repair. Mutation in versican causes Wagner syndrome (Kloeckener-Gruissem et al., 2013), characterized by chorioretinal atrophy, cataract, and retinal detachment. The molecular mechanisms for these ocular abnormalities are yet to be determined.

1.2.1.3 Cardiovascular development

During initial heart development, the atrioventricular (AV) cushion forms the AV septum and AV valves. Formation of AV cushions is facilitated by the deposition of ECM in the form of cardiac jelly. Endocardial cells covering the jelly then undergo epithelial-mesenchymal transition (EMT) populating the acellular AV cushion (Lockhart, Wirrig, Phelps, & Wessels, 2011). Cellular migration in AV vaulvogenesis is controlled by bone morphogenic protein- 2(BMP2) (Inai, Norris, Hoffman, Markwald, & Sugi, 2008) and multiple transforming growth factors (TGF) (Mercado-Pimentel & Runyan, 2007) and PGs regulate TGF signaling by sequestering the ligands for TGFβ receptors (Hausser, Gröning, Hasilik, Schönherr, & Kresse, 1994) (Kolb, Margetts, Sime, & Gauldie, 2001). Versican knockout mice (*hdf-/-*) die during embryonic stages with severe heart septal defects (Yamamura, Zhang, Markwald, & Mjaatvedt, 1997). Perlecan

knockout mice also exhibit similar phenotypes (Costell et al., 2002). Humans with SGBS, caused due to the mutation in glypican-3, develop cardiovascular malfunction (Lin, Neri, Hughes-Benzie, & Weksberg, 1999) and glypican-3 knockout mice exhibit high incidences of congenital heart defects (Ng et al., 2009). Mutations in glypican-6 causes autosomal recessive omodysplasia; a phenotype that involves defects in upper limbs and occasional cardiac defects (Campos-Xavier et al.). Genome-wide study of Tetralogy of Fallot linked the disease to single nucleotide polymorphisms in glypican-5 (Cordell et al., 2013). In all, these data demonstrate that altered PG environments disrupt cardiogenesis.

1.3. Renal Histology and Physiology

1.3.1 Epidemiology of Renal Disease in America

The kidney is a very important organ of homeostasis that excretes metabolic wastes produced in the body, maintains physiological fluid homeostasis, and regulates production of various vitamins and hormones. The Center for Disease Control and Prevention estimates that about 10% of the adult population in United States may have some form of chronic kidney disease (CDC). Kidney diseases are one of the top ten leading causes of death in Oklahoma (OSHD report, 2014). Proteinuria, abnormal loss of protein in urine, is a significant negative prognostic indicator of worsening kidney disease.

1.3.2 Renal Histology and Physiology

Kidneys are comprised of more than a million nephrons. The nephron consists of a glomerulus that filters the blood and a tubule system that reabsorbs or "reclaims" important molecules, including water, lost through the glomerular filter. As blood passes through the glomerular capillaries, the ultrafiltrate is produced via the glomerular basement membrane (GBM). This ultrafiltrate then passes into the proximal convoluted tubule where important proteins are re-absorbed/reclaimed by the scavenger receptors megalin and cubulin.

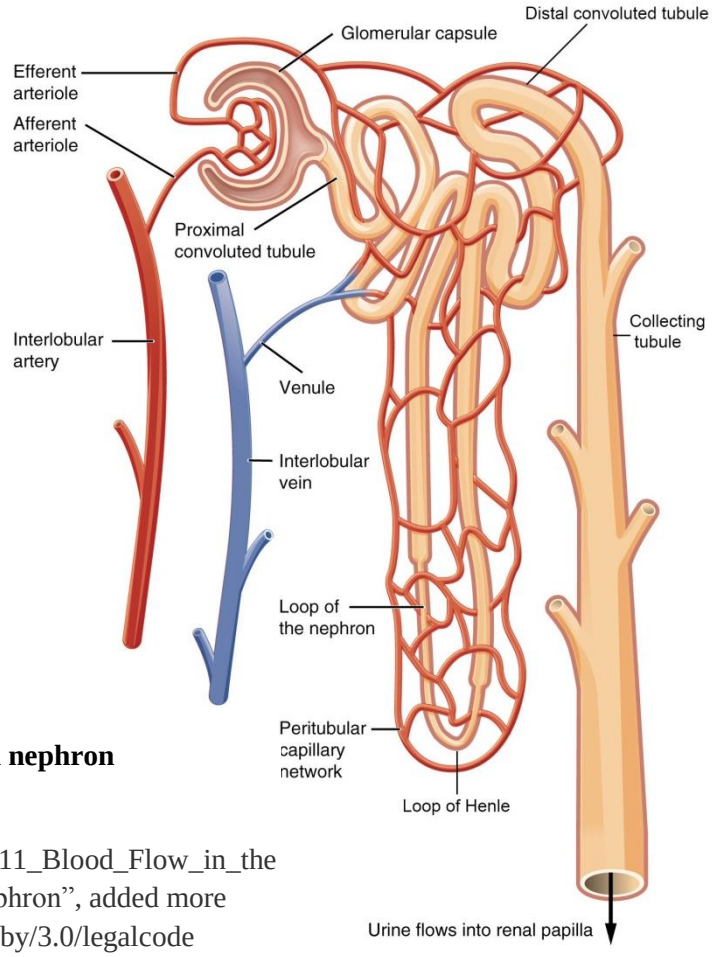

Figure 1. 3 Structure and components of a nephron

OpenStax College https://commons.wikimedia.org/wiki/File:2611_Blood_Flow_in_the_Nephron.jpg), "2611 Blood Flow in the Nephron", added more labels, https://creativecommons.org/licenses/by/3.0/legalcode

Histologically, the glomerulus resides within the renal corpuscle and constitutes the tuft of capillaries that are enclosed in visceral epithelial cells of Bowman's capsule. These cells are reflected within Bowman's capsule as the parietal layer thus enclosing Bowmen's space which is the initial site for collection of the newly formed ultrafiltrate. These visceral epithelial cells share a basement membrane with the glomerular endothelial cells in the glomerulus thus forming the GBM and are continuous with the epithelium of the proximal convoluted tubule outside the glomerulus. Another name for the visceral epithelial cells is podocytes. In addition to the capillary endothelium and podocytes in the glomerulus, interposed between glomerular

endothelial cells are mesangial cells that help in turning over of extracellular matrix of the GBM as well as in regulating glomerular blood flow. Blood enters the capillaries through afferent arteriole, which then flows through capillary tufts where most of the ultrafiltrate is generated and then the blood exits through the efferent arteriole. At this point, the blood flows into a peritubular capillary network comprised in some portions of a specialized network called the vasa-recta, this peritubular network is where the molecules, solutes, and water absorbed from the tubule system are drawn back into the blood and carried away via circulation.

Once created, the urinary ultrafiltrate then enters into the proximal convoluted tubule (PCT) that is lined by a simple cuboidal epithelium with apical microvilli and basal mitochondrial striations. About 95% of the kidney's reabsorption occurs in the PCT, the ultrafiltrate then passes through the loop of Henle (LH). In addition to reabsorption, small molecules like creatinine, uric acid, antibiotics, and diuretics are secreted into the lumen of PCT. In LH, potassium and other ions are reabsorbed thus increasing the tonicity of the medulla of the kidney. The maintenance of this medullary hypertonicity is very important for reabsorption of water from more distal portions of tubule lumen back into circulation. Once the ultrafiltrate passes LH, it reaches the distal Convoluted Tubule (DCT) where more urea and other solutes are secreted followed by pH modulation and water reabsorption in the collecting tubule system and ultimately collected in the renal pelvis and exit from the kidney via the ureter.

1.3.2.1. Glomerular Filtration Barrier and Glomerular Filtration

The glomerular filtration barrier consists of three distinct components: The capillary endothelium, specialized structure of the plasma membrane of the podocytes, and the GBM that is formed by both basement membranes of endothelium as well as podocytes (Figure 1.3). The glomerular capillary endothelium is fenestrated. Small molecules like creatinine, urea and other

metabolites in plasma can easily escape the capillaries through the fenestrations, but the fenestrations are not big enough for cellular passage.

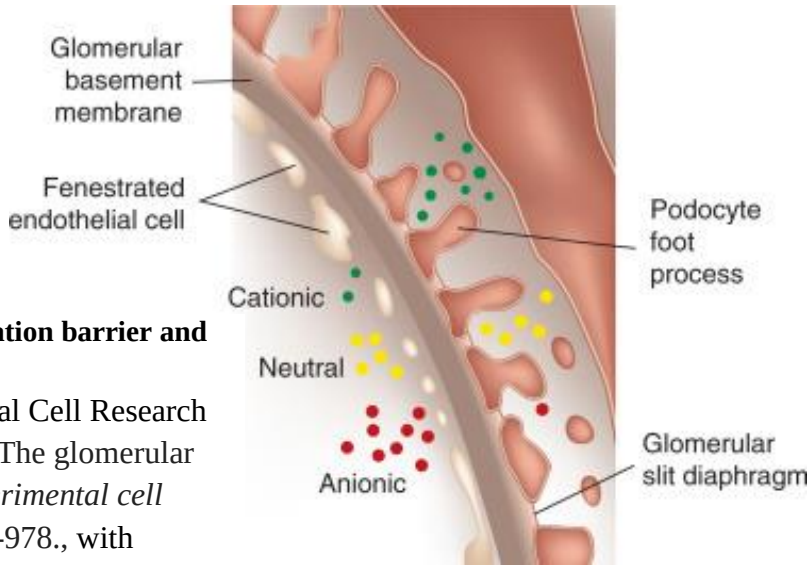

Figure 1. 4 Glomerular filtration barrier and glomerular filtration
Reprinted from Experimental Cell Research 318(9)., Miner, Jeffrey H. "The glomerular basement membrane." *Experimental cell research* 318.9 (2012): 973-978., with permission from Elsevier."

The GBM is fused basement membrane of that from the endothelium and podocytes. The GBM consists of laminins, type IV collagen, nidogens and HSPGs. The primary laminin in a fully formed GBM in laminin-521 (St John & Abrahamson, 2001) but other laminins are temporally expressed during various developmental stages of GBM (Sorokin et al., 1997). The PG component of GBM consists of HSPGs Agrin, perlecan and collagen XVIII (Miner, 2012). It has been hypothesized that HSPGs provide the anionic environment in GBM responsible for the glomerular permselectivity against proteins like albumin which are relatively negative in charge. However, recent evidences suggest that glomerular anionic environment is not the key player in glomerular filtration. Conditionally knockout mice for GAG binding sites of agrin and perlecan in podocytes do not show GBM defects and proteinuria (Goldberg, Harvey, Cunningham, Tryggvason, & Miner, 2009). In addition, when HSPGs were degraded using heparan degrading enzymes (van den Hoven et al., 2008) no proteinuria resulted. What these results highly suggest is

that alterations in GBM GAGs along are not sufficient to cause nephron dysfunction resulting in proteinuria. Recently Hausmann et al. (2010) have proposed that GBM acts as an electrophoretic sieve to get proteins to get back into serum from the urinary space.

The podocytes are specialized epithelial cells with foot process projections that interdigitate with those from itself and other podocytes where the intervening space between the foot processes is spanned with a specialize portion of plasma membrane referred to the filtration slit diaphragm. These slits are about 30-40nm wide and a are primary size exclusion sieves in the glomerulus (Schneeberger, Levey, McCluskey, & Karnovsky, 1975). The slit diaphragm has embedded in it the adhesion molecule ZO-1, nephrin, P-cadherin, CD2 associated protein, podocin, and Neph-1 all of which play important role in maintaining glomerular molecular selectivity as evidenced by biochemical as well as mutation studies of these proteins (Boute et al., 2000; Donoviel et al., 2001; Inoue et al., 2001; Reiser, Kriz, Kretzler, & Mundel, 2000; Ruotsalainen et al., 1999; Shih et al., 1999).

1.3.2.2. Scavenger Receptors and Tubular Reabsorption

Once the ultrafiltrate is produced, the myriad of proteins and vitamin binding molecules that got leaked are then primarily reabsorbed back into the blood by the PCT epithelium leaving little protein in the ultrafiltrate once it leaves the PCT. The microvilli in the luminal surface of PCT have scavenger receptors megalin and cubilin that uptake these lost proteins by endocytosis (Zhai et al., 2000).

Megalin (also known as LRP2) is low-density lipoprotein-related protein present in the PCT in the kidney. Megalin is 600KDa type I transmembrane protein with three distinct domains: a cytoplasmic tail, a single transmembrane domain, and an N-terminal extracellular domain. Mass spectrometric analysis of megalin showed heterogenous N-glycosylation in the N-terminal extracellular domain of megalin (Morelle et al., 2000). The extracellular domain of megalin has

four clusters of cystine-rich LDL receptor ligand binding repeats of which the second cluster consisting of the region from 1111- 1210 is identified as the primary site of ligand binding (Orlando et al., 1997). Megalin knockout mice have low molecular proteinuria (Leheste et al., 1999) indicating the importance of megalin in protein reabsorption in PCT. Multiple research groups have identified various macromolecules that can bind to megalin and can be detected in urine during megalin dysfunction (reviewed in (Christensen & Birn, 2002; Eshbach & Weisz, 2017).

Cubilin is a 400 kDa extracellular glycoprotein. Cubilin consists of 27 CUB (complement C1r/C1s, U epidermal growth factor, Bone Morphogenic Protein-1) domains that bind with the ligands. However, cubilin does not have any signal sequences for endocytosis. Another protein called amnionless forms a complex with cubilin and amnionless-cubilin complex acts as the endocytic scavenger receptor in proximal convoluted tubule (Amsellem et al., 2010). The endocytosis of amnionless-cubilin complex is megalin mediated and the two receptors work in conjunction with reabsorption of proteins in proximal convoluted tubule (Amsellem et al., 2010; Moestrup et al., 1998). Detection of cubilin specific ligands in the urine in megalin knockout mice also validates that amnionless-cubilin complex requires megalin for the internalization process (Amsellem et al., 2010).

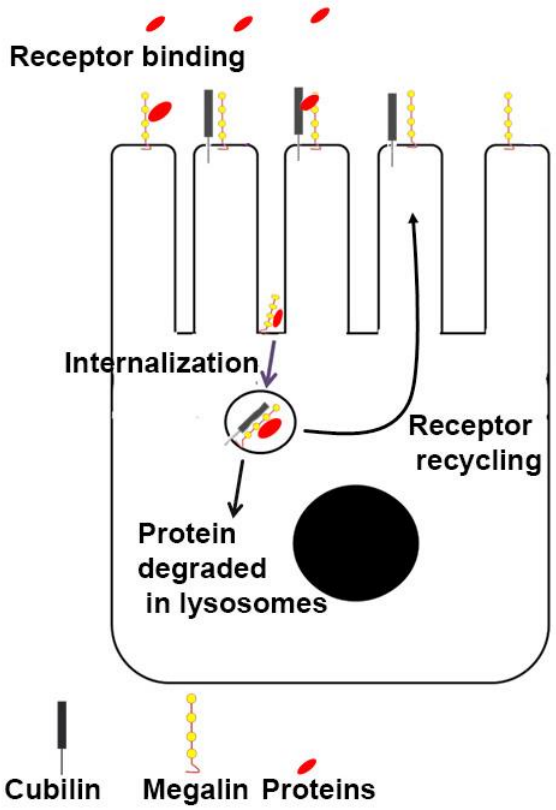

Figure 1. 5 Schematic diagram of receptor mediated reabsorption in PCT

Once the proteins get bound to scavenger receptor, the receptor is internalized by clathrin-mediated pathway (Fig 1.5). Internalization of the vesicle and transfer of those vesicles to the lysosome is mediated by Rab proteins, specifically, Rab5 helps with the internalization process (Bucci et al., 1992) and Rab7 mediates the transfer of endosomes to the lysosome (Vitelli et al., 1997). Concurrent with the process of internalization, the endosomes are acidified by vacuolar H+ ATPase coupled with voltage-gated chloride channel CCl5 (Mellman, Fuchs, & Helenius, 1986). The ligands are then degraded in lysosomes and the receptors are recycled to the apical microvilli for uptake of more ligands. The internalization process is shown to be regulated by phosphatidylinositide 3-kinase (PI3K), transformation growth factor beta-1(TGFβ−1) as well as angiotensin II (AT_2) (Gekle et al., 2003) (Brunskill, Stuart, Tobin, Walls, & Nahorski, 1998) (Caruso-Neves, Kwon, & Guggino, 2005). However, very little has been revealed in regards to

how PI3K regulates endocytosis. TGFβ-1 decreases protein binding and uptake and is postulated to inhibit megalin and/or cubilin function or other steps of the endocytosis (Gekle et al., 2003). AT2 regulates endocytosis through AT2 mediated phosphorylation of protein kinase B (PKB) (Caruso-Neves et al., 2005). Once the proteins are internalized, endocytic vesicles then fuse with lysosomes and the proteins are degraded, while the receptors are recycled back to the apical membranes for reabsorption of more proteins.

1.3.3. Proteinuria and Progression of Chronic Kidney Disease

Proteinuria, most notably albuminuria is a hallmark of renal pathology. Normal urine is virtually devoid of any protein, but various renal and non-renal insults result in proteinuria. Broadly, pathogenic mechanisms causing proteinuria can be grouped into three areas: increased filter load of proteins, defective glomerular filtration and defective tubular reabsorption process. Several pathological conditions can contribute to proteinuria. Apart from nephropathies, cardiovascular diseases, cancer, and infectious agents can also contribute to proteinuria. Proteinuria leads to an oversaturation of protein clearance in the PCT lumen leading to distal tubular damage, tubular epithelial cell activation, and inflammation thus compromising kidney function leading to progressive renal failure and end stage renal disease (Abbate, Zoja, & Remuzzi, 2006; Gorriz & Martinez-Castelao, 2012). Luminal transferrin induces secretion of inflammatory chemokines by PCT epithelium as well as by the cells in the glomerular mesangium (S. Tang et al., 2002). Albumin in the tubular lumen induces tubule-interstitial damage by inducing secretion of various chemokines and fibrotic mediators. Albumin overload activates complement C3 as well as induces TGFβ1, various mitogen-activated protein-dependent kinases and NF-κB pathway (Dixon & Brunskill, 2000; Donadelli, 2003; Sydney Tang, Sheerin, Zhou, Brown, & Sacks, 1999; Yard, Chorianopoulos, Herr, & van der Woude, 2001). Activated NF-kB stimulates secretion of various chemokines including RANTES (CCL5) (Zoja et al., 1998),

fractalkine (CX3CL1) (Donadelli, 2003) as well as monocyte chemoattractant protein-1 (MCP1/CCL2) (Y. Wang, Rangan, Tay, Wang, & Harris, 1999) which enhance the inflammatory response further damaging the kidney tubules as well as the glomerulus. The increase in TGFβ-1 causes increased ECM protein deposition and fibrosis in the tubular interstitium.

1.3.4. Proteoglycans in Glomerular Filtration and Tubular Reabsorption

In addition to the GBM proteoglycans agrin, perlecan, and collagen XVIII, kidneys express other membrane anchored PGs including glypicans, syndecans, CD44, and betaglycans (Rops et al., 2004). In the adult mature kidney, only glypican-1, glypican-3, syndecan-1 and syndecan-4 are expressed (Harvey, 2012). In addition, in the kidney GAGs are spatially distributed where HSPGs are predominant in the basement membranes while CSPGs are located in the extracellular matrix (Lensen et al., 2005).

In GBM, the endothelial glycocalyx includes a large and diverse number of PGs and other glycoproteins. Alterations in PGs are a consistent finding among many nephrotic human diseases and various animal models of kidney disease (van den Hoven et al., 2007). Increased heparanase levels and reduced glomerular HS is observed in multiple proteinuric kidney diseases including diabetic nephropathy, systematic lupus erythematous, minimal change diseases and membranous glomerulonephritis (Garsen, Lenoir, et al., 2016; C. J. Raats, Van Den Born, & Berden, 2000). Increased renal heparanase activity reduces HS levels in GBM and the endothelial glycocalyx during diabetic nephropathy (Garsen, Lenoir, et al., 2016) as well as in animal models of experimental glomerulonephritis (Garsen, Benner, et al., 2016). High amount of circulating anti-HS antibodies are correlated with proteinuria in SLE reaffirming the importance of HS in maintaining glomerular filtration barrier and other sections of the uriniferous tubule (Kim et al., 2017).

In the GBM, agrin, perlecan, and collagen XVIII are highly sulfated providing the net negative charge in the GBM. High-resolution reconstructive microscopic study shows two distinct layers of agrin in GBM each located closer to each constituent cell type that form the GBM (Suleiman et al., 2013) but how much Agrin is contributed by each individual cell type of the GBM is still debatable. Similar distribution for collagen XVIII has been observed in GBM with different isoforms being localized to the lamina rara externa near the podocytes (Kinnunen et al., 2011). Another proteoglycan, Collagen XV also localizes to the GBM and recently, it has been shown to be important for macrophage influx during renal ischemia (Zaferani et al., 2014). Agrin GAG chains are altered in a broad spectrum of kidney diseases associated with proteinuria while the expression of agrin core protein is unchanged (C. J. Raats et al., 2000). In contrast to these findings, experimental loss of podocyte-specific agrin and perlecan GAG deficit mice do not exhibit proteinuria (Goldberg et al., 2009; Harvey et al., 2007). In the former model, if the agrin core protein levels or localization are changed during GAG deficiency is yet to be explored.

The PCT basement membrane has a typical basement membrane consisting of agrin, perlecan, and collagen XVIII. Only the short isoform of collagen XVIII has been detected in the basement membrane of the PCT (Kinnunen et al., 2011). Other renal basement membranes illustrate differential expression of multiple agrin isoforms in comparison to the GBM (C. J. I. Raats et al., 1998). However, there is very little to no research on the specific PGs expressed by the PCT cells and their role in PCT function.

1.4. Pulmonary Histology and Physiology

1.4.1. Structural components in the lungs

The lung is a very dynamic tissue in regards to development and function with more than 300 million alveoli that are about 300 microns across. The alveoli are lined by alveolar epithelial cells (AEC) of two types: Type I and Type II. The Type I cells constitute about 95% of alveolar

wall surface area, whereas the Type II cells occupy rather small surface area of alveoli (Z. Chen et al., 2004). Type I cells are thin cells that have a fused basement membrane with the capillary endothelium. The Type I cells, the fused BM and the capillary endothelium collectively form the blood air barrier where gaseous exchange occurs. Type II cells are the stem cells that can convert into Type I cells as needed (Evans, Cabral, Stephens, & Freeman, 1975) and also the source various surfactant proteins (SP) that help reduce the surface tension, maintain air liquid interface as well as provide innate immunity. Hydrophobic SPs (SP-B and SP-C) maintain the air liquid interface and reduce the surface tension (Weaver & Conkright, 2001) while hydrophilic SPs (SP-A and SP-D) act in host defense (McCormack & Whitsett, 2002). Pulmonary macrophages within the alveolar lumen are the first line of defense. The extracellular space of alveolar wall is relatively sparse. It consists of an extracellular matrix (ECM) of collagens, elastin fibers, and proteoglycans and the resident fibroblasts is the principle cell that produces this ECM (Mercer & Crapo, 1990).

The pulmonary ECM comprises the fused basement membrane of the blood air barrier as well as the interstitial space (White, 2015). The BM in lungs is the primary site for the gas exchange and its biochemical composition allows for various key molecular events unique to the lung. Similar to other BM, the alveolar BM consists of collagen IV, laminins, nidogens, fibronectins and PGs (Dunsmore, 2008). Experimental degradation of GAG followed by differential staining showed HS as the predominating GAG in the alveolar BM while the capillary BM had HSPGs as well as CSPGs (Vaccaro & Brody, 1981; van Kuppevelt, Cremers, Domen, & Kuyper, 1984). PGs form the orderly arrangement of collagen fibers (Raspanti, Alessandrini, Ottani, & Ruggeri, 1997) and in-vitro digestion of GAGs results in decreased resistance and increased wet to dry ratio of rat lung strips (Jamal, Roughley, & Ludwig, 2001).

1.4.2. Innate Immunity in the Lungs

The anatomy, physiologic function, and environmental exposure of the lung parenchyma make them very prone to pathogens. The cumulative alveolar wall surface area, when expanded can reach more than 100 square meters (Colebatch & Ng, 1992), making the lungs one organ with the largest exposures to the external environment. The mucociliary transport mechanism in the trachea and upper bronchi gets rid of many of the pathogens and particles that get lodged in the mucosal surface of the conducting airways. Small particles, bacteria and viruses that are not cleared out by mucociliary transport reach the alveoli, where constantly patrolling alveolar macrophages phagocytize foreign antigens, particulates, and invading pathogens. In addition, Type II AEC produces surfactants (SP-A and SP-D) and other proteins into the alveolar air liquid interface that modulate the pulmonary defense mechanism. SP-A binds with rat alveolar macrophages *in-vitro* (Pison, Wright, & Hawgood, 1992) and stimulates macrophage migration by enhancing chemotaxis (Wright & Youmans, 1993) and phagocytosis (van Iwaarden, Welmers, Verhoef, Haagsman, & Van Golde, 1990).

1.4.2.1 Response to Lipopolysaccharide (LPS) in the Lungs

When lungs are exposed to microbial products, for example Lipopolysaccharide (LPS), the LPS forms a complex with LPS binding protein (LBP) (Tobias, Soldau, & Ulevitch, 1986) which is then recognized by CD14 (Tobias et al., 1993). LBP is required for initiation of the inflammatory response and to present LPS to CD14 (Jack et al., 1997). LBP is present in bronchoalveolar lavage fluid (BALF) at very low concentration but during inflammation, LBP levels increase (T. R. Martin et al., 1992) likely due to increased production from the hepatocytes (Ramadori, Meyer zum Buschenfelde, Tobias, Mathison, & Ulevitch, 1990), the type II AECs (Dentener et al., 2000), and the pulmonary artery smooth muscle cells (Wong et al., 1995). Cluster of differentiation (CD14) is a GPI-anchored membrane marker present in macrophages

and activated neutrophils (Haziot et al., 1988). The membrane associated CD14 binds and presents the LPS-LBP complex to the alveolar macrophages through Toll like Receptor 4 (TLR4) (Poltorak et al., 1998) via binding with heterodimeric complex formed by TLR4 and Myeloid differentiation protein (MD-2) (Park et al., 2009).

Upon binding of the CD14-LPS complex to MD2-TLR4 heterodimer, conformational change in the TLR4 recruits adapter proteins through interactions with various Toll-interleukin-1 receptor (TIR) domains to initiate the LPS signal pathways (Lu, Yeh, & Ohashi, 2008). There are two distinct LPS signaling pathways. The classical pathway involves adaptor proteins myeloid differentiation primary response gene 88 (MyD88) and the TIR domain-containing adaptor protein (TIRAP) (Fitzgerald et al., 2001) and the second MyD88-independent pathway involves adaptor proteins TIR domain-containing adaptor inducing IFN-β (TRIF) and TRIF-related adaptor molecule (TRAM) (Hoebe et al., 2003). Classical LPS signaling/Myd88 dependent pathway rapidly activates NF-κB signaling through pathway intermediates of the IL-1 receptor pathway that involves IL-1 receptor kinase-1 (IRAK1) and IRAK-4, to induce production of pro-inflammatory cytokines IL-1, IL-6, and IL-8 and the anti-inflammatory cytokine IL-10 (Thomas R. Martin & Frevert, 2005). The alternative pathway/Myd88 independent pathway was first proposed by Taro Kawai, Adachi, Ogawa, Takeda, and Akira (1999) when MyD88 mice failed to respond to LPS classically but still had NF-κB activation and mitogen-activated protein kinase (MAPK) signaling after LPS exposure. This slower alternative process involves activation of IRF3 with a late stage activation of MAPK and NF-κB pathway to induce a sustained and slower release of type I interferons (T. Kawai et al., 2001).

1.4.2.2. Inflammatory cells recruitment and progression of inflammation

Once the NF-kB is activated by LPS, a signaling cascade contributes further to the inflammatory process. Nuclear localization of NF-κB results in production and release of various

inflammatory cytokines including tumor necrosis factor- alpha (TNF–α) and macrophage inflammatory protein 2 (MIP-2), IL-6 and IL-12p40 from macrophages (Alcamo et al., 2001; N. Wang, Liang, & Zen, 2014). KC and MIP-2 increase leukocyte rolling, adhesion, and extravasation mediated by P-selectin (Zhang, Liu, Wang, & Thorlacius, 2001). P-selectin binds with P-selectin glycoprotein ligand-1 on the neutrophils and begins neutrophil tethering to the endothelial wall, while E-selectin is expressed later and mediates a slower and stable rolling (Bevilacqua, Stengelin, Gimbrone, & Seed, 1989). The stimulation from chemokines causes a shift from low affinity selectin mediated binding to high affinity integrin mediated high affinity binding and ultimately to arrest of neutrophil rolling (Simon, Hu, Vestweber, & Smith, 2000).

After the leukocyte arrest, "inside-out" signaling through β2 integrins causes conformational change in the β2 integrin further strengthening and spreading the adhesion via small GTPase intermediators (Wittchen, van Buul, Burridge, & Worthylake, 2005) and/or guanidine nucleotide exchange factors (Pasvolsky et al., 2007). Conformational change in integrins initiates "outside-in" signaling mediated by Src-like protein tyrosine kinases (PTK): Fgr and Hck (Giagulli et al., 2006). Firm tethering of neutrophils is followed by neutrophil diapedesis. Neutrophils crawl to nearest cellular junction, most commonly to the tri-cellular corners (Burns et al., 1997) and the junctions with reduced basement membrane matrix proteins (S. Wang et al., 2006). The extravasation of neutrophils occurs primarily in the para-cellular fashion in those junctions, interestingly, some neutrophils migrate in transcellular fashion through the endothelium (Carman & Springer, 2004).

While the neutrophils are paracellularly migrating, they encounter tight junctions (TJ) first followed by the adherens junction. TJs are formed by TJ proteins claudins, occludins and junctional adhesion molecules (JAM) that are tethered to Zonula Occludens-1 (ZO-1) intracellularly (Anderson & Van Itallie, 2009). The JAM proteins have affinity for various

integrins expressed by the leukocytes, and are translocated to endothelial apical surface during stimulation with pro-inflammatory molecules (Stamatovic, Sladojevic, Keep, & Andjelkovic, 2012), which allows JAM proteins to bind with integrins. JAM-A binds with β2 integrin LFA-1 (Ostermann, Weber, Zernecke, Schroder, & Weber, 2002) while JAM-B binds with α4β1 integrin VLA-4 (Cunningham, Rodriguez, Arrate, Tran, & Brock, 2002). The exact mechanisms how JAMs contribute to leukocyte transmigration are still debatable, but the inflammatory induction of JAMs redistribution and their affinity towards integrin indicate a mediating role of JAMs during the process of leukocyte extravasation.

Adherens junctions of the endothelial cells express VE-cadherin (cadherin 5) that regulate endothelial permeability and neutrophil transmigration (Gotsch et al., 1997). Phosphorylation of VE-cadherin (Gavard & Gutkind, 2006) results in conformational change in VE-cadherin causing intercellular gaps for diapedesis (Shaw, Bamba, Perkins, & Luscinskas, 2001). VE-cadherin can be phosphorylated by multiple pathways: integrin mediated pathway, adhesion molecules mediate pathway (Sarelius & Glading, 2015) and vascular endothelial growth factor (VEGF) mediated pathway (Xiao L. Chen et al., 2012; Gavard & Gutkind, 2006). Altered tight junction and adherens junctions increases endothelial permeability and leukocyte extravasation increasing leukocyte recruitment in the area.

1.4.2.3 Surfactant Proteins as immune-modulators in the lungs

SP-A modulates the LPS mediated inflammatory response *in vitro* in macrophage cell types by binding with soluble CD14 leading to a reduction in cellular secretion of tumor necrosis factor- alpha (TNF-α) (Borron et al., 2000; Sano et al., 1999), macrophage inflammatory protein-2, and nitric oxide (Borron et al., 2000). In normal lungs, there is a high ratio of SP-A: LBP favoring the binding of LPS to SP-A preventing further elicitation of the inflammatory response from LPS binding to LBP (Thomas R. Martin, 2000). During LPS exposure, SP-A is upregulated

in macrophages *in vitro* (Chroneos & Shepherd, 1995) as well as *in vivo* in mice challenged with intra-tracheal LPS (McIntosh, Swyers, Fisher, & Wright, 1996). Similarly, bronchoalveolar lavage fluid (BALF) SP-D level is elevated during LPS exposure (McIntosh et al., 1996). SP-D binds with bacterial LPS (Reinhardt et al., 2016; van Rozendaal et al., 1999) as well as with various microbes including *Eschereria Coli* (Kuan, Rust, & Crouch, 1992) *Klebsiella pneumoniae*, *Pseudomonas aeruginosa*, and *Legionella pneumophila* (Han & Mallampalli, 2015). The binding of SP-A and SP-D with microbes facilitates opsonization and phagocytosis of those pathogens by alveolar macrophages.

1.4.3. Proteoglycans in Pulmonary Pathology

1.4.3.1 Proteoglycans in pulmonary diseases

PGs are involved in multiple steps of maintaining pulmonary ECM homeostasis as well as pulmonary innate immunity. It has been long hypothesized and established that PGs contribute to pulmonary elasticity and alveolar stability by interacting and stabilizing collagen-elastin network in the ECM of lungs (Cavalcante et al., 2005), providing restrictive transendothelial fluid filtration (Negrini, Tenstad, & Wiig, 2003), and establishing a fluid repellent environment due to their anionic charges. Mouse models for various enzymes in PG assembly have distinct pulmonary phenotypes. *Ndst1* knockout mice die perinatally due to a respiratory distress like syndrome (Fan et al., 2000; Ringvall et al., 2000), most likely due to their inability to fully mature Type II AECs (Fan et al., 2000). *Hs6st-1* knockout mice develop alveolar enlargement (Habuchi et al., 2007). Glucuronic acid C5 epimerase (*Hsepi*) knockout mice poorly inflated their alveolar walls (Li et al., 2003).

Levels and composition of various PG subtypes are altered during experimental pulmonary pathology including bleomycin induced pulmonary fibrosis (Venkatesan, Ebihara, Roughley, & Ludwig, 2000; Venkatesan, Roughley, & Ludwig, 2002), LPS induced pulmonary

inflammation (Karlinsky, Bucay, Ciccolella, & Crowley, 1991), pulmonary emphysema (Konno et al., 1982; van Straaten et al., 1999), chronic obstructive pulmonary disease (Merrilees et al., 2008), idiopathic pulmonary fibrosis, and acute respiratory distress syndrome (Bensadoun, Burke, Hogg, & Roberts, 1996). Lung fibroblasts from bleomycin induced pulmonary fibrosis have increased levels of versican and HSPGs, which are upregulated even higher during TGF-β1 treatment (Venkatesan et al., 2002). Intratracheal administration of LPS increases amounts of hyaluronan and CSPGs while decreasing HSPGs levels in LPS challenged lungs (Karlinsky et al., 1991). Emphysematous lungs had diminished levels of hyaluronan (Konno et al., 1982) as well as decorin and biglycan in the peribronchial areas (van Straaten et al., 1999). Versican levels are upregulated in the alveolar walls during chronic obstructive pulmonary disease (Merrilees et al., 2008), acute respiratory disease syndrome and idiopathic pulmonary fibrosis (Bensadoun et al., 1996). The exact mechanisms how these proteoglycans contribute to diseases are current areas of research. It has been speculated that because of the structural and molecular diversity of PGs, they have widespread roles in disease development as well as in disease progression.

1.4.3.2 Proteoglycans in innate immunity

In regard to contribution of PGs in innate immunity, studies from various groups using various animal models clearly indicate that PGs can activate the TLRs, sequester chemokines and cytokines to regulate their release and biological activity as well as forming chemokine gradients, facilitate leukocyte adhesion and migration, regulate release of matrix metalloprotease (MMPs), and modulate the overall inflammatory process (See Fig 1.4).

Activation of TLRs

Decorin, biglycan, versican, hyaluronan and lumican are pro-inflammatory and activate toll like receptors. Decorin and biglycan can bind with SP-D (Groeneveld et al., 2005) as well. Decorin has multiple binding sites for SP-D. The sulfated GalNAc sugar in decorin binds to the carbohydrate recognition domain of SP-D while GAG deficient decorin core protein binds with

the collagen-like region of SP-D (Nadesalingam et al., 2003), the physiological significance of which is still unknown and is speculated to modulate the immune function of SP-D. Furthermore, decorin administration in decorin knockout mice activates MAPK pathway and upregulates expression of TNF-α and Il-12b and inhibits TGF-β mediated Il-10 protein upregulationby binding and sequestering TGF-β (Merline et al., 2011). Similar to decorin, biglycan stimulates TLR2 and TLR4 to activate MyD88 dependent NF-κB activation and upregulates *Tnf*-α and *Mip2* (Schaefer et al., 2005). Moreover, proinflammatory cytokines IL-1β and IL-6 can upregulate biglycan expression in macrophages (Schaefer et al., 2005) suggesting feedback of biglycan expression during inflammatory events.

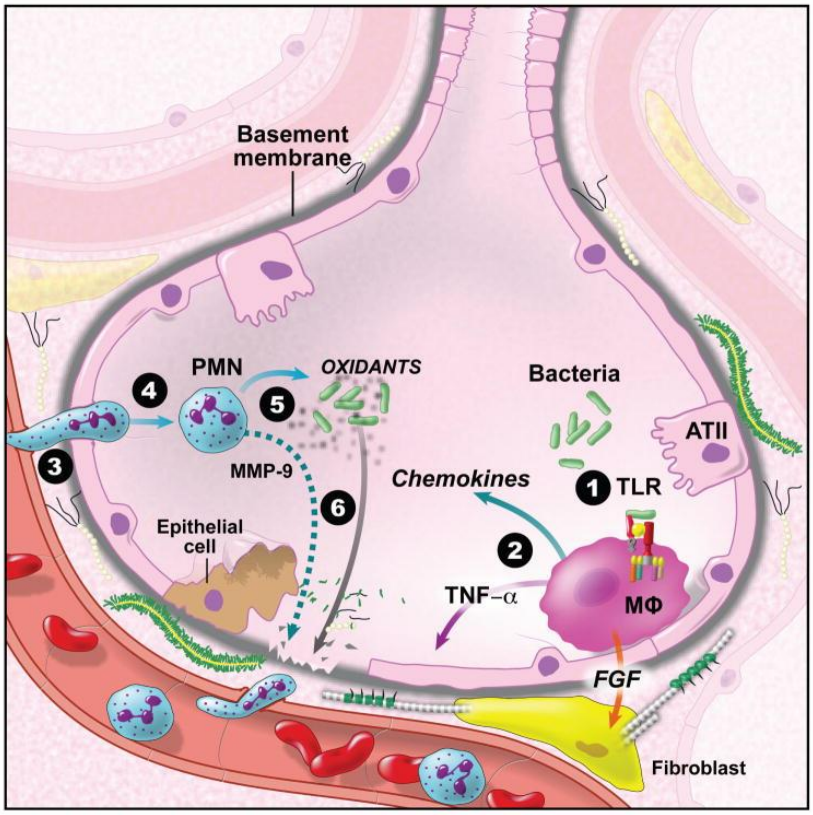

Figure 1. 6 Proteoglycans during pulmonary innate immunity
Reprinted from The Anatomical Record 293(6)., Gill, S., Wight, T. N., & Frevert, C. W. (2010). Proteoglycans: key regulators of pulmonary inflammation and the innate immune response to lung infection. *The Anatomical Record*, *293*(6), 968-981., with permission from Wiley-Liss, Inc

Hyaluronan fragments also activate TLR4 and enhance levels of MIP-2 and KC (Taylor et al., 2004). Lumican interacts with CD14 in the ECM and regulates TLR4 mediated upregulation of IL-6 and TNFa and Il1β during LPS stimulation (F. Wu et al., 2007). HS GAG chains themselves act as pro-inflammatory agents when injected intraperitoneal in the mice, by activating Tlr4 and *Tlr4* knockout mice fail to exhibit HSPG mediated systemic inflammatory response syndrome (Johnson, Brunn, & Platt, 2004).

GAG Interaction with Chemokines and Cytokines

Various chemokines can bind with GAG chains *in vitro* and *in vivo*. IL-8 and platelet factor-4 selectively bind with a subfraction of heparin *in vitro* (Witt & Lander, 1994). L. Wang, Fuster, Sriramarao, and Esko (2005) observed that reduction of HS GAG chains due to endothelial specific *Ndst1* mutation in mice reduced transport and transcytosis and surface expression of IL-8. NMR spectroscopy and surface topology from various research groups have already identified several other chemokines including MIP-1α (Witte Koopmann & Krangel, 1997), MIP-1β (W. Koopmann, Ediriwickrema, & Krangel, 1999),CXCL4 (Amara et al., 1999), RANTES (L. Martin et al., 2001), CXCL10 (Campanella, Lee, Sun, & Luster, 2003), and MCP1 (Lau et al., 2004) that have distinct GAG binding domains. *In silico* analysis for various chemokine oligomers have indicated four distinct GAG binding pockets (Lortat-Jacob, Grosdidier, & Imberty, 2002). S. Gill, Wight, and Frevert (2010) have compiled an extensive list of cytokines that interact with various GAG subtypes. Recently, using mutant chemokines that lack the GAG binding domain, it has been reaffirmed that GAG binding and oligomerization of chemokines is required for their activity (Proudfoot et al., 2003).

GAG Interactions during resolution of inflammation

Syndecans, more specifically the GAG chains of syndecans, present in AEC and bronchial epithelial surface are other important PGs in the lungs that modulate chemokines during

acute inflammation. Syndecan-4 knockout mice have increased response to LPS challenge and elevated MIP2 and KC levels compared with wild type mice (Tanino et al., 2012). A similar phenotype is observed with Syndecan-1 knockout mice. Syndecan-1 GAG chains sequester AEC secreted KC and MIP2. Under inflammatory and tissue injury situations MMP7 cleaves the syndecan ectodomain leading to their release from the cell surface in a phenomenon known as syndecan ectodomain shedding (Q. Li, Park, Wilson, & Parks, 2002). This shedding is thought to modulate the inflammatory response overall by sequestration of cytokines from their cognate receptors at the cell surface, by interference with the intact syndecan proteins binding their ligands preventing their signaling (Bass, Morgan, & Humphries, 2009), by producing local aggregations of active soluble complexes leading to local and restrictive activation of neutrophils (S. E. Gill et al., 2016), and/or by inducing the clearance of cytokines and resolution of neutrophilic inflammation from the formation and clearance of soluble complexes from the ECM (Hayashida, Parks, & Park, 2009).

GAG interaction in leukocyte adhesion and recruitment

The primary proteoglycan that mediate the process of leukocyte adhesion and migration are syndecans and glypicans in the glycocalyx, versican, hyaluronan, lumican, and part-time PG CD44 in the ECM, and agrin, perlecan, and collagen XVIII in the BM. The endothelial glycocalyx is very rich in surface proteoglycans, mostly syndecans and glypicans. Removal of HSPGs in endothelial glycocalyx using HS lyases prevents L-selectin on the neutrophils from binding to the endothelial cells, reduces leukocyte rolling velocity, and enhances the leukocyte adhesion (Constantinescu, Vink, & Spaan, 2003). Sulfated CS/DS chains of versican interact with adhesion molecules L-Selectin, P-selectin, and chemokines possibly facilitating leukocyte adhesion and transendothelial migration during inflammation (H. Kawashima et al., 2002). In liver sinusoids, hyaluronan binds with CD44 from neutrophils and facilitates neutrophil sequestration (McDonald et al., 2008). HS side chains of BM protein Collagen XVIII bind with

L-selectin and facilitate leukocyte migration (Hiroto Kawashima et al., 2003). Degradation products of BM PGs could also play role during acute inflammation in the lungs. Endostatin, a C-terminal Collagen XVIII fragment is elevated in BALF and plasma of patients with acute lung injury as wells as during LPS challenge and is associated with increased PMNs in the alveoli (Perkins et al., 2009). The contribution of other BM PGs in this process is still unknown; they are likely to affect the whole process similar to Collagen XVIII.

1.5. Objectives

The current research was focused to elucidate the roles of PGs during various disease pathologies. PGs are very diverse in nature and ubiquitously present controlling an array of signaling pathways for growth, differentiation, proliferation and maintenance of cells and the extracellular environment homeostasis. The diversity in PGs is contributed by the core proteins as well as the GAG chains associated with them. The very first diversity comes from PG core proteins themselves, as there are more than 35 known PG core proteins. The PG core proteins can have multiple GAG assembly sites that can contain GAGs of varying lengths and structures due to epimerization of uronic acids of repeating disaccharide chains. In addition, the possibility of sulfation at various positions in the GAG chain increases its negative charge and enhances the hydrophilic binding of the GAG chains with a relatively large variety of growth factors, chemokines, and signaling molecules. Trying to identify and delineate each and every molecule that PGs interact with is beyond the scope of any single set of studies. There has been a tremendous amount of research in the field of glycobiology to understand the roles PGs play during pathophysiology, however there are still mysteries. In this document the research is aimed at identifying the potential role of PGs and their GAGs in three areas of interest; first, human patients with spondylo-ocular syndrome, a rare genetic disorder affecting musculoskeletal system, sensorineural system, and cardiovascular system, were studied and the mutation causing the

disease were identified to be in *XYLT2*, the enzyme that catalyzes the first step of GAG chain assembly onto the PG core proteins. Further biochemical and molecular study on patient samples revealed a significant reduction in PG content and GAG chain modification on PG core proteins in those patients. Secondly, using *Xylt2* knockout mice model, the research investigated the role of PGs in renal protein homeostasis at the level of GBM filtration and in PCT protein reabsorption. Lastly, we explored how Xylt dependent GAGs contribute to pulmonary function and innate immunity using three distinctly different animal models: *Xylt2-/-*, conditional *Xylt1-/-*, and endothelial specific *Xylt1-/-*, by using state-of the art respiratory dynamics study as well as *in-vivo* LPS challenge.

References

Abbate, M., Zoja, C., & Remuzzi, G. (2006). How does proteinuria cause progressive renal damage? *J Am Soc Nephrol, 17*(11), 2974-2984. doi:10.1681/ASN.2006040377

Aebi, M. (2013). N-linked protein glycosylation in the ER. *Biochim Biophys Acta, 1833*(11), 2430-2437. doi:10.1016/j.bbamcr.2013.04.001

Aikio, M., Elamaa, H., Vicente, D., Izzi, V., Kaur, I., Seppinen, L., . . . Pihlajaniemi, T. (2014). Specific collagen XVIII isoforms promote adipose tissue accrual via mechanisms determining adipocyte number and affect fat deposition. *Proc Natl Acad Sci U S A, 111*(30), E3043-3052. doi:10.1073/pnas.1405879111

Alanay, Y., Superti-Furga, A., Karel, F., & Tuncbilek, E. (2006). Spondylo-ocular syndrome: a new entity involving the eye and spine. *Am J Med Genet A, 140*(6), 652-656. doi:10.1002/ajmg.a.31119

Albright, C. F., & Robbins, R. W. (1990). The sequence and transcript heterogeneity of the yeast gene ALG1, an essential mannosyltransferase involved in N-glycosylation. *J Biol Chem, 265*(12), 7042-7049.

Alcamo, E., Mizgerd, J. P., Horwitz, B. H., Bronson, R., Beg, A. A., Scott, M., . . . Baltimore, D. (2001). Targeted Mutation of TNF Receptor I Rescues the RelA-Deficient Mouse and Reveals a Critical Role for NF-κB in Leukocyte Recruitment. *The Journal of Immunology, 167*(3), 1592-1600. doi:10.4049/jimmunol.167.3.1592

Amara, A., Lorthioir, O., Valenzuela, A., Magerus, A., Thelen, M., Montes, M., . . . Arenzana-Seisdedos, F. (1999). Stromal cell-derived factor-1α associates with heparan sulfates through the first β-strand of the chemokine. *Journal of Biological Chemistry, 274*(34), 23916-23925. doi:10.1074/jbc.274.34.23916

Amsellem, S., Gburek, J., Hamard, G., Nielsen, R., Willnow, T. E., Devuyst, O., . . . Kozyraki, R. (2010). Cubilin is essential for albumin reabsorption in the renal proximal tubule. *J Am Soc Nephrol, 21*(11), 1859-1867. doi:10.1681/ASN.2010050492

Anderson, J. M., & Van Itallie, C. M. (2009). Physiology and Function of the Tight Junction. *Cold Spring Harbor Perspectives in Biology, 1*(2), a002584. doi:10.1101/cshperspect.a002584

Arikawa-Hirasawa, E., Wilcox, W. R., Le, A. H., Silverman, N., Govindraj, P., Hassell, J. R., & Yamada, Y. (2001). Dyssegmental dysplasia, Silverman-Handmaker type, is caused by functional null mutations of the perlecan gene. *Nat Genet, 27*(4), 431-434. doi:10.1038/86941

Aviezer, D., Hecht, D., Safran, M., Eisinger, M., David, G., & Yayon, A. (1994). Perlecan, basal lamina proteoglycan, promotes basic fibroblast growth factor-receptor binding, mitogenesis, and angiogenesis. *Cell, 79*(6), 1005-1013. doi:http://dx.doi.org/10.1016/0092-8674(94)90031-0

Babelova, A., Moreth, K., Tsalastra-Greul, W., Zeng-Brouwers, J., Eickelberg, O., Young, M. F., . . . Schaefer, L. (2009). Biglycan, a danger signal that activates the NLRP3 inflammasome via toll-like and P2X receptors. *J Biol Chem, 284*(36), 24035-24048. doi:10.1074/jbc.M109.014266

Bass, M. D., Morgan, M. R., & Humphries, M. J. (2009). Syndecans Shed Their Reputation as Inert Molecules. *Sci Signal, 2*(64), pe18-pe18. doi:10.1126/scisignal.264pe18

Bause, E. (1983). Structural requirements of N-glycosylation of proteins. Studies with proline peptides as conformational probes. *Biochem J, 209*(2), 331-336.

Bennett, E. P., Mandel, U., Clausen, H., Gerken, T. A., Fritz, T. A., & Tabak, L. A. (2012). Control of mucin-type O-glycosylation: a classification of the polypeptide GalNAc-transferase gene family. *Glycobiology, 22*(6), 736-756. doi:10.1093/glycob/cwr182

Bensadoun, E. S., Burke, A. K., Hogg, J. C., & Roberts, C. R. (1996). Proteoglycan deposition in pulmonary fibrosis. *Am J Respir Crit Care Med, 154*(6 Pt 1), 1819-1828. doi:10.1164/ajrccm.154.6.8970376

Berendsen, A. D., Fisher, L. W., Kilts, T. M., Owens, R. T., Robey, P. G., Gutkind, J. S., & Young, M. F. (2011). Modulation of canonical Wnt signaling by the extracellular matrix component biglycan. *Proceedings of the National Academy of Sciences of the United States of America, 108*(41), 17022-17027. doi:10.1073/pnas.1110629108

Bernfield, M., Gotte, M., Park, P. W., Reizes, O., Fitzgerald, M. L., Lincecum, J., & Zako, M. (1999). Functions of cell surface heparan sulfate proteoglycans. *Annu Rev Biochem, 68*, 729-777. doi:10.1146/annurev.biochem.68.1.729

Bernfield, M., Kokenyesi, R., Kato, M., Hinkes, M. T., Spring, J., Gallo, R. L., & Lose, E. J. (1992). Biology of the syndecans: a family of transmembrane heparan sulfate proteoglycans. *Annu Rev Cell Biol, 8*, 365-393. doi:10.1146/annurev.cb.08.110192.002053

Bevilacqua, M. P., Stengelin, S., Gimbrone, M. A., & Seed, B. (1989). Endothelial Leukocyte Adhesion Molecule 1: An Inducible Receptor for Neutrophils Related to Complement Regulatory Proteins and Lectins. *Science, 243*(4895), 1160-1165.

Borron, P., McIntosh, J. C., Korfhagen, T. R., Whitsett, J. A., Taylor, J., & Wright, J. R. (2000). Surfactant-associated protein A inhibits LPS-induced cytokine and nitric oxide production in vivo. *American Journal of Physiology-Lung Cellular and Molecular Physiology, 278*(4), L840-L847. doi:10.1152/ajplung.2000.278.4.L840

Boute, N., Gribouval, O., Roselli, S., Benessy, F., Lee, H., Fuchshuber, A., . . . Antignac, C. (2000). NPHS2, encoding the glomerular protein podocin, is mutated in autosomal recessive steroid-resistant nephrotic syndrome. *Nat Genet, 24*(4), 349-354. doi:10.1038/74166

Brown, D. S., & Eames, B. F. (2016). Emerging tools to study proteoglycan function during skeletal development. *Methods Cell Biol, 134*, 485-530. doi:10.1016/bs.mcb.2016.03.001

Brunskill, N. J., Stuart, J., Tobin, A. B., Walls, J., & Nahorski, S. (1998). Receptor-mediated endocytosis of albumin by kidney proximal tubule cells is regulated by phosphatidylinositide 3-kinase. *Journal of Clinical Investigation, 101*(10), 2140-2150.

Bucci, C., Parton, R. G., Mather, I. H., Stunnenberg, H., Simons, K., Hoflack, B., & Zerial, M. (1992). The small GTPase rab5 functions as a regulatory factor in the early endocytic pathway. *Cell, 70*(5), 715-728.

Burda, P., & Aebi, M. (1998). The ALG10 locus of Saccharomyces cerevisiae encodes the alpha-1,2 glucosyltransferase of the endoplasmic reticulum: the terminal glucose of the lipid-linked oligosaccharide is required for efficient N-linked glycosylation. *Glycobiology, 8*(5), 455-462.

Burgess, R. W., Nguyen, Q. T., Son, Y. J., Lichtman, J. W., & Sanes, J. R. (1999). Alternatively spliced isoforms of nerve- and muscle-derived agrin: their roles at the neuromuscular junction. *Neuron, 23*(1), 33-44.

Burns, A. R., Walker, D. C., Brown, E. S., Thurmon, L. T., Bowden, R. A., Keese, C. R., . . . Smith, C. W. (1997). Neutrophil transendothelial migration is independent of tight junctions and occurs preferentially at tricellular corners. *J Immunol, 159*(6), 2893-2903.

Campanella, G. S. V., Lee, E. M. J., Sun, J., & Luster, A. D. (2003). CXCR3 and Heparin Binding Sites of the Chemokine IP-10 (CXCL10). *Journal of Biological Chemistry, 278*(19), 17066-17074. doi:10.1074/jbc.M212077200

Campanelli, J. T., Gayer, G. G., & Scheller, R. H. (1996). Alternative RNA splicing that determines agrin activity regulates binding to heparin and alpha-dystroglycan. *Development, 122*(5), 1663-1672.

Campos-Xavier, A. B., Martinet, D., Bateman, J., Belluoccio, D., Rowley, L., Tan, T. Y., . . . Bonafé, L. (2009). Mutations in the Heparan-Sulfate Proteoglycan Glypican 6 (GPC6) Impair Endochondral Ossification and Cause Recessive Omodysplasia. *The American Journal of Human Genetics, 84*(6), 760-770. doi:10.1016/j.ajhg.2009.05.002

Capurro, M. I., Xiang, Y. Y., Lobe, C., & Filmus, J. (2005). Glypican-3 promotes the growth of hepatocellular carcinoma by stimulating canonical Wnt signaling. *Cancer Res, 65*(14), 6245-6254. doi:10.1158/0008-5472.can-04-4244

Carey, D. J. (1997). Syndecans: multifunctional cell-surface co-receptors. *Biochemical Journal, 327*(1), 1-16. doi:10.1042/bj3270001

Carman, C. V., & Springer, T. A. (2004). A transmigratory cup in leukocyte diapedesis both through individual vascular endothelial cells and between them. *J Cell Biol, 167*(2), 377-388. doi:10.1083/jcb.200404129

Caruso-Neves, C., Kwon, S. H., & Guggino, W. B. (2005). Albumin endocytosis in proximal tubule cells is modulated by angiotensin II through an AT2 receptor-mediated protein kinase B activation. *Proc Natl Acad Sci U S A, 102*(48), 17513-17518. doi:10.1073/pnas.0507255102

Cavalcante, F. S., Ito, S., Brewer, K., Sakai, H., Alencar, A. M., Almeida, M. P., . . . Suki, B. (2005). Mechanical interactions between collagen and proteoglycans: implications for the stability of lung tissue. *J Appl Physiol (1985), 98*(2), 672-679. doi:10.1152/japplphysiol.00619.2004

Chen, Xiao L., Nam, J.-O., Jean, C., Lawson, C., Walsh, Colin T., Goka, E., . . . Schlaepfer, David D. (2012). VEGF-Induced Vascular Permeability Is Mediated by FAK. *Developmental Cell, 22*(1), 146-157. doi:https://doi.org/10.1016/j.devcel.2011.11.002

Chen, Z., Jin, N., Narasaraju, T., Chen, J., McFarland, L. R., Scott, M., & Liu, L. (2004). Identification of two novel markers for alveolar epithelial type I and II cells. *Biochem Biophys Res Commun, 319*(3), 774-780. doi:10.1016/j.bbrc.2004.05.048

Christensen, E. I., & Birn, H. (2002). Megalin and cubilin: multifunctional endocytic receptors. *Nat Rev Mol Cell Biol, 3*(4), 256-266. doi:10.1038/nrm778

Chroneos, Z., & Shepherd, V. L. (1995). Differential regulation of the mannose and SP-A receptors on macrophages. *Am J Physiol, 269*(6 Pt 1), L721-726. doi:10.1152/ajplung.1995.269.6.L721

Clark, S. J., Keenan, T. D., Fielder, H. L., Collinson, L. J., Holley, R. J., Merry, C. L., . . . Bishop, P. N. (2011). Mapping the differential distribution of glycosaminoglycans in the adult human retina, choroid, and sclera. *Invest Ophthalmol Vis Sci, 52*(9), 6511-6521. doi:10.1167/iovs.11-7909

Colebatch, H. J., & Ng, C. K. (1992). Estimating alveolar surface area during life. *Respir Physiol, 88*(1-2), 163-170.

Constantinescu, A. A., Vink, H., & Spaan, J. A. E. (2003). Endothelial Cell Glycocalyx Modulates Immobilization of Leukocytes at the Endothelial Surface. *Arteriosclerosis, Thrombosis, and Vascular Biology, 23*(9), 1541-1547. doi:10.1161/01.atv.0000085630.24353.3d

Cordell, H. J., Töpf, A., Mamasoula, C., Postma, A. V., Bentham, J., Zelenika, D., . . . Goodship, J. A. (2013). Genome-wide association study identifies loci on 12q24 and 13q32 associated with Tetralogy of Fallot. *Hum Mol Genet, 22*(7), 1473-1481. doi:10.1093/hmg/dds552

Cortes, M., Baria, A. T., & Schwartz, N. B. (2009). Sulfation of chondroitin sulfate proteoglycans is necessary for proper Indian hedgehog signaling in the developing growth plate. *Development, 136*(10), 1697-1706. doi:10.1242/dev.030742

Costell, M., Carmona, R., Gustafsson, E., Gonzalez-Iriarte, M., Fassler, R., & Munoz-Chapuli, R. (2002). Hyperplastic conotruncal endocardial cushions and transposition of great arteries in perlecan-null mice. *Circ Res, 91*(2), 158-164.

Couchman, J. R. (2003). Syndecans: proteoglycan regulators of cell-surface microdomains? *Nat Rev Mol Cell Biol, 4*(12), 926-937. doi:10.1038/nrm1257

Couto, J. R., Huffaker, T. C., & Robbins, P. W. (1984). Cloning and expression in Escherichia coli of a yeast mannosyltransferase from the asparagine-linked glycosylation pathway. *Journal of Biological Chemistry, 259*(1), 378-382.

Cunningham, S. A., Rodriguez, J. M., Arrate, M. P., Tran, T. M., & Brock, T. A. (2002). JAM2 interacts with alpha4beta1. Facilitation by JAM3. *J Biol Chem, 277*(31), 27589-27592. doi:10.1074/jbc.C200331200

Daryadel, A., Haubitz, M., Figueiredo, M., Steubl, D., Roos, M., Mader, A., . . . Wagner, C. A. (2016). The C-Terminal Fragment of Agrin (CAF), a Novel Marker of Renal Function, Is Filtered by the Kidney and Reabsorbed by the Proximal Tubule. *PLoS One, 11*(7), e0157905. doi:10.1371/journal.pone.0157905

David, G., Lories, V., Decock, B., Marynen, P., Cassiman, J. J., & Van den Berghe, H. (1990). Molecular cloning of a phosphatidylinositol-anchored membrane heparan sulfate proteoglycan from human lung fibroblasts. *J Cell Biol, 111*(6 Pt 2), 3165-3176.

Day, J. M., Olin, A. I., Murdoch, A. D., Canfield, A., Sasaki, T., Timpl, R., . . . Aspberg, A. (2004). Alternative splicing in the aggrecan G3 domain influences binding interactions with tenascin-C and other extracellular matrix proteins. *J Biol Chem, 279*(13), 12511-12518. doi:10.1074/jbc.M400242200

De Cat, B., Muyldermans, S. Y., Coomans, C., Degeest, G., Vanderschueren, B., Creemers, J., . . . David, G. (2003). Processing by proprotein convertases is required for glypican-3

modulation of cell survival, Wnt signaling, and gastrulation movements. *J Cell Biol, 163*(3), 625-635. doi:10.1083/jcb.200302152

Dentener, M. A., Vreugdenhil, A. C., Hoet, P. H., Vernooy, J. H., Nieman, F. H., Heumann, D., . . . Wouters, E. F. (2000). Production of the acute-phase protein lipopolysaccharide-binding protein by respiratory type II epithelial cells: implications for local defense to bacterial endotoxins. *American journal of respiratory cell and molecular biology, 23*(2), 146-153.

Denzer, A. J., Schulthess, T., Fauser, C., Schumacher, B., Kammerer, R. A., Engel, J., & Ruegg, M. A. (1998). Electron microscopic structure of agrin and mapping of its binding site in laminin ‐ 1. *Embo j, 17*(2), 335-343. doi:10.1093/emboj/17.2.335

Desbordes, S. C., & Sanson, B. (2003). The glypican Dally-like is required for Hedgehog signalling in the embryonic epidermis of Drosophila. *Development, 130*(25), 6245-6255. doi:10.1242/dev.00874

Dixon, R., & Brunskill, N. J. (2000). Albumin stimulates p44/p42 extracellular-signal-regulated mitogen-activated protein kinase in opossum kidney proximal tubular cells. *Clinical Science, 98*(3), 295-301.

Donadelli, R. C. Z., M morigi, S Buelli, C Batani, S Tomasoni, D Corna, D Rottoli, A Benigni,M Abbate,G Remuzzi, and C Zoja. (2003). Protein Overload Induces Fractalkine Upregulation in Proximal Tubular Cells through Nuclear Factor B- and p38 Mitogen-Activated Protein Kinase-Dependent Pathways. *Journal of the American Society of Nephrology, 14*(10), 2436-2446. doi:10.1097/01.asn.0000089564.55411.7f

Donoviel, D. B., Freed, D. D., Vogel, H., Potter, D. G., Hawkins, E., Barrish, J. P., . . . Powell, D. R. (2001). Proteinuria and perinatal lethality in mice lacking NEPH1, a novel protein

with homology to NEPHRIN. *Mol Cell Biol, 21*(14), 4829-4836. doi:10.1128/MCB.21.14.4829-4836.2001

Drey, M., Sieber, C. C., Bauer, J. M., Uter, W., Dahinden, P., Fariello, R. G., & Vrijbloed, J. W. (2013). C-terminal Agrin Fragment as a potential marker for sarcopenia caused by degeneration of the neuromuscular junction. *Exp Gerontol, 48*(1), 76-80. doi:10.1016/j.exger.2012.05.021

Dunphy, W. G., & Rothman, J. E. (1983). Compartmentation of asparagine-linked oligosaccharide processing in the Golgi apparatus. *The Journal of Cell Biology, 97*(1), 270-275.

Dunsmore, S. E. (2008). Treatment of COPD: a matrix perspective. *Int J Chron Obstruct Pulmon Dis, 3*(1), 113-122.

Eames, B. F., Yan, Y. L., Swartz, M. E., Levic, D. S., Knapik, E. W., Postlethwait, J. H., & Kimmel, C. B. (2011). Mutations in fam20b and xylt1 reveal that cartilage matrix controls timing of endochondral ossification by inhibiting chondrocyte maturation. *PLoS Genet, 7*(8), e1002246. doi:10.1371/journal.pgen.1002246

Eickelberg, O., Centrella, M., Reiss, M., Kashgarian, M., & Wells, R. G. (2002). Betaglycan inhibits TGF-beta signaling by preventing type I-type II receptor complex formation. Glycosaminoglycan modifications alter betaglycan function. *J Biol Chem, 277*(1), 823-829. doi:10.1074/jbc.M105110200

Eshbach, M. L., & Weisz, O. A. (2017). Receptor-Mediated Endocytosis in the Proximal Tubule. *Annu Rev Physiol, 79*, 425-448. doi:10.1146/annurev-physiol-022516-034234

Evans, M. J., Cabral, L. J., Stephens, R. J., & Freeman, G. (1975). Transformation of alveolar Type 2 cells to Type 1 cells following exposure to NO2. *Experimental and Molecular Pathology, 22*(1), 142-150. doi:https://doi.org/10.1016/0014-4800(75)90059-3

Fan, G., Xiao, L., Cheng, L., Wang, X., Sun, B., & Hu, G. (2000). Targeted disruption of NDST-1 gene leads to pulmonary hypoplasia and neonatal respiratory distress in mice. *FEBS Lett, 467*(1), 7-11.

Farach-Carson, M. C., & Carson, D. D. (2007). Perlecan—a multifunctional extracellular proteoglycan scaffold. *Glycobiology, 17*(9), 897-905. doi:10.1093/glycob/cwm043

Filmus, J., Capurro, M., & Rast, J. (2008). Glypicans. *Genome Biol, 9*(5), 224. doi:10.1186/gb-2008-9-5-224

Fitzgerald, K. A., Palsson-McDermott, E. M., Bowie, A. G., Jefferies, C. A., Mansell, A. S., Brady, G., . . . O'Neill, L. A. (2001). Mal (MyD88-adapter-like) is required for Toll-like receptor-4 signal transduction. *Nature, 413*(6851), 78-83. doi:10.1038/35092578

Frank, C. G., & Aebi, M. (2005). ALG9 mannosyltransferase is involved in two different steps of lipid-linked oligosaccharide biosynthesis. *Glycobiology, 15*(11), 1156-1163. doi:10.1093/glycob/cwj002

Freeze, H. H., Esko, J. D., & Parodi, A. J. (2009). Glycans in Glycoprotein Quality Control. In nd, A. Varki, R. D. Cummings, J. D. Esko, H. H. Freeze, P. Stanley, C. R. Bertozzi, G. W. Hart, & M. E. Etzler (Eds.), *Essentials of Glycobiology*. Cold Spring Harbor (NY).

Gao, X. D., Tachikawa, H., Sato, T., Jigami, Y., & Dean, N. (2005). Alg14 recruits Alg13 to the cytoplasmic face of the endoplasmic reticulum to form a novel bipartite UDP-N-acetylglucosamine transferase required for the second step of N-linked glycosylation. *J Biol Chem, 280*(43), 36254-36262. doi:10.1074/jbc.M507569200

Garsen, M., Benner, M., Dijkman, H. B., van Kuppevelt, T. H., Li, J. P., Rabelink, T. J., . . . van der Vlag, J. (2016). Heparanase Is Essential for the Development of Acute Experimental Glomerulonephritis. *Am J Pathol, 186*(4), 805-815. doi:10.1016/j.ajpath.2015.12.008

Garsen, M., Lenoir, O., Rops, A. L., Dijkman, H. B., Willemsen, B., van Kuppevelt, T. H., . . . van der Vlag, J. (2016). Endothelin-1 Induces Proteinuria by Heparanase-Mediated

Disruption of the Glomerular Glycocalyx. *J Am Soc Nephrol, 27*(12), 3545-3551. doi:10.1681/ASN.2015091070

Gavard, J., & Gutkind, J. S. (2006). VEGF controls endothelial-cell permeability by promoting the beta-arrestin-dependent endocytosis of VE-cadherin. *Nat Cell Biol, 8*(11), 1223-1234. doi:10.1038/ncb1486

Gekle, M., Knaus, P., Nielsen, R., Mildenberger, S., Freudinger, R., Wohlfarth, V., . . . Christensen, E. I. (2003). Transforming growth factor-beta1 reduces megalin- and cubilin-mediated endocytosis of albumin in proximal-tubule-derived opossum kidney cells. *J Physiol, 552*(Pt 2), 471-481. doi:10.1113/jphysiol.2003.048074

Gesemann, M., Brancaccio, A., Schumacher, B., & Ruegg, M. A. (1998). Agrin Is a High-affinity Binding Protein of Dystroglycan in Non-muscle Tissue. *Journal of Biological Chemistry, 273*(1), 600-605. doi:10.1074/jbc.273.1.600

Gesemann, M., Cavalli, V., Denzer, A. J., Brancaccio, A., Schumacher, B., & Ruegg, M. A. (1996). Alternative splicing of agrin alters its binding to heparin, dystroglycan, and the putative agrin receptor. *Neuron, 16*(4), 755-767.

Giagulli, C., Ottoboni, L., Caveggion, E., Rossi, B., Lowell, C., Constantin, G., . . . Berton, G. (2006). The Src family kinases Hck and Fgr are dispensable for inside-out, chemoattractant-induced signaling regulating beta 2 integrin affinity and valency in neutrophils, but are required for beta 2 integrin-mediated outside-in signaling involved in sustained adhesion. *J Immunol, 177*(1), 604-611.

Gill, S., Wight, T. N., & Frevert, C. W. (2010). Proteoglycans: key regulators of pulmonary inflammation and the innate immune response to lung infection. *Anat Rec (Hoboken), 293*(6), 968-981. doi:10.1002/ar.21094

Gill, S. E., Nadler, S. T., Li, Q., Frevert, C. W., Park, P. W., Chen, P., & Parks, W. C. (2016). Shedding of Syndecan-1/CXCL1 Complexes by Matrix Metalloproteinase 7 Functions as

an Epithelial Checkpoint of Neutrophil Activation. *Am J Respir Cell Mol Biol, 55*(2), 243-251. doi:10.1165/rcmb.2015-0193OC

Gleghorn, L., Ramesar, R., Beighton, P., & Wallis, G. (2005). A Mutation in the Variable Repeat Region of the Aggrecan Gene (AGC1) Causes a Form of Spondyloepiphyseal Dysplasia Associated with Severe, Premature Osteoarthritis. *The American Journal of Human Genetics, 77*(3), 484-490. doi:10.1086/444401

Goldberg, S., Harvey, S. J., Cunningham, J., Tryggvason, K., & Miner, J. H. (2009). Glomerular filtration is normal in the absence of both agrin and perlecan-heparan sulfate from the glomerular basement membrane. *Nephrol Dial Transplant, 24*(7), 2044-2051. doi:10.1093/ndt/gfn758

Gorriz, J. L., & Martinez-Castelao, A. (2012). Proteinuria: detection and role in native renal disease progression. *Transplant Rev (Orlando), 26*(1), 3-13. doi:10.1016/j.trre.2011.10.002

Gotsch, U., Borges, E., Bosse, R., Boggemeyer, E., Simon, M., Mossmann, H., & Vestweber, D. (1997). VE-cadherin antibody accelerates neutrophil recruitment in vivo. *Journal of Cell Science, 110*(5), 583-588.

Groeneveld, T. W. L., Oroszlán, M., Owens, R. T., Faber-Krol, M. C., Bakker, A. C., Arlaud, G. J., . . . Roos, A. (2005). Interactions of the Extracellular Matrix Proteoglycans Decorin and Biglycan with C1q and Collectins. *The Journal of Immunology, 175*(7), 4715-4723. doi:10.4049/jimmunol.175.7.4715

Groffen, A. J. A., Buskens, C. A. F., van Kuppevelt, T. H., Veerkamp, J. H., Monnens, L. A. H., & van den Heuvel, L. P. W. J. (1998). Primary structure and high expression of human agrin in basement membranes of adult lung and kidney. *European Journal of Biochemistry, 254*(1), 123-128. doi:10.1046/j.1432-1327.1998.2540123.x

Habuchi, H., Nagai, N., Sugaya, N., Atsumi, F., Stevens, R. L., & Kimata, K. (2007). Mice deficient in heparan sulfate 6-O-sulfotransferase-1 exhibit defective heparan sulfate biosynthesis, abnormal placentation, and late embryonic lethality. *J Biol Chem, 282*(21), 15578-15588. doi:10.1074/jbc.M607434200

Halper, J. (2014). Proteoglycans and diseases of soft tissues. *Adv Exp Med Biol, 802*, 49-58. doi:10.1007/978-94-007-7893-1_4

Han, S., & Mallampalli, R. K. (2015). The Role of Surfactant in Lung Disease and Host Defense against Pulmonary Infections. *Annals of the American Thoracic Society, 12*(5), 765-774. doi:10.1513/AnnalsATS.201411-507FR

Hart, G. W., & West, C. M. (2009). Nucleocytoplasmic Glycosylation. In A. Varki, R. D. Cummings, J. D. Esko, H. H. Freeze, P. Stanley, C. R. Bertozzi, G. W. Hart, & M. E. Etzler (Eds.), *Essentials of Glycobiology* (2nd ed.). Cold Spring Harbor (NY).

Harvey, S. J. (2012). Models for studies of proteoglycans in kidney pathophysiology. *Methods Mol Biol, 836*, 259-284. doi:10.1007/978-1-61779-498-8_17

Harvey, S. J., Jarad, G., Cunningham, J., Rops, A. L., van der Vlag, J., Berden, J. H., . . . Miner, J. H. (2007). Disruption of glomerular basement membrane charge through podocyte-specific mutation of agrin does not alter glomerular permselectivity. *Am J Pathol, 171*(1), 139-152. doi:10.2353/ajpath.2007.061116

Hatano, S., Nagai, N., Sugiura, N., Tsuchimoto, J., Isogai, Z., Kimata, K., . . . Watanabe, H. (2017). Versican A-subdomain is required for its adequate function in dermal development. *Connect Tissue Res*, 1-13. doi:10.1080/03008207.2017.1324432

Hausmann, R., Kuppe, C., Egger, H., Schweda, F., Knecht, V., Elger, M., . . . Moeller, M. J. (2010). Electrical forces determine glomerular permeability. *J Am Soc Nephrol, 21*(12), 2053-2058. doi:10.1681/ASN.2010030303

Hausser, H., Gröning, A., Hasilik, A., Schönherr, E., & Kresse, H. (1994). Selective inactivity of TGF-β/decorin complexes. *FEBS Letters, 353*(3), 243-245. doi:10.1016/0014-5793(94)01044-7

Hayashida, K., Parks, W. C., & Park, P. W. (2009). Syndecan-1 shedding facilitates the resolution of neutrophilic inflammation by removing sequestered CXC chemokines. *Blood, 114*(14), 3033-3043. doi:10.1182/blood-2009-02-204966

Haziot, A., Chen, S., Ferrero, E., Low, M. G., Silber, R., & Goyert, S. M. (1988). The monocyte differentiation antigen, CD14, is anchored to the cell membrane by a phosphatidylinositol linkage. *J Immunol, 141*(2), 547-552.

Heinegard, D. (2009). Fell-Muir Lecture: Proteoglycans and more--from molecules to biology. *Int J Exp Pathol, 90*(6), 575-586. doi:10.1111/j.1365-2613.2009.00695.x

Hildebrand, A., Romaris, M., Rasmussen, L. M., Heinegard, D., Twardzik, D. R., Border, W. A., & Ruoslahti, E. (1994). Interaction of the small interstitial proteoglycans biglycan, decorin and fibromodulin with transforming growth factor beta. *Biochem J, 302 (Pt 2)*, 527-534.

Hoebe, K., Du, X., Georgel, P., Janssen, E., Tabeta, K., Kim, S. O., . . . Beutler, B. (2003). Identification of Lps2 as a key transducer of MyD88-independent TIR signalling. *Nature, 424*(6950), 743-748. doi:10.1038/nature01889

Inai, K., Norris, R. A., Hoffman, S., Markwald, R. R., & Sugi, Y. (2008). BMP-2 induces cell migration and periostin expression during atrioventricular valvulogenesis. *Dev Biol, 315*(2), 383-396. doi:10.1016/j.ydbio.2007.12.028

Inatani, M., Tanihara, H., Oohira, A., Honjo, M., & Honda, Y. (1999). Identification of a Nervous Tissue–Specific Chondroitin Sulfate Proteoglycan, Neurocan, in Developing Rat Retina. *Investigative Ophthalmology & Visual Science, 40*(10), 2350-2359.

Inatani, M., Tanihara, H., Oohira, A., Honjo, M., Kido, N., & Honda, Y. (2000). Upregulated expression of neurocan, a nervous tissue specific proteoglycan, in transient retinal ischemia. *Invest Ophthalmol Vis Sci, 41*(9), 2748-2754.

Inoue, T., Yaoita, E., Kurihara, H., Shimizu, F., Sakai, T., Kobayashi, T., . . . Yamamoto, T. (2001). FAT is a component of glomerular slit diaphragms. *Kidney Int, 59*(3), 1003-1012. doi:10.1046/j.1523-1755.2001.0590031003.x

Iozzo, R. V., & Murdoch, A. D. (1996). Proteoglycans of the extracellular environment: clues from the gene and protein side offer novel perspectives in molecular diversity and function. *FASEB J, 10*(5), 598-614.

Jack, R. S., Fan, X., Bernheiden, M., Rune, G., Ehlers, M., Weber, A., . . . Freudenberg, M. (1997). Lipopolysaccharide-binding protein is required to combat a murine gram-negative bacterial infection. *Nature, 389*(6652), 742-745.

Jamal, R. A., Roughley, P. J., & Ludwig, M. S. (2001). Effect of glycosaminoglycan degradation on lung tissue viscoelasticity. *American Journal of Physiology-Lung Cellular and Molecular Physiology, 280*(2), L306-L315. doi:10.1152/ajplung.2001.280.2.L306

Johnson, G. B., Brunn, G. J., & Platt, J. L. (2004). Cutting edge: an endogenous pathway to systemic inflammatory response syndrome (SIRS)-like reactions through Toll-like receptor 4. *J Immunol, 172*(1), 20-24.

Karlinsky, J. B., Bucay, P. J., Ciccolella, D. E., & Crowley, M. P. (1991). Effects of intratracheal endotoxin administration on hamster lung glycosaminoglycans. *Am J Physiol, 261*(2 Pt 1), L148-155. doi:10.1152/ajplung.1991.261.2.L148

Kawai, T., Adachi, O., Ogawa, T., Takeda, K., & Akira, S. (1999). Unresponsiveness of MyD88-Deficient Mice to Endotoxin. *Immunity, 11*(1), 115-122. doi:https://doi.org/10.1016/S1074-7613(00)80086-2

Kawai, T., Takeuchi, O., Fujita, T., Inoue, J. i., Muhlradt, P. F., Sato, S., . . . Akira, S. (2001). Lipopolysaccharide Stimulates the MyD88-Independent Pathway and Results in Activation of IFN-Regulatory Factor 3 and the Expression of a Subset of Lipopolysaccharide-Inducible Genes. *The Journal of Immunology, 167*(10), 5887-5894. doi:10.4049/jimmunol.167.10.5887

Kawashima, H., Atarashi, K., Hirose, M., Hirose, J., Yamada, S., Sugahara, K., & Miyasaka, M. (2002). Oversulfated chondroitin/dermatan sulfates containing GlcAbeta1/IdoAalpha1-3GalNAc(4,6-O-disulfate) interact with L- and P-selectin and chemokines. *J Biol Chem, 277*(15), 12921-12930. doi:10.1074/jbc.M200396200

Kawashima, H., Watanabe, N., Hirose, M., Sun, X., Atarashi, K., Kimura, T., . . . Miyasaka, M. (2003). Collagen XVIII, a Basement Membrane Heparan Sulfate Proteoglycan, Interacts with L-selectin and Monocyte Chemoattractant Protein-1. *Journal of Biological Chemistry, 278*(15), 13069-13076. doi:10.1074/jbc.M212244200

Keenan, T. D., Clark, S. J., Unwin, R. D., Ridge, L. A., Day, A. J., & Bishop, P. N. (2012). Mapping the differential distribution of proteoglycan core proteins in the adult human retina, choroid, and sclera. *Invest Ophthalmol Vis Sci, 53*(12), 7528-7538. doi:10.1167/iovs.12-10797

Kiani, C., Chen, L., Wu, Y. J., Yee, A. J., & Yang, B. B. (2002). Structure and function of aggrecan. *Cell Res, 12*(1), 19-32.

Kim, H. J., Hong, Y. H., Kim, Y. J., Kim, H. S., Park, J. W., Do, J. Y., . . . Lee, C. K. (2017). Anti-heparan sulfate antibody and functional loss of glomerular heparan sulfate proteoglycans in lupus nephritis. *Lupus, 26*(8), 815-824. doi:10.1177/0961203316678674

Kinnunen, A. I., Sormunen, R., Elamaa, H., Seppinen, L., Miller, R. T., Ninomiya, Y., . . . Pihlajaniemi, T. (2011). Lack of collagen XVIII long isoforms affects kidney podocytes,

whereas the short form is needed in the proximal tubular basement membrane. *J Biol Chem, 286*(10), 7755-7764. doi:10.1074/jbc.M110.166132

Kitagawa, H., Izumikawa, T., Uyama, T., & Sugahara, K. (2003). Molecular cloning of a chondroitin polymerizing factor that cooperates with chondroitin synthase for chondroitin polymerization. *J Biol Chem, 278*(26), 23666-23671. doi:10.1074/jbc.M302493200

Kloeckener-Gruissem, B., Neidhardt, J., Magyar, I., Plauchu, H., Zech, J.-C., Morle, L., . . . Berger, W. (2013). Novel VCAN mutations and evidence for unbalanced alternative splicing in the pathogenesis of Wagner syndrome. *Eur J Hum Genet, 21*(3), 352-356. doi:http://www.nature.com/ejhg/journal/v21/n3/suppinfo/ejhg2012137s1.html

Kolb, M., Margetts, P. J., Sime, P. J., & Gauldie, J. (2001). Proteoglycans decorin and biglycan differentially modulate TGF-beta-mediated fibrotic responses in the lung. *Am J Physiol Lung Cell Mol Physiol, 280*(6), L1327-1334. doi:10.1152/ajplung.2001.280.6.L1327

Kolset, S. O., Mann, D. M., Uhlin-Hansen, L., Winberg, J. O., & Ruoslahti, E. (1996). Serglycin-binding proteins in activated macrophages and platelets. *J Leukoc Biol, 59*(4), 545-554.

Kolset, S. O., Prydz, K., & Pejler, G. (2004). Intracellular proteoglycans. *Biochem J, 379*(Pt 2), 217-227. doi:10.1042/BJ20031230

Kolset, S. O., & Tveit, H. (2008). Serglycin--structure and biology. *Cell Mol Life Sci, 65*(7-8), 1073-1085. doi:10.1007/s00018-007-7455-6

Konno, K., Arai, H., Motomiya, M., Nagai, H., Ito, M., Sato, H., & Satoh, K. (1982). A biochemical study on glycosaminoglycans (mucopolysaccharides) in emphysematous and in aged lungs. *Am Rev Respir Dis, 126*(5), 797-801. doi:10.1164/arrd.1982.126.5.797

Koopmann, W., Ediriwickrema, C., & Krangel, M. S. (1999). Structure and function of the glycosaminoglycan binding site of chemokine macrophage-inflammatory protein-1β. *Journal of Immunology, 163*(4), 2120-2127.

Koopmann, W., & Krangel, M. S. (1997). Identification of a Glycosaminoglycan-binding Site in Chemokine Macrophage Inflammatory Protein-1α. *Journal of Biological Chemistry, 272*(15), 10103-10109. doi:10.1074/jbc.272.15.10103

Kornfeld, R., & Kornfeld, S. (1985). Assembly of Asparagine-Linked Oligosaccharides. *Annual Review of Biochemistry, 54*(1), 631-664. doi:10.1146/annurev.bi.54.070185.003215

Kuan, S. F., Rust, K., & Crouch, E. (1992). Interactions of surfactant protein D with bacterial lipopolysaccharides. Surfactant protein D is an Escherichia coli-binding protein in bronchoalveolar lavage. *The Journal of Clinical Investigation, 90*(1), 97-106. doi:10.1172/JCI115861

Lau, E. K., Paavola, C. D., Johnson, Z., Gaudry, J. P., Geretti, E., Borlat, F., . . . Handel, T. M. (2004). Identification of the glycosaminoglycan binding site of the CC chemokine, MCP-1: Implications for structure and function in vivo. *Journal of Biological Chemistry, 279*(21), 22294-22305. doi:10.1074/jbc.M311224200

LeClair, E. E., Mui, S. R., Huang, A., Topczewska, J. M., & Topczewski, J. (2009). Craniofacial skeletal defects of adult zebrafish Glypican 4 (knypek) mutants. *Dev Dyn, 238*(10), 2550-2563. doi:10.1002/dvdy.22086

Leheste, J. R., Rolinski, B., Vorum, H., Hilpert, J., Nykjaer, A., Jacobsen, C., . . . Willnow, T. E. (1999). Megalin knockout mice as an animal model of low molecular weight proteinuria. *Am J Pathol, 155*(4), 1361-1370. doi:10.1016/s0002-9440(10)65238-8

Lensen, J. F., Rops, A. L., Wijnhoven, T. J., Hafmans, T., Feitz, W. F., Oosterwijk, E., . . . van Kuppevelt, T. H. (2005). Localization and functional characterization of glycosaminoglycan domains in the normal human kidney as revealed by phage display-derived single chain antibodies. *J Am Soc Nephrol, 16*(5), 1279-1288. doi:10.1681/ASN.2004050413

Li, J.-p. (2010). Glucuronyl C5-Epimerase: An Enzyme Converting Glucuronic Acid to Iduronic Acid in Heparan Sulfate/Heparin Biosynthesis. In Z. Lijuan (Ed.), *Progress in Molecular Biology and Translational Science* (Vol. Volume 93, pp. 59-78): Academic Press.

Li, J.-P., Gong, F., Hagner-McWhirter, Å., Forsberg, E., Åbrink, M., Kisilevsky, R., . . . Lindahl, U. (2003). Targeted Disruption of a Murine Glucuronyl C5-epimerase Gene Results in Heparan Sulfate Lacking l-Iduronic Acid and in Neonatal Lethality. *Journal of Biological Chemistry, 278*(31), 28363-28366. doi:10.1074/jbc.C300219200

Lin, A. E., Neri, G., Hughes-Benzie, R., & Weksberg, R. (1999). Cardiac anomalies in the Simpson-Golabi-Behmel syndrome. *Am J Med Genet, 83*(5), 378-381.

Lindahl, U., Couchman, J., Kimata, K., & Esko, J. D. (2015). Proteoglycans and Sulfated Glycosaminoglycans. In rd, A. Varki, R. D. Cummings, J. D. Esko, P. Stanley, G. W. Hart, M. Aebi, A. G. Darvill, T. Kinoshita, N. H. Packer, J. H. Prestegard, R. L. Schnaar, & P. H. Seeberger (Eds.), *Essentials of Glycobiology* (pp. 207-221). Cold Spring Harbor (NY).

Litwack, E., Stipp, C., Kumbasar, A., & Lander, A. (1994). Neuronal expression of glypican, a cell-surface glycosylphosphatidylinositol-anchored heparan sulfate proteoglycan, in the adult rat nervous system. *The Journal of Neuroscience, 14*(6), 3713-3724.

Lockhart, M., Wirrig, E., Phelps, A., & Wessels, A. (2011). Extracellular matrix and heart development. *Birth Defects Res A Clin Mol Teratol, 91*(6), 535-550. doi:10.1002/bdra.20810

Lortat-Jacob, H., Grosdidier, A., & Imberty, A. (2002). Structural diversity of heparan sulfate binding domains in chemokines. *Proceedings of the National Academy of Sciences of the United States of America, 99*(3), 1229-1234. doi:10.1073/pnas.032497699

Lu, Y.-C., Yeh, W.-C., & Ohashi, P. S. (2008). LPS/TLR4 signal transduction pathway. *Cytokine, 42*(2), 145-151. doi:https://doi.org/10.1016/j.cyto.2008.01.006

Macri, L., Silverstein, D., & Clark, R. A. (2007). Growth factor binding to the pericellular matrix and its importance in tissue engineering. *Adv Drug Deliv Rev, 59*(13), 1366-1381. doi:10.1016/j.addr.2007.08.015

Margolis, R. K., Rauch, U., Maurel, P., & Margolis, R. U. (1996). Neurocan and phosphacan: two major nervous tissue-specific chondroitin sulfate proteoglycans. *Perspect Dev Neurobiol, 3*(4), 273-290.

Martin, L., Blanpain, C., Garnier, P., Wittamer, V., Parmentier, M., & Vita, C. (2001). Structural and functional analysis of the RANTES-glycosaminoglycans interactions. *Biochemistry, 40*(21), 6303-6318. doi:10.1021/bi002670n

Martin, T. R. (2000). Recognition of Bacterial Endotoxin in the Lungs. *American journal of respiratory cell and molecular biology, 23*(2), 128-132. doi:10.1165/ajrcmb.23.2.f189

Martin, T. R., & Frevert, C. W. (2005). Innate Immunity in the Lungs. *Proceedings of the American Thoracic Society, 2*(5), 403-411. doi:10.1513/pats.200508-090JS

Martin, T. R., Mathison, J. C., Tobias, P. S., Leturcq, D. J., Moriarty, A. M., Maunder, R. J., & Ulevitch, R. J. (1992). Lipopolysaccharide binding protein enhances the responsiveness of alveolar macrophages to bacterial lipopolysaccharide. Implications for cytokine production in normal and injured lungs. *J Clin Invest, 90*(6), 2209-2219. doi:10.1172/JCI116106

McCormack, F. X., & Whitsett, J. A. (2002). The pulmonary collectins, SP-A and SP-D, orchestrate innate immunity in the lung. *J Clin Invest, 109*(6), 707-712. doi:10.1172/JCI15293

McDonald, B., McAvoy, E. F., Lam, F., Gill, V., de la Motte, C., Savani, R. C., & Kubes, P. (2008). Interaction of CD44 and hyaluronan is the dominant mechanism for neutrophil sequestration in inflamed liver sinusoids. *J Exp Med, 205*(4), 915-927. doi:10.1084/jem.20071765

McIntosh, J. C., Swyers, A. H., Fisher, J. H., & Wright, J. R. (1996). Surfactant proteins A and D increase in response to intratracheal lipopolysaccharide. *Am J Respir Cell Mol Biol, 15*(4), 509-519. doi:10.1165/ajrcmb.15.4.8879185

Mellman, I., Fuchs, R., & Helenius, A. (1986). Acidification of the endocytic and exocytic pathways. *Annu Rev Biochem, 55*, 663-700. doi:10.1146/annurev.bi.55.070186.003311

Mercado-Pimentel, M. E., & Runyan, R. B. (2007). Multiple Transforming Growth Factor-β Isoforms and Receptors Function during Epithelial-Mesenchymal Cell Transformation in the Embryonic Heart. *Cells Tissues Organs, 185*(1-3), 146-156.

Mercer, R. R., & Crapo, J. D. (1990). Spatial distribution of collagen and elastin fibers in the lungs. *Journal of Applied Physiology, 69*(2), 756-765. doi:10.1152/jappl.1990.69.2.756

Merline, R., Moreth, K., Beckmann, J., Nastase, M. V., Zeng-Brouwers, J., Tralhao, J. G., . . . Schaefer, L. (2011). Signaling by the matrix proteoglycan decorin controls inflammation and cancer through PDCD4 and MicroRNA-21. *Sci Signal, 4*(199), ra75. doi:10.1126/scisignal.2001868

Merrilees, M. J., Ching, P. S., Beaumont, B., Hinek, A., Wight, T. N., & Black, P. N. (2008). Changes in elastin, elastin binding protein and versican in alveoli in chronic obstructive pulmonary disease. *Respir Res, 9*, 41. doi:10.1186/1465-9921-9-41

Miner, J. H. (2012). The glomerular basement membrane. *Exp Cell Res, 318*(9), 973-978. doi:10.1016/j.yexcr.2012.02.031

Mis, E. K., Liem, K. F., Kong, Y., Schwartz, N. B., Domowicz, M., & Weatherbee, S. D. (2014). Forward Genetics Defines Xylt1 as a Key, Conserved Regulator of Early Chondrocyte Maturation and Skeletal Length. *Dev Biol, 385*(1), 67-82. doi:10.1016/j.ydbio.2013.10.014

Moestrup, S. K., Kozyraki, R., Kristiansen, M., Kaysen, J. H., Rasmussen, H. H., Brault, D., . . . Verroust, P. J. (1998). The intrinsic factor-vitamin B12 receptor and target of teratogenic

antibodies is a megalin-binding peripheral membrane protein with homology to developmental proteins. *J Biol Chem, 273*(9), 5235-5242.

Morelle, W., Haslam, S. M., Ziak, M., Roth, J., Morris, H. R., & Dell, A. (2000). Characterization of the N-linked oligosaccharides of megalin (gp330) from rat kidney. *Glycobiology, 10*(3), 295-304. doi:10.1093/glycob/10.3.295

Munns, C. F., Fahiminiya, S., Poudel, N., Munteanu, M. C., Majewski, J., Sillence, D. O., . . . Hinsdale, M. E. (2015). Homozygosity for frameshift mutations in XYLT2 result in a spondylo-ocular syndrome with bone fragility, cataracts, and hearing defects. *Am J Hum Genet, 96*(6), 971-978. doi:10.1016/j.ajhg.2015.04.017

Nadesalingam, J., Bernal, A. L., Dodds, A. W., Willis, A. C., Mahoney, D. J., Day, A. J., . . . Palaniyar, N. (2003). Identification and Characterization of a Novel Interaction between Pulmonary Surfactant Protein D and Decorin. *Journal of Biological Chemistry, 278*(28), 25678-25687. doi:10.1074/jbc.M210186200

Nastase, M. V., Young, M. F., & Schaefer, L. (2012). Biglycan: a multivalent proteoglycan providing structure and signals. *J Histochem Cytochem, 60*(12), 963-975. doi:10.1369/0022155412456380

Negrini, D., Tenstad, O., & Wiig, H. (2003). Interstitial exclusion of albumin in rabbit lung measured with the continuous infusion method in combination with the wick technique. *Microcirculation, 10*(2), 153-165. doi:10.1038/sj.mn.7800180

Neill, T., Schaefer, L., & Iozzo, R. V. (2012). Decorin: a guardian from the matrix. *Am J Pathol, 181*(2), 380-387. doi:10.1016/j.ajpath.2012.04.029

Ng, A., Wong, M., Viviano, B., Erlich, J. M., Alba, G., Pflederer, C., . . . Saunders, S. (2009). Loss of glypican-3 Function Causes Growth Factor-dependent Defects in Cardiac and Coronary Vascular Development. *Dev Biol, 335*(1), 208-215. doi:10.1016/j.ydbio.2009.08.029

Nitkin, R. M., Smith, M. A., Magill, C., Fallon, J. R., Yao, Y. M., Wallace, B. G., & McMahan, U. J. (1987). Identification of agrin, a synaptic organizing protein from Torpedo electric organ. *The Journal of Cell Biology, 105*(6), 2471-2478. doi:10.1083/jcb.105.6.2471

O'Toole, J. J., Deyst, K. A., Bowe, M. A., Nastuk, M. A., McKechnie, B. A., & Fallon, J. R. (1996). Alternative splicing of agrin regulates its binding to heparin alpha-dystroglycan, and the cell surface. *Proc Natl Acad Sci U S A, 93*(14), 7369-7374.

Orlando, R. A., Exner, M., Czekay, R. P., Yamazaki, H., Saito, A., Ullrich, R., . . . Farquhar, M. G. (1997). Identification of the second cluster of ligand-binding repeats in megalin as a site for receptor-ligand interactions. *Proc Natl Acad Sci U S A, 94*(6), 2368-2373.

Ostermann, G., Weber, K. S., Zernecke, A., Schroder, A., & Weber, C. (2002). JAM-1 is a ligand of the beta(2) integrin LFA-1 involved in transendothelial migration of leukocytes. *Nat Immunol, 3*(2), 151-158. doi:10.1038/ni755

Paine-Saunders, S., Viviano, B. L., & Saunders, S. (1999). GPC6, a Novel Member of the Glypican Gene Family, Encodes a Product Structurally Related to GPC4 and Is Colocalized withGPC5on Human Chromosome 13. *Genomics, 57*(3), 455-458. doi:https://doi.org/10.1006/geno.1999.5793

Parisuthiman, D., Mochida, Y., Duarte, W. R., & Yamauchi, M. (2005). Biglycan modulates osteoblast differentiation and matrix mineralization. *J Bone Miner Res, 20*(10), 1878-1886. doi:10.1359/jbmr.050612

Park, B. S., Song, D. H., Kim, H. M., Choi, B. S., Lee, H., & Lee, J. O. (2009). The structural basis of lipopolysaccharide recognition by the TLR4-MD-2 complex. *Nature, 458*(7242), 1191-1195. doi:10.1038/nature07830

Pasvolsky, R., Feigelson, S. W., Kilic, S. S., Simon, A. J., Tal-Lapidot, G., Grabovsky, V., . . . Alon, R. (2007). A LAD-III syndrome is associated with defective expression of the Rap-

1 activator CalDAG-GEFI in lymphocytes, neutrophils, and platelets. *J Exp Med, 204*(7), 1571-1582. doi:10.1084/jem.20070058

Paulsson, M., Yurchenco, P. D., Ruben, G. C., Engel, J., & Timpl, R. (1987). Structure of low density heparan sulfate proteoglycan isolated from a mouse tumor basement membrane. *J Mol Biol, 197*(2), 297-313.

Pellegrini, M., Pilia, G., Pantano, S., Lucchini, F., Uda, M., Fumi, M., . . . Forabosco, A. (1998). Gpc3 expression correlates with the phenotype of the Simpson-Golabi-Behmel syndrome. *Developmental Dynamics, 213*(4), 431-439. doi:10.1002/(SICI)1097-0177(199812)213:4<431::AID-AJA8>3.0.CO;2-7

Perez, C., Gerber, S., Boilevin, J., Bucher, M., Darbre, T., Aebi, M., . . . Locher, K. P. (2015). Structure and mechanism of an active lipid-linked oligosaccharide flippase. *Nature, 524*(7566), 433-438. doi:10.1038/nature14953

Perin, J. P., Bonnet, F., Maillet, P., & Jolles, P. (1988). Characterization and N-terminal sequence of human platelet proteoglycan. *Biochem J, 255*(3), 1007-1013.

Perkins, G. D., Nathani, N., Richter, A. G., Park, D., Shyamsundar, M., Heljasvaara, R., . . . Thickett, D. R. (2009). Type XVIII collagen degradation products in acute lung injury. *Crit Care, 13*(2), R52. doi:10.1186/cc7779

Pison, U., Wright, J. R., & Hawgood, S. (1992). Specific binding of surfactant apoprotein SP-A to rat alveolar macrophages. *Am J Physiol, 262*(4 Pt 1), L412-417. doi:10.1152/ajplung.1992.262.4.L412

Poltorak, A., He, X., Smirnova, I., Liu, M. Y., Van Huffel, C., Du, X., . . . Beutler, B. (1998). Defective LPS signaling in C3H/HeJ and C57BL/10ScCr mice: mutations in Tlr4 gene. *Science, 282*(5396), 2085-2088.

Ponta, H., Sherman, L., & Herrlich, P. A. (2003). CD44: from adhesion molecules to signalling regulators. *Nat Rev Mol Cell Biol, 4*(1), 33-45. doi:10.1038/nrm1004

Proudfoot, A. E. I., Handel, T. M., Johnson, Z., Lau, E. K., LiWang, P., Clark-Lewis, I., . . . Kosco-Vilbois, M. H. (2003). Glycosaminoglycan binding and oligomerization are essential for the in vivo activity of certain chemokines. *Proceedings of the National Academy of Sciences of the United States of America, 100*(4), 1885-1890. doi:10.1073/pnas.0334864100

Raats, C. J., Van Den Born, J., & Berden, J. H. (2000). Glomerular heparan sulfate alterations: mechanisms and relevance for proteinuria. *Kidney Int, 57*(2), 385-400. doi:10.1046/j.1523-1755.2000.00858.x

Raats, C. J. I., Bakker, M. A. H., Hoch, W., Tamboer, W. P. M., Groffen, A. J. A., van den Heuvel, L. P. W. J., . . . van den Born, J. (1998). Differential Expression of Agrin in Renal Basement Membranes As Revealed by Domain-specific Antibodies. *Journal of Biological Chemistry, 273*(28), 17832-17838. doi:10.1074/jbc.273.28.17832

Ramadori, G., Meyer zum Buschenfelde, K. H., Tobias, P. S., Mathison, J. C., & Ulevitch, R. J. (1990). Biosynthesis of lipopolysaccharide-binding protein in rabbit hepatocytes. *Pathobiology, 58*(2), 89-94.

Raspanti, M., Alessandrini, A., Ottani, V., & Ruggeri, A. (1997). Direct Visualization of Collagen-Bound Proteoglycans by Tapping-Mode Atomic Force Microscopy. *Journal of Structural Biology, 119*(2), 118-122. doi:https://doi.org/10.1006/jsbi.1997.3865

Reinhardt, A., Wehle, M., Geissner, A., Crouch, E. C., Kang, Y., Yang, Y., . . . Seeberger, P. H. (2016). Structure binding relationship of human surfactant protein D and various lipopolysaccharide inner core structures. *Journal of Structural Biology, 195*(3), 387-395. doi:https://doi.org/10.1016/j.jsb.2016.06.019

Reiser, J., Kriz, W., Kretzler, M., & Mundel, P. (2000). The glomerular slit diaphragm is a modified adherens junction. *J Am Soc Nephrol, 11*(1), 1-8.

Reiss, G., te Heesen, S., Zimmerman, J., Robbins, P. W., & Aebi, M. (1996). Isolation of the ALG6 locus of Saccharomyces cerevisiae required for glucosylation in the N-linked glycosylation pathway. *Glycobiology, 6*(5), 493-498.

Ringvall, M., Ledin, J., Holmborn, K., van Kuppevelt, T., Ellin, F., Eriksson, I., . . . Forsberg, E. (2000). Defective heparan sulfate biosynthesis and neonatal lethality in mice lacking N-deacetylase/N-sulfotransferase-1. *J Biol Chem, 275*(34), 25926-25930. doi:10.1074/jbc.C000359200

Rops, A. L., van der Vlag, J., Lensen, J. F., Wijnhoven, T. J., van den Heuvel, L. P., van Kuppevelt, T. H., & Berden, J. H. (2004). Heparan sulfate proteoglycans in glomerular inflammation. *Kidney Int, 65*(3), 768-785. doi:10.1111/j.1523-1755.2004.00451.x

Rudolph, G., Kalpadakis, P., Bettecken, T., Lichtner, P., Haritoglou, C., Hergersberg, M., . . . Schmidt, H. (2003). Spondylo-ocular syndrome: a new entity with crystalline lens malformation, cataract, retinal detachment, osteoporosis, and platyspondyly. *American Journal of Ophthalmology, 135*(5), 681-687. doi:10.1016/s0002-9394(02)02155-4

Ruegg, M. A., Tsim, K. W., Horton, S. E., Kroger, S., Escher, G., Gensch, E. M., & McMahan, U. J. (1992). The agrin gene codes for a family of basal lamina proteins that differ in function and distribution. *Neuron, 8*(4), 691-699.

Ruotsalainen, V., Ljungberg, P., Wartiovaara, J., Lenkkeri, U., Kestila, M., Jalanko, H., . . . Tryggvason, K. (1999). Nephrin is specifically located at the slit diaphragm of glomerular podocytes. *Proc Natl Acad Sci U S A, 96*(14), 7962-7967.

Sano, H., Sohma, H., Muta, T., Nomura, S., Voelker, D. R., & Kuroki, Y. (1999). Pulmonary surfactant protein A modulates the cellular response to smooth and rough lipopolysaccharides by interaction with CD14. *J Immunol, 163*(1), 387-395.

Sanyal, S., & Menon, A. K. (2010). Stereoselective transbilayer translocation of mannosyl phosphoryl dolichol by an endoplasmic reticulum flippase. *Proc Natl Acad Sci U S A, 107*(25), 11289-11294. doi:10.1073/pnas.1002408107

Sarelius, I. H., & Glading, A. J. (2015). Control of vascular permeability by adhesion molecules. *Tissue Barriers, 3*(1-2), e985954. doi:10.4161/21688370.2014.985954

Sarrazin, S., Lamanna, W. C., & Esko, J. D. (2011). Heparan sulfate proteoglycans. *Cold Spring Harb Perspect Biol, 3*(7), a004952. doi:10.1101/cshperspect.a004952

Schaefer, L., Babelova, A., Kiss, E., Hausser, H. J., Baliova, M., Krzyzankova, M., . . . Grone, H. J. (2005). The matrix component biglycan is proinflammatory and signals through Toll-like receptors 4 and 2 in macrophages. *J Clin Invest, 115*(8), 2223-2233. doi:10.1172/JCI23755

Schmidt, H., Rudolph G Fau - Hergersberg, M., Hergersberg M Fau - Schneider, K., Schneider K Fau - Moradi, S., Moradi S Fau - Meitinger, T., & Meitinger, T. (2001). Retinal detachment and cataract, facial dysmorphism, generalized osteoporosis, immobile spine and platyspondyly in a consanguinous kindred--a possible new syndrome. *Clinical Genetics, 59*, 99-105.

Schneeberger, E. E., Levey, R. H., McCluskey, R. T., & Karnovsky, M. J. (1975). The isoporous substructure of the human glomerular slit diaphragm. *Kidney International, 8*(1), 48-52. doi:10.1038/ki.1975.75

Schwarz, F., & Aebi, M. (2011). Mechanisms and principles of N-linked protein glycosylation. *Curr Opin Struct Biol, 21*(5), 576-582. doi:10.1016/j.sbi.2011.08.005

Screaton, G. R., Bell, M. V., Jackson, D. G., Cornelis, F. B., Gerth, U., & Bell, J. I. (1992). Genomic structure of DNA encoding the lymphocyte homing receptor CD44 reveals at least 12 alternatively spliced exons. *Proceedings of the National Academy of Sciences of the United States of America, 89*(24), 12160-12164.

Shaw, S. K., Bamba, P. S., Perkins, B. N., & Luscinskas, F. W. (2001). Real-time imaging of vascular endothelial-cadherin during leukocyte transmigration across endothelium. *J Immunol, 167*(4), 2323-2330.

Shih, N. Y., Li, J., Karpitskii, V., Nguyen, A., Dustin, M. L., Kanagawa, O., . . . Shaw, A. S. (1999). Congenital nephrotic syndrome in mice lacking CD2-associated protein. *Science, 286*(5438), 312-315.

Shinomura, T., Nishida, Y., Ito, K., & Kimata, K. (1993). cDNA cloning of PG-M, a large chondroitin sulfate proteoglycan expressed during chondrogenesis in chick limb buds. Alternative spliced multiforms of PG-M and their relationships to versican. *Journal of Biological Chemistry, 268*(19), 14461-14469.

Shrimal, S., Cherepanova, N. A., & Gilmore, R. (2015). Cotranslational and posttranslocational N-glycosylation of proteins in the endoplasmic reticulum. *Semin Cell Dev Biol, 41*, 71-78. doi:10.1016/j.semcdb.2014.11.005

Simon, S. I., Hu, Y., Vestweber, D., & Smith, C. W. (2000). Neutrophil tethering on E-selectin activates beta 2 integrin binding to ICAM-1 through a mitogen-activated protein kinase signal transduction pathway. *J Immunol, 164*(8), 4348-4358.

Sleeman, J. P., Kondo, K., Moll, J., Ponta, H., & Herrlich, P. (1997). Variant exons v6 and v7 together expand the repertoire of glycosaminoglycans bound by CD44. *J Biol Chem, 272*(50), 31837-31844. doi:10.1074/jbc.272.50.31837

Sorokin, L. M., Pausch, F., Frieser, M., Kroger, S., Ohage, E., & Deutzmann, R. (1997). Developmental regulation of the laminin alpha5 chain suggests a role in epithelial and endothelial cell maturation. *Dev Biol, 189*(2), 285-300. doi:10.1006/dbio.1997.8668

St John, P. L., & Abrahamson, D. R. (2001). Glomerular endothelial cells and podocytes jointly synthesize laminin-1 and -11 chains. *Kidney Int, 60*(3), 1037-1046. doi:10.1046/j.1523-1755.2001.0600031037.x

Stagljar, I., te Heesen, S., & Aebi, M. (1994). New phenotype of mutations deficient in glucosylation of the lipid-linked oligosaccharide: cloning of the ALG8 locus. *Proc Natl Acad Sci U S A, 91*(13), 5977-5981.

Stamatovic, S. M., Sladojevic, N., Keep, R. F., & Andjelkovic, A. V. (2012). Relocalization of junctional adhesion molecule A during inflammatory stimulation of brain endothelial cells. *Mol Cell Biol, 32*(17), 3414-3427. doi:10.1128/mcb.06678-11

Stipp, C. S., Litwack, E. D., & Lander, A. D. (1994). Cerebroglycan: an integral membrane heparan sulfate proteoglycan that is unique to the developing nervous system and expressed specifically during neuronal differentiation. *J Cell Biol, 124*(1-2), 149-160.

Stum, M., Davoine, C. S., Vicart, S., Guillot-Noel, L., Topaloglu, H., Carod-Artal, F. J., . . . Nicole, S. (2006). Spectrum of HSPG2 (Perlecan) mutations in patients with Schwartz-Jampel syndrome. *Hum Mutat, 27*(11), 1082-1091. doi:10.1002/humu.20388

Sugumaran, G., Katsman, M., & Silbert, J. E. (1992). Effects of brefeldin A on the localization of chondroitin sulfate-synthesizing enzymes. Activities in subfractions of the Golgi from chick embryo epiphyseal cartilage. *J Biol Chem, 267*(13), 8802-8806.

Suleiman, H., Zhang, L., Roth, R., Heuser, J. E., Miner, J. H., Shaw, A. S., & Dani, A. (2013). Nanoscale protein architecture of the kidney glomerular basement membrane. *eLife, 2*, e01149. doi:10.7554/eLife.01149

Suzuki, O. T., Sertié, A. L., Der Kaloustian, V. M., Kok, F., Carpenter, M., Murray, J., . . . Passos-Bueno, M. R. (2002). Molecular Analysis of Collagen XVIII Reveals Novel Mutations, Presence of a Third Isoform, and Possible Genetic Heterogeneity in Knobloch Syndrome. *Am J Hum Genet, 71*(6), 1320-1329.

Takeuchi, H., Kantharia, J., Sethi, M. K., Bakker, H., & Haltiwanger, R. S. (2012). Site-specific O-Glucosylation of the Epidermal Growth Factor-like (EGF) Repeats of Notch: EFFICIENCY OF GLYCOSYLATION IS AFFECTED BY PROPER FOLDING AND

AMINO ACID SEQUENCE OF INDIVIDUAL EGF REPEATS. *J Biol Chem, 287*(41), 33934-33944. doi:10.1074/jbc.M112.401315

Tang, S., Leung, J. C., Tsang, A. W., Lan, H. Y., Chan, T. M., & Lai, K. N. (2002). Transferrin up-regulates chemokine synthesis by human proximal tubular epithelial cells: implication on mechanism of tubuloglomerular communication in glomerulopathic proteinura. *Kidney Int, 61*(5), 1655-1665. doi:10.1046/j.1523-1755.2002.00301.x

Tang, S., Sheerin, N. S., Zhou, W., Brown, Z., & Sacks, S. H. (1999). Apical Proteins Stimulate Complement Synthesis by Cultured Human Proximal Tubular Epithelial Cells. *Journal of the American Society of Nephrology, 10*(1), 69-76.

Tanino, Y., Chang, M. Y., Wang, X., Gill, S. E., Skerrett, S., McGuire, J. K., . . . Frevert, C. W. (2012). Syndecan-4 regulates early neutrophil migration and pulmonary inflammation in response to lipopolysaccharide. *Am J Respir Cell Mol Biol, 47*(2), 196-202. doi:10.1165/rcmb.2011-0294OC

Taylan, F., Costantini, A., Coles, N., Pekkinen, M., Heon, E., Siklar, Z., . . . Makitie, O. (2016). Spondyloocular Syndrome: Novel Mutations in XYLT2 Gene and Expansion of the Phenotypic Spectrum. *J Bone Miner Res, 31*(8), 1577-1585. doi:10.1002/jbmr.2834

Taylor, K. R., Trowbridge, J. M., Rudisill, J. A., Termeer, C. C., Simon, J. C., & Gallo, R. L. (2004). Hyaluronan fragments stimulate endothelial recognition of injury through TLR4. *J Biol Chem, 279*(17), 17079-17084. doi:10.1074/jbc.M310859200

Thiel, C., Schwarz, M., Peng, J., Grzmil, M., Hasilik, M., Braulke, T., . . . Korner, C. (2003). A new type of congenital disorders of glycosylation (CDG-Ii) provides new insights into the early steps of dolichol-linked oligosaccharide biosynthesis. *J Biol Chem, 278*(25), 22498-22505. doi:10.1074/jbc.M302850200

Tiedemann, K., Sasaki, T., Gustafsson, E., Gohring, W., Batge, B., Notbohm, H., . . . Reinhardt, D. P. (2005). Microfibrils at basement membrane zones interact with perlecan via fibrillin-1. *J Biol Chem, 280*(12), 11404-11412. doi:10.1074/jbc.M409882200

Tkachenko, E., Rhodes, J. M., & Simons, M. (2005). Syndecans: new kids on the signaling block. *Circ Res, 96*(5), 488-500. doi:10.1161/01.RES.0000159708.71142.c8

Tobias, P. S., Soldau, K., Kline, L., Lee, J. D., Kato, K., Martin, T. P., & Ulevitch, R. J. (1993). Cross-linking of lipopolysaccharide (LPS) to CD14 on THP-1 cells mediated by LPS-binding protein. *J Immunol, 150*(7), 3011-3021.

Tobias, P. S., Soldau, K., & Ulevitch, R. J. (1986). Isolation of a lipopolysaccharide-binding acute phase reactant from rabbit serum. *J Exp Med, 164*(3), 777-793.

Vaccaro, C. A., & Brody, J. S. (1981). Structural features of alveolar wall basement membrane in the adult rat lung. *The Journal of Cell Biology, 91*(2), 427-437. doi:10.1083/jcb.91.2.427

van den Hoven, M. J., Rops, A. L., Vlodavsky, I., Levidiotis, V., Berden, J. H., & van der Vlag, J. (2007). Heparanase in glomerular diseases. *Kidney Int, 72*(5), 543-548. doi:10.1038/sj.ki.5002337

van den Hoven, M. J., Wijnhoven, T. J., Li, J. P., Zcharia, E., Dijkman, H. B., Wismans, R. G., . . . van der Vlag, J. (2008). Reduction of anionic sites in the glomerular basement membrane by heparanase does not lead to proteinuria. *Kidney Int, 73*(3), 278-287. doi:10.1038/sj.ki.5002706

Van den Steen, P., Rudd, P. M., Dwek, R. A., & Opdenakker, G. (1998). Concepts and principles of O-linked glycosylation. *Crit Rev Biochem Mol Biol, 33*(3), 151-208. doi:10.1080/10409239891204198

van Iwaarden, F., Welmers, B., Verhoef, J., Haagsman, H. P., & Van Golde, L. (1990). Pulmonary surfactant protein A enhances the host-defense mechanism of rat alveolar macrophages. *Am J Respir Cell Mol Biol, 2*(1), 91-98.

van Kuppevelt, T. H., Cremers, F. P., Domen, J. G., & Kuyper, C. M. (1984). Staining of proteoglycans in mouse lung alveoli. II. Characterization of the Cuprolinic blue-positive, anionic sites. *Histochem J, 16*(6), 671-686.

van Rozendaal, B. A., van de Lest, C. H., van Eijk, M., van Golde, L. M., Voorhout, W. F., van Helden, H. P., & Haagsman, H. P. (1999). Aerosolized endotoxin is immediately bound by pulmonary surfactant protein D in vivo. *Biochim Biophys Acta, 1454*(3), 261-269.

van Straaten, J. F., Coers, W., Noordhoek, J. A., Huitema, S., Flipsen, J. T., Kauffman, H. F., . . . Postma, D. S. (1999). Proteoglycan changes in the extracellular matrix of lung tissue from patients with pulmonary emphysema. *Mod Pathol, 12*(7), 697-705.

Varki, A., & Kornfeld, S. (2015). Historical Background and Overview. In rd, A. Varki, R. D. Cummings, J. D. Esko, P. Stanley, G. W. Hart, M. Aebi, A. G. Darvill, T. Kinoshita, N. H. Packer, J. H. Prestegard, R. L. Schnaar, & P. H. Seeberger (Eds.), *Essentials of Glycobiology* (pp. 1-18). Cold Spring Harbor (NY).

Venkatesan, N., Ebihara, T., Roughley, P. J., & Ludwig, M. S. (2000). Alterations in large and small proteoglycans in bleomycin-induced pulmonary fibrosis in rats. *Am J Respir Crit Care Med, 161*(6), 2066-2073. doi:10.1164/ajrccm.161.6.9909098

Venkatesan, N., Roughley, P. J., & Ludwig, M. S. (2002). Proteoglycan expression in bleomycin lung fibroblasts: role of transforming growth factor-beta(1) and interferon-gamma. *Am J Physiol Lung Cell Mol Physiol, 283*(4), L806-814. doi:10.1152/ajplung.00061.2002

Veugelers, M., Cat, B. D., Muyldermans, S. Y., Reekmans, G., Delande, N., Frints, S., . . . David, G. (2000). Mutational analysis of the GPC3/GPC4 glypican gene cluster on Xq26 in patients with Simpson-Golabi-Behmel syndrome: identification of loss-of-function mutations in the GPC3 gene. *Hum Mol Genet, 9*(9), 1321-1328.

Veugelers, M., Vermeesch, J., Reekmans, G., Steinfeld, R., Marynen, P., & David, G. (1997). Characterization of Glypican-5 and Chromosomal Localization of HumanGPC5,a New

Member of the Glypican Gene Family. *Genomics*, *40*(1), 24-30. doi:https://doi.org/10.1006/geno.1996.4518

Vitelli, R., Santillo, M., Lattero, D., Chiariello, M., Bifulco, M., Bruni, C. B., & Bucci, C. (1997). Role of the small GTPase Rab7 in the late endocytic pathway. *Journal of Biological Chemistry*, *272*(7), 4391-4397.

Wang, L., Fuster, M., Sriramarao, P., & Esko, J. D. (2005). Endothelial heparan sulfate deficiency impairs L-selectin- and chemokine-mediated neutrophil trafficking during inflammatory responses. *Nat Immunol, 6*, 902. doi:10.1038/ni1233

https://www.nature.com/articles/ni1233#supplementary-information

Wang, N., Liang, H., & Zen, K. (2014). Molecular Mechanisms That Influence the Macrophage M1–M2 Polarization Balance. *Frontiers in Immunology*, *5*, 614. doi:10.3389/fimmu.2014.00614

Wang, S., Voisin, M. B., Larbi, K. Y., Dangerfield, J., Scheiermann, C., Tran, M., . . . Nourshargh, S. (2006). Venular basement membranes contain specific matrix protein low expression regions that act as exit points for emigrating neutrophils. *J Exp Med*, *203*(6), 1519-1532. doi:10.1084/jem.20051210

Wang, Y., Rangan, G. K., Tay, Y.-c., Wang, Y., & Harris, D. C. H. (1999). Induction of Monocyte Chemoattractant Protein-1 by Albumin Is Mediated by Nuclear Factor κB in Proximal Tubule Cells. *Journal of the American Society of Nephrology*, *10*(6), 1204-1213.

Watanabe, K., Yamada, H., & Yamaguchi, Y. (1995). K-glypican: a novel GPI-anchored heparan sulfate proteoglycan that is highly expressed in developing brain and kidney. *J Cell Biol, 130*(5), 1207-1218.

Waterson, J., Stockley, T. L., Segal, S., & Golabi, M. (2010). Novel duplication in glypican-4 as an apparent cause of Simpson-Golabi-Behmel syndrome. *Am J Med Genet A, 152A*(12), 3179-3181. doi:10.1002/ajmg.a.33450

Weaver, T. E., & Conkright, J. J. (2001). Function of surfactant proteins B and C. *Annu Rev Physiol, 63*, 555-578. doi:10.1146/annurev.physiol.63.1.555

White, E. S. (2015). Lung extracellular matrix and fibroblast function. *Ann Am Thorac Soc, 12 Suppl 1*, S30-33. doi:10.1513/AnnalsATS.201406-240MG

Wight, T. N., Kang, I., & Merrilees, M. J. (2014). Versican and the control of inflammation. *Matrix Biol, 35*, 152-161. doi:10.1016/j.matbio.2014.01.015

Witt, D. P., & Lander, A. D. (1994). Differential binding of chemokines to glycosaminoglycan subpopulations. *Current Biology, 4*(5), 394-400. doi:https://doi.org/10.1016/S0960-9822(00)00088-9

Wittchen, E. S., van Buul, J. D., Burridge, K., & Worthylake, R. A. (2005). Trading spaces: Rap, Rac, and Rho as architects of transendothelial migration. *Curr Opin Hematol, 12*(1), 14-21.

Wiweger, M. I., Avramut, C. M., de Andrea, C. E., Prins, F. A., Koster, A. J., Ravelli, R. B., & Hogendoorn, P. C. (2011). Cartilage ultrastructure in proteoglycan-deficient zebrafish mutants brings to light new candidate genes for human skeletal disorders. *J Pathol, 223*(4), 531-542. doi:10.1002/path.2824

Wong, H. R., Pitt, B. R., Su, G. L., Rossignol, D. P., Steve, A. R., Billiar, T. R., & Wang, S. C. (1995). Induction of lipopolysaccharide-binding protein gene expression in cultured rat pulmonary artery smooth muscle cells by interleukin 1 beta. *American journal of respiratory cell and molecular biology, 12*(4), 449-454.

Wright, J. R., & Youmans, D. C. (1993). Pulmonary surfactant protein A stimulates chemotaxis of alveolar macrophage. *American Journal of Physiology-Lung Cellular and Molecular Physiology, 264*(4), L338-L344. doi:10.1152/ajplung.1993.264.4.L338

Wu, F., Vij, N., Roberts, L., Lopez-Briones, S., Joyce, S., & Chakravarti, S. (2007). A novel role of the lumican core protein in bacterial lipopolysaccharide-induced innate immune response. *J Biol Chem, 282*(36), 26409-26417. doi:10.1074/jbc.M702402200

Wu, Y., Belenkaya, T. Y., & Lin, X. (2010). Dual Roles of Drosophila Glypican Dally-Like in Wingless/Wnt Signaling and Distribution. *480*, 33-50. doi:10.1016/s0076-6879(10)80002-3

Yamamura, H., Zhang, M., Markwald, R. R., & Mjaatvedt, C. H. (1997). A heart segmental defect in the anterior-posterior axis of a transgenic mutant mouse. *Dev Biol, 186*(1), 58-72. doi:10.1006/dbio.1997.8559

Yard, B. A., Chorianopoulos, E., Herr, D., & van der Woude, F. J. (2001). Regulation of endothelin‐1 and transforming growth factor‐β1 production in cultured proximal tubular cells by albumin and heparan sulphate glycosaminoglycans. *Nephrology Dialysis Transplantation, 16*(9), 1769-1775. doi:10.1093/ndt/16.9.1769

Yoon, J. H., & Halper, J. (2005). Tendon proteoglycans: biochemistry and function. *J Musculoskelet Neuronal Interact, 5*(1), 22-34.

Zaferani, A., Talsma, D. T., Yazdani, S., Celie, J. W., Aikio, M., Heljasvaara, R., . . . van den Born, J. (2014). Basement membrane zone collagens XV and XVIII/proteoglycans mediate leukocyte influx in renal ischemia/reperfusion. *PLoS One, 9*(9), e106732. doi:10.1371/journal.pone.0106732

Zhai, X. Y., Nielsen, R., Birn, H., Drumm, K., Mildenberger, S., Freudinger, R., . . . Gekle, M. (2000). Cubilin- and megalin-mediated uptake of albumin in cultured proximal tubule

cells of opossum kidney. *Kidney Int, 58*(4), 1523-1533. doi:10.1046/j.1523-1755.2000.00314.x

Zhang, X. W., Liu, Q., Wang, Y., & Thorlacius, H. (2001). CXC chemokines, MIP-2 and KC, induce P-selectin-dependent neutrophil rolling and extravascular migration in vivo. *Br J Pharmacol, 133*(3), 413-421. doi:10.1038/sj.bjp.0704087

Zielinska, D. F., Gnad, F., Wisniewski, J. R., & Mann, M. (2010). Precision mapping of an in vivo N-glycoproteome reveals rigid topological and sequence constraints. *Cell, 141*(5), 897-907. doi:10.1016/j.cell.2010.04.012

Zimmermann, D. R., & Ruoslahti, E. (1989). Multiple domains of the large fibroblast proteoglycan, versican. *Embo j, 8*(10), 2975-2981.

Zoja, C., Donadelli, R., Colleoni, S., Figliuzzi, M., Bonazzola, S., Morigi, M., & Remuzzi, G. (1998). Protein overload stimulates RANTES production by proximal tubular cells depending on NF-kappa B activation. *Kidney Int, 53*(6), 1608-1615. doi:10.1046/j.1523-1755.1998.00905.x

Table 1. 1 Clinical phenotype of known SOS phenotype patients

References	(Rudolph et al., 2003; Schmidt et al., 2001; Umair et al., 2017)					(Alanay et al., 2006; Umair et al., 2017)	(Munns et al, 2015)			(Taylan et al., 2016)			
Patients	II-6	II-7	II-5	II-4	II-3	Pat 1	Ind 1	Ind 2	Ind 3	I	II	III	IV
Mutation	p.Arg387Trp					p.Asp850His	p.Val232Glyfs*54		p.Ala174Profs*35	p.Arg730*	p.Arg563Gly	p.Arg563Gly	p.Leu605Pro
Parents	Con	Con	Con	Con	Con		Likely Con		non-con	Con	con	con	Con
Sex	M	M	F	M	M		M	Male	Male	F	F	M	M
Age	11	9	16	19	22	5	14	11	19	8	16	7	11
Height (Percentile)	90	10	3	75	10	<5	25-50	25-50	<5	Z-score -4.7	10-15	3	Z-score -1.9
Weight	>97	25	75	90	75	<5	NA	NA	NA	NA	NA	NA	NA
Ocular													
Amblyopia	NA	NA	NA	NA	NA	NA	+	+	NA	NA	NA	NA	NA
Anterior synechia of Iris	+	+	+	+	+	NA	NA	NA	NA	NA	NA	NA	NA
Atrophy of RPE	+	+	+	+	-	NA	NA	NA	NA	NA	NA	NA	NA
Band Keratophathy	-	-	+	-	-		NA	NA	NA	NA	NA	NA	NA
Cataract	+	+	+	+	+	+	+	NA	+	+	+	+	NA
Corneal clouding/Corneal opacity	NA	NA	+	NA	+	NA	-	NA	-	-	-	-	NA
Ectropian Uvea	NA	NA	NA	NA	NA	NA	NA	NA	NA	NA	+	NA	NA
Glaucoma	NA	NA	NA	NA	NA	NA	NA	NA	NA	+	NA	NA	NA
Melanosis of conjunctiva	-	-	+	-	-		NA	NA	NA	NA	NA	NA	NA
Microphthalmia	-	+	-	-	+	NA	NA	NA	NA	NA	NA	NA	NA
Nystagmus	NA	NA	NA	NA	NA	+	+	+	NA	+	NA	NA	-
Pigment	+	+	+	+	+	+	NA	NA	NA	NA	NA	NA	NA

abnormality													
Pthisis bulbi	-	-	-	-	+	NA	NA	NA	NA	NA	NA	NA	NA
Retinal Detachment	+	+	+	+	+	-	+	NA	+	-	-	-	NA
Thin retinal vessels			+	+		+	NA	NA	NA	NA	NA	NA	NA
Auditory													
Deafness	+	+	+	+	+	+	+	+	+	NA	+	+	+
Facial													
Facial Hypotonia	+	+	+	+	+	+	-	-	-	NA	NA	NA	NA
Craniofacial Dysmorphism	+	+	+	-	+								
Hyperthelorism	+	+	+	+	+	+	NA	NA	NA	NA	NA	NA	NA
Low Nasal Bridge	+	+	+	+	+		NA	NA	NA	NA	NA	NA	NA
Prognathism	+	+	+	+	+	NA	NA	NA	NA	NA	NA	NA	NA
Prominent nasal bridge	NA	NA	NA	NA	NA	+	NA	NA	NA	NA	NA	NA	NA
Large paranasal sinus	+	NA	NA	NA	NA	NA	NA	NA	NA	NA	NA	NA	NA
Mental													
Developmental Delay	-	-	-	-	-	+	+	+	-	+	NA	NA	NA
Intellectual disablity	-	-	-	-	-	+	+	+	-	+	NA	NA	NA
Musculoskeletal													
Atropic thenar muscle	+	-	-	-	-	NA	NA	NA	NA	NA	NA	NA	NA
BMD score	NA	NA	NA	NA	NA	NA	-2.5	NA	-5.8	-5.9	NA	-3	-4
Compression fractures	NA	NA	NA	NA	NA	NA	+	+	+	+	+	+	+
Disportionated short trunk	+	+	+	+	+	+	+	+	+	NA	NA	NA	NA

Hand/Finger abnormalities	+	-	-	-	_	NA	+	+	+	NA	NA	NA	NA
Joint hyperlaxity	-	-	-	-	-	+	-	-	-	NA	-	-	+
Kyphoscoliosis	+	+	+	+	+	+	-	-	-	+		+	+
Orthosis	NA	NA	NA	NA	NA	NA	NA	NA	NA	NA	NA	NA	+
Osteopenia	NA	NA	NA	NA	NA	NA	NA	NA	NA	NA	+	NA	NA
Osteoporosis	+	NA	NA	NA	NA	+	NA	NA	NA	NA	NA	NA	NA
Pectus Carinatum	NA	NA	NA	NA	NA	NA	NA	NA	NA	NA	NA	NA	+
pes planus	+	-	-	-	-	+	NA	NA	NA	NA	NA	NA	NA
Platyspondyly	+	+	+	+	+	+	+	+	NA	+	NA	NA	NA
Premature fractures	NA	NA	NA	NA	NA	NA	+	+	+	+	+	+	+
Reduced Lumbar Lordosis	+	+	+	+	+	NA	NA	NA	NA	NA	NA	NA	NA
Reduced Spinal mobility	+	+	+	+	+	NA	NA	NA	NA	NA	NA	NA	NA
Spontaneous fractures	NA	NA	NA	NA	NA	NA	+	+	+	NA	+	+	+
Integument													
Hyperextensibility	NA	NA	NA	NA	NA	+	NA	NA	NA	NA	NA	NA	NA
Heart													
Atrial septal defect/Patent foramen ovale	NA	NA	NA	NA	NA	NA	+	+	-	NA	-	-	NA
Dysplastic aortic valve	NA	NA	NA	NA	NA	NA	+	+	-	NA	-	-	NA
Mitral valve prolapse	NA	NA	NA	NA	NA	NA	+	+	-	NA	-	-	NA
VSD	+	-	-	-	-	+	-	-	-	NA	-	-	NA

Con: Consanguinous, non-con: non consaguinous, + Phenotype present, - Phenotype absent, NA phenotype not assessed

CHAPTER II

HOMOZYGOSITY FOR FRAMESHIFT MUTATIONS IN *XYLT2* RESULT IN A SPONDYLO-OCULAR SYNDROME WITH BONE FRAGILITY, CATARACTS, AND HEARING DEFECTS[1][2]

[1] Earlier version of this chapter has already been published as Munns, C. F., Fahiminiya, S., Poudel, N., Munteanu, M. C., Majewski, J., Sillence, D. O., . . . Hinsdale, M. E. (2015). Homozygosity for frameshift mutations in XYLT2 results in a spondylo-ocular syndrome with bone fragility, cataracts, and hearing defects. Am. J Hum Genet, 96(6), 971-978. doi:10.1016/j.ajhg.2015.04.017

[2] No permission required for use of published material in thesis/dissertation (see appendix I)

Abstract

Background Heparan and chondroitin/dermatan sulfated proteoglycans have a wide range of roles in cellular and tissue homeostasis including growth factor function, morphogen gradient formation, and co-receptor activity. Proteoglycan assembly initiates with a xylose monosaccharide covalently attached by either xylosyltransferase I or II.

Methods and Results Individuals 1 and 2 are brothers who presented with osteoporosis, cataracts, sensorineural hearing loss and mild learning defects. Whole exome sequence analyses showed that both individuals had a homozygous c.692dup mutation (NM_022167.3) in the xylosyltransferase II locus (*XYLT2*), causing reduced *XYLT2* mRNA and low circulating xylosyltransferase (XylT) activity. In an unrelated boy (individual 3) with a similar phenotype we noted low serum XylT activity. Sanger sequencing of *XYLT2* in this individual revealed a c.520del mutation in exon 2 that resulted in a frameshift and premature stop codon (p.Ala174Profs*35). Fibroblasts from individuals 1 and 2 showed a range of defects including reduced XylT activity, GAG incorporation of $^{35}SO_4$, and heparan sulfate proteoglycan assembly.

Conclusions We found that, in humans, XylT2 deficiency results in vertebral compression fractures, sensorineural hearing loss, eye defects and heart defects, a phenotype that is similar to the autosomal recessive disorder spondylo-ocular syndrome of unknown cause. This phenotype is different from what has been reported in individuals with linker enzyme deficiencies. These studies illustrate that the cells of the lens, retina, heart muscle, inner ear, and bone are dependent on XylT2 for proteoglycan assembly in humans.

2.1 Main

Proteoglycans (PGs) are a class of surface associated and extracellular matrix proteins that play a key role in many tissues (Esko, Kimata, & Lindahl, 2009; Sarrazin, Lamanna, & Esko, 2011). They are intimately involved in cellular homeostasis impacting many fundamental

biological processes ranging from growth factor function, morphogen gradient formation and co-receptor activity. The various PGs, except hyaluronic acid and keratan sulfate, share a common structure, consisting of a core protein on which glycosaminoglycan (GAG) disaccharide side chains are assembled. Two main groups of sulfated PGs, distinguished based on differences in GAG disaccharides, are heparan sulfate proteoglycan (HSPG) and chondroitin sulfate/dermatan proteoglycan (CS/DSPG)(Couchman & Pataki, 2012).

HSPGs and CS/DSPGs are very heterogeneous in regards to the types and number of GAG chains and the core protein modified; however, they share a common linker tetrasaccharide chain on which the GAG side chains are assembled on the core proteins. The first of these linker sugar residues is xylose, which is attached to a designated serine residue of the core protein by xylosyltransferases (XylTs). Two enzymes with XylT activity have been identified in humans, *XYLT1* and *XYLT2*(Gotting, Kuhn, Zahn, Brinkmann, & Kleesiek, 2000) and XylT activity is required for HSPG and CS/DSPG assembly(Hinsdale, 2013). Three additional sugar residues of the linker region are then added as galactose-galactose-glucuronic acid. Defects at each step of these sugar additions causes various autosomal recessive disorders (MIM604327, MIM606374)(Malfait et al., 2013; Schreml et al., 2014) illustrating the importance of PG in tissue homeostasis.

XylT1 and XylT2 are very similar in function, and are co-expressed in many tissues, but some temporal, spatial, and tissue-specific differences in expression exist(Eames et al., 2011; Hinsdale, 2013) and at the cellular level one or the other may be exclusively expressed(Cuellar, Chuong, Hubbell, & Hinsdale, 2007; Roch, Kuhn, Kleesiek, & Gotting, 2010). Predictably, reduced activity could differentially affect some tissues or developmental periods respective to the isoform affected. For example, in animal models and humans, impaired *XYLT1* function is associated with cartilage abnormalities due to defects in endochondral ossification and growth(Eames et al., 2011; Mis et al., 2014; Schreml et al., 2014) These observations suggest that

XYLT1 is critically important for growth cartilage and that its deficiency is not compensated for by *XYLT2* in this tissue.

The genetic syndromes characterized by osteoporosis, eye involvement with or without hearing impairment and intellectual disability include the osteoporosis pseudoglioma (OPPG (MIM 259770)) syndrome and spondylo-ocular syndrome (SOS (MIM 605822)). The majority of individuals with OPPG have mutations in low-density lipoprotein receptor-related protein 5. The first report of SOS described five affected members of a consanguineous family who had retinal detachment, cataract, facial dysmorphism, generalized osteoporosis, immobile spine and platyspondyly (Schmidt et al., 2001). Only one other family with SOS has been reported(Alanay, Superti-Furga, Karel, & Tuncbilek, 2006). The causative mutation for SOS is unknown.

This report describes 3 individuals from two unrelated families with a SOS-like phenotype including bone fragility, hearing impairment, heart septal defects and learning difficulties. Whole exome sequencing and Sanger sequence analyses revealed all individuals possess homozygous frameshift mutations in *XYLT2* that resulted in premature termination of transcription. Each of the mutated *XYLT2* loci results in decreased circulating XylT activity and fibroblasts from the individuals demonstrate reduced HS and CS assembly in PGs. These findings illustrate the unique role of XylT2 dependent PGs to tissue homeostasis. All affected family members or their legal guardians provided written informed consent and all studies were approved by the Sydney Children's Hospital Network Ethics Committee or Institutional Review Board of McGill University

The two index cases for this study are brothers from non-consanguineous healthy parents of European Australian descent (Figure 1A) evaluated at the Children's Hospital at Westmead in Westmead, Australia. Although non-consanguineous, there is a high likelihood of endogamy due to the geographical isolation of the parents region of origin. Individual 1 was born at 39 weeks

gestation by spontaneous vaginal delivery. Birth weight was 3990 grams (>90th centile), length 52 cm (90th centile) and occipito-frontal circumference 33.5 cm (10th centile). Examination at birth noted webbed neck and lymphedema of lower extremities. Investigations showed normal results for karyotype, comparative genomic hybridization micro-array, urine metabolic screen, TORCH screen and brain MRI.

At 18 months of age, individual 1 suffered a right femoral fracture and was found to have multiple vertebral compression fractures and generalized vertebral flattening (Figure 1D). Physical examination revealed a low posterior hairline, short webbed neck, posteriorly rotated and low-set ears, shield chest, undescended left testis (requiring orchidopexy), long fingers and toes and overriding second and third toes. Sclerae and teeth were normal. Dual-energy X-ray absorptiometry showed a low total body areal bone mineral density (BMD) Z-score of -1.8 and a low lumbar spine areal BMD, Z-score of -2.5. Treatment with intravenous pamidronate infusions was started at 20 months and resulted in reshaping of several vertebrae (Figure 1E). However, new vertebral compression fractures occurred despite therapy. At 14 years of age, he was fully ambulant, but he had an unsteady gait due to muscle weakness and poor vision (see below), and he had sustained five additional long-bone fractures.

In addition to musculoskeletal defects, this individual showed defects in cardiovascular and urinary systems. Echocardiography had detected an atrial septal defect that was surgically corrected at 8 years. It also revealed a mitral valve prolapse and dysplastic aortic valve. At 14 years of age, growth continued on the 25-50th centile for height and 20-50th for weight. He had a noticeable pectus carinatum with inferior depression and persistence of disproportionately long and slender fingers and toes, a low posterior hairline, short webbed neck, posteriorly rotated and low-set ears (Figure 1B). Ultrasound showed mild to moderately dilated bilateral distal ureters of uncertain etiology, but a normal appearance of kidneys, liver and biliary systems. However, he developed a perforated duodenal ulcer, which required surgical intervention.

Mild to moderate sensorineural hearing loss was diagnosed at 9 years of age and he was fitted with hearing aids. Ophthalmological examination showed amblyopia and nystagmus, and at 11 years of age he developed a spontaneous left retinal detachment that resulted in loss of vision in the affected eye. At 13 years, posterior sub-capsular cataracts were noted. Learning difficulties were confirmed at 6 years of age but difficult to assess formally because of visual and hearing disabilities. Subsequent assessments confirmed that he was functioning in the mild learning difficulty group.

Individual 2 had a clinical course very similar to that of individual 1, his brother. He had generalized vertebral flattening and compression fractures were detected at 3 and 12 months of age (Figure 1F). Thin cortices were discovered in metacarpal and phalanges and calvarial bones at 6 and 18 months of age (Figure 1C and K). Treatment with intravenous pamidronate was started at the age of 12 months. By 7 years of age, reshaping of some vertebral bodies was noted but new compression fractures were apparent (Figure 1G). Bilateral deformities (Figure 1H and I) and femoral fractures were apparent at the last follow up at 11 years of age (Figure 1J). At this age, he was ambulating independently. Growth continued along the 25-50th centile for height and 25th-75th centile for weight. Cardiac findings, sensorineural hearing loss, and urinary tract findings were identical to that of his brother. He underwent cardiac surgery and was fitted with hearing aids. Mild learning difficulties were noted at 6 years of age.

Both parents of individuals 1 and 2 were clinically normal. Neither the father nor mother had any unexplained fractures or musculoskeletal abnormalities at 40 and 39 years of age, respectively. Clinical examination of both parents, including anthropometry, was normal. Bone mineral densitometry by dual-energy X-ray absorptiometry and peripheral quantitative computed tomography were normal for the mother and elevated for the father (total body areal BMD Z-score 3.9).

To identify the disease-causing gene in this family, we performed whole exome sequencing on the genomic DNA of the affected individuals (see details in Supplemental Methods). After removing common variants, 327 and 301 variants were identified in individuals 1 and 2, respectively. The analysis of sequencing data did not reveal any rare variants within the 10 genes (*PTPN11*, *BRAF*, *HRAS*, *KRAS*, *MAPK1*, *MAPK2*, *SHOC2*, *RAF1*, *SOS1* and *RIT1*) already associated with Noonan syndrome or the known osteogenesis imperfecta genes (*CRTAP*, *LEPRE1*, *PPIB*, *SERPINH1*, *FKBP10*, *SP7*, *SERPINF1*, *BMP1*, *TMEM38B*, *IFITM5*, *WNT1*). The presence of the disease in two brothers with apparently healthy parents suggested an autosomal or X-linked recessive inheritance. Thus, we prioritized candidate genes with homozygous mutations shared by the two affected siblings this led to the identification of one frameshift insertion in *XYLT2* and one missense variant in each of 4 different genes (*FTSJ3*, *SLC38A10*, *CCDC57* and *SH3KBP1*) (Table S3).

Considering the function of these four latter genes, we concluded that they were unlikely to be responsible for the disease: The complete deletion of *SH3KBP1* (encoding CIN85) has been previously reported in a male individual with autism who did not show any dysmorphic features (Pinto et al., 2014). Furthermore, mice deficient of CIN85 expression were viable, fertile, and displayed no obvious structural abnormalities (Shimokawa et al., 2010). The *SLC38A10* variant (MAF: 0.001 in EVS) was not evolutionally conserved and predicted inconsequential to protein function by three different bioinformatics algorithms (Kumar, Henikoff, & Ng, 2009). A recent phenotypic screening of *Ccdc57* knockout mice revealed two significant abnormalities (hydrocephaly and abnormal hypodermis fat layer), which were not observed in our individuals. Finally, *FTSJ3* function is not fully characterized, but it may play a role in 18S rRNA synthesis (Morello et al., 2011) and no disease-related phenotype has been yet reported for this gene.

In contrast, several lines of evidence suggested *XYLT2* as the gene potentially responsible for the observed phenotypes. The homozygous frameshift insertion in *XYLT2* is the most

deleterious of the identified variants and most likely results in nonsense-mediated degradation of the mutant transcript and a consequent loss of XylT2. Notably, the closely related enzyme XYLT1 has previously been shown to be required for HSPG and CS/DSPG assembly, and a missense homozygous mutation in *XYLT1* resulted in an autosomal recessive short stature syndrome associated with intellectual disability [7].

Both individuals 1 and 2 harbor a homozygous frameshift insertion of C in exon 3 of *XYLT2* (NM_022167.3: c.692dup) that results in the loss of the last 634 amino acids of XYLT2 and insertion of 53 novel amino acids (p.Val232Glyfs*54) before a premature stop codon. The variant was located within about 23 Mb shared region of homozygosity (Supplemental Figure 1) and was not seen in our exome database (~1000 individuals), in the 1000Genomes database, dbSNP132, the EVS and the ExAC (~63,000 exomes of unrelated individuals) databases. The inserted sequence was confirmed by Sanger sequencing of genomic DNA from both boys (Figure 1A and Supplemental Figure 1). This mutation was further confirmed by sequence analyses of fibroblast XYLT2 mRNA (see below, Supplemental Figure 2). Analyses showed the parents were heterozygous for this mutation. All loci from the index individuals and parents were confirmed to be in the *XYLT2* gene by Sanger sequencing of *XYLT2* exon 3.

Affected individual serum and plasma XylT activity levels were determined to investigate the biochemical impact of the *XYLT2* mutation. Since platelets are a substantial source of XylT2 activity in serum, comparison of XylT activity in serum to plasma reflects an important cell-specific source of XylT2(Condac et al., 2009). As compared to adult control serum and plasma, individuals 1 and 2 had an approximately 75% and 57% drop in serum and plasma XylT activity, respectively (Figure 2A). Since age and pamidronate treatment may alter XylT levels, serum from age-match pamidronate-treated individuals with osteogenesis imperfecta were used as controls (Figure 2B). These findings show that the study individuals have substantial reductions in circulating XylT activity.

Dermal fibroblasts were isolated to further evaluate the genetic and resultant enzyme defect in individuals 1 and 2. Total XylT activity in cell lysates from these cultures cells showed the fibroblasts had an approximate 60% decrease for individual 1 and 45% decrease for individual 2 as compared to normal dermal fibroblasts (Figure 2C). Based on our previous findings that fibroblasts express both *XYLT1* and *XYLT2*(Cuellar et al., 2007), we suspected that the residual XylT activity is due to *XYLT1* expression. PG assembly was investigated in by immunohistochemistry and $^{35}SO_4$ incorporation assays. We examined HSPG assembly levels using GAG-specific antibody 10E4 performed as previously described(Condac et al., 2007). These results showed a qualitative decrease in HS GAG staining in the affected individuals' fibroblasts (Figure 2D). $^{35}SO_4$ incorporation by affected individuals' fibroblasts performed as described(Zhang, David, & Esko, 1995) with 25 uCi/ml for 24 hrs, showed a quantitative decrease of 60-65% in total $^{35}SO_4$ incorporation by the cells (Figure 2E). Chondroitinase ABC and heparitinase III digestion of the labeled PGs from these cells shows that both HS and CS are affected by the loss of XylT2 (Figure 2F) where in individual 1 there is 67% in loss of $^{35}SO_4$ with digestion. In all, these results confirm a significant defect in PG assembly due to the *XYLT2* mutation.

We suspected that the low *XYLT2* mRNA levels were due to premature translation termination leading to mRNA decay. To investigate, we cloned and sequenced *XYLT2* cDNA in triplicate from individual 2 fibroblasts. The sequence confirmed the cytosine insertion (c.692_693insC) in exon 3, the frame shift mutation, the addition of 53 non-conserved amino acids, and that the premature termination would severely truncate and disrupt a highly conserved portion of the protein resulting in a mature mutant protein lacking any of the predicted catalytic domain (see supplemental Figure 2). In support of premature termination and mRNA decay, expression analyses by quantitative real time RT-PCR showed the affected individuals' had a 75% decrease in *XYLT2* mRNA. Significantly, there was no change in any of the other

proteoglycan linker enzyme mRNA levels (Figure 2G) (see supplemental Table 2) including *XYLT1* confirming our earlier suspicion that the affected individuals' fibroblasts have residual XylT activity due to *XYLT1*. In all, these results demonstrate that the clinical observations in the affected individuals are due to a selective loss of XylT2 arising from a premature translational termination and likely mRNA decay.

After a mutation of *XYLT2* had been identified in individuals 1 and 2, an unrelated boy (individual 3) undergoing treatment with pamidronate and with phenotypic similarities to individuals 1 and 2 came to our attention. Individual 3 was born prematurely after 35 weeks of pregnancy. The parents are first cousins. Both parents and the two older siblings are healthy. Individual 3 sustained the first fracture, affecting the right femur, at the age of 18 months, and two more right femur fractures in the subsequent two years. When first examined at our institution at 3.9 years of age, he was very short (90 cm, corresponding to 5 cm below the 5^{th} percentile) and weight was low (12.2 kg, corresponding to 1.5 kg below the 5^{th} percentile). Limbs were straight with normal range of motion in the hip, but there was mild left hemiplegia with spasticity in the left lower extremity. Radiographs revealed multiple vertebral compression fractures (Figure 3). There was no dentinogenesis imperfecta and sclerae were white. Areal bone mineral density Z-score at the lumbar spine was -5.8. Treatment with intravenous pamidronate was started, which was associated with an increase in lumbar spine areal bone mineral density Z-score to -3.6 within 12 months. Bisphosphonate treatment was continued with varying protocols until 18 years of age, when lumbar spine areal bone mineral density Z-score was -1.4. Despite this treatment, he sustained a total of 10 lower extremity fractures and he was never able to walk independently. At the time of the last follow-up (at 19 years of age), he was using a wheelchair for all mobility; height was 145 cm and weight 48 kg.

Apart from musculoskeletal issues, a hearing deficit was noted at 10 years of age in individual 3 and hearing aids were fitted. Bilateral cataract was diagnosed at 12 years of age and

treated with removal of the lenses. At 15 years of age, retinal detachment occurred in the right eye. No heart or lung abnormalities had been noted. He attended regular school, with normal academic performance.

Given the noted phenotypic similarities to individuals 1 and 2, we measured serum XylT activity in individual 3. As XylT activity was similar to that of 1 and 2 (Figure 2B), we performed Sanger sequencing of *XYLT2* in individual 3. This revealed that individual 3 was homozygous for a c.520del mutation in exon 2 that resulted in a frameshift and premature stop codon Ala174Profs*35 (Figure 3A).

The skeletal phenotype of these boys resembles those of a sibship described as SOS (Table S1) (Schmidt et al., 2001). The only other recognized disorder to be associated with vertebral compression fractures and eye disease is Osteoporosis-pseudoglioma syndrome (OPPG) (MIM 259770) due to mutations in *LRP5*. However, OPPG involves ocular defects due to hyperplasia of the vitreous, corneal opacity, and secondary glaucoma(Teebi, Al-Awadi, Marafie, Bushnaq, & Satyanath, 1988) and growth plate abnormalities causing dwarfism in some individuals(De Paepe, Leroy, Nuytinck, Meire, & Capoen, 1993; Somer, Palotie, Somer, Hoikka, & Peltonen, 1988). Our cases also showed variable stature, with the first two cases having normal stature and the third, significant short stature suggesting variable impact on growth cartilage. However, the chest wall deformity seen in cases 1 and 2 may reflect dysplastic growth of costal cartilages. It should be noted that short bones are found in both zebra fish and mice harbouring hypomorphic *Xylt1* alleles(Eames et al., 2011), and in these mice, no *Xylt2* expression was detected in articular cartilage tissue suggesting that articular cartilage GAG assembly is highly XylT1 dependent. These findings suggest that XylT1 and XylT2 can impact cartilage but the effect maybe variable depending on the location of the cartilage and the type of cartilage. This indicates that we would not expect XylT2 deficiency to affect articular cartilage, but growth plate cartilage might require both XylT1 and XylT2 activity. Therefore, defects in *XYLT1* or those in

the remaining enzymatic steps of linker assembly would be expected to affect growth cartilage, and this is supported by observations made in individuals with hypomorphic mutations in *XYLT1* and mutations in *B4GALT7* (beta1,4-galacosyltransferase 7), *B3GALT6* (beta1,3-galactosyltransferase 6), and *B3GAT3* (beta1,3-glucuronyltransferase 3)(glucuronyltransferase I) who have significant short stature(Baasanjav et al., 2011; Malfait et al., 2013; Nakajima et al., 2013) (MIM606374) (MIM604327). Given the variable growth seen in our three cases, further assessment of XYLT1 and XYLT2 expression in the growth plate is required.

In summary, we have shown that a frameshift mutation of *XYLT2* truncates XylT2 eliminating the catalytic domain and results in severe XylT deficiency as demonstrated in reduced serum and plasma XylT activity and giving rise to defects in musculoskeletal, myocardial, ocular, inner ear, and central nervous system tissues where *XYLT1* expression fails to compensate. This indicates that XylT2 is critical for PG assembly in these tissues.

2.2 Web Resources

CNV database, http://dgvbeta.tcag.ca/gb2/gbrowse/dgv2_hg19/

Human Gene Mutation Database; http://www.hgmd.org/

Online Mendelian Inheritance in Man (OMIM), http://www.omim.org

UCSC database, version hg19, http://www.genome.ucsc.edu/

The 1000 genomes database: http://www.1000genomes.org

Exome Aggregation Consortium (ExAC), Cambridge, MA (URL: http://exac.broadinstitute.org) [date (October, 2014) accessed].

Exome Variant Server, NHLBI GO Exome Sequencing Project (ESP): http://evs.gs.washington.edu/EVS/, v.0.0.14, June 20, 2012

2.3 Supplemental Methods

2.3.1 Whole Exome Capture

Whole exome sequencing was performed on 3 µg of genomic DNA of each individual at Genome Quebec Innovation Center, Montreal, Canada. Briefly, exonic sequences were captured

using the SureSelect Human Exome Kit V.4 (Agilent Technologies, Inc., Santa Clara, CA). Enriched libraries were then sequenced on Illumina Hiseq 2000 sequencer, generating 100 base pair paired-end reads for each sample. The bioinformatic analysis of exome sequencing data was carried out as previously described (Fahiminiya et al., 2014; Fahiminiya et al., 2013). In brief, mapping reads against the human reference genome (hg19), local realignment around small insertions or deletions (indels), depth of coverage calculation and the reads duplication removal were performed using the BWA (v. 0.5.9) (Li & Durbin, 2009), Genome Analysis Toolkit (McKenna et al., 2010) and Picard tools (http://picard.sourceforge.net), respectively. The mean read depth for the consensus-coding sequence was 99X (II-1) and 122X (II-2), and 95% of bases were covered by ≥10 reads. The genetic variations (SNVs and indels) were detected using Samtools (v. 0.1.17) (Li et al., 2009) and mpileup and were annotated with an in-house annotation pipeline that uses ANNOVAR and custom scripts. The potential damaging effect of variants was predicted using SIFT [18], PolyPhen-2 [19], MutationTaster [20]. To differentiate novel variants from common polymorphisms and sequencing artifacts, exonic (frameshift indels, nonsense, missense) and canonical splice site variants with minor allele frequency of more than 1% in public databases (1000Genomes or in the Exome Variant Server (EVS)) or seen in >10 individuals in our in-house exome database were filtered out. Candidate genes having shared homozygous mutations between the two patients were selected and were manually examined using the Integrative Genomics Viewer (IGV) (Robinson et al., 2011).

All loci from index patients and parents were confirmed to be in the *XYLT2* gene by Sanger sequencing of *XYLT2* exon 3 amplification by polymerase chain reaction followed by direct sequencing using an Applied Biosystems 3730xl sequencer (Applied Biosystems, Foster City, CA, USA). Sequence traces were aligned with GenBank reference sequence NM_022167.2.

2.3.2 Cell Culture

Dermal fibroblasts from the patients and parents were grown in Fibroblast Growth Kit-Low Serum (ATCC-PCS-221-041) supplemented with 1% Penicillin/Streptomycin at 37^0 C and 5% CO_2 in humidified environment. Commercial primary dermal fibroblasts from ATCC (PCS-201-012) adult were used as the control and grown in same culture condition. Confluent cells were trypsinized using 0.05% Trypsin for 5 minutes at 37^0 C and passaged 1:10. No cells were grown more than passage 10.

2.3.3 RNA isolation, cDNA synthesis and real-time PCR (RT-PCR)

RNA was isolated from near to confluent cells from vented T75 flasks using TRIzol reagent (Cat # 15596-018, Life Technologies), treated with DNase I (Cat # M0303S, NEB) and then cleaned up using TRIzol reagent. Five μg of RNA was used to generate cDNA using superscript III cDNA synthesis kit (Cat # 18080-051, Invitrogen) or MMLV reverse transcriptase using random hexamers primers. Quantitative real time PCR was performed on 1:5 diluted cDNA using gene specific primers as listed in table I. GAPDH expression was used for normalization on each plate. Each sample was analyzed in triplicates and comparative gene expression was determined using $2^{-\Delta\Delta}$ Ct method (Livak & Schmittgen, 2001). Three independent experiments were conducted for each target and the mean and standard deviation were calculated. Many primers sets available from Origene.

2.3.4 Determination of xylosyltransferase activity

The protocol to determine Xylosyltransferase activity has been described elsewhere(Condac et al., 2009). Normal control serum and plasma were from four normal adult males. For age-sex matched controls, these were patients with osteogenesis imperfecta and being treated with pamidronate. Patient and control plasma was isolated from potassium EDTA treated blood. In brief, serum (10 μl) and cell lysates (50μl) were incubated in a total reaction volume of 100 μl containing 25mM 2-(4-morpholino)-ethane sulfonic acid, pH 6.5, 25 μl KCl, 5mMs of KF,

MnCl2 and Mgcl2 with 1.13 μm UDP-[14C]-D-Xylose 150-250 mCi/mol (Perkin Elmer, Waltham, WA), 7.46 μm UDP-D-Xylose (Carbosource, University of Georgia, Atlanta, GA) and 160 μm of bikunin acceptor peptide (Biosynthesis, Lewisville, TX) for one hour at 37^0C. Keeping the tubes on ice for 5 minutes stopped the reaction. 1.5 mg BSA was added to the reaction as a carrier and the reaction was precipitated using 500 μl of 10% trichloroacetic acid 4% phosphotungstic acid by incubation on ice for one hour. The tubes were centrifuged and the pellets were washed with 750 μl of 5% trichloroacetic acid, incubating for 15 minutes on ice and centrifuging at 12,000 X g. The final pellet was dissolved in 400 μl of 1 N NaOH. Radioactivity in the resuspension was measured using scintillation counter. One unit of enzyme activity represents incorporation of 1 μmol xylose/min into the acceptor peptide. For serum, the enzyme activity was calculated as mU/L and for cell lysates; the enzyme activity was calculated as mU/mg of protein in the lysate. All the samples were run in triplicates and the mean and the standard deviation were calculated.

2.4 Figures and Legends

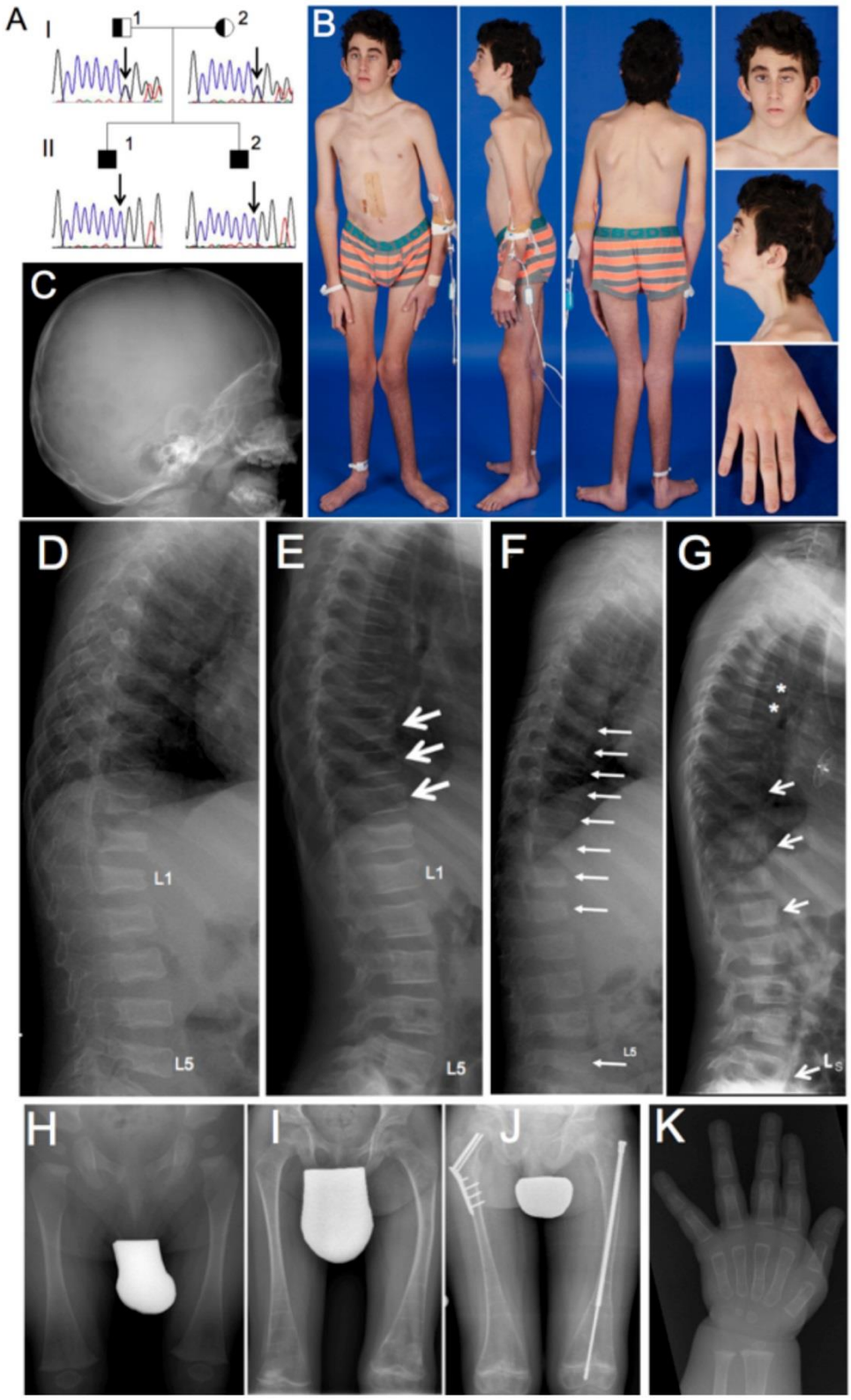

Figure 2. 1 Clinical and Radiological Findings in Individuals 1 and 2

(A) Pedigree and results of Sanger sequencing in individual 1 (II-1) and individual 2 (II-2). (B) Clinical aspect of individual 1 at 14 years of age. (C) Calvarial bone is thin (18 months). The dens axis appears normal. (D) Lateral spine radiograph of individual 1 at the age of 18 months. All thoracic and lumbar vertebrae are deformed or fractured. (E) At 7 years of age (after 3 years of pamidronate treatment), some vertebral bodies have undergone marked reshaping, indicated by arrows. (F) Lateral spine radiograph of individual 2 at the age of 12 months. Several vertebrae are deformed or fractured, indicated by arrows. (G) After 6 years of pamidronate treatment (age 7 years), some vertebral bodies have reshaped (arrows), but new compression fractures have developed in other vertebra (asterisks). (H) to (J) Femur radiographs of individual 2 at 6 months, 8 years and 11 years of age, respectively. Despite pamidronate treatment, femoral deformities and at least 3 fractures developed, necessitating hardware insertion. (K) Hand radiographs in individual 2 at 6 months of age, showing thin cortices. (The clinical evaluations of patients 1 and 2 were performed by Craig F. Munns and Andrew Biggin at Institute of Endocrinology and Diabetes, The Children's hospital at Westmead, NSW Australia, and bioinformatics study was performed by Somaya Fahiminiya, and Jacek Majewski at Department of Human Genetics, McGill University)

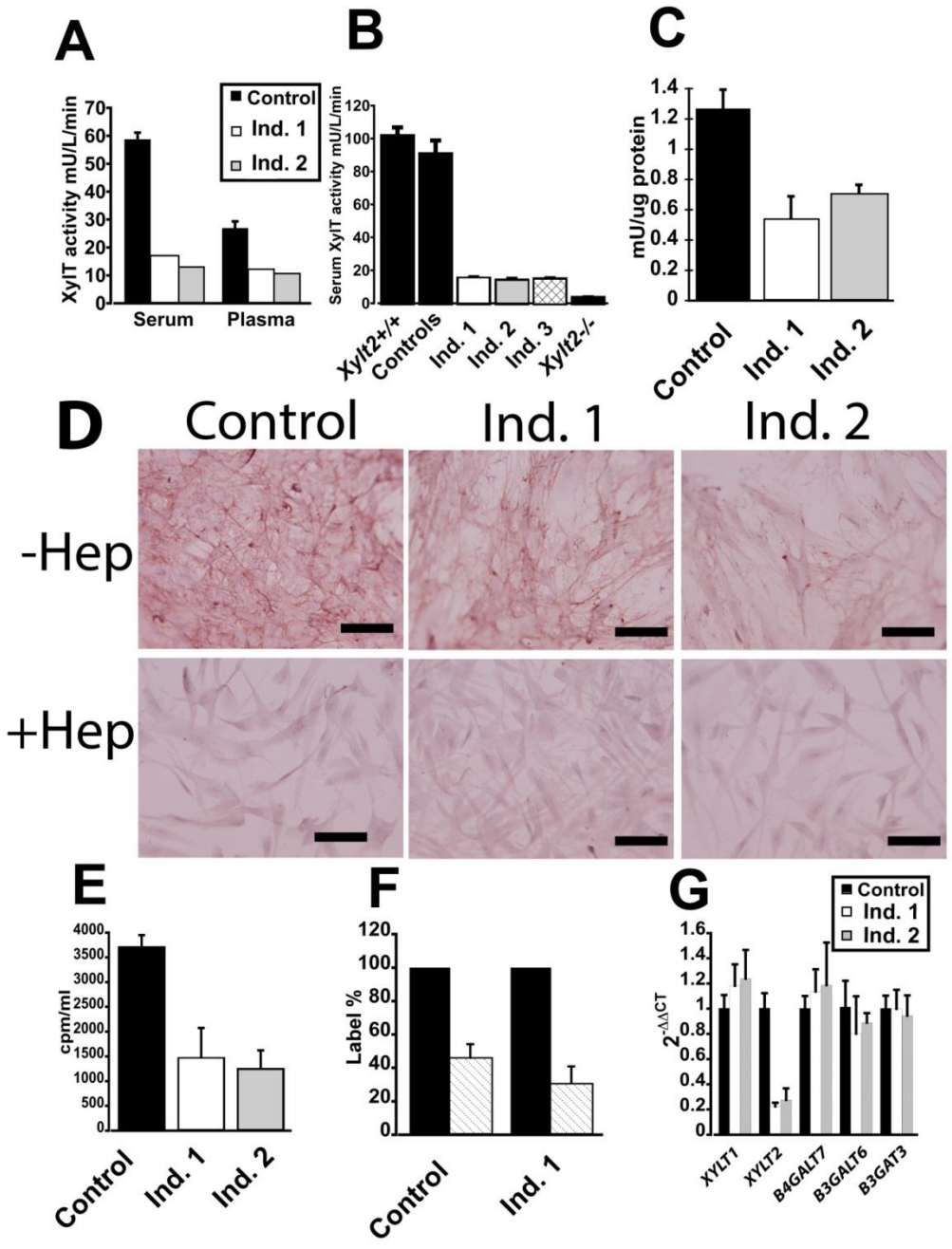
A
XylT activity mU/L/min
70
60
50
40
30
20
10
0
Serum
Plasma
Control
Ind. 1
Ind. 2
B
Serum XylT activity mU/L/min
120
100
80
60
40
20
0
Xylt2+/+ Controls
Ind. 1
Ind. 2
Ind. 3
Xylt2-/-
C
mU/ug protein
1.4
1.2
1
0.8
0.6
0.4
0.2
0
Control
Ind. 1
Ind. 2
D
Control
Ind. 1
Ind. 2
-Hep
+Hep
E
cpm/ml
4000
3500
3000
2500
2000
1500
1000
500
0
Control
Ind. 1
Ind. 2
F
Label %
120
100
80
60
40
20
0
Control
Ind. 1
G
Control
Ind. 1
Ind. 2
2-ΔΔCT
1.6
1.4
1.2
1
0.8
0.6
0.4
0.2
0
XYLT1
XYLT2
B4GALT7
B3GALT6
B3GAT3

Figure 2. 2 Reduced XylT activity in Affected Individuals

(A) Individual 1 (Ind. 1) and individual 2 (Ind. 2) serum and plasma XylT activity as compared to adult male controls (n=4). (B) Serum XylT activity in individuals 1, 2 and 3 as compared to age-matched controls (n=4). XylT levels in wild type (*Xylt2*+/+) and in our XylT2 deficient (*Xylt2*-/-) mice (Condac et al., 2007) are also illustrated (n = 3 each) for comparison, error bars represent standard deviation. Total XylT activity was assayed using published protocols(Condac et al., 2009) and for the study individuals' values, these represent the mean of triplicate measurements. (C) XylT activity in dermal fibroblast lysate. Values are means of triplicate measurements and error bars are the standard deviation. (D) Immunohistochemistry for HS shows affected individuals' fibroblasts have reduced levels of HS illustrated by reduced red staining that is subsequently removed with heparitinase III digestion. Scale bars are 100 μm. –Hep is undigested cells, +Hep is heparitinase III digested cells. (E) Sulfate incorporation assays by study individual fibroblasts shows a reduction in ^{35}S incorporation where individual 1 is 60% and individual 2 is 66% reduced as compared to control fibroblasts. (F) Shows digestion of eluted ^{35}S labeled GAGs from control fibroblasts of 54% and individual 1 of 67% with chondroitinase ABC and heparitinase III in hashed bars. Undigested labeled GAGs are set at 100% in black bars. (G) Real-time quantitative reverse transcription PCR of fibroblast mRNA for proteoglycan linker enzymes done in triplicate. Individual 1 fibroblasts had a 77% decrease and individual 2 fibroblasts had a 72% decrease in *XYLT2* mRNA. Values are means of triplicate measurements, normalized to GAPDH, and error bars are the standard deviation. Control mRNA is from normal dermal fibroblasts.

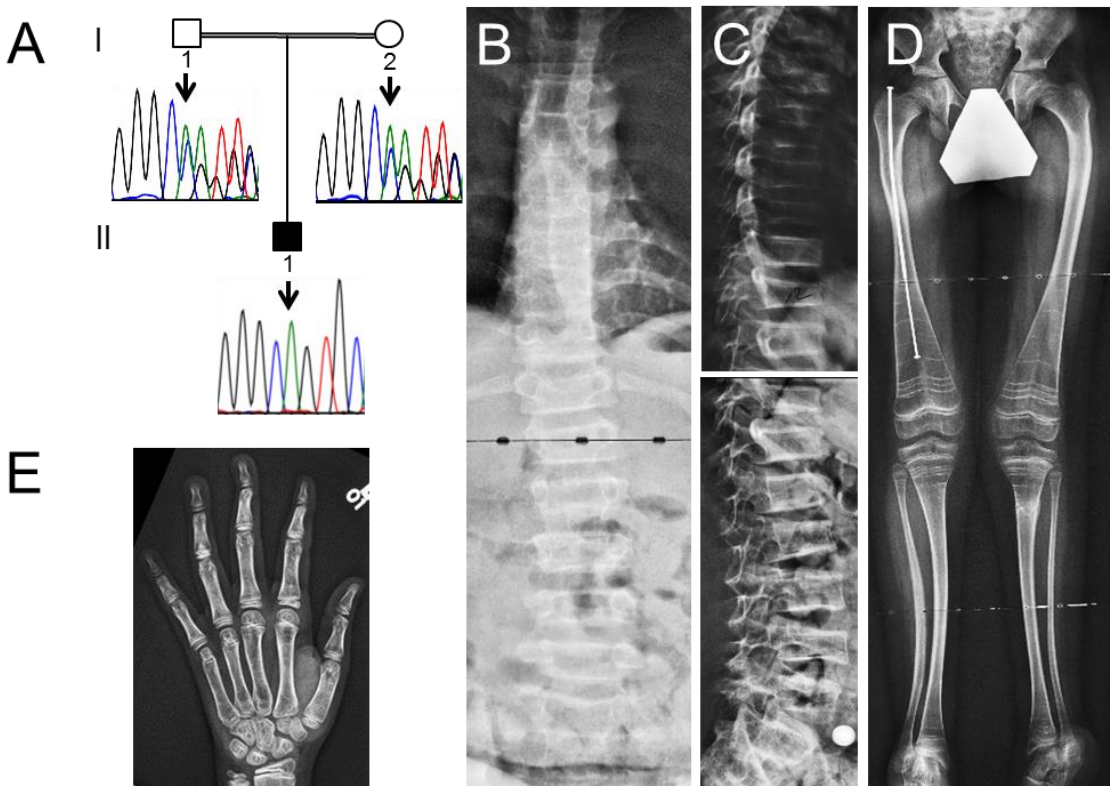

Figure 2. 3 Clinical and Radiological Findings in Individual 3.

(A) Results of Sanger sequencing. Individual 3 (II-1 in the pedigree) is homozygous for a c.520del mutation in *XYLT2*, the parents are heterozygous for this deletion. (B) Antero-posterior radiograph of the spine. Most vertebrae appear decreased in height. (C) Lateral spine radiograph showing severe vertebral compression fractures. (D) Mild deformities of the lower deformities. The right femur has been rodded following fracture. The metaphyseal lines that are prominent in distal femurs and proximal tibias are due to treatment with intravenous pamidronate infusions. (E) Radiograph of the left hand and wrist, showing somewhat thin cortices. The clinical evaluations of patients 1 and 2 were performed by Craig F. Munns and Andrew Biggin at Institute of Endocrinology and Diabetes, The Children's hospital at Westmead, NSW Australia, and bioinformatics study was performed by Somaya Fahiminiya, and Jacek Majewski at Department of Human Genetics, McGill University)

Table 2. 1Comparison between patients Ind.1, Ind. 2, Ind. 3 and Spondylo-Ocular syndrome (Schmidt et al., 2001)

	Ind. 1	Ind. 2	Ind. 3	SOS
Normal height	+	+	+	+
Vertebral compression fractures	+	+	+	+
Long-bone fractures	+	+	+	-
Flat feet	+	+	+	+
Cataract	+	+	+	+
Retinal detachment	+	-	+	+
Heart defect	+	+	n.r.	+/-
Hearing loss	+	+	+	-
Ureter dilatation	+	+	n.r.	n.r.

n.r., not reported. Ind.1, individual 1; Ind. 2, individual 2; Ind. 3, individual 3

Table 2. 2 RT-PCR primers and accession numbers for gene targets

Gene	Forward Primer	Reverse primer	NCBI Accession number
XYLT1	accgagatatgaatttcttgaagtca	aggccctgcttccgaatg	NM_022166
XYLT2	gggtgagacccgcttcct	gcatcatctttcctgagaggtagtt	NM_022167
GALT7	tgacaagaccgccacacc	gtcctgagcctgagcaatatg	NM_007255
GALT6	cctaggtcaggccgttgagtt	gcggtcagtcctggattca	NM_080605
GAT3A	gccaactgcactcgggtact	cctgcttcatcttgggcttct	NM_012200

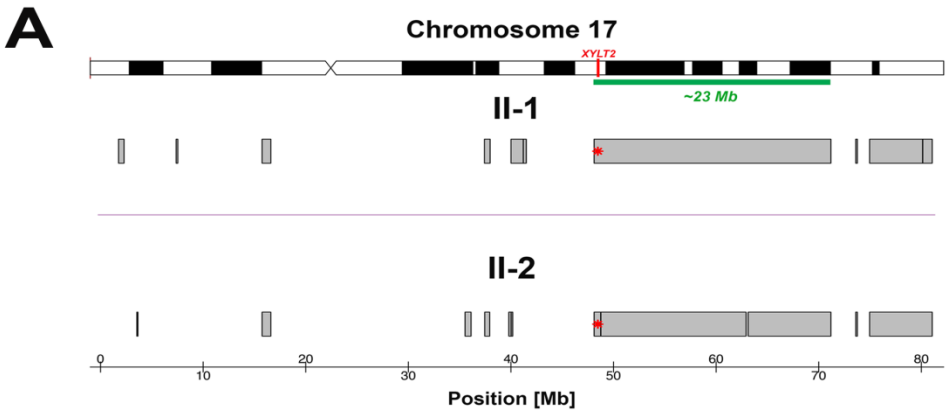
A
Chromosome 17
XYLT2
~23 Mb
II-1
II-2
0
10
20
30
40
50
60
70
80
Position [Mb]

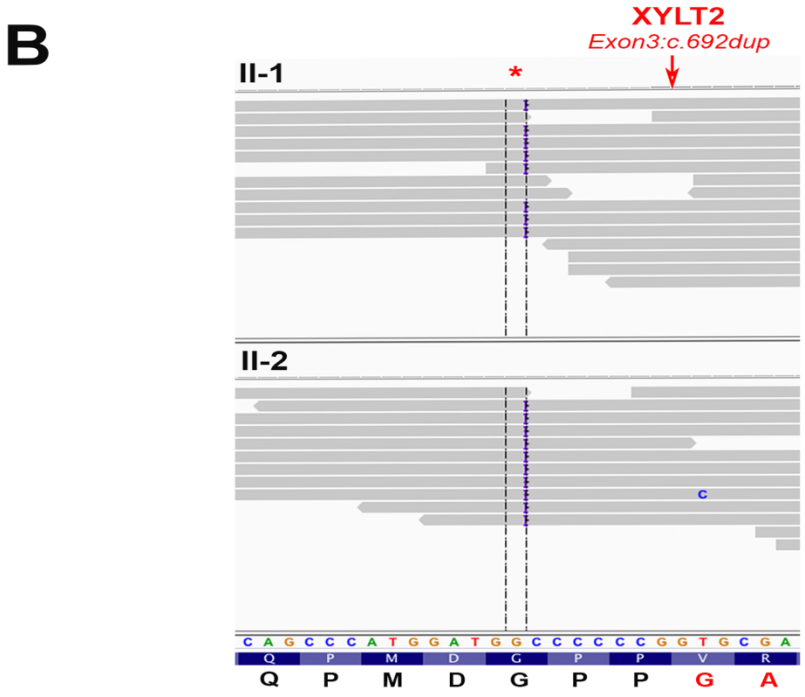
B
XYLT2
Exon3:c.692dup
II-1
II-2
C A G C C C A T G G A T G G C C C C C C C G G T G C G A
Q P M D G P P V R
Q P M D G P P G A

Figure 2. 4 Mutation Analysis of Individual 1 and 2.

(A) The gray bars show the location of the region of homozygosity on chromosome 17 for individuals 1 (II-1) and 2 (II-2). The ~23Mb shared region of homozygosity surrounding *XYLT2* is indicated with the green bar. *XYLT2* is located on chromosome 17 and in both individuals harbour a homozygous mutation at genomic position 4,843,186 (highlighted by a red asterisk). B) The IGV snapshot shows the position of the homozygous single-nucleotide duplication in *XYLT2* (NM_022167: c.692dup) (red arrow) that is shared by the two patients. The gray bars are 100 bp paired-end reads that mapped to the human reference genome (hg19) using BWA aligner. The insertion introduces a stop codon 54 residues downstream (p.Val232Glyfs*54) as shown in figure 2.5 below. In the lower part of figure, the reference DNA sequence, the reference protein sequence (two shades of blue) and protein predicted from variant coding sequence are illustrated where the variant sequence is in red.

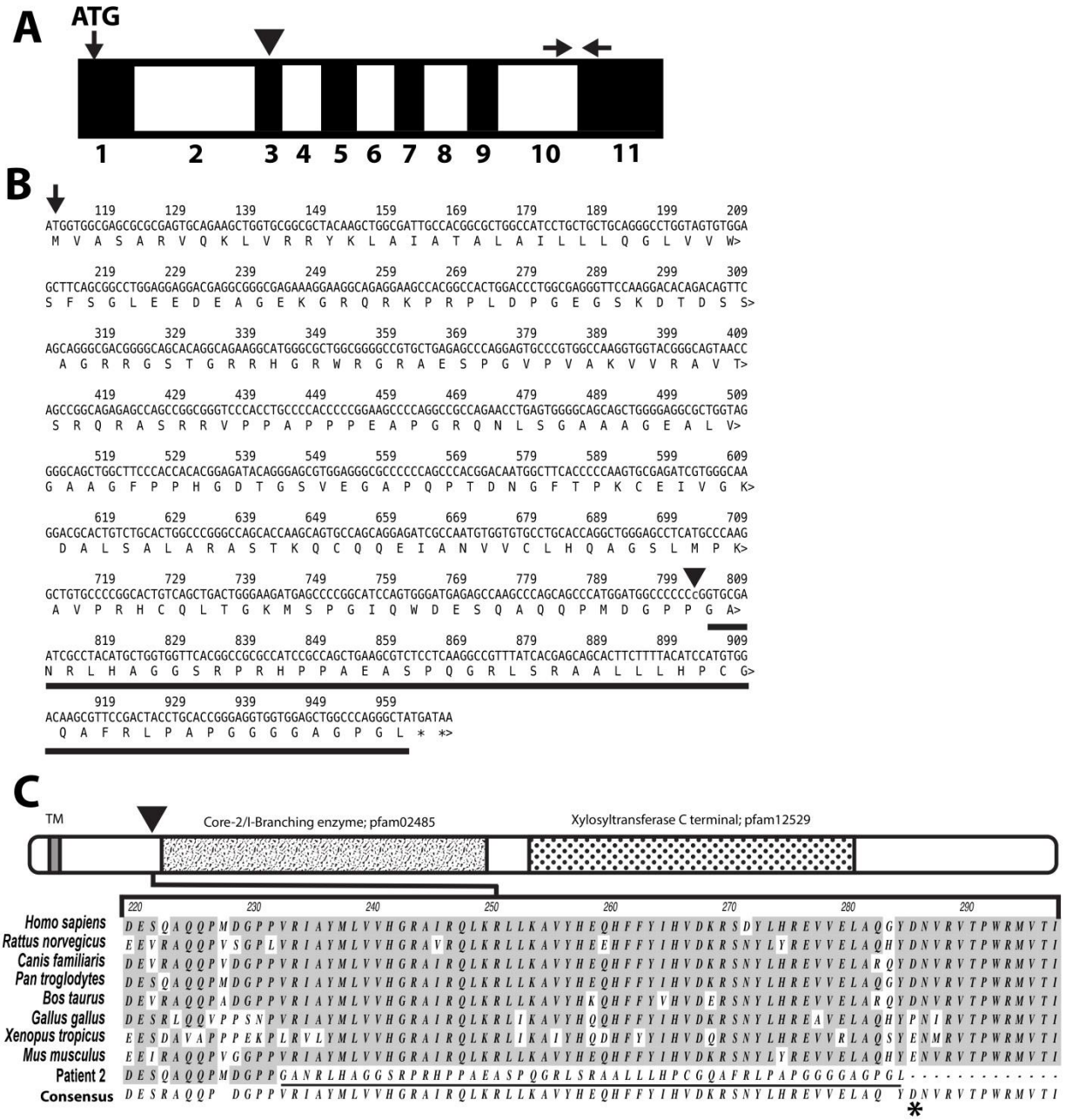
A
ATG
1 2 3 4 5 6 7 8 9 10 11
B
119 129 139 149 159 169 179 189 199 209
ATGGTGGCGAGCGCGCGAGTGCAGAAGCTGGTGCGGCGCTACAAGCTGGCGATTGCCACGGCGCTGGCCATCCTGCTGCTGCAGGGCCTGGTAGTGTGGA
M V A S A R V Q K L V R R Y K L A I A T A L A I L L L Q G L V V W>
219 229 239 249 259 269 279 289 299 309
GCTTCAGCGGCCTGGAGGAGGACGAGGCGGGCGAGAAAGGAAGGCAGAGGAAGCCACGGCCACTGGACCCTGGCGAGGGTTCCAAGGACACAGACAGTTC
S F S G L E E D E A G E K G R Q R K P R P L D P G E G S K D T D S S>
319 329 339 349 359 369 379 389 399 409
AGCAGGGCGACGGGGCAGCACAGGCAGAAGGCATGGGCGCTGGCGGGGCCGTGCTGAGAGCCCAGGAGTGCCCGTGGCCAAGGTGGTACGGGCAGTAACC
A G R R G S T G R R H G R W R G R A E S P G V P V A K V V R A V T>
419 429 439 449 459 469 479 489 499 509
AGCCGGCAGAGAGCCAGCCGGCGGGTCCCACCTGCCCCACCCCCGGAAGCCCCAGGCCGCCAGAACCTGAGTGGGGCAGCAGCTGGGGAGGCGCTGGTAG
S R Q R A S R R V P P A P P P E A P G R Q N L S G A A A G E A L V>
519 529 539 549 559 569 579 589 599 609
GGGCAGCTGGCTTCCCACCACACGGAGATACAGGGAGCGTGGAGGGCGCCCCCCAGCCCACGGACAATGGCTTCACCCCCAAGTGCGAGATCGTGGGCAA
G A A G F P P H G D T G S V E G A P Q P T D N G F T P K C E I V G K>
619 629 639 649 659 669 679 689 699 709
GGACGCACTGTCTGCACTGGCCCGGGCCAGCACCAAGCAGTGCCAGCAGGAGATCGCCAATGTGGTGTGCCTGCACCAGGCTGGGAGCCTCATGCCCAAG
D A L S A L A R A S T K Q C Q Q E I A N V V C L H Q A G S L M P K>
719 729 739 749 759 769 779 789 799 809
GCTGTGCCCCGGCACTGTCAGCTGACTGGGAAGATGAGCCCCGGCATCCAGTGGGATGAGAGCCAAGCCCAGCAGCCCATGGATGGCCCCCCcGGTGCGA
A V P R H C Q L T G K M S P G I Q W D E S Q A Q Q P M D G P P G A>
819 829 839 849 859 869 879 889 899 909
ATCGCCTACATGCTGGTGGTTCACGGCCGCGCCATCCGCCAGCTGAAGCGTCTCCTCAAGGCCGTTTATCACGAGCAGCACTTCTTTTACATCCATGTGG
N R L H A G G S R P R H P P A E A S P Q G R L S R A A L L L H P C G>
919 929 939 949 959
ACAAGCGTTCCGACTACCTGCACCGGGAGGTGGTGGAGCTGGCCCAGGGCTATGATAA
Q A F R L P A P G G G G A G P G L * *>
C
TM
Core-2/I-Branching enzyme; pfam02485
Xylosyltransferase C terminal; pfam12529
220 230 240 250 260 270 280 290
Homo sapiens
Rattus norvegicus
Canis familiaris
Pan troglodytes
Bos taurus
Gallus gallus
Xenopus tropicus
Mus musculus
Patient 2
Consensus

Figure 2. 5 mRNA analysis of conserved amino acids in mutated region of XYLT2 in Ind 1 and 2

(A) Alternating black and white boxes with indicated numbers indicate exons within the cDNA with exon 1 being black. Translational initiation codon ATG is indicated. Black arrow head indicates site of shared mutation for individual I and individual 2. Black horizontal arrows indicate position of real-time PCR primers using for expression analyses B) Top is cDNA sequence from individual I and individual 2 with translation below. Translational initiation codon ATG indicated by the black arrow. Black arrow head indicates cytosine insertion. Black bar indicates start of aberrant protein sequence ending in two stop codons indicated by asterisks. C) Diagram shows known domain structure of XylT2. Transmembrane domain is shown in N-terminal region, TM. Triangle shows location of insertion and frame shift and underlined amino acids in patient protein are those due to frame shift mutation. Dotted domain shows predicted catalytic domain. Resulting translational termination is indicated by asterisk. Inserted 53 non-conserved amino acids and non-consensus to multiple species is shown demonstrating total loss of consensus after frame shift. (These sequencing and alignment experiments were performed with the help of Dr Steve Hartson and OSU Protein/DNA Core.)

Table 2. 3 Bioinformatics analysis in Ind.1 and Ind.2

Supplementary Data Table III	Genomic Position hg19				
	chr17:48431826	chr17:61902289	chr17:79225239	chr17:80136979	chrX:19725093
Consequence	frameshift insertion	Missense variant	Missense variant	Missense variant	Missense variant
Reference allele	GCCCCCC	C	G	C	C
Alternative allele	GCCCCCCC	A	A	T	T
Individual-1	Hom	Hom	Hom	Hom	Hom
Individual-2	Hom	Hom	Hom	Hom	Hom
BioType of transcript	Nonsense mediated_decay	Protein coding	Protein coding	Protein coding	Protein coding
Accession Number	NM_022167	NM_017647	NM_138570	NM_198082	NM_001024666
cDNA Change	c.692_693insC	c.712G>T	c.2119C>T	c.1298G>A	c.185G>A
Protein Change	p.P231fs	p.A238S	p.L707F	p.R433H	p.R62Q
Gene name	XYLT2	FTSJ3	SLC38A10	CCDC57	SH3KBP1
#prev seen in-house database	0	0	1	3	0
dbSNP: rsID	-	0	rs200011449	rs200450321	-
MAF from 1000 genomes	0	0	0	0	0
EVS MAF	0	0	0.0012	0.001107	0
ExAC MAF	0	0	0.001504	0.0007	0.000008
SIFT score	Not provided	0.02	0.13	0	0.03
Polyphen2 score	Not provided	0.928	0	0.715	0.105
Mutation Taster prediction	Not provided	Disease Causing	Polymorphism	Disease causing	Disease causing

References

Alanay, Y., Superti-Furga, A., Karel, F., & Tuncbilek, E. (2006). Spondylo-ocular syndrome: a new entity involving the eye and spine. *Am J Med Genet A, 140*(6), 652-656. doi:10.1002/ajmg.a.31119

Baasanjav, S., Al-Gazali, L., Hashiguchi, T., Mizumoto, S., Fischer, B., Horn, D., . . . Hoffmann, K. (2011). Faulty initiation of proteoglycan synthesis causes cardiac and joint defects. *Am J Hum Genet, 89*(1), 15-27. doi:10.1016/j.ajhg.2011.05.021

Condac, E., Dale, G. L., Bender-Neal, D., Ferencz, B., Towner, R., & Hinsdale, M. E. (2009). Xylosyltransferase II is a significant contributor of circulating xylosyltransferase levels and platelets constitute an important source of xylosyltransferase in serum. *Glycobiology, 19*(8), 829-833. doi:10.1093/glycob/cwp058

Condac, E., Silasi-Mansat, R., Kosanke, S., Schoeb, T., Towner, R., Lupu, F., . . . Hinsdale, M. E. (2007). Polycystic disease caused by deficiency in xylosyltransferase 2, an initiating enzyme of glycosaminoglycan biosynthesis. *Proc Natl Acad Sci U S A, 104*(22), 9416-9421. doi:10.1073/pnas.0700908104

Couchman, J. R., & Pataki, C. A. (2012). An introduction to proteoglycans and their localization. *The journal of histochemistry and cytochemistry, 60*(12), 885-897.

Cuellar, K., Chuong, H., Hubbell, S. M., & Hinsdale, M. E. (2007). Biosynthesis of chondroitin and heparan sulfate in chinese hamster ovary cells depends on xylosyltransferase II. *J Biol Chem, 282*(8), 5195-5200. doi:10.1074/jbc.M611048200

De Paepe, A., Leroy, J. G., Nuytinck, L., Meire, F., & Capoen, J. (1993). Osteoporosis-pseudoglioma syndrome. *Am J Med Genet, 45*(1), 30-37. doi:10.1002/ajmg.1320450110

Eames, B. F., Yan, Y. L., Swartz, M. E., Levic, D. S., Knapik, E. W., Postlethwait, J. H., & Kimmel, C. B. (2011). Mutations in fam20b and xylt1 reveal that cartilage matrix controls timing of endochondral ossification by inhibiting chondrocyte maturation. *PLoS Genet, 7*(8), e1002246. doi:10.1371/journal.pgen.1002246

Esko, J. D., Kimata, K., & Lindahl, U. (2009). Proteoglycans and Sulfated Glycosaminoglycans. In nd, A. Varki, R. D. Cummings, J. D. Esko, H. H. Freeze, P. Stanley, C. R. Bertozzi, G. W. Hart, & M. E. Etzler (Eds.), *Essentials of Glycobiology* (2nd ed.). Cold Spring Harbor (NY).

Fahiminiya, S., Al-Jallad, H., Majewski, J., Palomo, T., Moffatt, P., Roschger, P., . . . Rauch, F. (2014). A Polyadenylation Site Variant Causes Transcript-Specific BMP1 Deficiency and Frequent Fractures in Children. *Hum Mol Genet*. doi:10.1093/hmg/ddu471

Fahiminiya, S., Majewski, J., Mort, J., Moffatt, P., Glorieux, F. H., & Rauch, F. (2013). Mutations in WNT1 are a cause of osteogenesis imperfecta. *Journal of medical genetics*. doi:10.1136/jmedgenet-2013-101567

Gotting, C., Kuhn, J., Zahn, R., Brinkmann, T., & Kleesiek, K. (2000). Molecular cloning and expression of human UDP-d-Xylose:proteoglycan core protein beta-d-xylosyltransferase and its first isoform XT-II. *J Mol Biol, 304*(4), 517-528. doi:10.1006/jmbi.2000.4261

Hinsdale, M. E. (2013). Xylosyltransferase I, II. In P. K. H. Professor Naoyuki Taniguchi, Professor Minoru Fukuda, Professor Hisashi Narimatsu, Dr. Yoshiki Yamaguchi and Dr. Takashi Angata (Ed.), Handbook of Glycosyltransferases and Related Genes. Springer-Verlag Berlin Heidelberg: SpringerReference, www.springerreference.com;. Retrieved from http://link.springer.com/referencework/10.1007/978-4-431-54240-7/page/4. doi:DOI: 10.1007/SpringerReference_332097 2013-04-26 05:43:46 UTC

Kumar, P., Henikoff, S., & Ng, P. C. (2009). Predicting the effects of coding non-synonymous variants on protein function using the SIFT algorithm. *Nature Protocols, 4*(7), 1073-1082. doi:DOI 10.1038/nprot.2009.86

Li, H., & Durbin, R. (2009). Fast and accurate short read alignment with Burrows-Wheeler transform. *Bioinformatics (Oxford, England), 25*(14), 1754-1760.

Li, H., Handsaker, B., Wysoker, A., Fennell, T., Ruan, J., Homer, N., . . . Durbin, R. (2009). The Sequence Alignment/Map format and SAMtools. *Bioinformatics (Oxford, England), 25*(16), 2078-2079.

Livak, K. J., & Schmittgen, T. D. (2001). Analysis of relative gene expression data using real-time quantitative PCR and the 2(-Delta Delta C(T)) Method. *Methods, 25*(4), 402-408. doi:10.1006/meth.2001.1262

Malfait, F., Kariminejad, A., Van Damme, T., Gauche, C., Syx, D., Merhi-Soussi, F., . . . De Paepe, A. (2013). Defective initiation of glycosaminoglycan synthesis due to B3GALT6 mutations causes a pleiotropic Ehlers-Danlos-syndrome-like connective tissue disorder. *Am J Hum Genet, 92*(6), 935-945. doi:10.1016/j.ajhg.2013.04.016

McKenna, A., Hanna, M., Banks, E., Sivachenko, A., Cibulskis, K., Kernytsky, A., . . . DePristo, M. A. (2010). The Genome Analysis Toolkit: A MapReduce framework for analyzing next-generation DNA sequencing data. *Genome Research, 20*(9), 1297-1303. doi:DOI 10.1101/gr.107524.110

Mis, E. K., Liem, K. F., Kong, Y., Schwartz, N. B., Domowicz, M., & Weatherbee, S. D. (2014). Forward Genetics Defines Xylt1 as a Key, Conserved Regulator of Early Chondrocyte Maturation and Skeletal Length. *Dev Biol, 385*(1), 67-82. doi:10.1016/j.ydbio.2013.10.014

Morello, L. G., Coltri, P. P., Quaresma, A. J., Simabuco, F. M., Silva, T. C., Singh, G., . . . Zanchin, N. I. (2011). The human nucleolar protein FTSJ3 associates with NIP7 and functions in pre-rRNA processing. *PLoS One, 6*(12), e29174. doi:10.1371/journal.pone.0029174

Nakajima, M., Mizumoto, S., Miyake, N., Kogawa, R., Iida, A., Ito, H., . . . Ikegawa, S. (2013). Mutations in B3GALT6, which encodes a glycosaminoglycan linker region enzyme, cause a spectrum of skeletal and connective tissue disorders. *Am J Hum Genet, 92*(6), 927-934. doi:10.1016/j.ajhg.2013.04.003

Pinto, D., Delaby, E., Merico, D., Barbosa, M., Merikangas, A., Klei, L., . . . Scherer, S. W. (2014). Convergence of genes and cellular pathways dysregulated in autism spectrum disorders. *Am J Hum Genet, 94*(5), 677-694. doi:10.1016/j.ajhg.2014.03.018

Robinson, J. T., Thorvaldsdottir, H., Winckler, W., Guttman, M., Lander, E. S., Getz, G., & Mesirov, J. P. (2011). Integrative genomics viewer. *Nature Biotechnology, 29*(1), 24-26. doi:Doi 10.1038/Nbt.1754

Roch, C., Kuhn, J., Kleesiek, K., & Gotting, C. (2010). Differences in gene expression of human xylosyltransferases and determination of acceptor specificities for various proteoglycans. *Biochem Biophys Res Commun, 391*(1), 685-691. doi:10.1016/j.bbrc.2009.11.121

Sarrazin, S., Lamanna, W. C., & Esko, J. D. (2011). Heparan sulfate proteoglycans. *Cold Spring Harb Perspect Biol, 3*(7), a004952. doi:10.1101/cshperspect.a004952

Schmidt, H., Rudolph G Fau - Hergersberg, M., Hergersberg M Fau - Schneider, K., Schneider K Fau - Moradi, S., Moradi S Fau - Meitinger, T., & Meitinger, T. (2001). Retinal detachment and cataract, facial dysmorphism, generalized osteoporosis, immobile spine and platyspondyly in a consanguinous kindred--a possible new syndrome. *Clinical Genetics, 59*, 99-105.

Schreml, J., Durmaz, B., Cogulu, O., Keupp, K., Beleggia, F., Pohl, E., . . . Ozkinay, F. (2014). The missing "link": an autosomal recessive short stature syndrome caused by a hypofunctional XYLT1 mutation. *Hum Genet, 133*(1), 29-39.

Shimokawa, N., Haglund, K., Holter, S. M., Grabbe, C., Kirkin, V., Koibuchi, N., . . . Dikic, I. (2010). CIN85 regulates dopamine receptor endocytosis and governs behaviour in mice. *Embo j, 29*(14), 2421-2432. doi:10.1038/emboj.2010.120

Somer, H., Palotie, A., Somer, M., Hoikka, V., & Peltonen, L. (1988). Osteoporosis-pseudoglioma syndrome: clinical, morphological, and biochemical studies. *Journal of medical genetics, 25*(8), 543-549.

Teebi, A. S., Al-Awadi, S. A., Marafie, M. J., Bushnaq, R. A., & Satyanath, S. (1988). Osteoporosis-pseudoglioma syndrome with congenital heart disease: a new association. *Journal of medical genetics, 25*(1), 32-36.

Zhang, L. J., David, G., & Esko, J. D. (1995). Repetitive Ser-Gly Sequences Enhance Heparan-Sulfate Assembly in Proteoglycans. *Journal of Biological Chemistry, 270*(45), 27127-27135. doi:DOI 10.1074/jbc.270.45.27127

CHAPTER III

REDUCED PROTEOGLYCANS IN THE KIDNEY CAUSES PROTEINURIA DUE TO BOTH TUBULE AND GLOMERULAR ABNORMALITIES

Abstract

Background: Proteoglycans (PGs) are ubiquitously present in most of cells. Xylosyltransferase assembles a xylose molecule onto the serine residue of PG core protein to initiate assembly of glycosaminoglycan (GAG), and it exists in two isoforms; XylT1 and XylT2. We have previously shown that in *Xylt2-/-* mice PGs are important determinants of liver homeostasis and deficiency of liver GAGs causes hepatobiliary fibrosis and biliary cystic disease. The kidneys of *Xylt2-/-* mice have glomerular basement membrane changes, fibrosis and tubule dilation even though the remaining XylT1 isoform contributes to substantial XylT activity. Based on our observation in *Xylt2-/-* mice, we hypothesized that GAG levels are significant components in renal nephron function. We used the *Xylt2-/-* mouse model as well as *in-vitro* proximal tubule cells with reduced GAG to study involvement of PGs and their GAGs in glomerular filtration as well as tubular reabsorption in the kidney.

Methods: Renal functional parameters assessed in the mice were blood urea nitrogen (BUN), urine osmolality, urine creatinine levels, urinary albumin ELISA, and western blotting. Ultrastructural changes in the GBM were visualized via transmission electron microscopy (TEM) and polyethyleneimine based detection of GBM charge distribution. For *in-vitro* BSA uptake studies, extracellular GAGs were removed from proximal tubule derived cell lines using GAG lyases enzymes as well as by CRISPR-Cas9 mediated mutagenesis followed by uptake of Biotinylated-BSA.

Results: *Xylt2-/-* mice have increased progressive BUN, proteinuria, and in older mice, renal failure. TEM study of various kidney sections shows ultrastructural changes in the glomerulus, specifically thickening of GBM, podocyte feet process effacement, and a decrease in anionic charge in GBM. Histological study and TEM of kidney tubules show tubule dilatation of multiple kidney tubule segments and formation of basal

membrane separation from the basement membrane in proximal convoluted tubule epithelium. In-vitro studies in proximal tubule derived cell lines show decrease in albumin uptake due to decreased GAGs.

Conclusions: These findings in the indicate that XylT2-dependent GAG assembly onto core proteins is important in nephron homeostasis. Deficiency of GAGs results in ultrastructural and functional defects in the glomerular basement membrane and proximal convoluted tubule, and that these changes disrupt how well the nephron handles protein.

3.1 Introduction

Chronic kidney disease is one of the most prevalent diseases in America. Currently, according to CDC the prevalence rate for CKD is 14.85% of the population and is projected to stay the same until the year 2020, the prevalence is higher at 43.38%, among individuals 65 years and older (CDC, 2017). Medicare dollars exceeded $50 billion for treatment of CKD in patients over 65 years of age. This represents 20% of the total budget for Medicare (USRDS, 2017). In 2014, over 678,000 patients with end-stage kidney disease required treatment with dialysis and/or transplant in the U.S. Albuminuria, or clinically more commonly referred to as proteinuria, is considered a hallmark of CKD as two thirds of patients with CKD stage 4 have some degree of albuminuria (CDC, 2017). Proteinuria is a single independent risk factor and predictor of CKD progression (Ardissino et al., 2004; Staples & Wong, 2010).

The role of proteinuria in progression of CKD is multifaceted. An increase in albumin to creatinine ratio in patients with CKD signals a significant increase in the risk for end stage renal disease (ESRD)(Carrero et al., 2017), whereas a decline in proteinuria is a positive prognostic indicator in patients with any kidney disease (Inker et al., 2014). Therefore, lowering proteinuria is always considered an important clinical treatment goal in patients with kidney disease (De

Jong, Navis, & de Zeeuw, 1999; Group, 1997; Ruggenenti et al., 2008; Vogt, Waanders, Boomsma, de Zeeuw, & Navis, 2008). Experimentally, animal models and *in-vitro* cell culture models have made significant contributions to our mechanistic understanding of how proteinuria develops and the effects of proteinuria on renal physiology (Cravedi & Remuzzi, 2013).

Most progressive renal diseases with clinical proteinuria have defective glomerular filtration of the plasma. Glomerular filtration depends on a specific arrangement of structures generated by the capillary endothelium and the podocytes lining Bowman's Space. This glomerular filtration barrier consists of the glomerular endothelial cells and their basement membrane plus the podocytes and their basement membrane. The combination of basement membranes constitutes the glomerular basement membrane (GBM). The GBM is highly anionic in nature due to presence of heparan sulfate proteoglycans (HSPGs) (Kanwar & Farquhar, 1979), which have been postulated to electrochemically repel and exclude the bulk of plasma proteins from leaking into Bowman's Space, however, podocyte specific deletion of agrin and perlecan proteoglycans in mice fails to induce proteinuria despite decreases in glomerular anionic sites (Goldberg, Harvey, Cunningham, Tryggvason, & Miner, 2009; Harvey et al., 2007). This led to a new model by Hausmann et al. (2010) that states extracellular electric potential differences created in part by PGs determines glomerular filtration selectivity. Therefore, although charge repulsion may not be the phenomenon, PGs are still important components of glomerular filtration.

If protein should transit the GBM, which some invariably does, then its reabsorption occurs in the proximal convoluted tubule (PCT) by the scavenger receptors megalin and cubilin (Christensen & Birn, 2002). The reabsorption process appears to occur through a standard receptor mediated endocytosis of receptor binding, receptor internalization, and lysosome mediated degradation of the captured protein and receptor recycling to the membrane (Terryn et al.). Mutations in megalin and cubilin are associated with low molecular weight proteinuria in

humans as well is animal models (Weyer et al., 2011). PCT epithelial cells express membrane anchored PGs at the luminal surface. PGs have been shown to bind albumin *in-vitro* (Hattori, Kimura, Seyrek, & Dubin, 2001), and albumin has been shown to regulate heparanase expression in PCT (Masola et al., 2011). Podocyte specific deletion of HS N-deacetylase and sulfotransferase (*Ndst1*) in mice ultimately leads to mild proteinuria and intracellular vacuoles in PCT at 9 month of age and abundant amounts of lysosome in the epithelium. In addition, these mice have podocyte foot process effacement and abnormal podocyte adhesion to Bowman's capsule (Sugar et al., 2014).

In the kidney, PGs, especially HSPGs agrin and perlecan, form a major portion of glomerular basement membrane and contribute to glomerular permselectivity (Borza, 2017; Groffen et al., 1998; Miner, 2012) and most recently have been shown to activate complement by recruiting factor H to the GBM during kidney pathology (Borza, 2017; Clark et al., 2013). HSPGs are also present in the endothelial glycocalyx, which when damaged results in nephrotic diseases (Garsen et al., 2016; Salmito et al., 2015; Salmon & Satchell, 2012). Membrane associated PGs syndecans and glypicans are differentially expressed during various stages of kidney development as well as in adult kidneys (Harvey, 2012). Despite the fact that PGs are integral components of the kidney ECM, and are altered in multiple renal diseases, the mechanistic contribution by PGs to overall nephron homeostasis is poorly understood. We have previously described a XylT2 deficient mouse model (*Xylt2-/-*) with a polycystic disease phenotype, having wide spread biliary cysts and liver fibrosis (Condac et al., 2007). In the kidney, these mice present with occasionally dilated kidney tubules, mild fibrotic changes, and hydronephrosis at later stages and decrease in glycosylation of selective PGs (Condac et al., 2007). Using this unique animal model of GAG reduction due to XylT2 deficiency (*Xylt2-/-*), we are focusing on the mechanistic roles of PGs in nephron homeostasis. In these mice, we assessed renal function by measuring BUN, urinary albumin, creatinine, vasopressin response, and plasma creatinine in *Xylt2-/-* mice. Furthermore,

we characterize the impact of these changes on kidney structure by histology and ultrastructure by transmission electron microscopy. These investigations establish that, XylT2 deficiency results in proteinuria and an age-related decline in renal function associated with ultrastructural defects in the kidney glomerulus and PCT. Further characterization of PGs and albumin uptake by PCT cell lines demonstrate that GAGs are mechanistically important for protein reclamation by the PCT. These studies show that PGs/GAGs in the GBM are vital for maintaining GBM ultrastructure and function and that GAGs are important to PCT function.

3.2. Methods

3.2.1 Animals and Cell types

Generation of *Xylt2-/-* mice has been described already (Condac et al., 2007). Xylt2-/- mice were backcrossed with 129/Sv mice for 8 generations. Mice were kept in ABSL2 barrier facility with *ad libitum* amount of food and water intake. All the procedures and protocols were approved by Institutional Animal Use and Care Protocol. Opossum Proximal convoluted cells (OK) cells (ATCC# CRL-1840) and human proximal convoluted tubule cells (HK-2) cells (ATCC# CRL-2190) were purchased from ATCC. Cells were grown in EMEM (Biowhittaker#12-611) supplemented with bovine growth serum (Hyclone# SH30541.03), L-glutamine (Gibco# 25030164), and penicillin/streptomycin (Gibco#10378016) and maintained at 37° C with 5% CO_2 in the humidified environment. 293T cells were purchased from GenHunter (Cat# Q401) and maintained on DMEM (Gibco#11965092) supplemented with BGS, L-glutamine and penicillin/streptomycin. For biotinylated bovine serum albumin uptake studies, cells were switched into defined media (Serum free EMEM supplemented with L-glutamine, penicillin/streptomycin, 10 μg/ml insulin (Sigma#I6634) and 10 mg/ml Fetuin (Sigma# F3004)).

3.2.2 Antibodies and reagents

Antibodies used for the study are goat anti albumin, rabbit anti β2-microglobulin, and rabbit anti transferrin (Abcam, Cambridge, MA, USA), mouse anti heparan sulfate stub antibody epitope 10E4 (Amsbio Cambridge, MA, USA), mouse anti megalin H-10 (Santacruz , Dallas, TX, USA), mouse anti Gapdh (Ambion, Foster City, CA, USA). Horse-radish peroxidase conjugated secondary antibodies used for the study were goat anti rabbit IgG, rabbit anti goat IgG, and goat anti mouse IgG (Calbiochem, , San Diego, CA, USA) and goat anti mouse IgG/IgM (Seracare, Milford, MA, USA). Biotinylated BSA was purchased from Vector laboratories (Cat# B-2007). Polyethylenamide (PEI) – 25KDa form was purchased from Polysciences, Warrington, PA, USA. *Bacteroides* Heparitinase III was purchased from New England Biolabs, Ipswich, MA, USA and Chondroitinase ABC from *Proteus vulgaris* was purchased from Seikagaiku, Japan.

3.2.3. Urine collection and analysis

Urine was collected by micturition over the petri dish method as described by Watts (1971). Briefly, mice were held over a weigh boat and induced to urinate by applying massaging and gentle trans-abdominal pressure over the urinary bladder. Urine was collected and stored at -80° until further analysis. For Coomassie blue staining, 1 μl of urine was diluted 1:10 and electrophoresed into SDS-PAGE and stained with Coomassie staining for 5 minutes followed by several washings with destaining solution (40% methanol, 10 %glacial acetic acid in ddH_20) until bands were clearly visible. For Western blotting, 1 μl of urine was subjected to SDS-PAGE followed by transfer to PVDF membrane. Membranes were blocked with 5% milk in TBST overnight followed by incubation with specific primary antibodies diluted in blocking buffer for one hour at room temperature. The antibody dilutions were; albumin (1:3,000), transferrin (1:5,000), β2 microglobulin (1:5,000). The membranes were washed and incubated with species specific horse radish peroxide labelled secondary antibody (1:50,000) in blocking buffer.

Chemiluminescence was detected using SuperSignal West Pico (Thermo Scientifc # 34580) followed by imaging in Amersham 600 imager (GE life technologies).

3.2.4. Transmission electron microscopy

Mice were anesthetized using isoflurane. Kidneys were collected and trimmed into roughly 1 mm^3 cubes and fixed with half strength Karnavosky's fixative (2.5% glutaraldehyde, 2% paraformaldehyde in 0.1M sodium cacodylate buffer) for two hours. Tissues were then washed with 0.1M sodium cacodylate buffer, PH 7.2 followed by fixation with osmium tetroxide. Stained tissues were then washed again with cacodylate buffer and dehydrated in increasing concentrations of ethanol. Tissues were then washed with propylene oxide three times and equilibrated to a 1:1 mix of propylene oxide: epoxy resin overnight. The propylene oxide was allowed to evaporate for 24 hours and tissues were embedded in polymerizing epoxy resin at 60°C overnight. The embedded blocks were then trimmed, sectioned, mounted and stained with uranyl acetate and lead citrate followed by observation in transmission electron microscope.

3.2.5. Anionic labeling

Mice were injected with Polyethyleneimine intravenously. Kidneys were harvested and processed for TEM as described previously. TEM pictures were taken for GBM and number of anionic sites were counted using NIH Image J software. Total length of GBM in particular image was measured using freehand tool in NIH Image J software. TEM scale bar was used for reference to estimate nm length of GBM. The numbers of anionic sites were normalized to the length of GBM. A minimum of 5 images were counted for each mouse.

3.2.6. Vasopressin challenge

The mice received an intraperitoneal injection of desmopressin (DDAVP, Sigma-V1005) at 1.0 ng/g BW and urine osmolality. Two hours after desmopressin challenge urine osmolality was measured using Micro Osmometer from Precision Systems Inc. (Natick, MA 01760)

(Takahashi et al., 2000). Percentage change in urine osmolality was calculated using pre-injection urine osmolality as baseline level.

3.2.7 *In vitro* BSA uptake studies

Cells were let to grow to confluency. After confluency, extracellular proteoglycans were digested with Heparitinase III or Chondroitinase ABC overnight in defined media. Biotinylated BSA uptake assays were performed by supplementing the defined media with Biotinylated BSA (100 mg/ml) for 2 hours. Cells were washed with PBS three times and collected in 100 µl Radio-immunoprecipitation lysis buffer. Cell lysate was subjected to SDS-PAGE followed by transfer into PVDF membrane. Membranes were incubated with horse-radish peroxidase conjugated streptavidin followed by chemiluminescence. Gapdh was used as loading control.

3.2.8 Immunohistochemistry

The rotocol for Immunohistochemistry (IHC) has been described previously (Condac et al., 2007). Kidney paraffin sections were used in IHC for Megalin (Lrp2) and cells grown in glass coverslips were used in IHC for HSPGs. Sections/cells were fixed in 4% Paraformaldehyde and washed twice with 1X wash buffer followed by treatment with 0.1M glycine and blocking of indigenous peroxide with 0.3% H2O2 in Methanol. Antigen unmasking was performed in kidney sections by boiling in 10mM sodium citrate buffer. Tissues/cells were then washed twice with wash buffer and blocked with 3% BSA for 1 hour followed by incubation with primary antibodies megalin (1:100) or anti-HSPG (1:200) overnight in 1% BSA in wash buffer. Cells were washed with wash buffer three times followed by incubation with HRP labeled goat anti-mouse IgG or IgG/IgM (1:100 in 1%BSA in wash buffer). Immunostaining was performed by using NOVA Red-HRP substrate (Vector Biologicals) and counterstained with hematoxylin.

3.2.9 CRISPR mediated knockout of XYLT2 in HK2 cells

CRISPR mediated gene mutation was induced by using lentiviral gene delivery system. LentiCRISPR v2 vector was a gift from Feng Zhang (addgene plasmid# 52961). Oligonucleotides for the guide RNA targeted to Exon 2 of XYLT2 were generated using Massachusetts Institute of Technology CRISPR design tool (tools.genome-engineering.org). Oligonucleotides were annealed and cloned into LentiCRISPR v2 vector as previously described (Sanjana, Shalem, & Zhang, 2014). Briefly, lentiCRISPRv2 plasmid was digested with *Bsm*BI and gel purified. The guide RNA oligonucleotides were annealed using T4 ligase followed by ligation of linearized plasmid with guide RNA oligonucleotide. The resulting plasmid was transformed into stbl3 bacteria to produce plasmid vector. 293T cells were transfected with lentiCRISPR v2 vector using calcium phosphate precipitation method. Twelve hours post-transfection, cells were switched to serum free medium. Virus particles were collected 48 hours later, centrifuged at 3000 rpm for 5 minutes and supernatant was used for transfection of HK-2 cells using polybrene (Sigma#107689). Cells at about 60% confluency were transfected with virus containing media in presence of polybrene (8ug/ml final concentration) for 8 hours. After 8 hours, cells were switched to selection media with puromycin (1ug/ml) for 48 hours. Post selection, cells were trypsinized and clonally selected to a 96 well plate using serial dilutions. The wells with single colony were identified and expanded for screening and characterization of mutation. DNA was isolated from isolated single cell clones and the region with mutation was PCR amplified. Using restriction mapping with *Nci*I digestion, the clones were screened for the mutation and further characterized by XYLT activity measurement and immunohistochemistry for HSPG GAGs.

3.2.10 Real-time RTPCR

Total RNA was isolated from kidney tissues and cells using TRIzol reagent (Cat # 15596-018, Life Technologies), contaminant DNA degraded by DNase I treatment using 1 units of DNase I (Cat # M0303S, NEB), followed by TRIzol reagent extraction one more time.

Complementary DNA (cDNA) was prepared from five micrograms of RNA using Moloney Murine Leukemia Virus (M-MuLV) from NEB (Cat# M0235). Real-time RTPCR was performed on 1:5 diluted cDNA using gene specific primers listed in table 1. Relative gene expression was determined using $2^{-\Delta\Delta CT}$ method (Livak & Schmittgen, 2001). GAPDH was used as housekeeping gene for human cDNA while beta actin was used as reference for mouse cDNA. Primers for human and mouse megalin and cubilin were ordered from Origene.A list of primers used for the experiment are provided in Table 3.1.

3.2.11 Measurement of XylT activity

The protocol for measurement of xylosyltransferase activity in cultured cells has been previously described (Munns et al., 2015). Cells were trypsinized and after trypsin inactivation using complete growth media, cells were washed with PBS three times and frozen as cell pellets. Cell pellets were sonicated in sucrose lysis buffer containing 250mM sucrose, 20mM Tris HCl pH 7.5, 10mM Sodium azide, 1μg/ml Leupeptin, 0.5 μg/ml Pepstatin A, and 200 μM PMSF. The supernatant after centrifugation was used for XylT activity measurement. XylT assay was performed in presence of 25 μM MES pH 6.5, 25 μM KCl, 5 μM KF, 5 μM $MgCl_2$, and 5 μM $MnCl_2$ with ^{14}C UDP Xylose (1.97 μM) and cold UDP Xylose (7.46 μM) as donor substrate and Bikunin Peptide (160 μM) as acceptor peptide. The mixture was incubated at 37 C for one hour followed by 10% tricholoroacetic acid (TCA)/ 4% phosphotungstic acid (PTA) precipitation of bikunin peptide with bovine serum albumin as carrier. The pellets were then washed twice with 5% TCA on ice. The incorporated radioactivity in the pellet was measured using scintillation counter. Protein amount in sucrose lysis buffer was used for normalization of XylT activity. One unit of enzyme activity represented amount of micromoles of ^{14}C UDP-Xylose incorporated per minute by 1 mg of protein in cell lysate. The K_m for Bikunin peptide with UDP-xylose has been already determined in given condition (Condac et al., 2009).

3.2.12 Statistical analysis

Statistical analysis was performed using SAS JMP 12.0 software. Two-tailed unpaired t-test were performed while comparing two groups whereas one way-ANOVA was used when comparing more than two groups followed by Tukey's honestly significance difference as post-hoc test to compare differences among the groups.

3.4 Results

3.4.1 Proteoglycan deficient *Xylt2-/-* mice have renal function defects

PGs are altered during various kidney pathologies. Renal functions are measures of severity of renal diseases. Renal function in *Xylt2-/-* mice, similar to patients, was evaluated by measuring blood urea nitrogen (BUN), urine to plasma creatinine ratio (U: P_{CT}), plasma electrolyte concentrations, and albuminuria. *Xylt2-/-* mice have progressive disease with elevated BUN levels (Fig 3.1 A) and reduced U:P_{CT} ratio (Fig 3.1 D). Analysis of plasma electrolytes shows normal plasma K^+, Cl^-, and Na^+ levels, but plasma albumin level is elevated significantly (Table 3.2) possibly due to dehydration from kidney water loss. In addition, as early as 3 months of age, *Xylt2-/-* mice develop proteinuria consisting of a significantly higher urinary albumin as detected by ELISA and Western blotting (Fig 3.1. B &F), and by Coomassie staining in later stages (Fig 3.1. C). Increases in BUN, reduced U: P_{CT}, and proteinuria are clinical indications of renal disease progression. Based on these data, we hypothesized that XylT2 deficiency in mice impairs renal function including renal protein handling. To determine if there was an impaired vasopressin response in *Xylt2-/-* mice, we performed a vasopressin challenge in *Xylt2-/-* mice.

3.4.2. Xylt2-/- mice have blunted response to desmopressin challenge

One primary function of the kidney is to help regulate hydration status under changing environments or conditions. The ability of the kidney to conserve and retrieve water for normal water balance is a critical function which requires the kidney to respond to pituitary vasopressin

by retaining urinary water leading to more concentrated urine. Our observations indicate that *Xylt2-/-* mice have renal function defects including significantly reduced urine osmolality (Fig 3.2 A). A decreased urine osmolality indicates an inability of kidneys to concentrate urine or reabsorb water in the collecting duct. Water deprivation studies or a vasopressin challenge with intraperitoneal injection of a vasopressin analogue, desmopressin are classically used to assess the kidney's ability to concentrate the urine. Desmopressin challenge in *Xylt2-/-* mice showed that two hours after desmopressin challenge the *Xylt2-/-* mice failed to elevate urine osmolality while the *Xylt2+/+* mice had a two fold increase in urine osmolality in response to desmopressin (Fig 3.2 B). These findings indicate that *Xylt2-/-* mice kidneys lack a normal response to vasopressin suggesting a primary renal defect in this physiologic pathway. Next we performed ultrastructural studies of kidney using transmission electron microscopy.

3.4.3 Xylt2-/- have ultra-structural defects in the glomerulus

Given that *Xylt2-/-* had increased proteinuria, a glomerular and possibly a PCT defect might be responsible, therefore we performed TEM on kidneys from *Xylt2-/-* and *Xylt2+/+* to study ultrastructural changes in the glomerular filtration barrier. We first visualized the glomerular basement membrane (GBM), glomerular capillaries, and podocytes. While the glomerular ultrastructure was normal in *Xylt2+/+* mice, the *Xylt2-/-* kidneys show a thickened GBM and effacement of podocyte foot processes (Fig 3.3 B-F). Our findings are in agreement with previous literature on glomerular changes during PKD (Lager, Qian, Bengal, Ishibashi, & Torres, 2001). Occasional thickening of GBM and foot process effacement are associated with proteinuria in human PKD patients (Katz, Hakki, Miller, & Finkelstein, 1989) as well as in the animal model of ADPKD (Lager et al., 2001).

Since XylT2 deficiency causes defective glycosylation of PG core proteins, we hypothesized that the changes in GBM ultrastructure are due to the altered glycosylation of PG core proteins in the GBM. The highly negative charge of the sulfated GAGs in the GBM can be

readily assessed by how much cationic dye like polyethyleneimine (PEI) they retain. This can be visualized as electron dense bodies by TEM (Rada & Carlson, 1991). We measured the charge distribution in GBM using PEI and found a significant reduction in numbers of anionic sites in *Xylt2-/-* GBM as compared to wildtype at 3-4 months of age while no GBM ultrastructural defects were yet developed (Fig 3.3 G-K). Real-time RTPCR on *Xylt2-/-* kidneys showed no difference in mRNA expression of basement membrane associated PGs at 3 months of age (Fig 3.4.). These results suggest a normal level of GBM PGs but with reduced GAG content.

As a result at least one source of proteinuria in *Xylt2-/-* mice is a defected GBM. However, mouse models of deletion of agrin and perlecan GAG sites in mice has generated mixed results with no clear correlation between reduced GBM anionic sites, proteinuria, and foot process effacement (Goldberg et al., 2009) suggesting that the changes in GBM ultrastructure and GBM charge distribution is not likely the only cause of proteinuria in *Xylt2-/-* mice. This led us to hypothesize that the *Xylt2-/-* mice may have alterations in PCT structure and protein reabsorption that may be contributing to the development of overt proteinuria. In addition, GAGs could act as a co-receptor for albumin uptake by the PCT as described above. To test our hypothesis, we first performed histopathological analyses of various kidney tubules as well as ultrastructural TEM of proximal convoluted tubules.

3.4.4 Xylt2-/- mice have tubule dilatation and structural deformity in PCT

Immunohistochemistry was performed on paraffin embedded kidney sections to detect various kidney tubule structures. Proximal convoluted tubules are LTA positive, Tamm-Horsefall (TH) is a unique glycoprotein of the thick ascending loop of Henle while DBA lectin is a collecting duct specific marker. Using these tools, we observed that tubules identified by all three types of lectins were dilated in *Xylt2-/-* mice (Fig 3.5 A-C). To further characterize the tubular ultrastructure, we performed TEM of PCT of the *Xylt2-/-* mice and wild type controls. While the *Xylt2+/+* mice had normal PCT structures (Fig 3.5 G), *Xylt2-/-* kidneys although at low

frequency within an animal, *Xylt2-/-* mice consistently showed some deformed PCT epithelial attachments to its basement membrane, with visible intracellular spaces between the BM and the epithelial plasma membrane (Fig 3.5 H).

These observations led us to speculate that defective PCT structure may be a contributing factor for the development of proteinuria in *Xylt2-/-* mice in addition to altered GBM biology. Most of the proteins that inadvertently pass through the GBM are reabsorbed back into the blood via scavenger receptors megalin and cubilin present in luminal surface of PCT epithelium (Christensen, Birn, Storm, Weyer, & Nielsen, 2012). We hypothesized that deficiency in GAGs results in altered megalin and cubilin expression or function in the *Xylt2-/-* kidneys. To test our hypothesis, we used real-time RTPCR and immunohistochemistry to detect megalin and cubilin expression in *Xylt2-/-* kidneys. Surprisingly, *Xylt2-/-* kidneys had no change in Megalin and Cubilin mRNA expression (Fig 3.5 I). Immunohistochemistry for Megalin also did not revealed any significant alteration in staining pattern for megalin in *Xylt2-/-* Kidneys (Fig 3.5 J, K). To identify if reduced GAGs in the PCT had any role PCT protein resorption, we investigated the effect of GAG deficiency or loss in protein uptake by PCT epithelium by using in-vitro biotinylated albumin uptake assay.

3.4.5 Tubular re-absorption is reduced in proteoglycan deficiency

We speculated that GAG deficiency in PCT might affect protein absorption process in PCT. To investigate on how protein uptake is altered during GAG deficiency, we used two different types of PCT derived cell lines; Opossum PCT derived cell lines (OK cells) and human PCT derived cell lines (HK-2 cells). Immunohistochemistry for HSPG in cells grown on coverslips after digestion with Heparitinase III showed a visible reduction in HSPGs (Fig 3.6 B) when compared to undigested controls (Fig 3.6 A). Significantly, when these cells were challenged with albumin uptake, we found a significant reduction of BSA uptake in the cells when the HSPG GAGs were removed (Fig 3.6 C, D). Similar observations were made when

CSPG GAGs were removed by using chondroitinase ABC (Fig 3.6 E, F). These results suggest that the GAGs on the apical surface of the cells are important mediators of albumin reabsorption in proximal convoluted cells.

We used similar strategies using a second tubule epithelial cell line HK-2 cells to test if the mechanism was similar cell lines. We first established that the uptake in HK-2 cells is mediated by megalin by treating the cells with inhibitor of megalin mediated uptake, receptor-associated protein (RAP), and allowing for BSA uptake. We found a reduced uptake of albumin in the cells treated with RAP (Fig 3.6 G, H) confirming a role of megalin in protein resorption in these cells. We then performed uptake assay in HK-2 cells by digesting the extracellular GAGs. Similar to the OK cells, there was a significant decrease in BSA uptake when GAGs were digested, with more pronounced effect due to CSPG digestion (Fig 3.6 I, J). Those data strongly suggest that GAGs are important for in the process of albumin uptake. We next tested our hypothesis by another approach of reducing GAGs by eliminating XylT activity similar to what is occurring in the *Xylt2-/-* mice.

3.4.6. CRISPR mediated Knockdown of XYLT2 in PCT HK-2 cell line reduces albumin uptake

We induced CRISPR-Cas9 mediated gene mutation in XYLT2 in HK-2 cells and performed albumin uptake assay to measure how much PCT epithelial cell albumin resorption is impaired with XYLT2 deficiency. To validate our findings from the *in vitro* uptake studies with digestion of OK and HK-2 cells and to better investigate the impact of XylT2 deficiency on proteinuria, we used CRISPR-Cas9 system to create *XYLT2* deficient HK-2 cells. Cells were screened for functional loss of *XYLT2* by immunostaining for HSPGs as well as by loss of XylT activity. CRISPR targeted HK-2 cells (B10) had a visible reduction in surface HSPG staining (Fig 7 B) and a significantly lower XYLT activity (Fig 7 C) as compared with wild type HK-2 cells. Next, we performed biotinylated-BSA uptake studies in B10 and compared the uptake of albumin

with untransfected HK-2 cells. Our data shows that clone B10 had lower albumin uptake by Western blotting and densitometry analyses (Fig 7 D, E). These findings further validate our earlier findings that loss of GAGs disrupts albumin uptake.

3.4 Discussion

Patients with autosomal dominant polycystic kidney disease (ADPKD) have alterations in the PG sulfation and levels leading to alterations in the renal extracellular matrix environment (Ehara, Carone, McCarthy, & Couchman, 1994; Husson et al., 2004; Lelongt, Carone, & Kanwar, 1988). We have previously shown that PG deficient *Xylt2-/-* mice develop liver cysts and fibrosis (Condac et al., 2007). These mice also develop mild renal fibrosis and hydronephrotic kidneys at later stages and have defective glycosylation of some PGs similar to the liver (Condac et al., 2009). The findings that *Xylt2-/-* mice develop renal tubule dilatation, fibrosis, and PKD like phenotype (Condac et al., 2007) suggest that GAGs are important for the maintenance of normal renal extracellular matrix environment and renal function. In this paper, using *in-vivo* and *in-vitro* studies, we show that reduction in renal extracellular GAG chains results in proteinuria and that these changes can be attributed to both biochemical and structural alterations. Our findings that *Xylt2-/-* mice develop podocyte foot processes effacement and thickening of the GBM are in agreement with the observations on *Sulf1* and *Sulf2* knockout mice (Schumacher et al., 2011; Takashima et al., 2016). However, we know that loss of negative charge or even foot process effacement is not absolutely causative of proteinuria given previous reports on GBM agrin and perlecan in mouse models (Goldberg et al., 2009) and in mouse models of podocyte specific *Extl-1* and *Ndst-1* knockout mice (Chen et al., 2008; Sugar et al., 2014). These findings indicate that GBM GAGs may not be the sole contributor to albumin handling by the kidney as previously thought. In fact, another possibility could be that the agrin and perlecan knockout mice may have defective glomerular filtration, but the PCT reabsorption of albumin is efficient enough to result in minimal or no proteinuria at all. Since *Xylt2-/-* mice are globally GAG deficit, unlike podocyte

specific knockout, deficiency of GAGs on other PGs could augment the proteinuria by decreasing the tubular reabsorption process. Our findings show that membrane associated PGs glypican-1 and syndecan-4 expression, which are involved during kidney pathologies (Ishiguro et al., 2001; Stahl et al.; Yung et al., 2001), is downregulated in XylT2 deficient kidneys. Our data suggests that in *Xylt2-/-* mice alterations in membrane associated PG core proteins, especially syndecan-4 and glypican-1, in addition to the GBM associated GAGs contribute to proteinuria.

In addition to the GBM defects, this paper investigates the function of GAGs in tubular epithelium and their contribution to the development of proteinuria. PGs have been shown to bind albumin *in-vitro* (Hattori et al., 2001), and albumin has been shown to regulate heparanase expression in PCT (Masola et al., 2011). Podocyte specific deletion of HS N-deacetylase and sulfotransferase (*Ndst1*) in mice ultimately leads to mild proteinuria and intracellular vacuoles in PCT at 9 month of age and abundant amounts of lysosome in the epithelium. In addition, these mice have podocyte foot process effacement and abnormal podocyte adhesion to Bowman's capsule (Sugar et al., 2014). Here we show that, by *in-vitro* uptake assay, deficiency of GAGs hinders albumin uptake in PCT cells. To further explore the mechanism, we used human PCT derived HK-2 cells. We first established that albumin uptake in HK-2 cells is megalin mediated by using classical megalin ligand inhibitor; Receptor associated protein (RAP). Using multiple GAG deficiency models, we show that GAGs are important in mediating albumin uptake by two different PCT cell lines. Our findings also show that the expression of megalin and cubilin were not altered during GAG deficiency in mouse kidneys. Therefore, our results suggest the possibility of direct functional interaction of GAGs with the megalin-cubilin endocytosis complex.

3.6 Conclusion

In this paper, using GAG deficient *Xylt2-/-* mice as well as an *in-vitro* GAG deficiency model, we show that PGs and their GAGs are important components of renal pathophysiology. It

is well established that GAGs in the GBM contribute to glomerular filtration even-though the exact mechanisms are still debatable. Our findings that GAG deficiency results in podocyte foot process effacement and thickening of glomerular basement membranes reaffirm that PGs and their GAGs are required for maintenance of GBM ultrastructure. We also show that with XylT2 deficiency the expression of membrane associated PGs glypican-1 and syndecan-4 changes in the kidney. In addition to establishing roles of GAGs in GBM structure, our results also broaden the idea that GAGs in the PCT regulate protein reabsorption. Using *In-vitro* uptake studies, we show that GAGs are required in PCT for proper albumin uptake. In all, we can conclude that If there are pathologic reductions in GAGs in GBM accompanied by decreased or loss of GAGs in PCT, then proteinuria can develop as the protein lost through the GMB overloads uptake mechanisms in the PCT and GAG deficit PCT cells cannot efficiently reclaim plasma proteins lost through the defective GBM. The end result is overt proteinuria with damage to downstream tubular epithelium, leading to progression of chronic kidney pathology in *Xylt2-/-* deficit kidneys.

3.7. Figures and Figure Legends

Table 3. 1 RT-PCR primers and accession numbers for gene targets

Gene	Forward Primer	Reverse Primer	NCBI accession No.	Source
Xylt2	gggtgagacccgcttcct	gcatcatctttcctgagaggtagtt	NM_145828.3	
Xylt1	gaacagctgcaggtactaccaat	gaatcggtcagcaaggaagtaga	NM_175645	
Lrp2	ccaatggactcactctggacct	gaatggaaggcagtgctgatgac	NM_001081088.1	Origene
Cubn	tccgcttcacatcagatggcag	ccttcccaatctcaactgctcc	NM_001081084.3	Origene
Sdc4	gccactggataaccacatcc	cttccagttccttgggtcct	NM_011521.2	
Gpc1	gtgccttccgggacctatat	gtctcctcaaggtgcaggtt	NM_016696.5	
Actb	gctctggctcctagcaccat	ccaccgatccacacagagtact	NM_007393.5	
LRP2	gtctaaccgcactgtgatagcc	cggaagtttcctcccaatgtgg	NM_004525.2	Origene
CUBN	cctaccattgctccaggtgctt	atgagccacgtacagtccactc	NM_001081.3	Origene

Table 3. 2 Analysis of Plasma electrolytes and albumin in Xylt2-/- mice

Test		**Xylt2+/+**	**Xylt2-/-**
Plasma K^+	mmol/l	7.2 ± 2.6, n=7	6.0 ± 0.5, n=6
Plasma Cl^-	mmol/l	115.8 ± 4.6, n=8	111.3 ± 2.5, n=7
Plasma Na^+	mmol/l	136.1 ± 6.6, n=8	133.1 ± 2.5, n=7
Plasma BUN	mg/dl	20.9 ± 4.3, n=8	31.9 ± 10.3, n=7, (p=0.0162)
Plasma Albumin	g/dl	2.3 ± 0.2, n=8	2.6 ± 0.2, n=7, (p=0.0155)
Urine Cr	mg/dl	101.5 ± 26.0	69.9 ± 16.1
Urine Osmolality		2463.7 ± 245.9, n=8	2094.3 ± 809.1, n=7

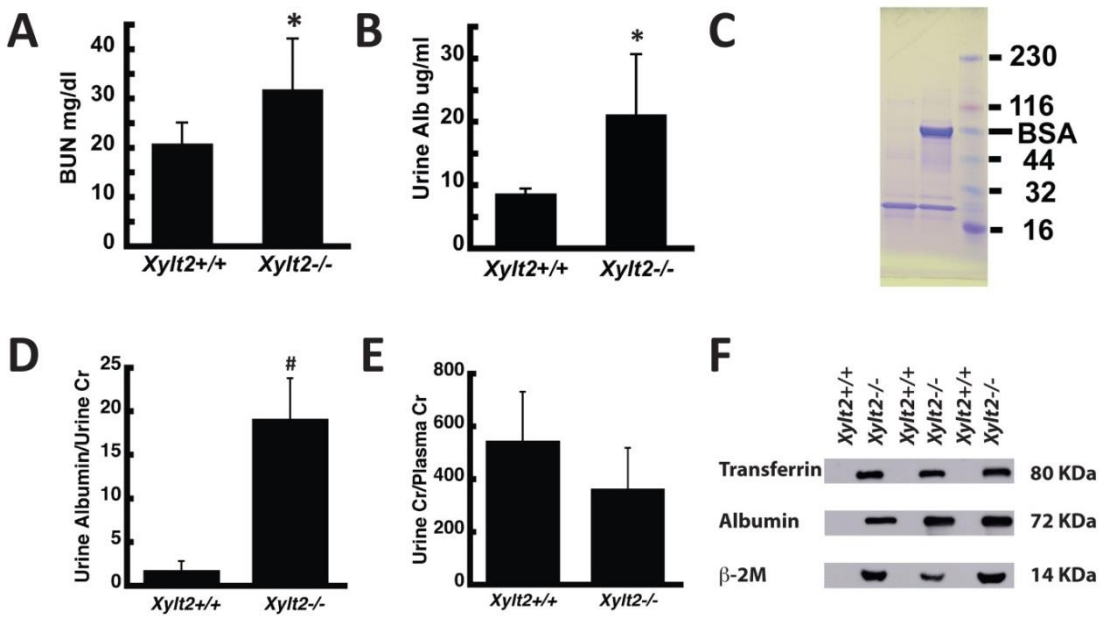

Figure 3. 1 Xylt2-/- mice have renal function defects

Various renal function parameters were assessed in Xylt2-/- mice. (A) Blood Urea Nitrogen (BUN) (n= 8 *Xylt2*+/+; 7 *Xylt2-/-*). (B-D) Urinary albumin in *Xylt2-/-* mice as measured by (B) Albumin ELISA at 3-4 months (n= 8 *Xylt2*+/+; 5 *Xylt2-/-*), (C) Coomassie staining at 7-8 months (n=3 each), and (D) normalized urinary albumin to creatinine (n= 8 *Xylt2*+/+; 5 *Xylt2-/-*). (E) Trend of reduced urinary to plasma creatinine ratio (n=7 *Xylt2*+/+; 5 *Xylt2-/-*, p=0.06).(F) Western blotting of urine showing presence of various proteins specifically reabsorbed by PCT cells (*$p<0.05$, #$p<0.01$). (Part of these experiments were conducted by Eduard Condac, Beatrix Forencz, and Maria Cristina Munteanu and analyzed by the author.)

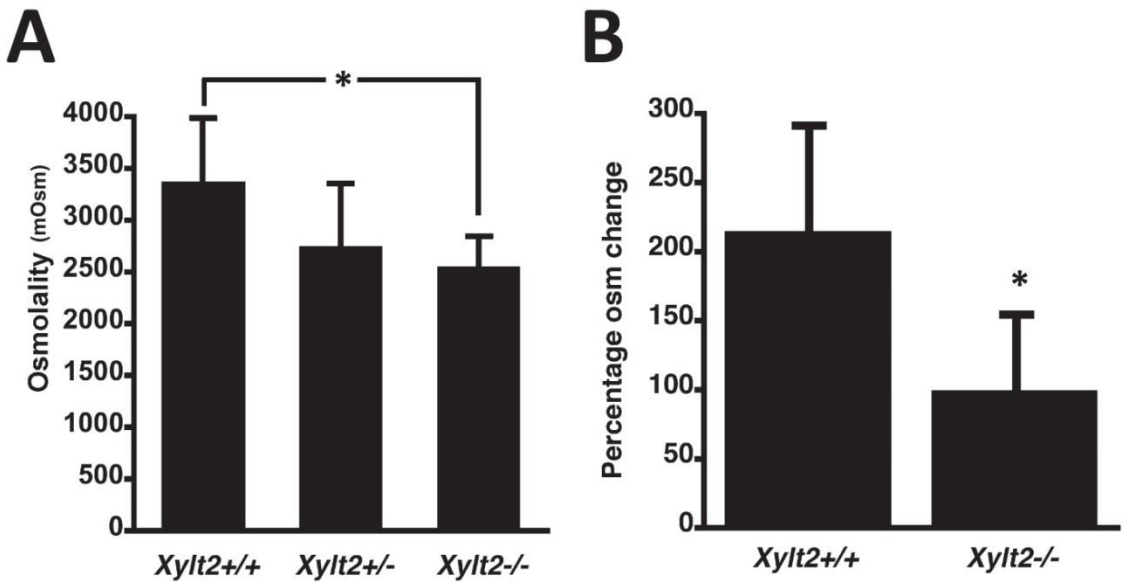

Figure 3. 2 Xylt2-/- mice have a blunted response to desmopressin (DDAVP) challenge.

3.5- 4 months old female mice were injected with DDAVP intraperitoneally and urine osmolality was measured after two hours and change in urine osmolality was calculated. T_0 indicated urine osmolality before intraperitoneal injection of DDAVP; (A) shows decreased urine osmolality at T_0 in *Xylt2-/-* mice (n= 10 *Xylt2+/+;* 7 *Xylt2+/-*; 6 *Xylt2-/-*; *p<0.05); (B) shows no change in percentage osmolality change after two hours post DDAVP challenge in Xylt2-/- mice while Xylt2+/+ mice had two fold change in urine osmolality. (n= 6 *Xylt2+/+*; 4 *Xylt2-/-*; *p<0.05). (This experiment was conducted by Eduard Condac and analyzed by the author.)

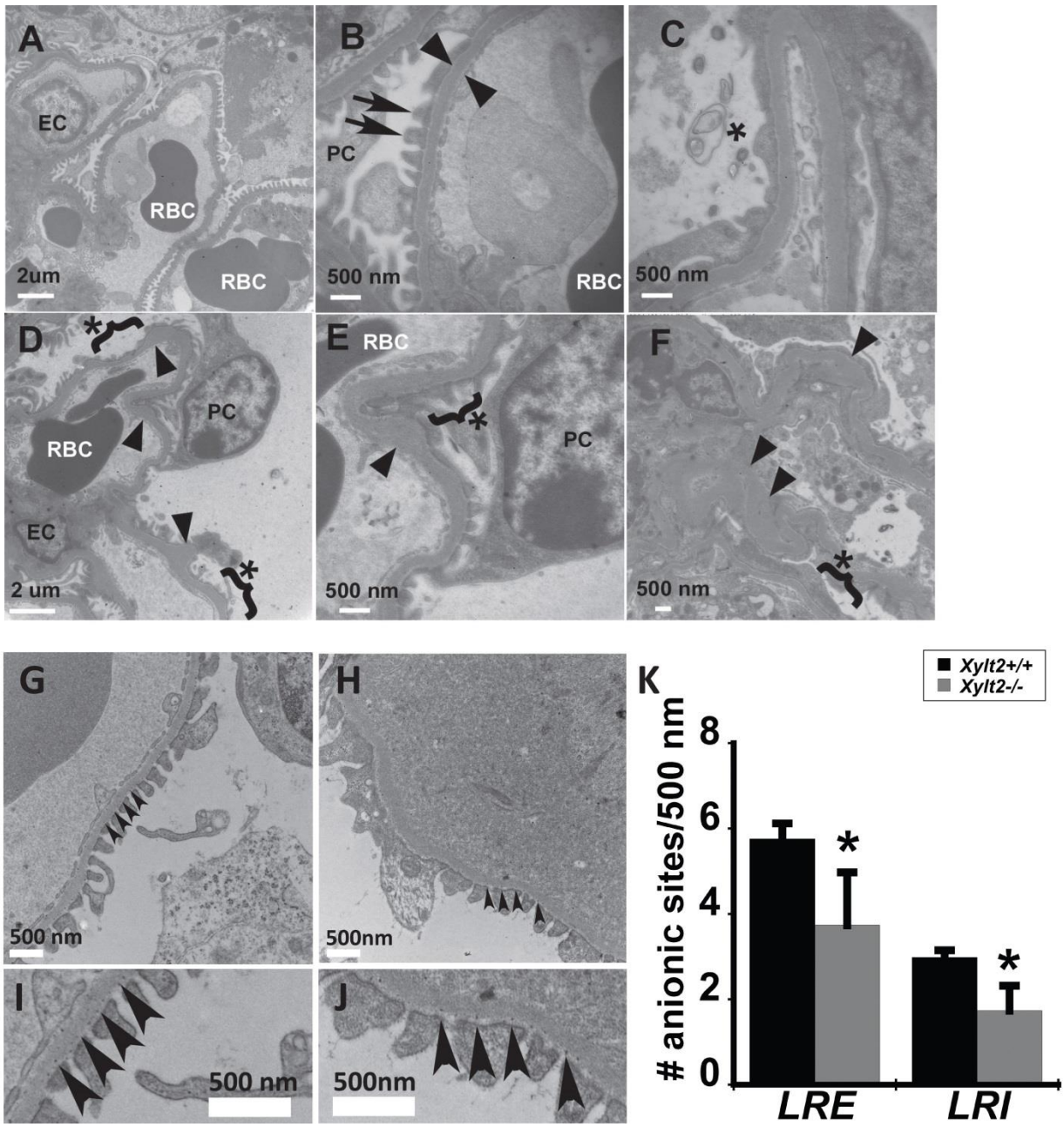
A
EC
RBC
RBC
2um
B
PC
500 nm
RBC
C
500 nm
D
RBC
PC
EC
2 um
E
RBC
PC
500 nm
F
500 nm
G
500 nm
H
500nm
I
500 nm
J
500nm
K
Xylt2+/+
Xylt2-/-
anionic sites/500 nm
0
2
4
6
8
*
*
LRE
LRI

Figure 3. 3 Xylt2-/- mice have glomerular basement membrane defects.

Transmission Electron Microscopy (TEM) was performed in kidneys from 7-8 months old mice. (A-B) *Xylt2+/+* mice had normal glomerular basement membrane (GBM) thickness (between arrowheads) and podocyte feet processes (shown by arrows) as revealed by TEM. (C-F); *Xylt2-/-* mice showed a distinct effacement of podocyte feet processes (shown by asterisk), as well as occasionally thickened GBM (shown by arrowheads). Mice were injected with PEI and kidneys harvested and processed for TEM. (G-J) Representative electron micrographs of GBM of *Xylt2+/+* (G) and *Xylt2-/-* (H) injected with PEI. (I) and (J) show higher magnification of (G and (H), respectively. (K) Enumeration of anionic sites in the Lamina Rara Externa (LRE) and Lamina Rara Interna (LRI). (n= 4 *Xylt2+/+;* 3 *Xylt2-/-*, *$p<0.05$). EC: Endothelium, RBC: Red Blood cells, PC: Podocytes. (These experiments were performed with the help of Robert Silasi-Mansat at Oklahoma Medical Research Foundation)

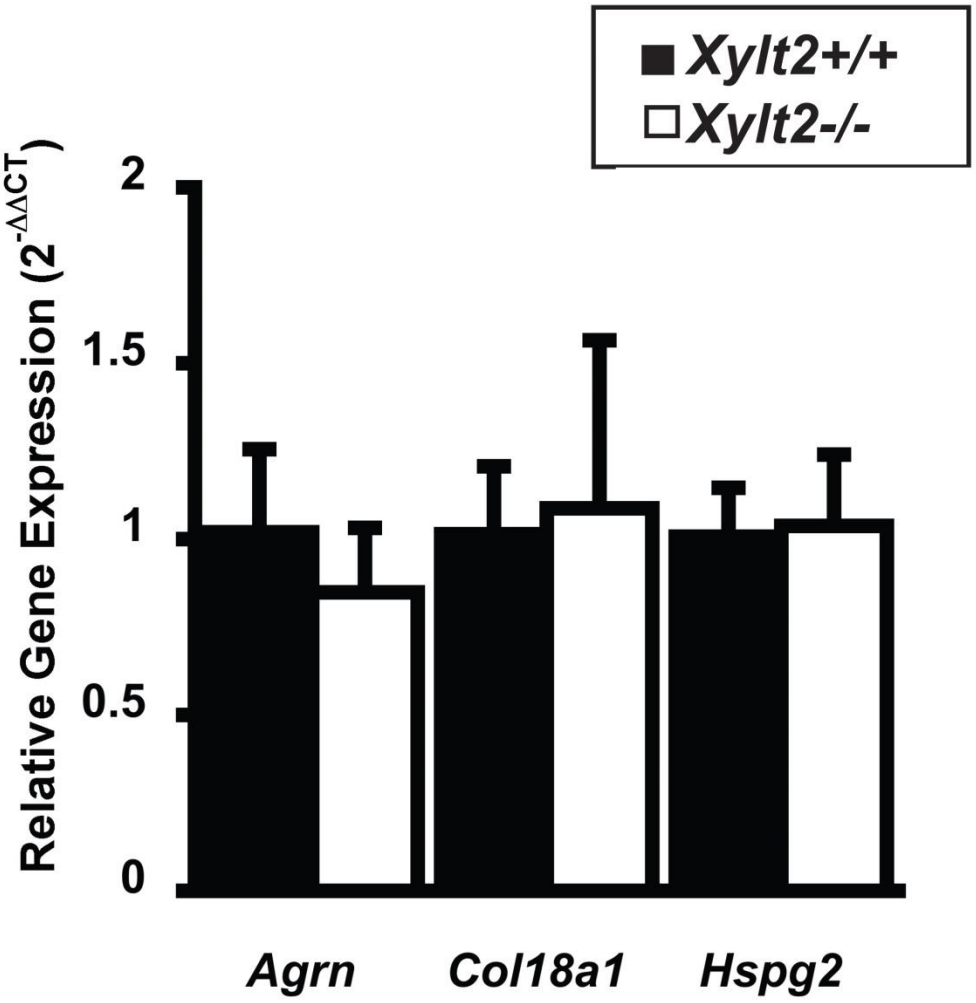

Figure 3. 4 Expression of GBM associated PGs is not altered in Xylt2-/- mice.

Real-time RTPCR was performed in kidneys of Xylt2-/- mice to measure mRNA expression levels of GBM associated PGs. There was no difference in mRNA expression of GBM associated PGs in Xylt2 deficient kidneys when compared to Xylt2+/+ kidneys (n=4 each genotype).

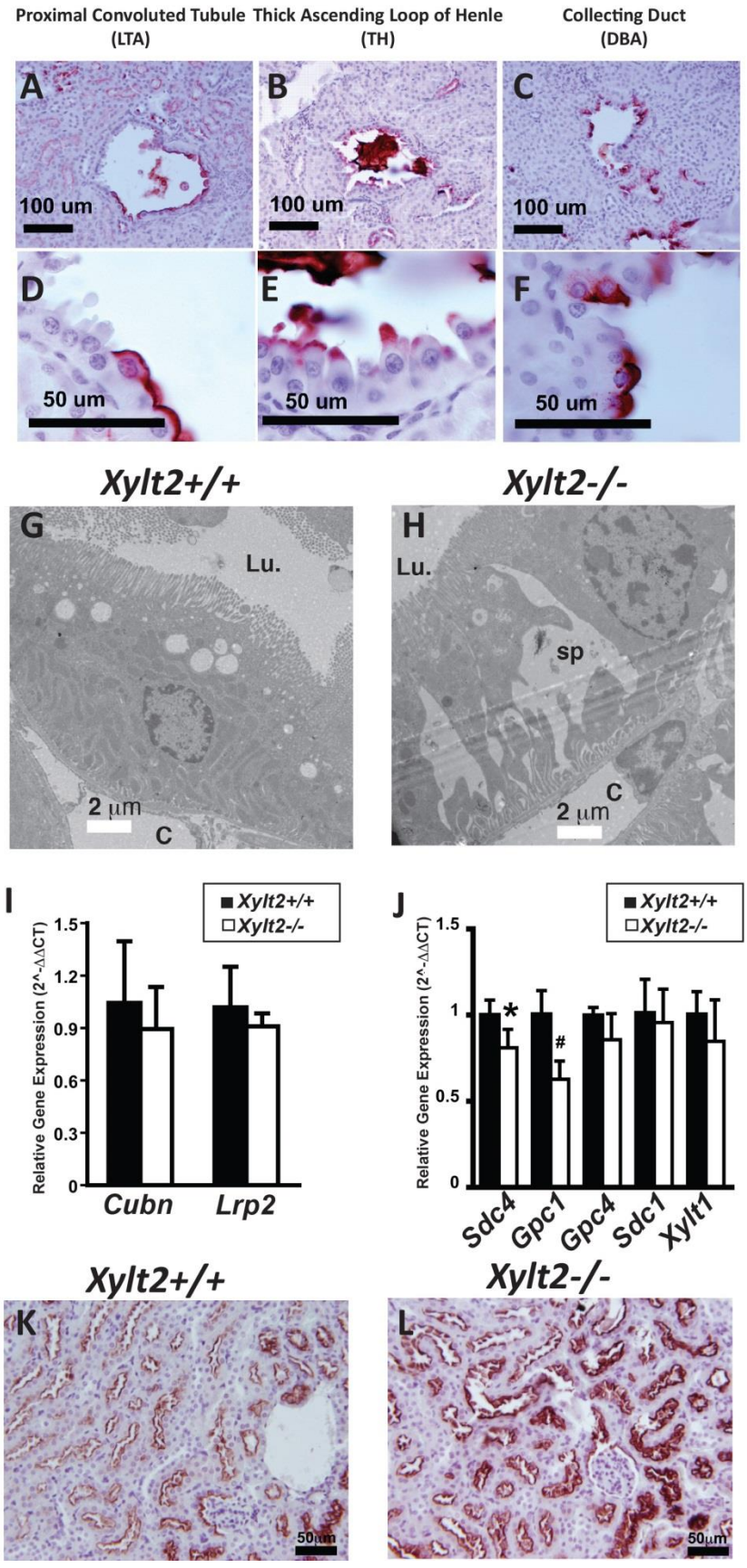
Proximal Convoluted Tubule (LTA)
Thick Ascending Loop of Henle (TH)
Collecting Duct (DBA)
A
B
C
100 um
100 um
100 um
D
E
F
50 um
50 um
50 um
Xylt2+/+
Xylt2-/-
G
Lu.
2 µm
C
H
Lu.
sp
C
2 µm
I
Xylt2+/+
Xylt2-/-
Relative Gene Expression (2^-ΔΔCT)
1.5
1.2
0.9
0.6
0.3
0
Cubn
Lrp2
J
Xylt2+/+
Xylt2-/-
Relative Gene Expression (2^-ΔΔCT)
1.5
1
0.5
0
*
#
Sdc4
Gpc1
Gpc4
Sdc1
Xylt1
Xylt2+/+
Xylt2-/-
K
L
50µm
50µm

Figure 3. 5 Xylt2-/- mice have tubular dilatation and ultrastructural deformities.

A-F; Five micrometer sections of kidneys were immunostained with tubule specific lectin to detect various tubule segments. (A), (B), and (C) show dilatation of proximal convoluted tubule, thick ascending loop of Henle, and Collecting tubule, respectively as identified by tubule specific lectins. (D),(E), and (F); higher magnification of A, B and C, respectively. (G-H) representative TEM structure of proximal convoluted tubule showing ultrastructural chanes in PCT epithelium at 7-8 months of age. (G) *Xylt2*+/+ PCT shows normal architecture and (H) *Xylt2*-/- PT shows intracellular spaces. (I) Relative mRNA expression for scavenger receptors megalin and cubilin in *Xylt2*-/- kidneys (n= 4). (J) Relative mRNA expression of membrane associated PGs in *Xylt2*-/- kidneys (n=4 each genotype). (K-L) Immunohistochemistry of megalin in *Xylt2*+/+ (K) and *Xylt2*-/- (L) kidneys (n=3 each genotype)., LTA; Lotus tetragonolobus Agglutinin, TH; Tamm-Horsefall, DBA; Dolichos Biflorus Agglutinin, Lu; Lumen of Proximal convoluted tubule, Sp; Intracellular spaces, C; Capillary, *$p<0.05$; #$p<0.01$

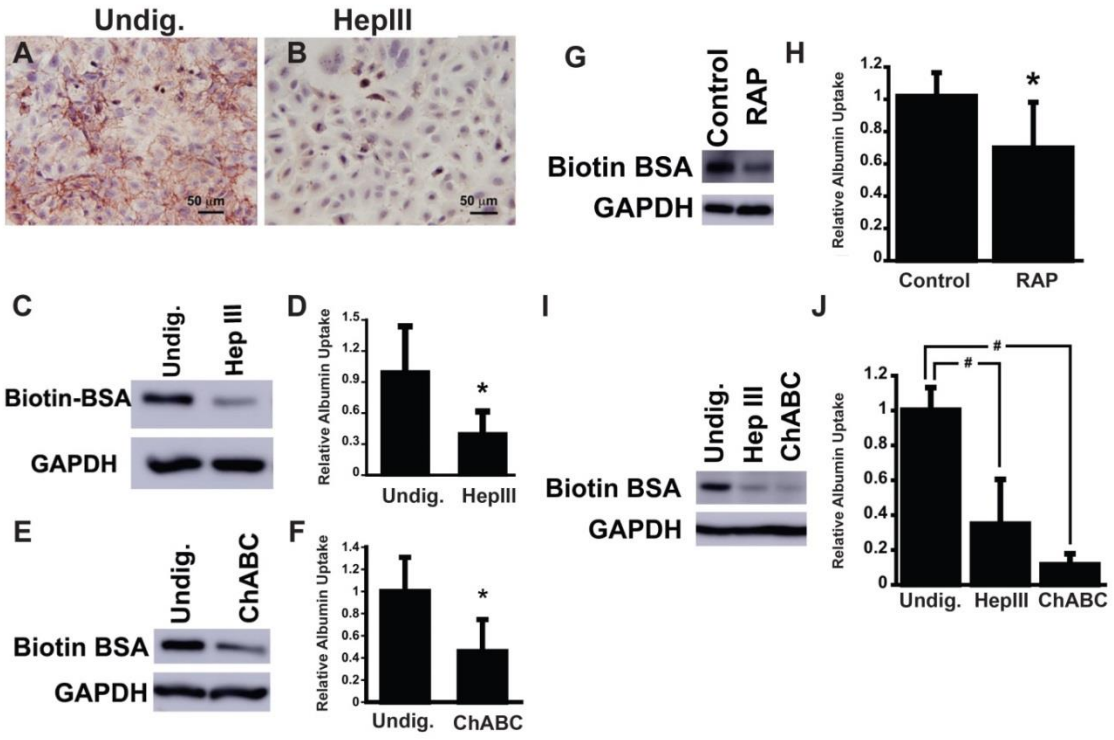

Figure 3. 6 Absence of extracellular GAGs in-vitro reduces exogenous albumin uptake in different proximal tubule cell lines

(A –F; OK Cells, G-J; HK-2 cells) Extracellular HSPGs or CSPGs were digested from cells in vitro and uptake of Biotinylated albumin performed for 2 hours in serum-free condition. (A-B) Decreased levels of HSPGs GAGs in HepIII treated OK cells when compared to the undigested cells. (C to J) Western blotting followed by densitometry analyses to measure albumin uptake during GAG deficiency in PCT derived cells. (C-D) Reduced uptake of BSA by OK cells lacking HSPGs (n= 4 each). (E-F) Reduced uptake of BSA by OK cells lacking CSPGs (n= 4). (G-H) Reduced uptake of albumin by HK-2 cells treated with megalin specific ligand RAP by (n=3 each) (I-J) Reduced uptake of BSA by HK-2 cells lacking HSPGs or CSPGs by (n= 4 each) (RAP: Receptor-associated protein, Undig. Undigested, HepIII: Heparinase III digested; ChABC: Chondroitinase ABC digested, *$p<0.05$, #$p<0.01$

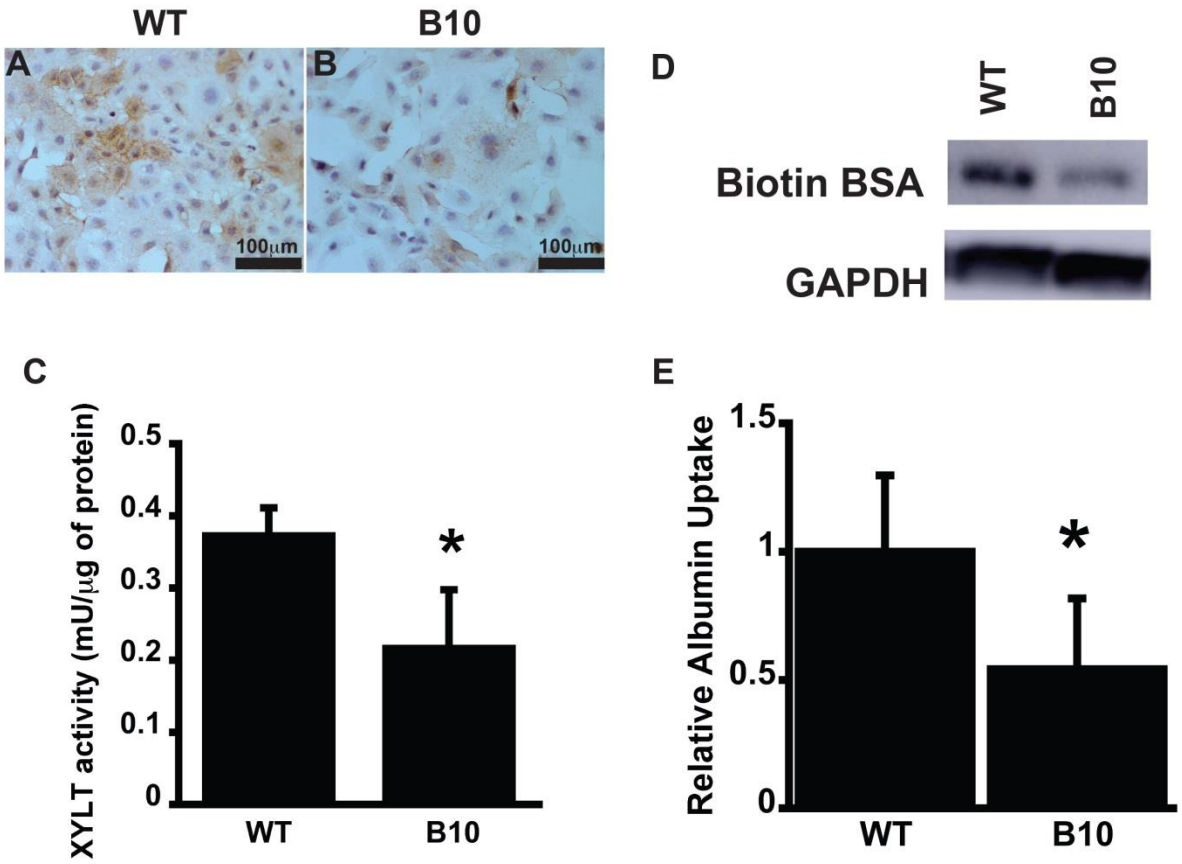

Figure 3. 7 CRISPR targeted mutation in XYLT2 caused albumin uptake in HK-2 cells. HK-2 cells were transfected with lentivirus particle packaged with CRISPR-Cas9 vector targeted to exon 2 of XYLT2 followed by functional effect of mutation and subsequent BSA uptake studies. (A-B) Immunohistochemistry shows decreased in HSPG GAG in mutant HK-2 cells (B) when compared to WT cells (A). (C) Decreased XYLT activity in mutant HK-2 cells when compared to WT cells (n= 3 WT, 4 B10) (D-E) Decreased albumin uptake by XYLT2 deficient HK-2 cells by (D) western blotting and (E) densitometry analysis (n= 5 each, *$p<0.05$).

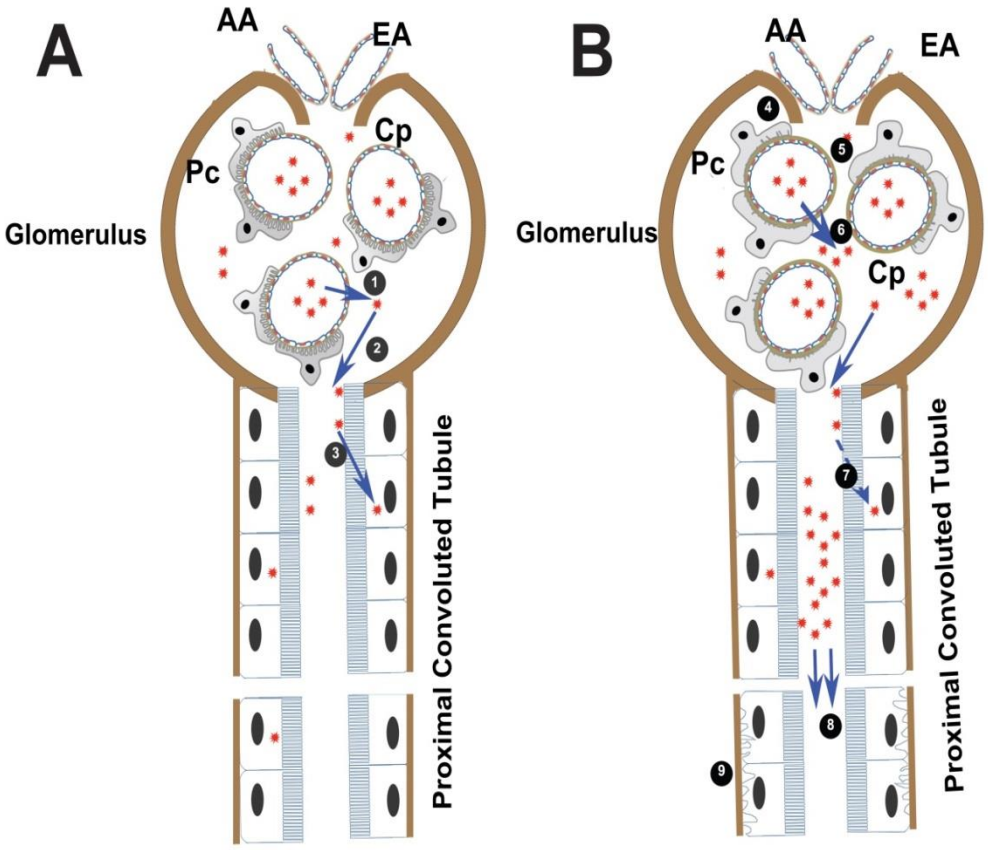

Figure 3. 8 Proposed model of development of proteinuria in Xylt2-/- mice

(A); In normal mice, some albumin transgresses (1) the glomerular filter and then enters (2) into the proximal convoluted tubule lumen where most of the proteins are reabsorbed (3) by endocytic receptors megalin and cubilin in the apical surface of PCT. (B); Xylt2-/- mice develop effacement of podocyte feet processes (4) and thickening of glomerular basement membrane (5) and disrupted glomerular filtration barrier leading to excessive leakage of proteins (6) into the proximal tubule lumen where deficiency of GAGs in luminal surface reduces protein uptake efficiency of PCT (7) and results in overt proteinuria (8). Furthermore, as the mice become older, around 7-8 months, basal surface of PCT develops detachment of basal surface from BM to form intracellular spaces (9) and dilatation of kidney tubules. AA; Afferent arteriole, EA; Efferent arteriole, Pc; Podocytes, Cp;Capillary

References:

Ardissino, G., Testa, S., Dacco, V., Vigano, S., Taioli, E., Claris-Appiani, A., . . . Montini, G. (2004). Proteinuria as a predictor of disease progression in children with hypodysplastic nephropathy. Data from the Ital Kid Project. *Pediatr Nephrol, 19*(2), 172-177. doi:10.1007/s00467-003-1268-0

Borza, D. B. (2017). Glomerular basement membrane heparan sulfate in health and disease: A regulator of local complement activation. *Matrix Biol, 57-58*, 299-310. doi:10.1016/j.matbio.2016.09.002

Carrero, J. J., Grams, M. E., Sang, Y., Ärnlöv, J., Gasparini, A., Matsushita, K., . . . Coresh, J. (2017). Albuminuria changes and subsequent risk of end-stage renal disease and mortality. *Kidney International, 91*(1), 244-251. doi:10.1016/j.kint.2016.09.037

CDC. (2017). Chronic Kidney Disease Surveillance System—United States. Retrieved from http://www.cdc.gov/ckd

Chen, S., Wassenhove-McCarthy, D. J., Yamaguchi, Y., Holzman, L. B., van Kuppevelt, T. H., Jenniskens, G. J., . . . McCarthy, K. J. (2008). Loss of heparan sulfate glycosaminoglycan assembly in podocytes does not lead to proteinuria. *Kidney Int, 74*(3), 289-299. doi:10.1038/ki.2008.159

Christensen, E. I., & Birn, H. (2002). Megalin and cubilin: multifunctional endocytic receptors. *Nat Rev Mol Cell Biol, 3*(4), 256-266. doi:10.1038/nrm778

Christensen, E. I., Birn, H., Storm, T., Weyer, K., & Nielsen, R. (2012). Endocytic receptors in the renal proximal tubule. *Physiology (Bethesda), 27*(4), 223-236. doi:10.1152/physiol.00022.2012

Clark, S. J., Ridge, L. A., Herbert, A. P., Hakobyan, S., Mulloy, B., Lennon, R., . . . Day, A. J. (2013). Tissue-specific host recognition by complement factor H is mediated by differential activities of its glycosaminoglycan-binding regions. *J Immunol, 190*(5), 2049-2057. doi:10.4049/jimmunol.1201751

Condac, E., Dale, G. L., Bender-Neal, D., Ferencz, B., Towner, R., & Hinsdale, M. E. (2009). Xylosyltransferase II is a significant contributor of circulating xylosyltransferase levels and platelets constitute an important source of xylosyltransferase in serum. *Glycobiology, 19*(8), 829-833. doi:10.1093/glycob/cwp058

Condac, E., Silasi-Mansat, R., Kosanke, S., Schoeb, T., Towner, R., Lupu, F., . . . Hinsdale, M. E. (2007). Polycystic disease caused by deficiency in xylosyltransferase 2, an initiating enzyme of glycosaminoglycan biosynthesis. *Proc Natl Acad Sci U S A, 104*(22), 9416-9421. doi:10.1073/pnas.0700908104

Cravedi, P., & Remuzzi, G. (2013). Pathophysiology of proteinuria and its value as an outcome measure in chronic kidney disease. *Br J Clin Pharmacol, 76*(4), 516-523. doi:10.1111/bcp.12104

De Jong, P. E., Navis, G., & de Zeeuw, D. (1999). Renoprotective therapy: titration against urinary protein excretion. *Lancet, 354*(9176), 352-353. doi:10.1016/s0140-6736(99)90122-8

Ehara, T., Carone, F. A., McCarthy, K. J., & Couchman, J. R. (1994). Basement membrane chondroitin sulfate proteoglycan alterations in a rat model of polycystic kidney disease. *Am J Pathol, 144*(3), 612-621.

Garsen, M., Lenoir, O., Rops, A. L., Dijkman, H. B., Willemsen, B., van Kuppevelt, T. H., . . . van der Vlag, J. (2016). Endothelin-1 Induces Proteinuria by Heparanase-Mediated Disruption of the Glomerular Glycocalyx. *J Am Soc Nephrol, 27*(12), 3545-3551. doi:10.1681/ASN.2015091070

Goldberg, S., Harvey, S. J., Cunningham, J., Tryggvason, K., & Miner, J. H. (2009). Glomerular filtration is normal in the absence of both agrin and perlecan-heparan sulfate from the glomerular basement membrane. *Nephrol Dial Transplant, 24*(7), 2044-2051. doi:10.1093/ndt/gfn758

Groffen, A. J. A., Buskens, C. A. F., van Kuppevelt, T. H., Veerkamp, J. H., Monnens, L. A. H., & van den Heuvel, L. P. W. J. (1998). Primary structure and high expression of human agrin in basement membranes of adult lung and kidney. *European Journal of Biochemistry, 254*(1), 123-128. doi:10.1046/j.1432-1327.1998.2540123.x

Group, T. G. (1997). Randomised placebo-controlled trial of effect of ramipril on decline in glomerular filtration rate and risk of terminal renal failure in proteinuric, non-diabetic nephropathy. The GISEN Group (Gruppo Italiano di Studi Epidemiologici in Nefrologia). *Lancet, 349*(9069), 1857-1863.

Harvey, S. J. (2012). Models for studies of proteoglycans in kidney pathophysiology. *Methods Mol Biol, 836*, 259-284. doi:10.1007/978-1-61779-498-8_17

Harvey, S. J., Jarad, G., Cunningham, J., Rops, A. L., van der Vlag, J., Berden, J. H., . . . Miner, J. H. (2007). Disruption of glomerular basement membrane charge through podocyte-specific mutation of agrin does not alter glomerular permselectivity. *Am J Pathol, 171*(1), 139-152. doi:10.2353/ajpath.2007.061116

Hattori, T., Kimura, K., Seyrek, E., & Dubin, P. L. (2001). Binding of Bovine Serum Albumin to Heparin Determined by Turbidimetric Titration and Frontal Analysis Continuous Capillary Electrophoresis. *Analytical Biochemistry, 295*(2), 158-167. doi:https://doi.org/10.1006/abio.2001.5129

Hausmann, R., Kuppe, C., Egger, H., Schweda, F., Knecht, V., Elger, M., . . . Moeller, M. J. (2010). Electrical forces determine glomerular permeability. *J Am Soc Nephrol, 21*(12), 2053-2058. doi:10.1681/ASN.2010030303

Husson, H., Manavalan, P., Akmaev, V. R., Russo, R. J., Cook, B., Richards, B., . . . Ibraghimov-Beskrovnaya, O. (2004). New insights into ADPKD molecular pathways using combination of SAGE and microarray technologies. *Genomics, 84*(3), 497-510. doi:10.1016/j.ygeno.2004.03.009

Inker, L. A., Levey, A. S., Pandya, K., Stoycheff, N., Okparavero, A., & Greene, T. (2014). Early Change in Proteinuria as a Surrogate Endpoint for Kidney Disease Progression: An Individual Patient Meta-analysis. *American journal of kidney diseases : the official journal of the National Kidney Foundation, 64*(1), 74-85. doi:10.1053/j.ajkd.2014.02.020

Ishiguro, K., Kadomatsu, K., Kojima, T., Muramatsu, H., Matsuo, S., Kusugami, K., . . . Muramatsu, T. (2001). Syndecan-4 Deficiency Increases Susceptibility to κ-Carrageenan–Induced Renal Damage. *Laboratory investigation, 81*(4), 509-516.

Kanwar, Y. S., & Farquhar, M. G. (1979). Presence of heparan sulfate in the glomerular basement membrane. *Proceedings of the National Academy of Sciences, 76*(3), 1303-1307.

Katz, S., Hakki, A., Miller, A., & Finkelstein, S. (1989). Ultrastructural tubular basement membrane lesions in adult polycystic kidney disease. *Annals of Clinical & Laboratory Science, 19*(5), 352-359.

Lager, D. J., Qian, Q., Bengal, R. J., Ishibashi, M., & Torres, V. E. (2001). The pck rat: a new model that resembles human autosomal dominant polycystic kidney and liver disease. *Kidney Int, 59*(1), 126-136. doi:10.1046/j.1523-1755.2001.00473.x

Lelongt, B., Carone, F. A., & Kanwar, Y. S. (1988). Decreased de novo synthesis of proteoglycans in drug-induced renal cystic disease. *Proc Natl Acad Sci U S A, 85*(23), 9047-9051.

Livak, K. J., & Schmittgen, T. D. (2001). Analysis of relative gene expression data using real-time quantitative PCR and the 2(-Delta Delta C(T)) Method. *Methods, 25*(4), 402-408. doi:10.1006/meth.2001.1262

Masola, V., Gambaro, G., Tibaldi, E., Onisto, M., Abaterusso, C., & Lupo, A. (2011). Regulation of heparanase by albumin and advanced glycation end products in proximal tubular cells. *Biochimica et Biophysica Acta (BBA) - Molecular Cell Research, 1813*(8), 1475-1482. doi:https://doi.org/10.1016/j.bbamcr.2011.05.004

Miner, J. H. (2012). The glomerular basement membrane. *Exp Cell Res, 318*(9), 973-978. doi:10.1016/j.yexcr.2012.02.031

Munns, C. F., Fahiminiya, S., Poudel, N., Munteanu, M. C., Majewski, J., Sillence, D. O., . . . Hinsdale, M. E. (2015). Homozygosity for frameshift mutations in XYLT2 result in a spondylo-ocular syndrome with bone fragility, cataracts, and hearing defects. *Am J Hum Genet, 96*(6), 971-978. doi:10.1016/j.ajhg.2015.04.017

Rada, J. A., & Carlson, E. C. (1991). Anionic site and immunogold quantitation of heparan sulfate proteoglycans in glomerular basement membranes of puromycin aminonucleoside nephrotic rats. *The Anatomical Record, 231*(1), 35-47. doi:10.1002/ar.1092310106

Ruggenenti, P., Perticucci, E., Cravedi, P., Gambara, V., Costantini, M., Sharma, S. K., . . . Remuzzi, G. (2008). Role of remission clinics in the longitudinal treatment of CKD. *J Am Soc Nephrol, 19*(6), 1213-1224. doi:10.1681/asn.2007090970

Salmito, F. T., de Oliveira Neves, F. M., Meneses, G. C., de Almeida Leitao, R., Martins, A. M., & Liborio, A. B. (2015). Glycocalyx injury in adults with nephrotic syndrome: Association with endothelial function. *Clin Chim Acta, 447*, 55-58. doi:10.1016/j.cca.2015.05.013

Salmon, A. H., & Satchell, S. C. (2012). Endothelial glycocalyx dysfunction in disease: albuminuria and increased microvascular permeability. *J Pathol, 226*(4), 562-574. doi:10.1002/path.3964

Sanjana, N. E., Shalem, O., & Zhang, F. (2014). Improved vectors and genome-wide libraries for CRISPR screening. *Nat Methods, 11*(8), 783-784. doi:10.1038/nmeth.3047

Schumacher, V. A., Schlotzer-Schrehardt, U., Karumanchi, S. A., Shi, X., Zaia, J., Jeruschke, S., . . . Ai, X. (2011). WT1-dependent sulfatase expression maintains the normal glomerular filtration barrier. *J Am Soc Nephrol, 22*(7), 1286-1296. doi:10.1681/ASN.2010080860

Stahl, K., Hegermann, J., Njau, F., Schroder, P., Staggs, L. B., Hanke, N., . . . Haller, H. Knockdown of Glypican-1 and 5 isoforms causes proteinuria and glomerular injury in zebrafish (Danio rerio).

Staples, A., & Wong, C. (2010). Risk Factors for Progression of Chronic Kidney Disease. *Current opinion in pediatrics, 22*(2), 161-169. doi:10.1097/MOP.0b013e328336ebb0

Sugar, T., Wassenhove-McCarthy, D. J., Esko, J. D., van Kuppevelt, T. H., Holzman, L., & McCarthy, K. J. (2014). Podocyte-specific deletion of NDST1, a key enzyme in the sulfation of heparan sulfate glycosaminoglycans, leads to abnormalities in podocyte organization in vivo. *Kidney International, 85*(2), 307-318. doi:10.1038/ki.2013.281

Takahashi, N., Chernavvsky, D. R., Gomez, R. A., Igarashi, P., Gitelman, H. J., & Smithies, O. (2000). Uncompensated polyuria in a mouse model of Bartter's syndrome. *Proceedings of the National Academy of Sciences, 97*(10), 5434-5439. doi:10.1073/pnas.090091297

Takashima, Y., Keino-Masu, K., Yashiro, H., Hara, S., Suzuki, T., van Kuppevelt, T. H., . . . Nagata, M. (2016). Heparan sulfate 6-O-endosulfatases, Sulf1 and Sulf2, regulate glomerular integrity by modulating growth factor signaling. *Am J Physiol Renal Physiol, 310*(5), F395-408. doi:10.1152/ajprenal.00445.2015

Terryn, S., Tanaka, K., Lengelé, J.-P., Olinger, E., Dubois-Laforgue, D., Garbay, S., . . . Devuyst, O. (2016). Tubular proteinuria in patients with HNF1α mutations: HNF1α drives endocytosis in the proximal tubule. *Kidney International, 89*(5), 1075-1089. doi:10.1016/j.kint.2016.01.027

USRDS. (2017). US Renal Data System 2016 Annual Data Report: Epidemiology of Kidney Disease in the United States. *Am J Kidney Dis, 69*(3s1), A4. doi:10.1053/j.ajkd.2017.01.036

Vogt, L., Waanders, F., Boomsma, F., de Zeeuw, D., & Navis, G. (2008). Effects of dietary sodium and hydrochlorothiazide on the antiproteinuric efficacy of losartan. *J Am Soc Nephrol, 19*(5), 999-1007. doi:10.1681/asn.2007060693

Watts, R. H. (1971). A simple capillary tube method for the determination of the specific gravity of 25 and 50 micro l quantities of urine. *Journal of Clinical Pathology, 24*(7), 667-668.

Weyer, K., Storm, T., Shan, J., Vainio, S., Kozyraki, R., Verroust, P. J., . . . Nielsen, R. (2011). Mouse model of proximal tubule endocytic dysfunction. *Nephrol Dial Transplant, 26*(11), 3446-3451. doi:10.1093/ndt/gfr525

Yung, S., Woods, A., Chan, T. M., Davies, M., Williams, J. D., & Couchman, J. R. (2001). Syndecan-4 up-regulation in proliferative renal disease is related to microfilament organization. *The FASEB Journal, 15*(9), 1631-1633. doi:10.1096/fj.00-0794fje

CHAPTER IV

XYLOSYLTRANSFERASE I DEFICIENCY RESULTS IN DECREASED PULMONARY FUNCTION AND EXACERBATED RESPONSE TO LIPOPOLYSACCHARIDE INDUCED ACUTE LUNG INJURY

Abstract

The lung's Extracellular matrix (ECM) is responsible for maintaining tissue structural integrity as well as a significant component of the air-blood gas exchanged. Proteoglycans (PGs) are integral components of the ECM. PGs consist of PG core proteins covalently linked with glycosaminoglycan (GAG) chains. The assembly of GAG chains onto the PG core protein is initiated by addition of xylose to specified serine residues of the PG core protein by xylosyltransferase (XylT) that consists of two distinct isoforms: XylT1 and XylT2. Though XylT2 is the predominant XylT isoform in the lungs, XylT2 deficient mice have normal lung function. We investigated on the role of the minor isoform XylT1 in pathophysiology of the lungs. To investigate their role in maintenance of pulmonary ECM and function, we measured multiple key physiologic parameters of respiratory function in novel conditional *Xylt1* knockout mice. The data suggest that loss of the XylT1 dependent GAGs on the PGs affects respiratory function in multiple areas of the lung. Furthermore, challenging XylT1 deficient mice with lipopolysaccharide (LPS) causes an exacerbated response associated with decrease PG core protein mRNA expression, altered surfactant protein, and cluster of differentiation 14 (Cd14) expressions and hyperactivation of Tlr4 mediated NFkB signaling. Together, our data suggest that PGs and the XylT1 dependent GAGs associated with them are important for maintaining pulmonary dynamics and also pulmonary innate defense mechanisms via a previous unknown mechanism of regulation of surfactant proteins and Cd14.

4.1 Introduction

The alveolar extracellular region comprises the fused BMs of epithelial and endothelial cells and the extracellular matrix (ECM). Proteoglycans (PGs) are O-serine glycoconjugated proteins that have a core protein covalently assembled with glycosaminoglycan (GAGs) chain(s) bridged to the core protein by a linker tetrasaccharide structure. PGs are present in the ECM, basement membrane (BM), surface of alveolar epithelial cells (AEC), and also in the endothelial

glycocalyx of the capillary lumen. In the ECM, PGs stabilize the collagen and elastin fibers to maintain alveolar stability and pulmonary elasticity(Cavalcante et al., 2005; Fust, LeBellego, Iozzo, Roughley, & Ludwig, 2005), maintain pulmonary fluid equilibrium by providing a highly charged fluid repellent environment, and restricting transendothelial fluid transport(Negrini, Passi, & Moriondo, 2008), as well as sequestering various growth factors and ligands involved in many signaling pathways (Babelova et al., 2009; Neill, Schaefer, & Iozzo, 2012; Schaefer et al., 2005).

The biology and nature of PGs is tightly regulated to maintain respiratory homeostasis and with disease shifts in levels, types, and location of PGs occurs to reestablish functional homeostasis (Blackwood, Cantor, Moret, Mandl, & Turino, 1983; Fust et al., 2005; Karlinsky, Bucay, Ciccolella, & Crowley, 1991; Merrilees et al., 2008). Animal knockouts for various enzymes in the PG assembly have defective alveolar formation (Habuchi et al., 2007), respiratory distress(Ringvall et al., 2000) and defective maturation of AEC II cells resulting in failure of these cells to secret surfactant proteins(Fan et al., 2000).

Despite the fact that PGs are potential regulators of pathophysiology in the lungs, there is lack of information on the exact mechanism of how the PGs regulate, and are regulated, during pulmonary disease. Study of such complex physiological functions requires in vivo models. Therefore, development of animal models to investigate the impact of alterations in PGs and their effect during respiratory disease is needed. Current animal models for the study of PG GAG chain alterations either die at early embryo stage (Habuchi et al., 2007) and/or perinatally (Fan et al., 2000; Ringvall et al., 2000). Fortuitously, the *Xylt2* knockout mice have a late onset of cystic liver and alterations in kidney pathology and lack any distinct pulmonary phenotype even though *Xylt2* is the predominant transcript of the two isoforms in the lungs. (Condac et al., 2007). For XylT1, there exists a mouse model with a hypomorphic *Xylt1* allele, which has skeletal defects and early chondrocyte maturation. Some neonatal mice do not make it to adulthood. No pulmonary

phenotype was found in this mouse (Mis et al., 2014). In this paper, we present a novel conditional *Xylt1* knockout animal model with a distinct pulmonary phenotype demonstrating role of XylT1 dependent PGs in lung homeostasis. Our findings establish that, though being the minor XylT isoform in the lungs, XylT1 dependent GAGs are important in respiratory homeostasis as well as in respiratory innate immunity. Therefore, this XylT1 deficient mouse model is a unique mouse model to study the pathophysiologic and homeostatic impact of respiratory PGs.

4.2 Materials and Methods

4.2.1. Animals

Generation of Xylt2-/- (*Xylt2-/-*) mice has been described already (Condac et al., 2007). *Xylt2-/-* mice were backcrossed to 129/S6SvEvTac mice for 8 generations. Targeted *Xylt1-/-* mice were generated using similar technique as previously described (Condac et al., 2007). Targeting homology arms were generated using bacterial artificial chromosome (BAC) fragment containing the *Xylt1* locus. But briefly, the construct was generated by ligating *FLP* recombination sites to surround a neomycin selection cassette (*Neo*) of which were inserted into intron 1 of the *Xylt1* locus. In addition, *loxP* sites were inserted 5' to exon 1 and 3' to *Neo*. Once homologous recombination was confirmed by Southern blot analyses in the ES cells (See Fig. 4.1), the *Neo* cassette was removed using the *FLP* recombination sites (data not shown). This creates an intact *Xylt1* locus that when exposed to *Cre* recombinase will delete exon 1 creating a null *Xylt1* allele. Gene targeting in E14 ES cells, zygote injection and chimera production was done using previously described techniques (Condac et al., 2007).

4.2.2 Induction of *Xylt1* deletion in *Xylt1* targeted mice

*Xylt1*targeted mice (*Xylt1 fl/fl*) were backcrossed to B6.Cg-Tg (CAG-cre/Esr1*) 5Amc/J, (*CaggCre+*) for 9 generations this line is on a C57Bl/6J background. This generated the global deletion model for *(Xylt1 fl/fl; CaggCre+)*. In addition, for endothelial specific knock out of *Xylt1*, the *Xylt1 fl/fl* mice were crossbred with VE-Cadherin-Cre (Jackson laboratory#006137) to

generate conditional *Xylt1* targeted (*Xylt1 fl/fl; VECre+)* mice for endothelial deletion of *Xylt1*. Both the *CaggCre+* and the *VECre+* mice are tamoxifen responsive Cre recombinase. For inducing conditional deletion globally of *Xylt1* (*Xylt1-/-;CaggCre+)*, mice were either injected with 1mg/Kg BW dose of tamoxifen citrate (US pharmacopeia) for 5 days or fed tamoxifen containing diet (Envigo, USA) for 15 days post weaning, followed by 15 days of tamoxifen withdrawal period. Initial body weights were recorded daily then they were recorded twice a week during and after the tamoxifen exposure to monitor body weight changes due to tamoxifen. Littermate CaggCre- (*Xylt1 fl/fl; CaggCre-*) mice exposed to tamoxifen were used as controls.

Xylt2 and *Xylt1* VE-cadherin double knockout mice (*Xylt2-/-; Xylt1-/-; VECre+)* were generated by crossbreeding *Xylt2+/-* with VE-cadherin-Cre Xylt1 knockout mice (*Xylt1-/-; VECre+*) followed by tamoxifen exposure post weaning. Littermate VECre+ (*Xylt2+/-; Xylt1fl/fl; VECre+*) mice were used as controls. Littermate control mice went through same diet regimen as of conditional knockout animals. Mice were kept in BSL2 barrier facility with ad libitum amount of food and water intake. All the procedures and protocols were approved by Institutional Animal Use and Care Protocol.

4.2.3 Pulmonary functions measurement

Mice were anaesthetized using a mixture of Xylazine (10mg/kg) and Ketamine (80mg/Kg) and Tracheostomy was performed by ventral midline cervical incision to expose trachea followed by insertion and ligation of an18 gauge cannula into the trachea. Lung function measurements were performed in tracheostomized mice using SCIREQ FlexiVent (Montreal, Canada). The instrument and techniques have been already compared and validated with other types of mechanical ventilator systems (Vanoirbeek et al., 2010). Ventilation was performed by using a tidal volume of 10 ml/Kg, respiration of 150 breaths/minute and positive end-expiratory pressure of 2 Cm.H_2O. Six types of respiratory maneuvers were performed: Deep Inflation (DI),

Snapshot (SS), broadband force oscillation technique (FOT), pressure volume loops generated by stepwise-volume regulated breathing (PVs-V), and negative pressure force expiration (NPFE).

DI was performed by using a single breathing event with a pressure of 30 Cm.H_2O with achievement of plateau in three seconds and maintenance for several seconds to determine inspiratory capacity (IC). During SS, a standardized single sinusoidal waveform was used to determine resistance (R), elastance (E) and compliance (C) of total respiratory system. During broadband FOT, a wide range of frequencies from 1 to 20 Hertz involving frequencies below and above subject's breathing frequency were used to determine Newtonian resistance (Rn), tissue damping (G), and tissue elastance (H). PVs-V was used to measure quasi-static compliance (Cst) to estimate intrinsic elastic properties of lungs and chest. The NPFE maneuver was performed by application of sudden negative pressure to the lungs to measure forced expiratory volume (FEV), forced expiratory flow (FEF), forced vital capacity (FVC), and peak expiratory flow (PEF). A coefficient of determination of 0.95 was used to exclude erroneous readings. The resulting parameters were analyzed using Flexiware v7.0 software. An average of three measurements was used as the final value for the parameters for each mouse.

4.2.4. Histopathology and trichrome staining

Mice were euthanized using isoflurane and lungs were infused with 500 microliters of 4% paraformaldehyde. Whole plunk was then fixed in 4% paraformaldehyde overnight followed by trimming and embedding in paraffin cassettes. Five micrometer thick sections were made and stained with H & E staining and Sirius red staining using previously described protocol (Condac et al., 2007).

4.2.5. Intranasal LPS challenge

Mice were anaesthetized with Xylazine and Ketamine. LPS from E coli O111:B4 (Sigma#L630) was administered intranasally at a dose of 5 mg/Kg BW in a final volume of 50 µl/

mouse with each 5-10 µl drop alternating between two nostrils. After 24 hours, mice were sacrificed and tissues were harvested and flash frozen in liquid nitrogen.

4.2.6. Collection and analysis of bronchoalveolar lavage fluid (BALF)

Twenty four hours after LPS administration, mice were euthanized using isoflurane and tracheostomy was performed. Lungs were inflated with 750 ul of PBS twice to collect BALF. BALF was centrifuged at 4000x g for 5 minutes at 4C. The supernatant was harvested for protein analysis. Total BALF cells were counted using haemocytometer. To estimate the total number of red blood cells, hypotonic RBC lysis buffer was used to lyse red blood cells in the BALF and cells remaining in BALF were counted again. The cell count after RBC lysis was subtracted from cell count before RBC lysis. An aliquot of resuspended cells was centrifuged in cytospin slides for differential leukocyte counting. Protein content in BALF was estimated by BCA reagent using manufacturer's protocol.

4.2.7. Cytokine array in BALF

Cytokine array in BALF was performed using RayBiotech mouse cytokine array -C3 kit (RayBiotech, Norcorss, GA, USA) according to manufacturer's protocol. Briefly, the membranes were wetted and capture antibodies were added and incubated for 2 hours. 500 ul of BALF was applied to the membrane and incubated overnight at 4C with rocking followed by washing and incubation with streptavidin conjugated secondary antibody. The membranes were washed and Chemiluminescence was detected using GE Amersham 600 imager after incubation of membrane with Chemiluminescence substrate provided with the kit. Post-imaging densitometric analysis was performed using NIH-Image J software using Positive control spots in the membrane as reference spots to compare expression in two different membranes.

4.2.8. Real-time RTPCR

The protocol for real-time RTPCR has already been described in section 3.2.10. Primers used for the experiments are listed in table 4.1.

4.2.9. Protein Isolation and Western blotting

Flash frozen lung tissues were homogenized into 1:10 volume of RIPA lysis buffer with protease and phosphatase inhibitors. Homogenates were incubated on ice for 1 hour followed by centrifugation at 10,000 rpm for 30 mins at 4^0C and supernatant collected for further analysis. Protein concentration was measured using BCA assay (Thermo Scientific) as per manufacturer's instruction. 25-50 micrograms of protein were subjected for Western blotting as described in section 3.2.7. List of primary and secondary antibodies are available on Table 4.2 with sources and dilutions used for the experiment. For western blotting of PG proteins, samples were incubated with either Chondroitinase ABC (Seikagaiku) or Heparitinase III (NEB) overnight to digest the GAG chains before SDS PAGE.

4.2.10 Statistical Analysis

Statistical analysis was performed as described in section 3.2.12.

4.3 Results

4.3.1. XylT1 deficient mice have altered pulmonary dynamics

Lungs express both isoforms *Xylt1* and *Xylt2*, with XylT2 contributing 70% of XylT activity in the lungs (Sivasami, manuscript in preparation). However, *Xylt2* knockout mice have normal lung morphology and histology and do not show any alterations in respiratory parameters (Sivasami, manuscript in preparation). Given that PGs are critical to the function of ECM and basement membrane homeostasis and that the XylT2 deficient mice lack a pulmonary defect. XylT1 must be critical to pulmonary homeostasis. There is the possibility that XylT2 and XylT1 have differential substrate specificities and potentially unique cellular differences in expression.

Therefore, we hypothesized that the lesser isoform *Xylt1* is more important to respiratory homeostasis.

To test our hypothesis, we assessed mechanical and pulmonary function in conditional *Xylt1* knockout mice. These investigations using Deep Inflation perturbation showed an overall decrease in inspiratory capacity of *Xylt1-/-;CaggCre+* mice for both females and males (Fig 4.2 A). Snapshot perturbation showed an increase in total lung resistance (Rrs), elastance (Ers) and decrease in compliance (Crs) of *Xylt1-/-; CaggCre+* mice and compared to controls (Fig 4.2 C, D, and E). To identify the mechanical reasons for the abnormal flexiVent findings, broadband FOT perturbation was used to measure Newtonian resistance (Rn), tissue damping (G) and tissue elastance (H). *Xylt1-/-; CaggCre+* male mice had an increase in all three parameters while the females had an increasing trend for Rn (Fig 4.2 E) but G and H were significantly higher than littermate controls similar to the males (Fig 4.2 F and G). PVs-P perturbation was used to estimate lung static compliance (Cst) during the fully inflated position. In both genders, Cst was significantly reduced in *Xylt1-/-; CaggCre+* mice compared to their littermate controls (Fig 4.2 H). To further understand the mechanism and degree of fibrosis, lungs were examined histopathologically.

4.3.2. XylT1 deficient mice have mild increase in fibrosis in the lungs and reduced expression of PG core proteins

Increase in total lung resistance (Rrs), decrease in inspiratory capacity (IC), decreased compliance (Crs), increased tissue damping (G) and tissue elastance (H) are typical characteristic of fibrosis in the lungs (Vanoirbeek et al., 2010). To measure the extent of fibrosis in *Xylt1-/-; CaggCre+* mice, we examined the lungs for fibrotic changes by Mason's trichrome staining. While the lungs from littermate controls had normal gross histological structures (Fig 4.3 A and C), gross and histological structures in *Xylt1* deficient lungs were relatively normal except for some mild to almost absent fibrosis around peribronchial areas (Fig 4.3 B and D).

We then performed real-time RTPCR in the lungs to measure levels of various PG related genes. Real-time RTPCR showed a significant reduction in mRNA levels of *Xylt1* in *Xylt1-/-;CaggCre+* mice lungs while *Xylt2* mRNA expression was unchanged (Fig 4.3 E) confirming that the conditional deletion of *Xylt1* had occurred. We also observed a significant reduction in mRNA level expression of surface associated PGs Syndecan-1 and Syndecan-4, which facilitate clearance of chemokines from the lungs after inflammatory insult (Li, Park, Wilson, & Parks, 2002; Tanino et al., 2012). Based on these observations, we hypothesized that *Xylt1-/-;CaggCre+* mice are more susceptible to LPS induced acute lung injury than wild type mice. To test our hypothesis, we challenged the mice with intranasal LPS and analyzed the BALF as well as lung tissue for the severity of inflammation.

4.3.3 *Xylt1* conditional knockout mice have exacerbated response to LPS induced acute lung injury

Xylt1-/-;CaggCre+ mice were challenged with intranasal *E. coli* LPS at 5 mg/Kg BW dose in a total volume of 50 µl. At 24 hours post inoculation, body weight changes, BALF and lung tissues were analyzed for severity of inflammation. We saw significantly higher cellular infiltration in the alveolar space of the *Xylt1-/-;CaggCre+* mice as revealed by increased BALF cell count (Fig 4.4 A). Measurement of total protein accumulation in the BALF showed significantly higher protein amount in the BALF from the Xylt1 conditional knockout mice when compared with wild-type littermates (Fig 4.4 B). There was also an overall increase in BALF RBC numbers (Fig 4.4 C) and a visibly higher sanguineous color of the BALF from *Xylt1-/-;CaggCre+* mice (Fig 4.4 D), suggesting a vascular permeability defect.. These findings strongly suggest that innate immunity regulation or control is compromised in the XylT1 deficient lungs when challenged with LPS.

To understand the mechanism of increased susceptibility to LPS in *Xylt1-/-; CaggCre+* mice, we performed cytokine array in BALF collected from LPS challenged mice. Since both

males and females share similar phenotypes, investigations on mechanisms were focused only on male cohorts. Figure 4.5 E and F show the results from BALF cytokine array analyses of *Xylt1fl/fl;CaggCre-* and *Xylt1-/-;CaggCre+* mice, respectively. There was an increase in BALF levels of the neutrophil chemoattractants, Mip2 and Vcam1 (Fig 4.4 E and F). Surprisingly, in the BALF of *Xylt1-/-;CaggCre+* mice, the pro-inflammatory cytokines Il-1β and Tnf-α levels were unchanged while Il-12 and Il-6 levels were decreased. Furthermore, anti-inflammatory cytokine Il-10 was unchanged in the *Xylt1-/-;CaggCre+* BALF. We did observed changes in other cytokines that were indirectly related to the innate and adaptive immune responses (see Table 4.3 and 4.4). To validate the source of these changes at the gene expression level, we next performed real-time RTPCR on LPS challenged lung tissue.

4.3.4 *Xylt1* conditional knockout mice had increased proinflammatory cytokine expression in the lungs

Lung tissue real-time RTPCR on LPS challenged mice showed about a 70% loss in *Xylt1* mRNA expression in *Xylt1-/-; CaggCre+* mice (Fig 4.5 A) thus again confirming deletion of the *Xylt1* locus. The mRNA level expression of *Xylt2* was also significantly downregulated in *Xylt1-/-;CaggCre+* mice lung (Fig 4.5 A). Measurement of mRNA levels of various cytokines showed that the expression of neutrophil chemoattractant Mip-2 (*Cxcl3*) was upregulated in the lungs while KC (*Cxcl1*) was unchanged (Fig 4.5 C) correlating with the cytokine levels in BALF (Fig 4.5 B); however, *Vcam-1* expression was significantly reduced in *Xylt1-/-; CaggCre+* mice (Fig 4.5 C) as opposed to the observation of increased BALF Vcam-1 levels (Fig 4.4 F), indicating a post-transcriptional and/or post-translational regulation of Vcam-1 levels. Similar to *Vcam-1*, we saw contrasting results between mRNA levels expression of lung *Il-1b* and its protein level in the BALF (Fig 4.5 B). Expression of *Il-12b* was reduced (Fig 4.5 B), correlating with reduced protein level in the BALF of *Xylt1-/-;CaggCre+* mice, however, the smaller subunit of Il-12, *Il-12a* was upregulated in the lungs of *Xylt1-/-; CaggCre+* mice (Fig 4.5 and C). Other pro-inflammatory

cytokines *Il-6*, and *Tnfa* mRNA and anti-inflammatory cytokine *Il-10* mRNA expressions were unaltered in *Xylt1-/-; CaggCre*+ mice lungs correlating with BALF levels (Fig 4.5 B). These findings suggest a pro-inflammatory environment in the Xylt1 deficient lungs.

4.3.5. *Xylt1* conditional knockout mice show vascular permeability defects

Since *Xylt1-/-; CaggCre*+ mice had no differential increased in any cell type in the alveolar space despite having an overall increase in total cellular infiltration including RBCs, the findings indicate a vascular permeability change in the pulmonary endothelium. To investigate this we examined the levels of Vegfa protein in the BALF and mRNA in the lung tissue. We did not see any change in Vegfa levels in the BALF, but *Vegfa* mRNA levels were downregulated in the *Xylt1-/-; CaggCre*+ mice after LPS treatment (Fig 4.5 C) suggesting a propensity for increased permeability in the tissue.

4.3.6. Exacerbated response to LPS challenge in conditional Xylt1 knockout is mediated by increased TLR4 signaling

Given that LPS stimulates innate immunity via Tlr4 receptor by activating NF-κB signaling pathway (Poltorak et al., 1998), we performed real-time RTPCR expression of *Cd14* and *Tlr4* mRNA levels in lung tissue from *Xylt1-/-; CaggCre*+ mice and saw significant upregulation of *Cd14* and *Tlr4* mRNA levels (Fig 4.6 A). LPS mediated Tlr4 activation subsequently activates NF-κB through Myd88 dependent signaling and MAPK through MyD88 independent signaling through Erk1/2 pathway. Next we measured phosphorylation levels of the p65 subunit of NF-κB pathway as well as Erk1/2 of MAPK pathway to assess the activity of those pathways. Although we saw a decrease in total NF-κB in *Xylt1-/-; CaggCre*+ mice lungs, there was a significant increase in Ser536 phosphorylation of NF-κB as compared with littermate controls (Fig 4.6 B). Western blotting of phosphorylated Erk1/2 showed no changes in the Erk1/2 activity levels in *Xylt1-/-; CaggCre*+ mice compared to littermate controls (Fig 4.6 C).

These findings suggest that the exacerbated response to LPS during *Xylt1* deficiency is due to upregulation of NF-κB signaling pathway mediated through MyD88 dependent signaling.

PGs are important modulators of multiple steps know important in inflammatory cell recruitment and the initiation of an innate immune response (Gill, Wight, & Frevert, 2010). PGs known to affect these processes are ECM PGs decorin, versican, biglycan, and lumican, as well as surface associated PGs syndecan-1 and syndecan-4. Since these are all candidate effectors of the lung phenotype in the *Xylt1-/-; CaggCre+* mice, we began our investigations into identifying candidate core proteins. We performed western blotting for decorin to look at levels and glycosylation of decorin in lung tissue of the *Xylt1-/-; CaggCre+* mice. We did not see any difference in either the glycosylation of decorin (Fig 4.6 D) or the total protein levels suggesting decorin is not likely involved in the phenotype observed in *Xylt1-/-; CaggCre+* mice. Biglycan and syndecans 1 and 4 mRNA level expression in unchallenged *Xylt1-/-; CaggCre+* mice were found to be decreased as compared to those PGs in the unchallenged *Xylt1-/-; CaggCre+* mice (Fig 4.3 E). However, syndecan-1 and syndecan-4 may be mechanistically involved after LPS exposure in *Xylt1-/-; CaggCre+* mice, since real-time RTPCR measurements show an increase in Syndecan-1 and Syndecan-4 mRNA levels in XylT1 deficient lungs to the levels of littermate controls (Fig 4.5 A). These findings suggest that syndecan levels are more affected in XylT1 deficiency and possibly contribute to exacerbation of LPS induce acute lung injury.

4.3.7 Xylt1 deficiency causes alterations in surfactant biology in the lungs

Our next question was how the surfactant proteins are affected during Xylt1 deficiency since alterations in GAGs in HS N-deactylase and sulfotransferase (*Ndst*-1) knockout mice resemble neonatal respiratory distress syndrome in mice associated with defective AEC type 2 cells and a decrease in phospholipid content in the lungs.(Fan et al., 2000) Therefore, we hypothesized that the surfactant proteins (Sp) are altered in Xylt1 deficient lungs. To test our hypothesis, we performed real-time RTPCR and western blotting to investigate Sp-D and Sp-A

levels in the lungs. We observed a significant reduction in mRNA expression of Sp-A and Sp-D in the XylT1 deficient lungs (Fig 4.7 A). Furthermore, upon LPS exposure, the wild type mice had a significant upregulation of Sp-D while there was a trend of upregulation of Sp-A as compared to wild type mice unexposed (Fig 4.7 B). Interestingly, even after LPS challenge, XylT1 deficient lungs fail to upregulate the Sp-D mRNA expression (Fig 4.7 C) as the wild type mice do. However, when comparing Sp-D protein levels in the lungs, XylT1 deficient lungs had significantly higher Sp-D protein levels (Fig 4.7 D) suggesting an abnormality in Sp-D secretion by the AECs. It has been already proven that GAG deficiency can result in defective surfactant secretion as seen in *Ndst-1* knockout mice (Fan et al., 2000). Our findings indicate that, during GAG deficiency due to loss of XylT1, after LPS exposure, there are increased levels of Sp-D protein in the lungs, but the mRNA is downregulated, suggestive of a mechanism of disrupted Sp-D secretion from the lung cells into the BALF. Although this hypothetically makes sense, we have yet to determine how reduced GAGs would prohibit Sp-D secretion and this needs to be further investigated.

4.3.8 Real-RTPCR on XylT isoforms in the lungs cell type indicates likelihood of Xylt2 dominancy

Since there is a differential expression of the XylT isoforms in multiple cell types and tissues (Condac et al., 2007; Cuellar, Chuong, Hubbell, & Hinsdale, 2007) we next wanted to investigate the cell-type expression pattern of XylT isoforms in various pulmonary cell types with the idea to identify candidate cell types affected in the *Xylt1-/-; CaggCre+* mice. We measured mRNA expression of *Xylt1* and *Xylt2* in the lung tissue as well as in the various cell types present in the lungs to identify those cell type(s) critically dependent on *Xylt1* expression. We performed real-time RTPCR for relative mRNA expression levels of *Xylt1* and *Xylt2* on RNA from mouse AEC type I, AEC type II, pulmonary fibroblasts (All a generous gift from Dr. Lin Liu of the Oklahoma Center for Respiratory and Infectious Diseases Center and director of its Molecular Biology Core) and primary human coronary artery endothelial cells (a kind gift from Dr. Pamela

Lovern). We observed a dominant expression of *Xylt2* over *Xylt1* ranging from two to 12 folds in various cell types present in the lungs, and we saw a higher expression of *Xylt2* in endothelial cells (Fig 4.8). Assuming that the primers for both *Xylt2* and *Xylt1*have similar efficiencies, we can speculate a likelihood of dominance of *Xylt2* expression in various lung cell types. The data needs to be further verified by measuring residual XylT activity in lung tissues of Xylt1 knockout mice and/or by measuring protein levels of XylT isoforms in the lungs and various lung cell types. However, given our results in the *Xylt1-/-; CaggCre*+ mice, though likely being the minor isoform, *Xylt1* must have a significant role in GAG assembly in the lungs such that there might be specific core proteins dependent on XylT1 that are critical to pulmonary homeostasis.

4.3.9 Endothelial proteoglycans do not contribute for maintenance of pulmonary dynamics

To investigate the specific roles that endothelial XylT1 dependent GAGs have in pulmonary function, we generated endothelial specific *Xylt1* knockout mice and performed respiratory function analysis similar as to that for the *Xylt1-/-; CaggCre*+ mice. Interestingly, we observed no change in respiratory dynamics in endothelial specific *Xylt1* knockout mice except for Rrs and G (Fig 4.9 B and F), however, when *Xylt2* was deleted in all cell types in conjunction with an endothelial specific deletion of *Xylt1*, a similar FlexiVent phenotype was observed as seen in the total conditional *Xylt1* knockout mice (i.e. *Xylt1-/-; CaggCre*+ mice) (Fig 4.9) suggesting that the phenotype in *Xylt1-/-; CaggCre*+ mice is not exclusively arising from altered endothelial GAG levels but likely due to a loss of GAGs in the cells that make up the blood air exchange barrier including the endothelial cells and that the phenotype in the *Xylt1-/-; CaggCre*+ mice is more due to decreased GAG levels in this barrier than anything else. Critical to elucidating these relationships are future mouse lines that have a specific deficiency of *Xylt1* in endothelial cells and AEC type I cells.

4.5. Discussion

Here in this paper we show that XylT1 deficiency causes altered pulmonary dynamics as well pulmonary innate immunity in response to an endotoxin challenge. PGs provide architectural support to form collagen fibers (Raspanti, Alessandrini, Ottani, & Ruggeri, 1997) and removal of GAGs in-vitro results in lung tissue increased resistance (Jamal, Roughley, & Ludwig, 2001). Our findings that *Xylt1-/-; CaggCre+* mice have altered pulmonary dynamics support that PGs are important mediators of pulmonary dynamics and elasticity. Findings from SS perturbation in FlexiVent® analyses show that *Xylt1-/-; CaggCre+* mice have an overall increase in resistance and a decrease in the compliance of the lungs. The increase in resistance is correlated with increase in airway resistance as well as lung tissue resistance suggesting that in the *Xylt1* knockout mice glycosylation defects in the upper airways and lung parenchyma contribute to the pulmonary abnormalities and thus XylT1 dependent GAGs are important in these areas for pulmonary functionOur findings are in concord with previous findings that *in-vitro* removal of chondroitin sulfate GAGs results in increased pulmonary resistance(Jamal et al., 2001). In addition this gives insight in possible roles of GAGs in maintaining airway resistance. Other factors including substrate specificity of the XylT isoforms and possible interactions between the XylT isoforms could also contribute to the phenotype. This needs to be further investigated.

Our findings also show that *Xylt1* knockout mice have decrease pulmonary compliance and increased pulmonary elastance. The increased elastance or stiffneess of the lungs should be considered with decreased compliance as pulmonary compliance is inversesly correlated with pulmonary compliance. The decrease in compliance in *Xylt1* knockout mice could be a result from the decreased quasistatic compliance of the lungs due to fibrotic change. It has been already been shown that PG deficiency due to XylT2 deficiency causes fibrosis in the liver and a mild increase in fibrosis in the kidney in *Xylt2* knockout mice (Condac et al., 2007). Here, we show

that in in *Xylt1-/-; CaggCre+* mice, there is a very mild to no increase in collagen deposition in peribronchial areas. The increase in resistance associated with a decrease in compliance and this slight increase in collagen deposition in peribronchial regions suggests that physiologic changes from *Xylt1* deletion could in part be due to fibrotic change of the lungs, but it does not fully explain the phenotype. Deficiency of GAGs or PG core proteins results in biological dysfunction by altering their bioavailability and biochemical characteristics (Rühland et al., 2007). Our findings show that during XylT1 deficiency, expression of various PG core proteins is altered. These changes could be impacting tissue homeostasis. Moreover, the findings indicate that the presence of GAG chains may play an important role in expression of the PG core proteins syndecan-1, syndecan-4, and biglycan, subsequently affecting their bioavailability and susequent physiological function. Lastly, we speculate that levels of the additional surfactants like Sp-B and Sp-C may be affected and leading to increased resistence and elastance and decresased sompliance. This is under investigation.

Our *in-vivo* LPS challenge experiments show that XylT1 deficiency exacerbates the response to LPS challenge. The increase in inflammation likely results from an increase in NF-κB-p65 phosphorylation which coorelates with a decrease in *Sftpd* and increases in *Cd14* and *Tlr4* mRNA expression. In addition, this augmented response is associated with decrease in mRNA expression of PG core proteins Syndecan-1, Syndecan-4,and Biglycan. LPS induces innate immune response via Tlr4 mediated activation of NF-kB through activation of Myd88 dependent pathway (Lu, Yeh, & Ohashi, 2008). We saw an increase in expression of basal levels of *Cd14* in XylT1 deficient lungs, and during LPS challenge, *Cd14* is upregulated even higher with LPS challenge when compared with the controls. This is significant since Cd14 facilitates the binding of LPS to the surface Tlr4 to induce activation of inflammatory reaction (Frey et al., 1992). These findings demonstrate that one cause of augmented LPS response during XylT1 deficiency is due to increased NF-kB activation.

We also observed that the levels of surfactant proteins, especially Sp-D is downregulated in *Xylt1-/-; CaggCre+* lungs. During LPS exposure, the levels of surfactant proteins normally rise to opsonize and facilitate the phagocytosis of unbound LPS in the lungs. Sp-D specifically acts to quell the repsonse to LPS by binding to multiple components of Tlr4 signaling including Tlr4 itself. Similar to studies from others, we observed a normal surfactant expression increase in Sp-D in response to LPS in control mice (Gaunsbaek, Rasmussen, Beers, Atochina-Vasserman, & Hansen, 2013; Yamazoe et al., 2008) . However, in the XylT1 deficient mice, the levels of surfactant proteins Sp-A and Sp-D failed to upregulate to wildtype levels after LPS exposure. We speculate that the defective glycosylation may lead to reduced protein folding in the endoplasmic reticulum leading to defective secretion of Sp-D. Since Sp-D is known to have a lectin binding domain, this domain when inappropriately exposed to other misfolded proteins may inappropriatly aggregate and not be secreted properly. This in combination with high *Cd14* levels creates an envrionment of increased Tlr4 pathway activation due to the inability of lung defense mechanism to neutralize unbound LPS leading to higher occupancy of Tlr4 and a hyperstimulation Tlr4 pathway by LPS.

The relatively low amounts of PGs Syndecan-1 and Syndecan-4 play an additional role in this proinflammatory environment. Syndecan-1 and Syndecan-4 are known to shed their ectodomains with the GAGs during inflammation in the lungs. This ectodomain then can bind with the neutrophil chemoattractants and facilitate the clearance of the cytokines, eventually leading towards resolution of the inflammatory environment (Li et al., 2002; Tanino et al., 2012). Decreased levels of Syndecan-1 and Syndecan-4 in the XylT1 deficient lungs will directly reduce clearance of these chemokines from the alveolar space leading to more cellular influx and likely prolonged recruitment. Moreover, during LPS exposure, *Xylt2* mRNA is also downregulated in XylT1 deficient mice, likely causing an adiditonal reductions in GAG assembly on syndecan PG core proteins during this inflammatory challenge.

Our observations from the 24 hour LPS challenge indicate that the levels of various cytokines in the BALF do not always correlate with the mRNA expression levels in the lung tissue suggesting post-transcriptional controls. This should not be surprising since cytokine levels are highly regulated during inflammation (Ilyin et al., 2000). For example, in LPS challenged Dcn knockout mice, downregulation of *Il10* mRNA is proposed to be due to an autofeedback mechanism as a response to high levels of Il10 protein (Merline et al., 2011). Our findings also suggest that XylT1 deficiency causes decreased vascular permeability as revealed by decreased expression of *Vegfa* and *Vcam1*. This is likely to cause a greater influx of neutrophils, activated macrophages, and other cells from the peripheral circulation. Accompanying these cells are plasma proteins that exudate into the alveolar space during LPS stimulation (Lu et al., 2008). All these factors in combination can significantly alter the cytokine profile in XylT1 knockout mice after LPS challenge. This mechanism is still under investigation.

4.6. Conclusion

In this paper, we show that lung PGs are required for maintenance of normal lung physiologic function and innate immunity and that it is dependent on XylT1. We show that during XylT1 deficiency, expression of biglycan, syndecan-1 and syndecan-4 are downregulated in lung tissue likely impacting function and innate immunity responses. We show that XylT1 deficient mice have reduced pulmonary function as revealed by measurements of respiratory mechanics. We also show that XylT1 deficient lungs have an augmented inflammatory response due to increased NF-κB activation. This results as a consequence of decreased levels of surfactant protein-D, elevated levesl of Cd14, and decreased levels of Syndecan-1 and Syndecan-4. During LPS exposure, the low surfactant and high Cd14 levels in the lung decreases the normal LPS clearance process leading to hyperactivation of Tlr4 mediated NF-kB pathway ultimately resulting in higher levels of pro-inflammatory cytokine Il-1b, and neutrophil chemoattractant Mip2, and Vcam1 in the lungs. The low levels of syndecans in the lungs also slows the clearance

of neutrophil chemoattractant Mip2 causing a more sustained recruitment and prolonged influx of leukocytes into the alveolar space. The end result is an exacerbated leukocyte influx which further compromises lung function during pathogen challenge. In summary, in this paper we further expand the role of GAGs in pulmonary physiology and innate immunity. The expectation is this impact of GAGs is mediated by direct impact on the fucntion of specifc PGs and by indirect effects at the levels of cellular organelles and receptor activation. Future studies will be directed at these important questions.

4.7. Figures and Figure legends

Table 4. 1 RT-PCR primers and accession numbers for gene targets

Gene	Forward Primer	Reverse Primer	NCBI accession No./Source
Xylt2	gggtgagacccgcttcct	gcatcatctttcctgagaggtagtt	NM_145828.3
Xylt1	gaacagctgcaggtactacccaat	gaatcggtcagcaaggaagtaga	NM_175645
Actb	gctctggctcctagcaccat	ccaccgatccacacagagtact	NM_007393.5
Ccl2	gctacaagaggatcaccagcgg	gtctggacccattccttcttgg	NM_011333.3
Il10	cggttagcagtatgttgtccagc	cgggaagacaataactgcaccc	NM_010548.2
Cxcl1	tccagagcttgaaggtgttgcc	aaccaagggagcttcagggtca	NM_008176.3
Il1b	ctttgaagttgacggaccc	tgagtgatactgcctgcctg	(Mandrekar, Ambade, Lim, Szabo, & Catalano, 2011)
Il6	acaaccacggccttccctactt	cacgatttcccagagaacatgtg	(Mandrekar et al., 2011)
Tnfa	caccaccatcaaggactcaa	aggcaacctgaccactctcc	(Mandrekar et al., 2011)
Ccl5	ctcaccatatggctcggaca	cgactgcaagattggagcac	NM_013653.3
Ccl17	tgccatcgtgtttctgactgt	atggccttgggtttttcacc	NM_011332.3
Csf2rb	gcaggcttcttgctgagcaaca	ggaagttgctctgtggattcgg	NM_001358854.1
Cxcl3	ccagacagaagtcatagccac	cttcatcatggtgaggggctt	NM_203320.3
Ifng	gaactggcaaaaggatggtgac	ttgttgctgatggcctgattg	NM_008337.4
Il1a	gcttgagtcggcaaagaaatc	gagagagatggtcaatggcaga	NM_010554.4
Il3	gaagctcccagaacctgaact	tctccttggctttccacgaat	NM_010556.4
Il12a	acgagagttgcctggctactag	cctcatagatgctaccaaggcac	NM_008351.3
Il12b	gaactcacaggtggaggtcag	aggaacgcacctttctggtta	NM_001303244.1
Il17a	ggactctccaccgcaatgaa	tttccctccgcattgacaca	NM_010552.3
Pf4	ccagctcatagccaccctgaa	ggcagctgatacctaactctcca	NM_019932.4
Vcam1	ctcttacctgtgcgctgtga	cttcagggaatgagtagacctcc	NM_011693.3
Vegfa	ccctggctttactgctgtacct	cttgatcacttcatgggacttctg	NM_001287058.1
Sftpa1	cagtgtgattgggagaaacca	ggcttccggcacaaacttc	NM_023134
Sftpd	gtgagaagggtgatccaggtttg	gttcgccagcagagccattc	NM_009160
Cd14	gaatctaccgaccatggagc	actttcctcgtctagctcgc	NM_009841.4
Sdc1	tagtgggcctcatctttgct	tgccttcgtccttcttcttc	(Nairn et al., 2007)
Sdc4	gccactggataaccacatcc	cttccagttccttgggctct	(Nairn et al., 2007)
Tlr4	agcttctccaatttttcagaacttc	tgagaggtggtgtaagccatgc	NM_021297.3
Bgn	gtacaggttgggcttaggtcaca	cagaaaactcaggctcccattc	NM_007542.5
Dcn	gggctggcacagcataagtatat	cccaactgcggagatgttgt	NM_001190451.2
Vcan	gttgggatgcttgctggtat	gctccatgtcgtctgcagta	(Nairn et al., 2007)

Table 4. 2 List of antibodies used

Protein/ Ab clone	Antibody Source	Host Species	Dilution
Dcn (LF113)	Larry Fisher, NIH	Rabbit	1:5,000
Sp-D (C6)	SantaCruz Biotechnology	Mouse	1:250
NFkB-p65	Cell Signaling Technology	Rabbit	1:1,000
phospho p65	Cell Signaling Technology	Rabbit	1:1,000
Erk 1/2	Cell signaling Technology	Rabbit	1:1,000
phospho erk 1/2	Cell Signaling Technology	Rabbit	1:1,000
Gapdh	Ambion	Mouse	1:10,000
anti-mouse-HRP	Calbiochem	Goat	1:50,000
anti-rabbit- HRP	Calbiochem	Goat	1:50,000

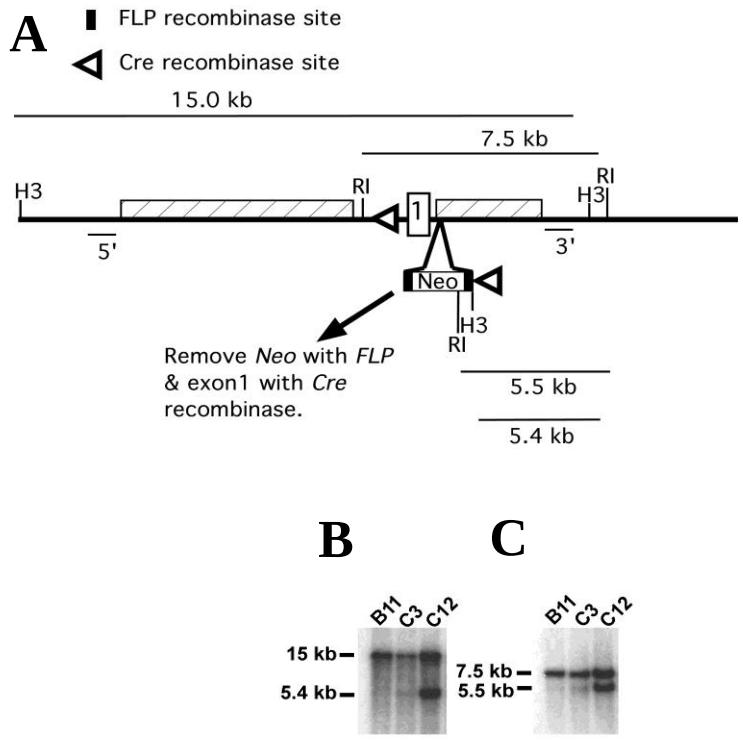

Figure 4. 1 Generation of Conditional Xylt1 knockout mouse model.

(A) Targeting scheme of *Xylt1* locus. Exon 1, white box numbered 1, can be deleted conditionally using *Cre* recombinase. 5' and 3' are probes used for Southern blot analyses. (B) Southern blot analysis of ES cell genomic DNA digested with Hind III restriction enzyme and probed with 3' probe. This probe detects the 15 kb wild type H3 fragment and the 5.4 kb targeted fragment due to the homologous recombination and insertion into the *Xylt1* locus of a new H3 site as part of the neomycin selection cassette. (C) Same DNAs as in B digested with *EcoRI* and probed with same probe. In this case, wild type band is 7.5 kb and targeted band is 5.5 kb due to the presence of an RI site in the neomycin cassette. Therefore, C12 has *Xylt1* conditionally targeted. A probe 5' to the locus has confirmed these results. Note that C3 appears to have some targeted cells in it and may be a mixed clone. Construct design was by Dr. Hinsdale's laboratory. The ES cell clones and founder mice were generated by the Animal Models Core Facility of University of North Carolina at Chapel Hill, director Dr. Randy Thrasher.

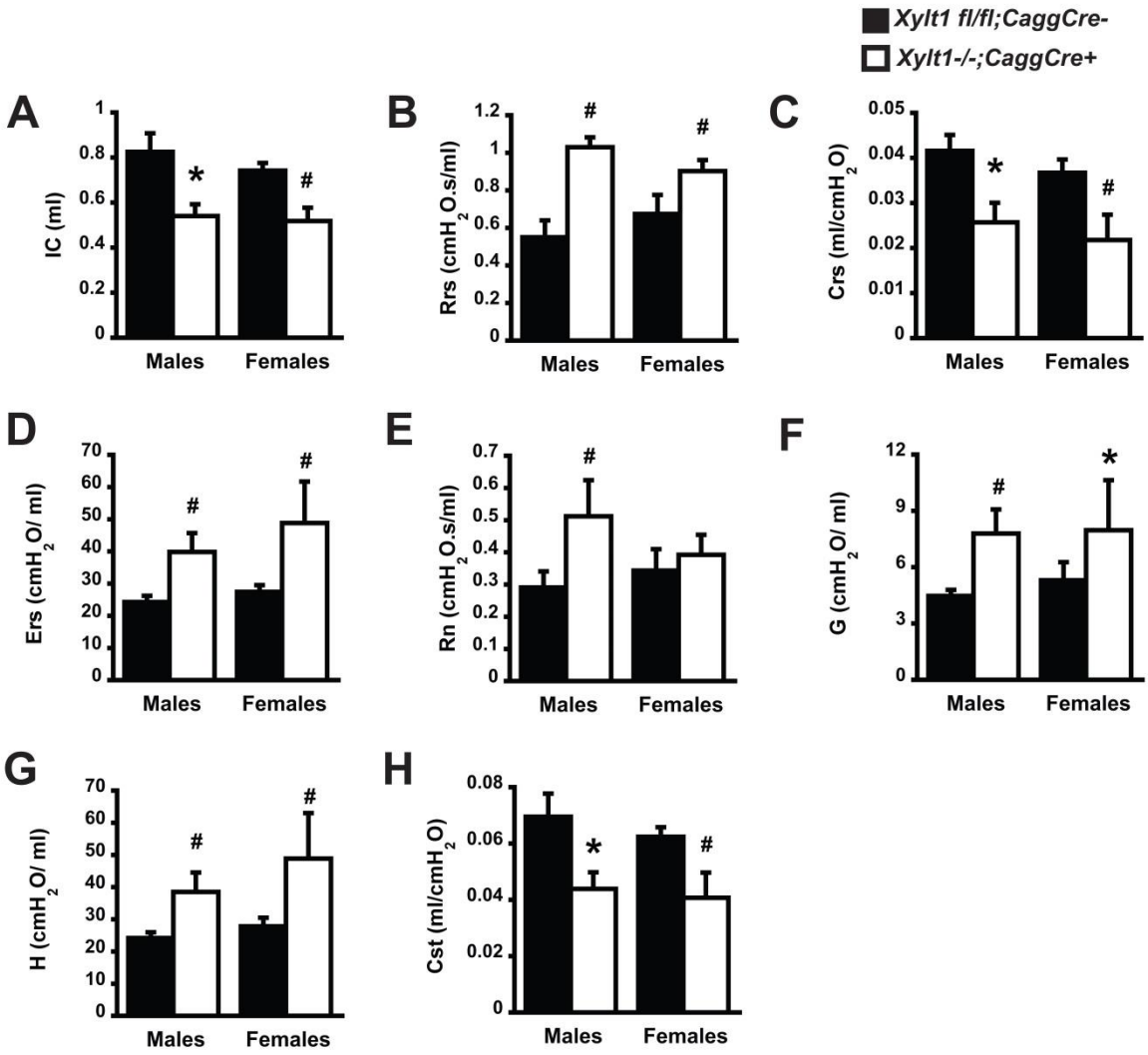

Figure 4. 2 XylT1 deficient mice have decreased pulmonary function.

Pulmonary function parameters were assessed in *Xylt1* conditional knockout mice (*Xylt1-/-; CaggCre+*) using four different perturbations in Scireq Flexivent ®. (A) reduced inspiratory capacity, (B) increased resistance, (C) decreased compliance, (D) increased elastance, (E) increased Newtonian resistance, (F) increased tissue damping, (G) increased tissue elastance (H) increased static compliance, and (I) trend of decrease in hysteresis area in *Xylt1-/-; CaggCre+* mice. (n= 8 *Xylt1 fl/fl;CaggCre-*; 7 *Xylt1-/-;CaggCre+*; *p<0.05, #p<0.01). (This experiment was conducted by Pulavendran Sivasmi and Mallika Achanta and analyzed by the author.)

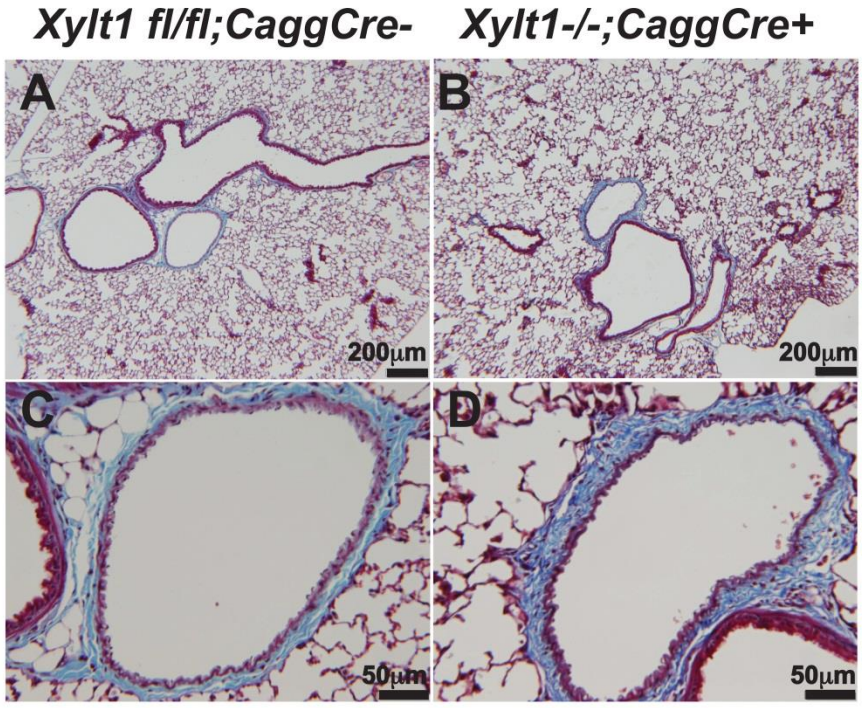
Xylt1 fl/fl;CaggCre-
Xylt1-/-;CaggCre+
A
B
200μm
200μm
C
D
50μm
50μm

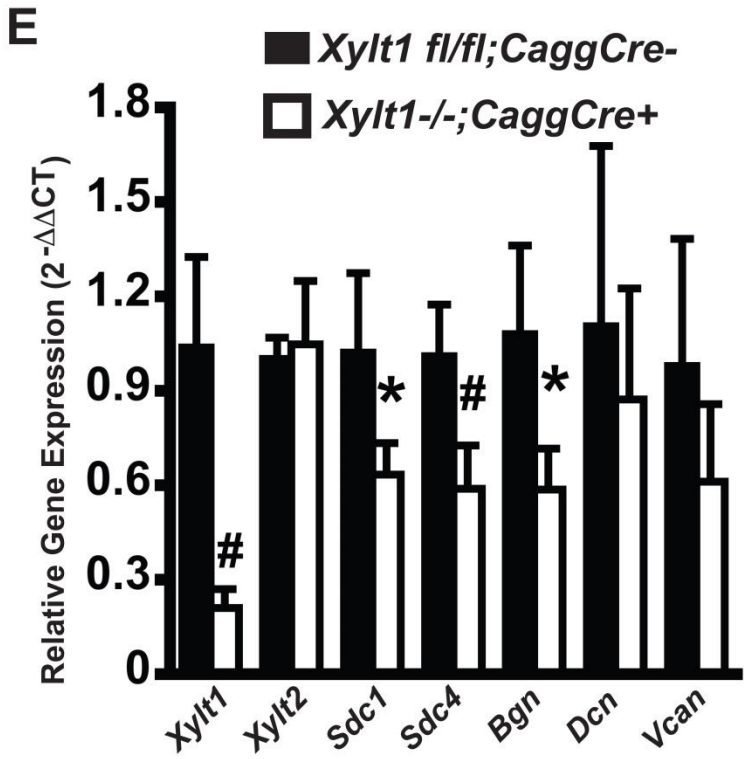
E
Xylt1 fl/fl;CaggCre-
Xylt1-/-;CaggCre+
Relative Gene Expression (2-ΔΔCT)
1.8
1.5
1.2
0.9
0.6
0.3
0
#
*
#
*
Xylt1
Xylt2
Sdc1
Sdc4
Bgn
Dcn
Vcan

Figure 4. 3 XylT1 deficient male mice have mild increase in fibrosis in peribronchial area and reduced PG core protein expression

(A-D) Representative images of trichrome staining of lung sections. (A) Control mice normal liver histology with very little collagen around the peribronchial area while (B) *Xylt1-/-; CaggCre+* mice with mild increase in collagen deposition around peribronchial area. (C) and (D) show magnification of (A) and (B) respectively. (E) Reduction in *Xylt1, Syndecan-1, and Syndecan-4* mRNA in *Xylt1-/-; CaggCre+* mice while *Xylt2* mRNA is unchanged (n= 6 *Xylt1 fl/fl; CaggCre-,* 5 *Xylt1-/-; CaggCre+*, *p<0.05, #p<0.01).

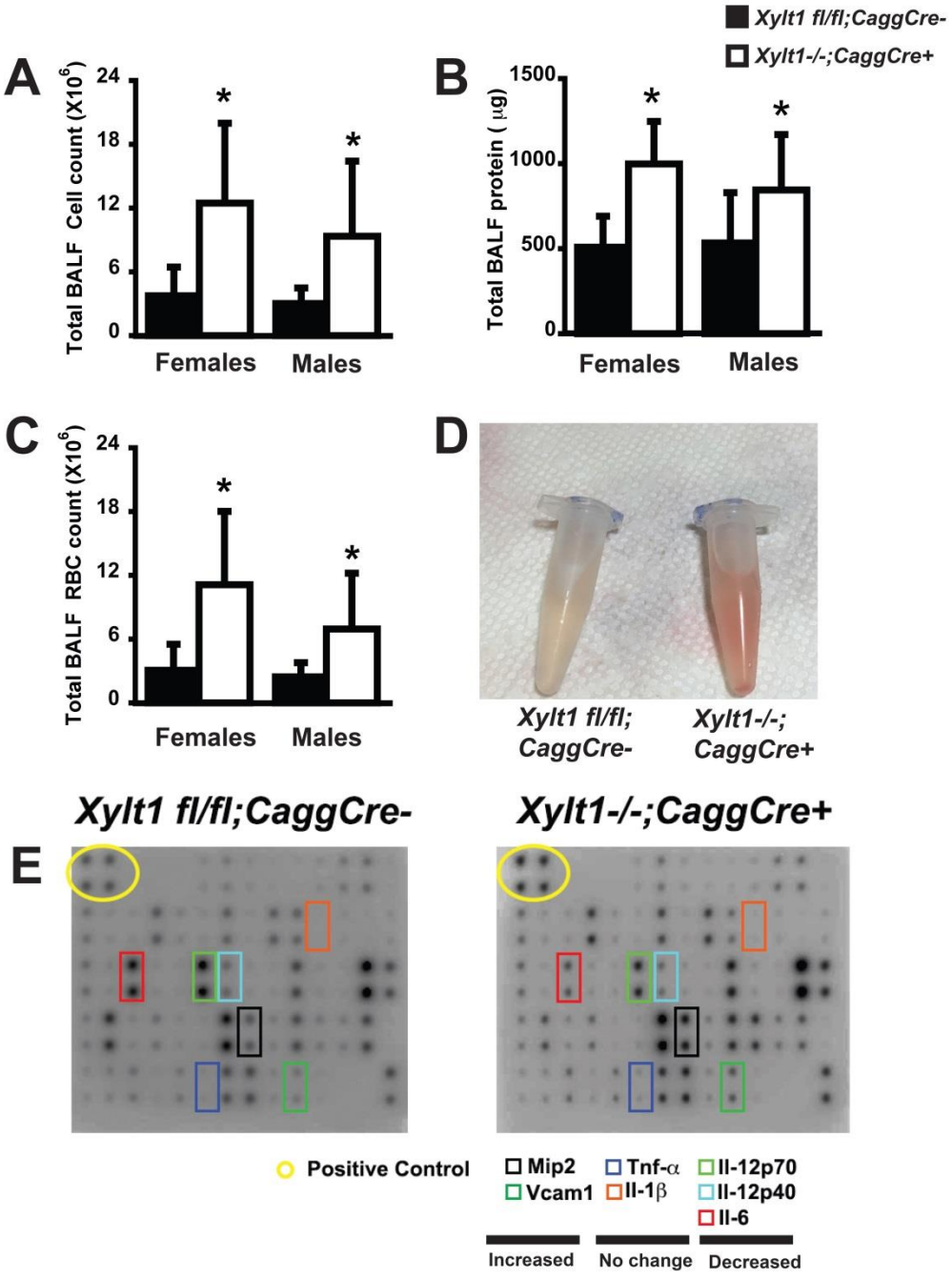
Xylt1 fl/fl;CaggCre-
Xylt1-/-;CaggCre+
A
Total BALF Cell count (X10^6)
24
18
12
6
0
*
*
Females
Males
B
Total BALF protein (μg)
1500
1000
500
0
*
*
Females
Males
C
Total BALF RBC count (X10^6)
24
18
12
6
0
*
*
Females
Males
D
Xylt1 fl/fl; CaggCre-
Xylt1-/-; CaggCre+
E
Xylt1 fl/fl;CaggCre-
Xylt1-/-;CaggCre+
Positive Control
Mip2
Vcam1
Tnf-α
Il-1β
Il-12p70
Il-12p40
Il-6
Increased
No change
Decreased

Figure 4. 4 XylT1 deficient male mice have exacerbated response to LPS induced acute lung injury and increased levels of neutrophil chemo-attractants in BALF

Mice were challenged with intranasal LPS and BALF collected and analyzed after 24 hours. (A) total BALF cell count, (B) total BALF protein amount, (C) total BALF red blood cell count and (D) visibly more reddish color of BALF from *Xylt1-/-; CaggCre+* mice in comparison to littermate controls. (n= 7 *Xylt1 fl/fl;CaggCre-*, 7 *Xylt1-/-;CaggCre+*, *p<0.05). (E and F) altered cytokines in BALF of *Xylt1-/-; CaggCre+* mouse. Panel (E) array results for littermate controls and panel (F) array result for *Xylt1-/-; CaggCre+* mice. Legends on the bottom are grouped according to respective changes, yellow circles show positive controls used for comparing data from the two membranes. A detailed result of cytokine array is provided in Table 3 and 4.

Table 4. 3 Result of BALF cytokine Array (Cytokines with altered protein levels in BALF of Xylt1-/-; CaggCre+ mice)

Cytokines with low levels in *Xylt1* knockout (Cut-off <25% change from controls)		
Cytokine	*Xylt1 fl/fl; CaggCre-*	*Xylt1-/-; CaggCre+*
IL-6	1	0.19
MCP1	1	0.29
IL-12 p40/p70	1	0.36
CCL5	1	0.41
CD40	1	0.47
IL5	1	0.52
CCL17	1	0.55
IL-1a	1	0.57
CXCL9	1	0.61
Axl	1	0.62
IL-3	1	0.63
Ltn	1	0.65
IL-12 p70	1	0.65
IFN-g	1	0.7

Cytokines with high levels in *Xylt1* knockout (Cut-off >25% change from controls)		
Cytokine	*Xylt1 fl/fl; CaggCre-*	*Xylt1-/-; CaggCre+*
CX3CL1	1	1.25
CXCL13	1	1.29
IGFBP-6	1	1.3
IGFBP-5	1	1.33
IL-13	1	1.37
IL-17a	1	1.37
VCAM-1	1	1.69
MIP-2	1	1.78
IL-3rb	1	1.96
CXCL4	1	3.52

Table 4. 4 Result of BALF cytokine Array (Cytokines with no Change in BALF protein levels in Xylt1-/-; CaggCre+ mice

Cytokine	*Xylt1 fl/fl; CaggCre-*	*Xylt1-/-; CaggCre+*
MCP-5	1	0.77
GM-CSF	1	0.78
Leptin	1	0.797
IL4	1	0.816
CCL25	1	0.819
M-CSF	1	0.827
I-309	1	0.861
CXCL16	1	0.866
CD30 Ligand	1	0.871
IL-1b	1	0.897
IL-2	1	0.904
TIMP-1	1	0.92
TNF R1	1	0.921
IL-9	1	0.922
SDF-1a	1	0.926
IL-10	1	0.926
MIP-1g	1	0.934
CCL24	1	0.953

Cytokine	*Xylt1 fl/fl; CaggCre-*	*Xylt1-/-; CaggCre+*
FasL	1	0.975
CD30	1	1.012
CCL11	1	1.038
MIP-3a	1	1.044
TNFa	1	1.052
MIP-1a	1	1.06
LIX	1	1.061
TNF RII	1	1.096
Leptin R	1	1.103
L-Selectin	1	1.118
CRG-2	1	1.124
VEGF-A	1	1.137
IGFBP-3	1	1.151
P-Selectin	1	1.161
TPO	1	1.179
GCSF	1	1.202
MIP-3b	1	1.214
CCL27	1	1.227

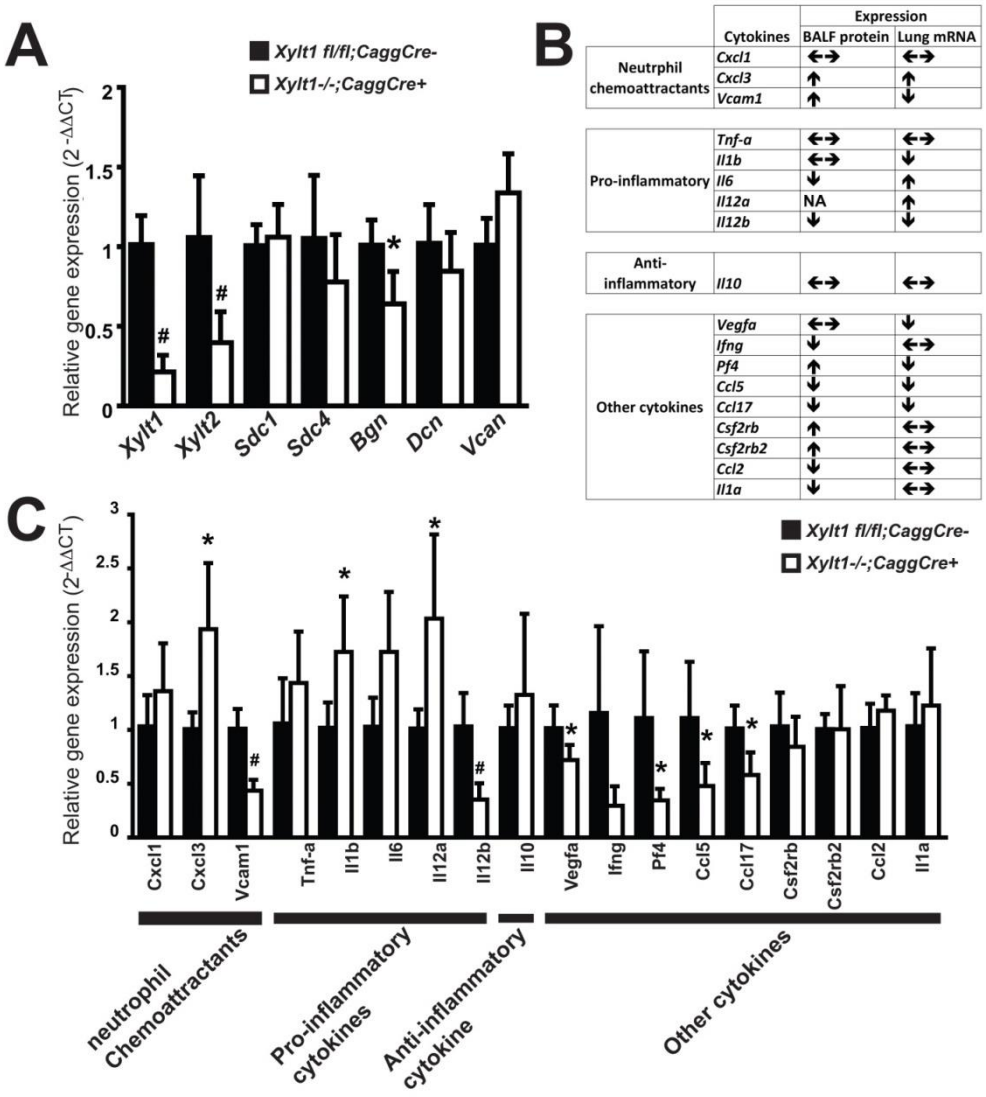

Figure 4. 5 Xylt1 deficient lungs have increased inflammation in the lungs.

Realtime RTPCR was performed in lungs tissue from LPS challenged *Xylt1-/-; CaggCre+* mice. (A) mRNA levels of *Xylt1* and *Xylt2*, syndecan-1, and syndecan-4 in *Xylt1-/-; CaggCre+* lungs; (B) various cytokines at their protein level in the BALF and mRNA level in the lungs; (C) mRNA levels of neutrophil chemoattractants, pro-inflammatory cytokine, anti-inflammatory cytokine and other cytokines (n= 4-5 *Xylt1 fl/fl;CaggCre-;* 4-6 *Xylt1-/-;CaggCre+*, *p<0.05, #p<0.01).

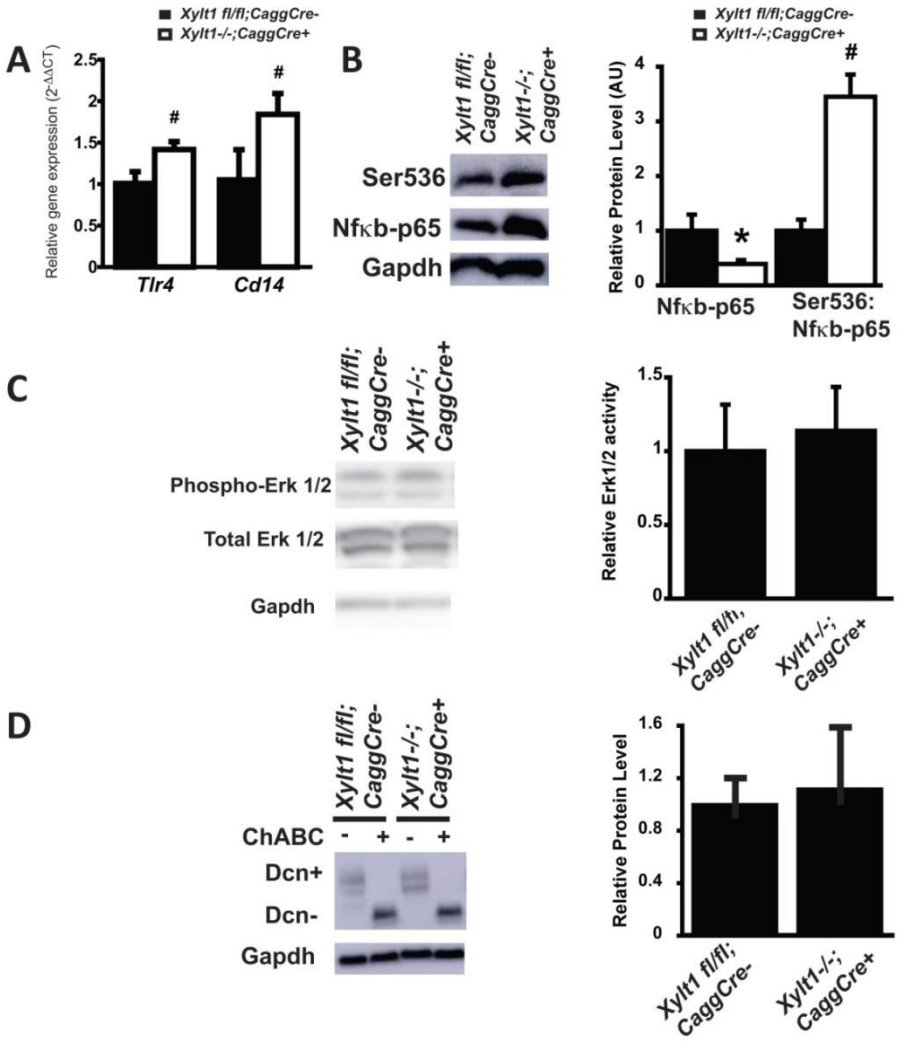

Figure 4. 6 Exacerbated response to LPS challenge in conditional *Xylt1* knockout is mediated by increased TLR4 signaling.

(A) mRNA level expression of *Cd14* and Tl*r4* (n=5 each), (B) Ser536 phosphorylation of Nfκb-p65 (n= 3 *Xylt1 fl/fl;CaggCre-,* 4 *Xylt1-/-;CaggCre+*); (C) Erk1/2 activity measured by Western blotting (n= 4 *Xylt1 fl/fl;CaggCre-*, 5 *Xylt1-/-;CaggCre+*); (D) Protein levels and glycosylation pattern of Decorin (n= 4 each genotype) in *Xylt1-/-; CaggCre+* when compared to compared to littermate controls. Dcn+; decorin with GAG chain, Dcn-; decorin without GAG chains, ChABC; Chondroitinase ABC (*p<0.01; #p<0.05).

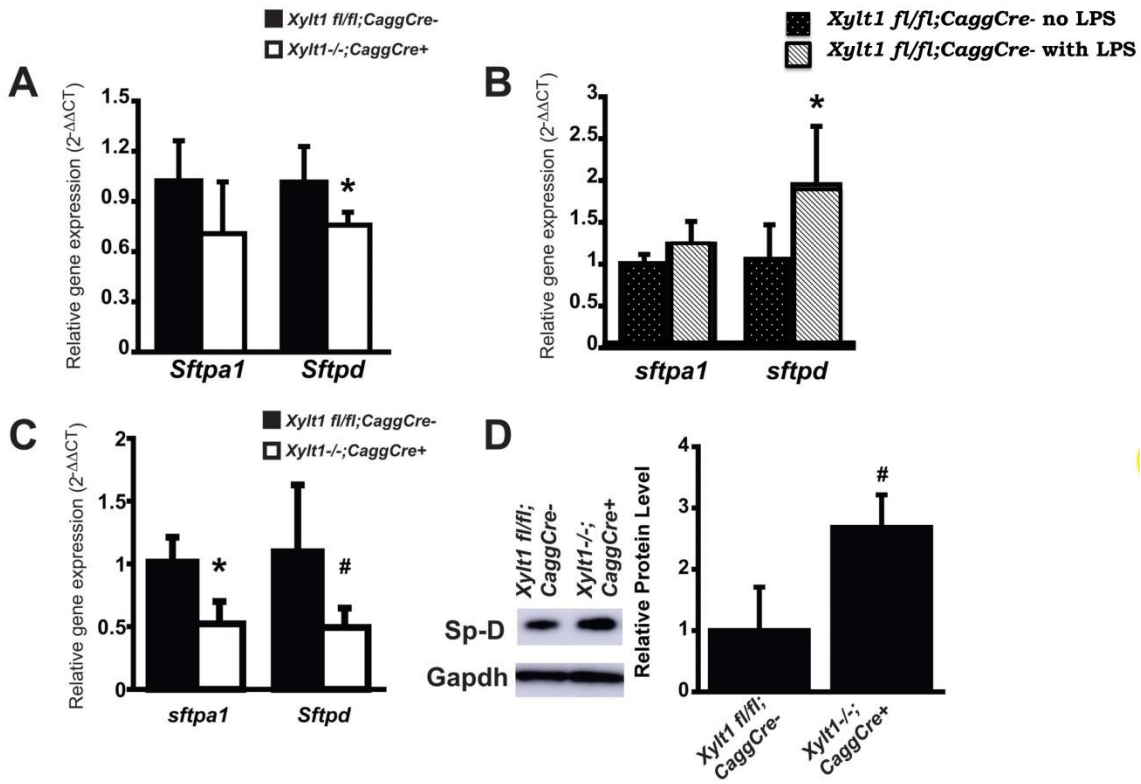

F**igure 4. 7 XylT1 deficient cells have altered surfactant A and D biology.**

Real-time RTPCR was performed in lung tissue from *Xylt1-/-;CaggCre+* mice to measure levels of surfactant protein A and D. (A) Levels of Sp-D mRNA in *Xylt1-/-;CaggCre+* mice when compared with littermate controls (n= 6 *Xylt1 fl/fl;CaggCre-*, 5 *Xylt1-/-;CaggCre+*). (B) Levels of surfactant protein D mRNA in littermate control mice after LPS treatment (n= 6 controls, 5 LPS). (C) Levels of Sp-A and Sp-D mRNA in *Xylt1-/-;CaggCre-* mice after LPS treatment when compared with littermate controls (n= 5 *Xylt1fl/fl; CaggCre-*, 6 *Xylt1-/-;CaggCre+*). (D) Surfactant D protein levels in *Xylt1-/-;CaggCre-* mice after LPS treatment (n= 4 each genotype).

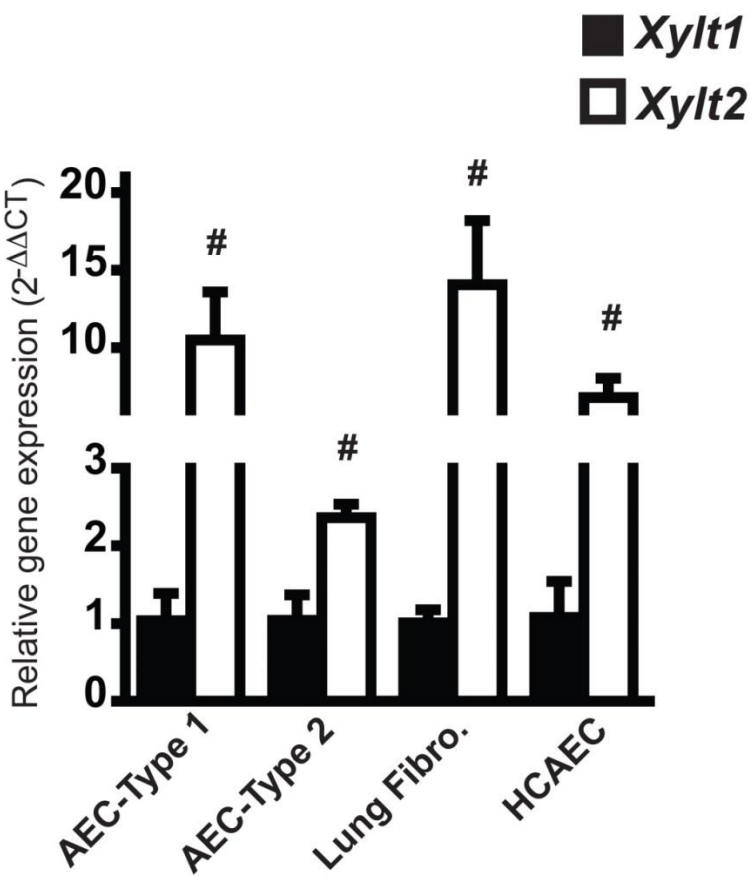

Figure 4. 8 mRNA expression level of XylT isoforms in lungs shows likelihood of dominancy of XylT2 in lungs.

Various cell types present in mouse lungs and human coronary artery endothelium were used for real-time RTPCR experiment. Fig shows that AEC type 1, lung fibroblasts and endothelial cells have around 10 fold higher expression of *Xylt2* as compared to *Xylt1*, while AEC type 2 had only about 2 fold higher mRNA expression of *Xylt2* as compared to *Xylt1* (n=3 each, #$p<0.01$) (This experiment was conducted by Yurong Liang at Oklahoma Center for Respiratory and Infectious Disease- Molecular Biology Core, and analyzed by the author.)

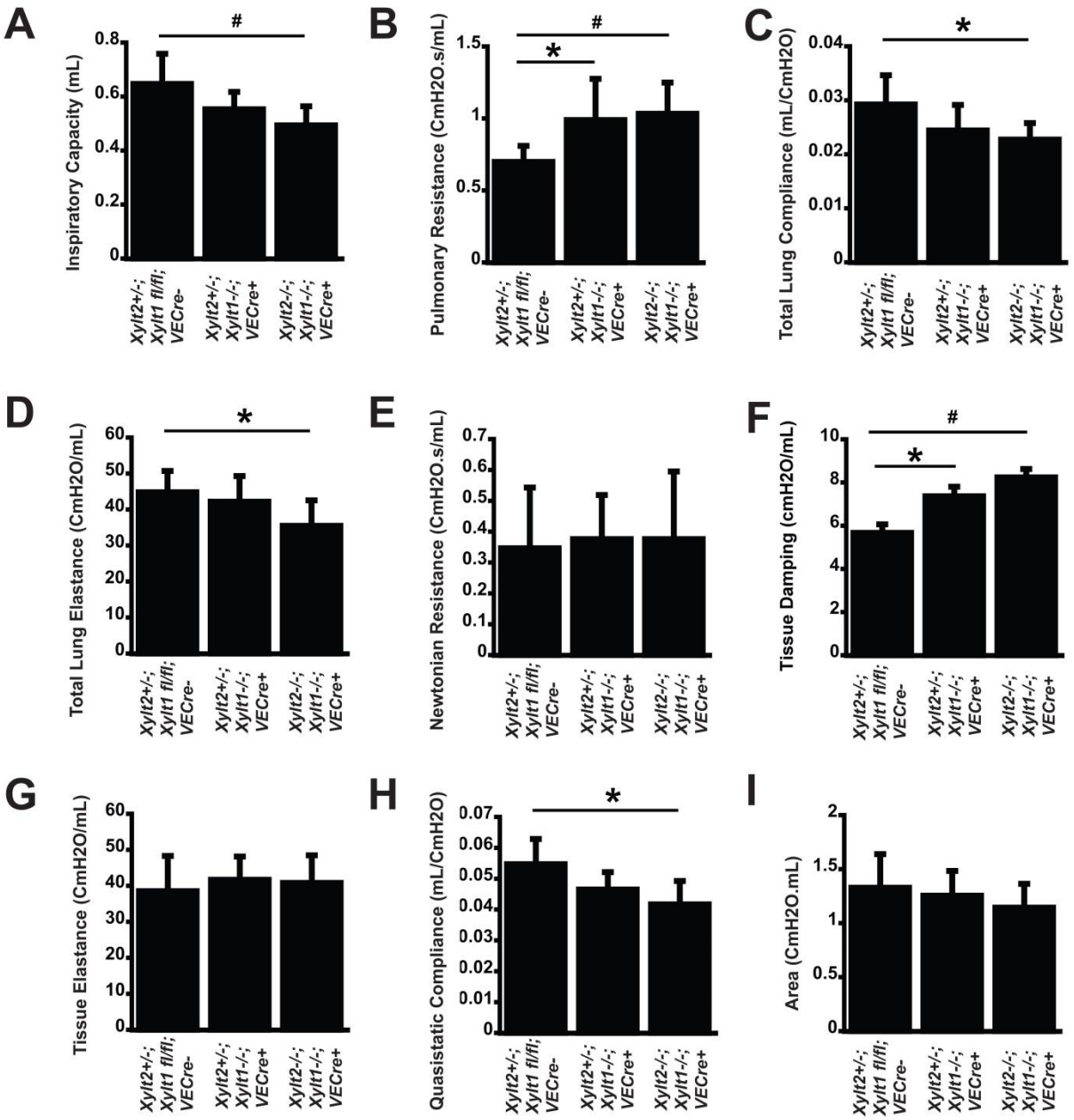
A
Inspiratory Capacity (mL)
0.8
0.6
0.4
0.2
0
#
B
Pulmonary Resistance (CmH2O.s/mL)
1.5
1
0.5
0
#
*
C
Total Lung Compliance (mL/CmH2O)
0.04
0.03
0.02
0.01
0
*
D
Total Lung Elastance (CmH2O/mL)
60
50
40
30
20
10
0
*
E
Newtonian Resistance (CmH2O.s/mL)
0.7
0.6
0.5
0.4
0.3
0.2
0.1
0
F
Tissue Damping (cmH2O/mL)
10
8
6
4
2
0
#
*
G
Tissue Elastance (CmH2O/mL)
60
50
40
30
20
10
0
H
Quasistatic Compliance (mL/CmH2O)
0.07
0.06
0.05
0.04
0.03
0.02
0.01
0
*
I
Area (CmH2O.mL)
2
1.5
1
0.5
0
Xylt2+/-; Xylt1 fl/fl; VECre-
Xylt2+/-; Xylt1-/-; VECre+
Xylt2-/-; Xylt1-/-; VECre+

Figure 4. 9 Altered pulmonary dynamics in conditional Xylt1 knockout mice is not due to proteoglycans of endothelial origin.

Pulmonary function parameters were assessed in Xylt1 conditional knockout mice using four different perturbations in Scireq Flexivent ®. (A) No change in Inspiratory capacity of *Xylt2+/-;Xylt1-/-;VECre+* mice, while *Xylt2-/-;Xylt1-/-;VECre+* mice had reduced inspiratory capacity. (B) Increased resistance in *Xylt2+/-;Xylt1-/-;VECre+* and Xylt2-/-;Xylt1-/-;VECre+ mice. (C-D) No change in compliance and elastance in *Xylt2+/-;Xylt1-/-;VECre+*, while Xylt2-/-;Xylt1-/-;VECre+ mice had reduced compliance and increased elastance. (E-G) No change in Newtonian resistance, increased tissue damping and, no change in tissue elastance, respectively in both *Xylt2+/-;Xylt1-/-;VECre+* and *Xylt2-/-;Xylt1-/-;VECre+* mice. (H) No change in static compliance in *Xylt2+/-;Xylt1-/-;VECre+* mice, while *Xylt2-/-;Xylt1-/-;VECre+* mice had reduced static compliance. (I) No change in hysteresis area in both *Xylt2+/-;Xylt1-/-;VECre+* and *Xylt2-/-;Xylt1-/-;VECre+* mice. (n= 9 *Xylt2+/-;Xylt1 fl/fl;VECre+*; 9 *Xylt2+/-;Xylt1-/-VECre+*; 7 *Xylt2-/-;Xylt1-/-;VECre+*, *p<0.05, #p<0.01).

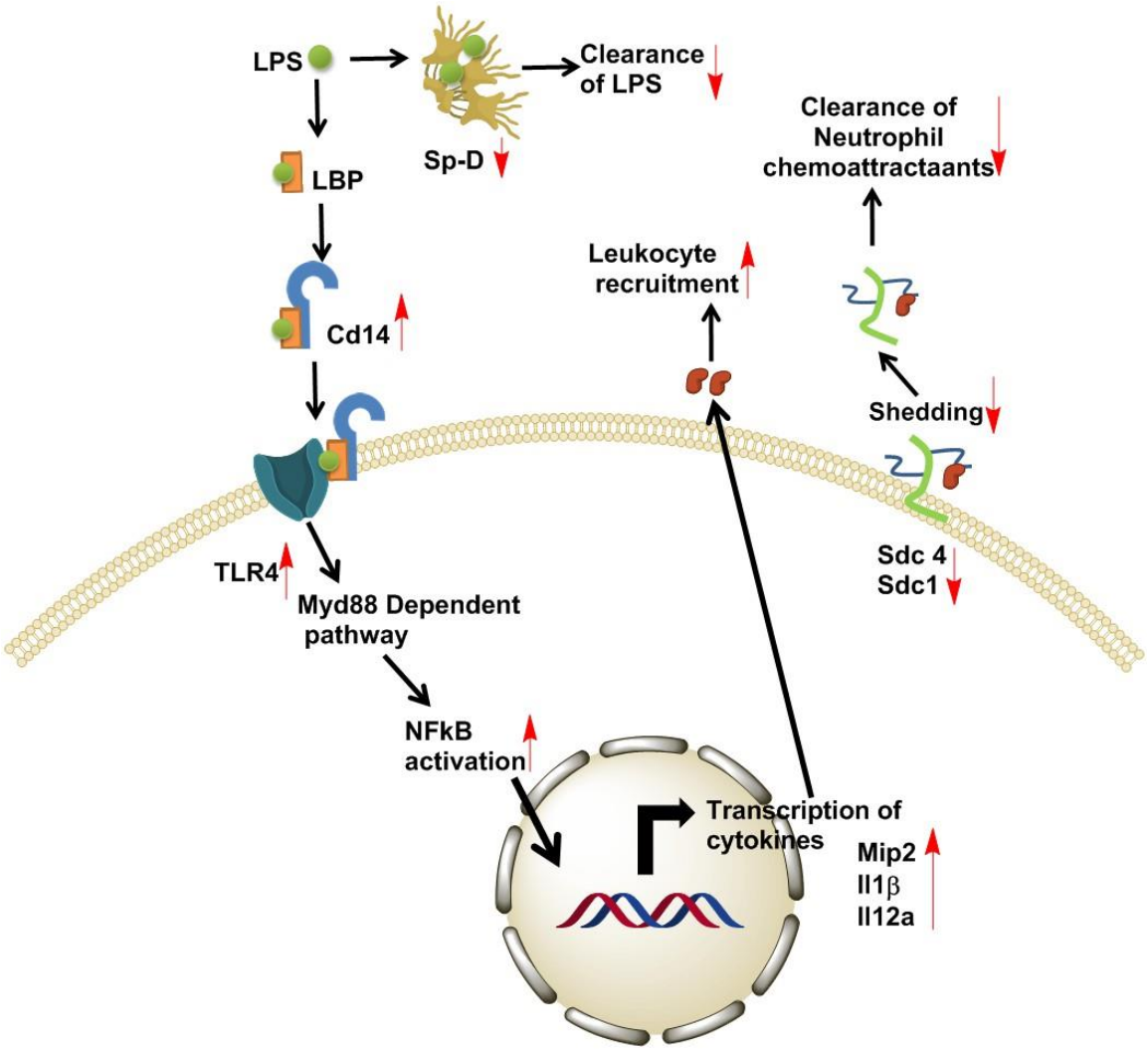
LPS
Clearance of LPS
Sp-D
LBP
Cd14
Leukocyte recruitment
Clearance of Neutrophil chemoattractaants
Shedding
Sdc 4
Sdc1
TLR4
Myd88 Dependent pathway
NFkB activation
Transcription of cytokines
Mip2
Il1β
Il12a

Figure 4. 10 Proposed model of augmented LPS response in *Xylt1* deficient mice.

XylT1 deficiency results in increased susceptibility to LPS by three mechanisms. First, XylT1 deficiency results in decreased expression and possibly defective secretion of Sp-D in the alveolar space resulting in decreased surfactant mediated clearance of LPS, causing sustained presence of LPS in the lungs, which is then available for inflammatory signaling. Second, XylT1 deficiency causes increased Cd14 levels in the lungs, contributing to enhanced LPS mediated TLR4 activation, which then subsequently hyper stimulates the NFkB activation resulting in increased expression and production of neutrophil chemoattractant Mip2 and pro-inflammatory cytokines Il1b and Il12a causing increased leukocyte recruitment in the alveolar space. Third, XylT1 deficiency causes decreased expression of syndecans in the AEC cell surface, creating less syndecans available for shedding and subsequent clearance of neutrophil chemoattractant and resulting in delayed neutrophils clearance.

References

Babelova, A., Moreth, K., Tsalastra-Greul, W., Zeng-Brouwers, J., Eickelberg, O., Young, M. F., . . . Schaefer, L. (2009). Biglycan, a danger signal that activates the NLRP3 inflammasome via toll-like and P2X receptors. *J Biol Chem, 284*(36), 24035-24048. doi:10.1074/jbc.M109.014266

Blackwood, R. A., Cantor, J. O., Moret, J., Mandl, I., & Turino, G. M. (1983). Glycosaminoglycan synthesis in endotoxin-induced lung injury. *Proc Soc Exp Biol Med, 174*(3), 343-349.

Cavalcante, F. S., Ito, S., Brewer, K., Sakai, H., Alencar, A. M., Almeida, M. P., . . . Suki, B. (2005). Mechanical interactions between collagen and proteoglycans: implications for the stability of lung tissue. *J Appl Physiol (1985), 98*(2), 672-679. doi:10.1152/japplphysiol.00619.2004

Condac, E., Silasi-Mansat, R., Kosanke, S., Schoeb, T., Towner, R., Lupu, F., . . . Hinsdale, M. E. (2007). Polycystic disease caused by deficiency in xylosyltransferase 2, an initiating enzyme of glycosaminoglycan biosynthesis. *Proc Natl Acad Sci U S A, 104*(22), 9416-9421. doi:10.1073/pnas.0700908104

Cuellar, K., Chuong, H., Hubbell, S. M., & Hinsdale, M. E. (2007). Biosynthesis of chondroitin and heparan sulfate in chinese hamster ovary cells depends on xylosyltransferase II. *J Biol Chem, 282*(8), 5195-5200. doi:10.1074/jbc.M611048200

Fan, G., Xiao, L., Cheng, L., Wang, X., Sun, B., & Hu, G. (2000). Targeted disruption of NDST-1 gene leads to pulmonary hypoplasia and neonatal respiratory distress in mice. *FEBS Lett, 467*(1), 7-11.

Frey, E., Miller, D., Jahr, T. G., Sundan, A., Bazil, V., Espevik, T., . . . Wright, S. (1992). Soluble CD14 participates in the response of cells to lipopolysaccharide. *Journal of Experimental Medicine, 176*(6), 1665-1671.

Fust, A., LeBellego, F., Iozzo, R. V., Roughley, P. J., & Ludwig, M. S. (2005). Alterations in lung mechanics in decorin-deficient mice. *Am J Physiol Lung Cell Mol Physiol, 288*(1), L159-166. doi:10.1152/ajplung.00089.2004

Gaunsbaek, M. Q., Rasmussen, K. J., Beers, M. F., Atochina-Vasserman, E. N., & Hansen, S. (2013). Lung Surfactant Protein D (SP-D) Response and Regulation During Acute and Chronic Lung Injury. *Lung, 191*(3), 295-303. doi:10.1007/s00408-013-9452-x

Gill, S., Wight, T. N., & Frevert, C. W. (2010). Proteoglycans: key regulators of pulmonary inflammation and the innate immune response to lung infection. *Anat Rec (Hoboken), 293*(6), 968-981. doi:10.1002/ar.21094

Habuchi, H., Nagai, N., Sugaya, N., Atsumi, F., Stevens, R. L., & Kimata, K. (2007). Mice deficient in heparan sulfate 6-O-sulfotransferase-1 exhibit defective heparan sulfate biosynthesis, abnormal placentation, and late embryonic lethality. *J Biol Chem, 282*(21), 15578-15588. doi:10.1074/jbc.M607434200

Ilyin, S. E., González-Gómez, I., Romanovicht, A., Gayle, D., Gilles, F. H., & Plata-Salamán, C. R. (2000). Autoregulation of the interleukin-1 system and cytokine–cytokine interactions in primary human astrocytoma cells. *Brain Research Bulletin, 51*(1), 29-34. doi:https://doi.org/10.1016/S0361-9230(99)00190-2

Jamal, R. A., Roughley, P. J., & Ludwig, M. S. (2001). Effect of glycosaminoglycan degradation on lung tissue viscoelasticity. *American Journal of Physiology-Lung Cellular and Molecular Physiology, 280*(2), L306-L315. doi:10.1152/ajplung.2001.280.2.L306

Karlinsky, J. B., Bucay, P. J., Ciccolella, D. E., & Crowley, M. P. (1991). Effects of intratracheal endotoxin administration on hamster lung glycosaminoglycans. *Am J Physiol, 261*(2 Pt 1), L148-155. doi:10.1152/ajplung.1991.261.2.L148

Li, Q., Park, P. W., Wilson, C. L., & Parks, W. C. (2002). Matrilysin Shedding of Syndecan-1 Regulates Chemokine Mobilization and Transepithelial Efflux of Neutrophils in Acute Lung Injury. *Cell, 111*(5), 635-646. doi:https://doi.org/10.1016/S0092-8674(02)01079-6

Lu, Y.-C., Yeh, W.-C., & Ohashi, P. S. (2008). LPS/TLR4 signal transduction pathway. *Cytokine, 42*(2), 145-151. doi:https://doi.org/10.1016/j.cyto.2008.01.006

Mandrekar, P., Ambade, A., Lim, A., Szabo, G., & Catalano, D. (2011). An essential role for MCP-1 in alcoholic liver injury: regulation of pro-inflammatory cytokines and hepatic steatosis. *Hepatology (Baltimore, Md.), 54*(6), 2185-2197. doi:10.1002/hep.24599

Merline, R., Moreth, K., Beckmann, J., Nastase, M. V., Zeng-Brouwers, J., Tralhao, J. G., . . . Schaefer, L. (2011). Signaling by the matrix proteoglycan decorin controls inflammation and cancer through PDCD4 and MicroRNA-21. *Sci Signal, 4*(199), ra75. doi:10.1126/scisignal.2001868

Merrilees, M. J., Ching, P. S., Beaumont, B., Hinek, A., Wight, T. N., & Black, P. N. (2008). Changes in elastin, elastin binding protein and versican in alveoli in chronic obstructive pulmonary disease. *Respir Res, 9*, 41. doi:10.1186/1465-9921-9-41

Mis, E. K., Liem, K. F., Kong, Y., Schwartz, N. B., Domowicz, M., & Weatherbee, S. D. (2014). Forward Genetics Defines Xylt1 as a Key, Conserved Regulator of Early Chondrocyte Maturation and Skeletal Length. *Dev Biol, 385*(1), 67-82. doi:10.1016/j.ydbio.2013.10.014

Nairn, A. V., Kinoshita-Toyoda, A., Toyoda, H., Xie, J., Harris, K., Dalton, S., . . . Linhardt, R. J. (2007). Glycomics of Proteoglycan Biosynthesis in Murine Embryonic Stem Cell Differentiation. *Journal of proteome research, 6*(11), 4374-4387. doi:10.1021/pr070446f

Negrini, D., Passi, A., & Moriondo, A. (2008). The role of proteoglycans in pulmonary edema development. *Intensive Care Med, 34*(4), 610-618. doi:10.1007/s00134-007-0962-y

Neill, T., Schaefer, L., & Iozzo, R. V. (2012). Decorin: a guardian from the matrix. *Am J Pathol, 181*(2), 380-387. doi:10.1016/j.ajpath.2012.04.029

Poltorak, A., He, X., Smirnova, I., Liu, M. Y., Van Huffel, C., Du, X., . . . Beutler, B. (1998). Defective LPS signaling in C3H/HeJ and C57BL/10ScCr mice: mutations in Tlr4 gene. *Science, 282*(5396), 2085-2088.

Raspanti, M., Alessandrini, A., Ottani, V., & Ruggeri, A. (1997). Direct Visualization of Collagen-Bound Proteoglycans by Tapping-Mode Atomic Force Microscopy. *Journal of Structural Biology, 119*(2), 118-122. doi:https://doi.org/10.1006/jsbi.1997.3865

Ringvall, M., Ledin, J., Holmborn, K., van Kuppevelt, T., Ellin, F., Eriksson, I., . . . Forsberg, E. (2000). Defective heparan sulfate biosynthesis and neonatal lethality in mice lacking N-deacetylase/N-sulfotransferase-1. *J Biol Chem, 275*(34), 25926-25930. doi:10.1074/jbc.C000359200

Rühland, C., Schönherr, E., Robenek, H., Hansen, U., Iozzo, R. V., Bruckner, P., & Seidler, D. G. (2007). The glycosaminoglycan chain of decorin plays an important role in collagen fibril formation at the early stages of fibrillogenesis. *FEBS Journal, 274*(16), 4246-4255. doi:10.1111/j.1742-4658.2007.05951.x

Schaefer, L., Babelova, A., Kiss, E., Hausser, H. J., Baliova, M., Krzyzankova, M., . . . Grone, H. J. (2005). The matrix component biglycan is proinflammatory and signals through Toll-like receptors 4 and 2 in macrophages. *J Clin Invest, 115*(8), 2223-2233. doi:10.1172/JCI23755

Tanino, Y., Chang, M. Y., Wang, X., Gill, S. E., Skerrett, S., McGuire, J. K., . . . Frevert, C. W. (2012). Syndecan-4 regulates early neutrophil migration and pulmonary inflammation in response to lipopolysaccharide. *Am J Respir Cell Mol Biol, 47*(2), 196-202. doi:10.1165/rcmb.2011-0294OC

Vanoirbeek, J. A. J., Rinaldi, M., De Vooght, V., Haenen, S., Bobic, S., Gayan-Ramirez, G., . . . Janssens, W. (2010). Noninvasive and Invasive Pulmonary Function in Mouse Models of Obstructive and Restrictive Respiratory Diseases. *American journal of respiratory cell and molecular biology, 42*(1), 96-104. doi:10.1165/rcmb.2008-0487OC

Yamazoe, M., Nishitani, C., Takahashi, M., Katoh, T., Ariki, S., Shimizu, T., . . . Kuroki, Y. (2008). Pulmonary surfactant protein D inhibits lipopolysaccharide (LPS)-induced

inflammatory cell responses by altering LPS binding to its receptors. *J Biol Chem, 283*(51), 35878-35888. doi:10.1074/jbc.M807268200

CHAPTER V

CONCLUSION

Our research has focused on understanding the importance of XylT to organ, tissue, and cellular homeostasis. By investigating deficient patients, mouse models, and cellular models we can begin to comprehend the significance of expression patterns of the XylT isoforms and what specific physiologic states depend on them. Furthermore what organs, tissues, and cell types depend on isoform specific glycosylation. We performed whole exome sequencing followed by Sanger sequencing to identify causative mutation of spondylo-ocular syndrome (SOS), a rare congenital human disease with developmental defects in multiple organ systems including musculoskeletal, sensorineural, and cardiovascular system, to be homozygous frameshift mutations in *XYLT2* in two related and a third unrelated individual. We also used *Xylt1* and *Xylt2* knockout mouse model to investigate on roles of PGs and their GAGs in pulmonary and renal homeostasis, respectively. Finally, we manipulated GAG levels in vitro to mechanistically view how loss of these molecules impacts cellular uptake of protein.

The first part of this research involved identifying the mutations responsible for SOS. We reported the mutation to be in *XYLT2*. We identified the mutation by sequencing and characterized the mutation molecularly by showing decreased mRNA expression of *XYLT2* and biochemically by showing decreased glycosylation of HSPGs in the patient fibroblasts, by overall reduced XYLT activity in the patient serum, plasma, and fibroblasts, and by reduced sulfate incorporation in patient fibroblasts. We also showed that the mRNA expression of *XYLT1* is unchanged in the patients suggesting no compensatory mechanism exists between the two XYLT isoforms. Assessment of the known patients considering their specific mutations and following up with detailed and chronologic clinical assessments in the future will help us to delineate more of the isoform specificity in the function of various organs as well as in glycosylation of multiple PGs with age. This in comparison to the age-related changes we see in the *Xylt2-/-* mice is of interest.

The second part of this research involved loss of XylT2 in mouse and the associated impact on renal function. The research was based on previous findings that *Xylt2-/-* mice had mild

fibrosis in the kidney, dilatations of kidney tubules, defective glycosylation of selective PGs in the kidney, and progressive renal disease resulting into renal failure at older age. We investigated on how XylT2 deficiency contributes to kidney pathology by analyzing the kidneys for functional, ultrastructural, and molecular changes during XylT2 deficiency. Similar to human XYLT2 deficient patient fibroblasts, we did not see any compensatory increase in *Xylt1* mRNA in *Xylt2-/-* mice kidneys. Our findings show that XylT2 is the predominant Xylt in the kidney and XylT2 mediated glycosylation is important for maintenance of glomerular and tubular ultrastructure and function. We show that XylT2 deficiency results in proteinuria associated with alterations in glomerular ultrastructure. Using an in-vitro model, we also show that GAGs and XYLT2 are required for proper functioning of the proximal convoluted tubule, i.e. reabsorption of proteins transgressing the glomerular filtration barrier. We also reported that some membrane associated PG core protein mRNA expression is downregulated in *Xylt2-/-* mice identifying novel roles of these membrane associated PGs and their GAGs in nephron homeostasis. Our findings also might indicate some glycosylation mediated regulation of membrane associated PG core protein expression. Future research should focus on understanding the mechanism by which GAGs regulate the protein handling process, most importantly in the PCT, and how GAGs might be playing in regulation of core protein expression in the kidney. Answers to these questions will bring new insight into how proteinuria develops and progresses during CKD and reciprocally may identify candidate therapeutics for reducing proteinuria during CKD.

The third part of this research investigated the role of XylT1 dependent PGs in pulmonary mechanics and innate immunity using a *Xylt1* conditional knockout mouse model. Similar to kidneys, various diseases and pathological conditions of the lungs are associated with alterations in PGs expression and their glycosylation. Here, we show that *Xylt1* deletion results in changes in PG expression in the lungs and is associated with increased resistance and decreased compliance of the lungs. Our preliminary findings suggest that the alterations in pulmonary dynamics are less likely to come solely from the reduced chest wall mechanics, pulmonary

fibrosis, or due to endothelium PGs. We also show that *Xylt1* deficiency predisposes the lungs to elevated responses to LPS induced acute lung injury by over-stimulation of NFκB pathway, and possibly by decreasing surfactant associated protein-D and increasing cluster of differentiation 14 expressions. During LPS exposure, levels of *Xylt2* mRNA also decrease in XylT1 deficient lungs suggesting regulation of *Xylt2* by LPS induced transcription factors thus further impacting some XylT2 dependent glycosylation of PG core proteins. The regulation of XylT isoforms is largely unknown, and understanding how these isoforms are regulated during health and disease should be one primary focus of future research.

In summary, we show that XylT isoforms could have overlapping functions in the development and maintenance of multiple organ and tissue systems yet there can be niches of function where predominance of expression does not always indicate critical influence and that compensatory changes in seemingly redundant isoforms are not guaranteed even within the same tissue or cell type..

APPENDICES

Appendix I: Author permission from Elsevier

Title: Homozygosity for Frameshift Mutations in XYLT2 Result in a Spondylo-Ocular Syndrome with Bone Fragility, Cataracts, and Hearing Defects

Author: Craig F. Munns,Somayyeh Fahiminiya,Nabin Poudel,Maria Cristina Munteanu,Jacek Majewski,David O. Sillence,Jordan P. Metcalf,Andrew Biggin,Francis Glorieux,François Fassier,Frank Rauch,Myron E. Hinsdale

Publication: The American Journal of Human Genetics

Publisher: Elsevier

Date: 4 June 2015

Appendix II: Cd14 Expression during LPS challenge in the lungs

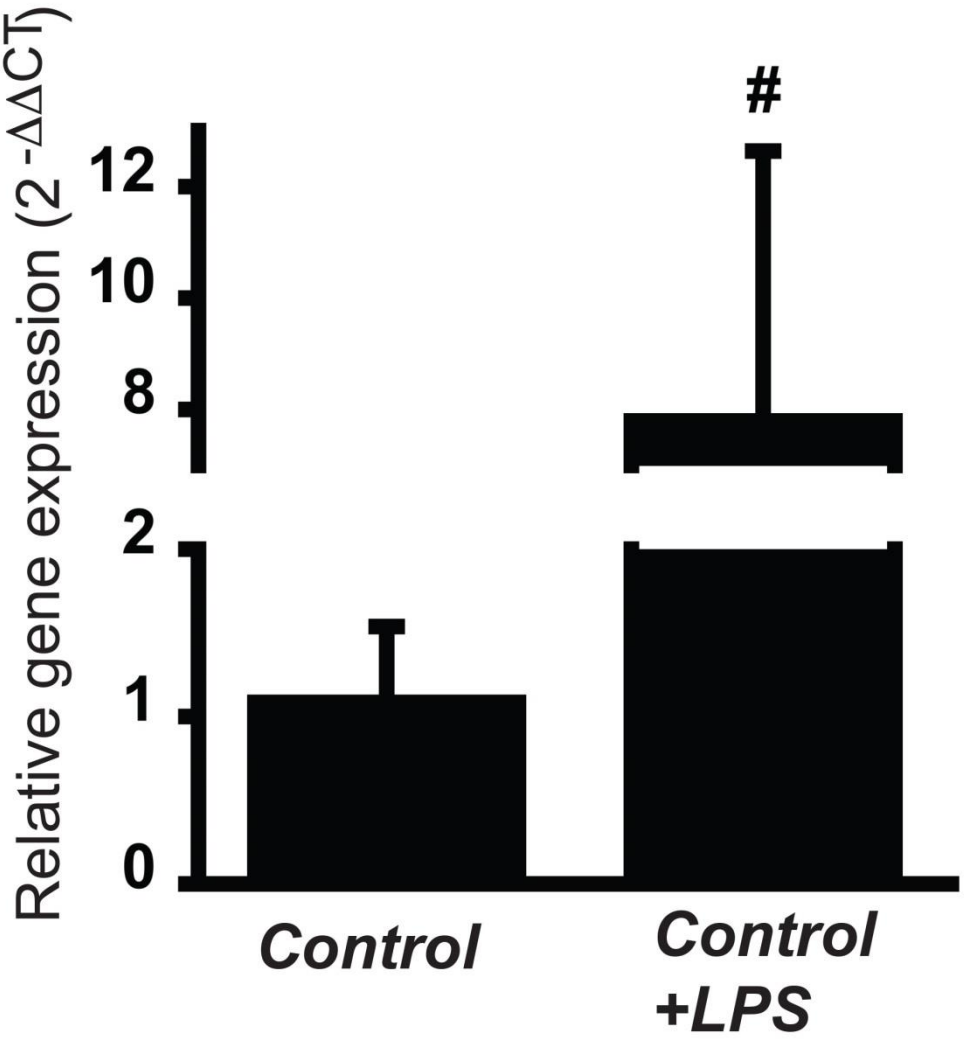

Realtime RT-PCR was performed in lungs from LPS challenged mice to detect changes in levels of Cd14 mRNA after LPS challenge. Our data shows a significant increase in cd14 mRNA levels after LPS challenge in mice.

Appendix III: Xylt1 in mouse lungs and cell types in bleomycin induced fibrosis

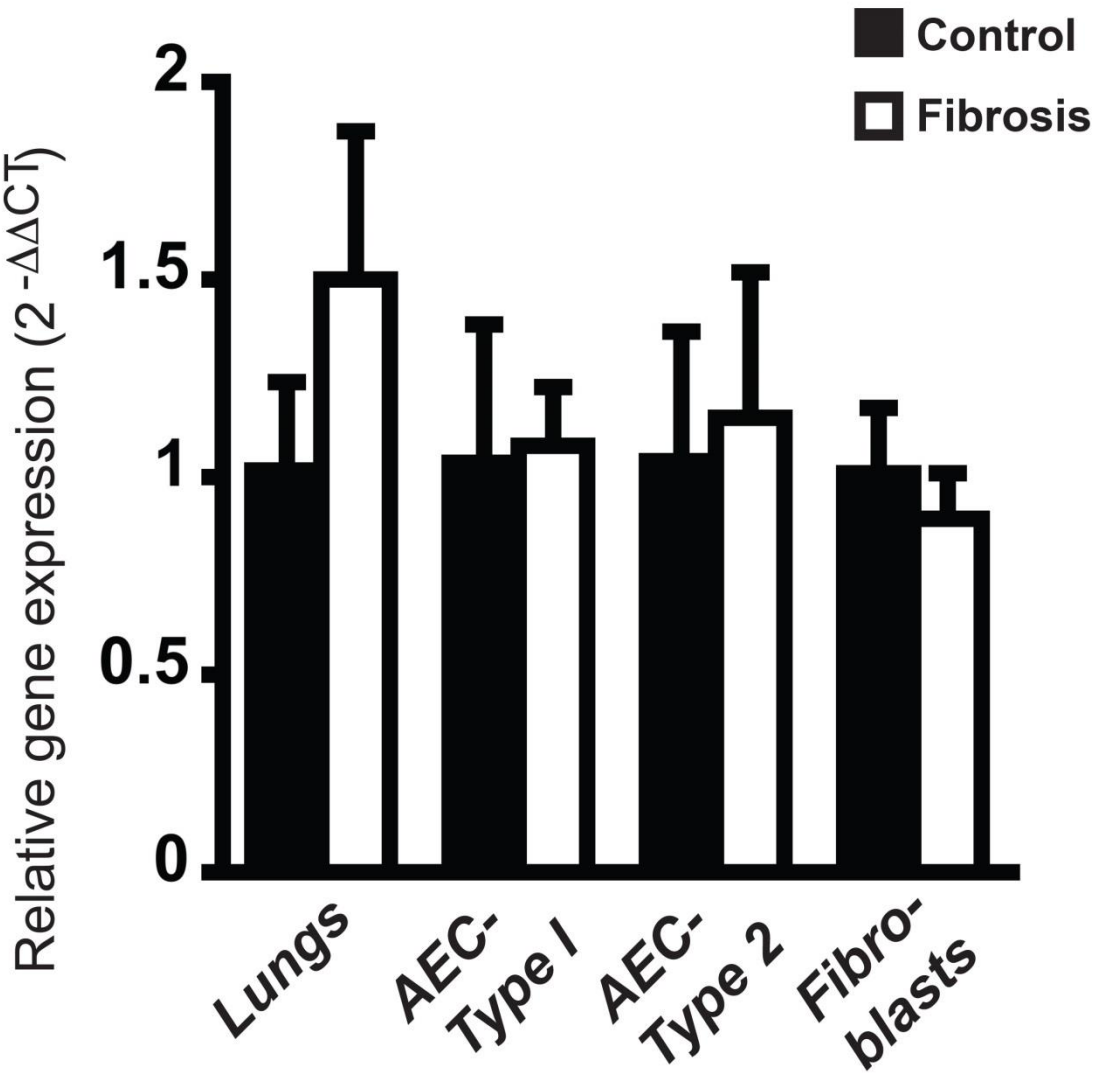

Realtime PCR was performed to measure changes in levels of *Xylt1* in mouse model of bleomycin induced pulmonary fibrosis. Our data indicates that bleomycin induced pulmonary fibrosis does not alter expression of *Xylt1* mRNA in various lung cell types. (This experiment was conducted by Yurong Liang at Oklahoma Center for Respiratory and Infectious Disease-Molecular Biology Core.)

Appendix IV: Xylt2 expression in mouse lungs and cell types in bleomycin induced fibrosis

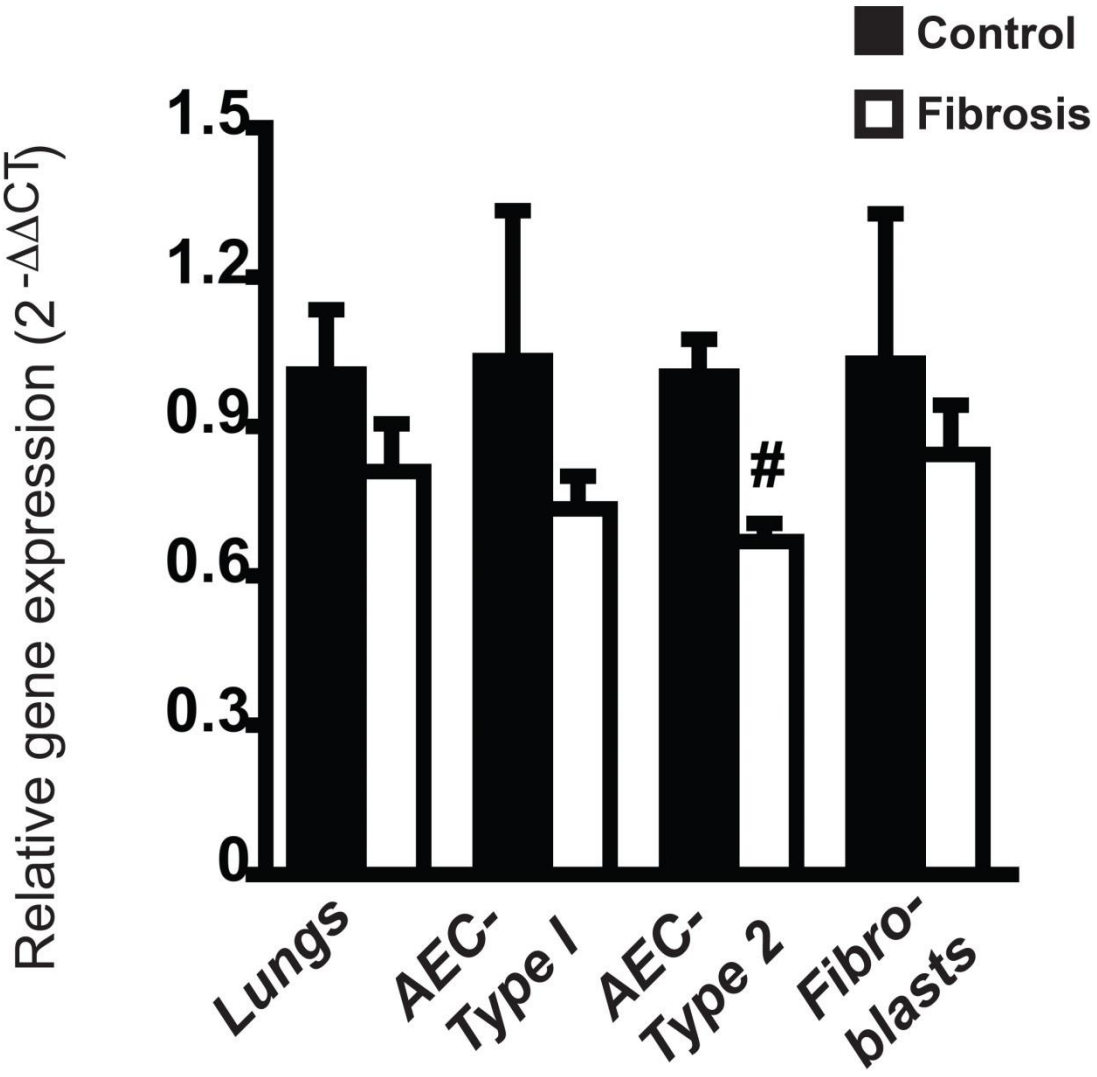

Realtime PCR was performed to measure changes in levels of *Xylt1* in mouse model of bleomycin induced pulmonary fibrosis. Our data indicates that bleomycin induced pulmonary fibrosis does not alter expression of *Xylt1* mRNA in the lung cell types except in type 2 alveolar epithelial cells. (This experiment was conducted by Yurong Liang at Oklahoma Center for Respiratory and Infectious Disease- Molecular Biology Core.)

VITA

Nabin Poudel

Candidate for the Degree of

Doctor of Philosophy

Thesis: Clinical, Cellular, and Biochemical Consequences of Xylosyltransferase Deficiency: Impact of Isoforms and Cellular Expression

Major Field: Veterinary Biomedical Sciences

Biographical:

Education:

Completed the requirements for the Doctor of Philosophy/ in Veterinary Biomedical Sciences at Oklahoma State University, Stillwater, Oklahoma in May, 2018.

Completed the requirements for the Bachelor of Veterinary Science and Animal Husbandry at Tribhuvan University, Nepal in 2009

Experience:
Graduate Teaching Associate (August 2011- May 2018)

Professional Memberships:
American Society of Nephrology
American Society of Biochemistry and Molecular Biology